ISSN 0021-9673

VOL. 516 NO. 2 SEPTEMBER 21, 1990
THIS ISSUE COMPLETES VOL. 516

JOURNAL OF CHROMATOGRAPHY

INTERNATIONAL JOURNAL ON CHROMATOGRAPHY, ELECTROPHORESIS AND RELATED METHODS

ELSEVIER

JOURNAL OF CHROMATOGRAPHY

Scope. The *Journal of Chromatography* publishes papers on all aspects of chromatography, electrophoresis and related methods. Contributions consist mainly of research papers dealing with chromatographic theory, instrumental development and their applications. The section *Biomedical Applications*, which is under separate editorship, deals with the following aspects: developments in and applications of chromatographic and electrophoretic techniques related to clinical diagnosis or alterations during medical treatment; screening and profiling of body fluids or tissues with special reference to metabolic disorders; results from basic medical research with direct consequences in clinical practice; drug level monitoring and pharmacokinetic studies; clinical toxicology; analytical studies in occupational medicine.

Submission of Papers. Manuscripts (in English; *four* copies are required) should be submitted to: The Editor of *Journal of Chromatography*, P.O. Box 681, 1000 AR Amsterdam, The Netherlands, or to: The Editor of *Journal of Chromatography, Biomedical Applications*, P.O. Box 681, 1000 AR Amsterdam, The Netherlands. Review articles are invited or proposed by letter to the Editors. An outline of the proposed review should first be forwarded to the Editors for preliminary discussion prior to preparation. Submission of an article is understood to imply that the article is original and unpublished and is not being considered for publication elsewhere. For copyright regulations, see below.

Subscription Orders. Subscription orders should be sent to: Elsevier Science Publishers B.V., P.O. Box 211, 1000 AE Amsterdam, The Netherlands, Tel. 5803 911, Telex 18582 ESPA NL. The *Journal of Chromatography* and the *Biomedical Applications* section can be subscribed to separately.

Publication. The *Journal of Chromatography* (incl. *Biomedical Applications*) has 37 volumes in 1990. The subscription prices for 1990 are:

J. Chromatogr. (incl. *Cum. Indexes, Vols. 451–500*) + *Biomed. Appl.* (Vols. 498–534):
Dfl. 6734.00 plus Dfl. 1036.00 (p.p.h.) (total *ca.* US$ 3885.00)

J. Chromatogr. (incl. *Cum. Indexes, Vols. 451–500*) only (Vols. 498–524):
Dfl. 5616.00 plus Dfl. 756.00 (p.p.h.) (total *ca.* US$ 3186.00)

Biomed. Appl. only (Vols. 525–534):
Dfl. 2080.00 plus Dfl. 280.00 (p.p.h.) (total *ca.* US$ 1180.00).

Our p.p.h. (postage, package and handling) charge includes surface delivery of all issues, except to subscribers in Argentina, Australia, Brasil, Canada, China, Hong Kong, India, Israel, Malaysia, Mexico, New Zealand, Pakistan, Singapore, South Africa, South Korea, Taiwan, Thailand and the U.S.A. who receive all issues by air delivery (S.A.L. — Surface Air Lifted) at no extra cost. For Japan, air delivery requires 50% additional charge; for all other countries airmail and S.A.L. charges are available upon request. Back volumes of the *Journal of Chromatography* (Vols. 1–497) are available at Dfl. 195.00 (plus postage). Claims for missing issues will be honoured, free of charge, within three months after publication of the issue. Customers in the U.S.A. and Canada wishing information on this and other Elsevier journals, please contact Journal Information Center, Elsevier Science Publishing Co. Inc., 655 Avenue of the Americas, New York, NY 10010. Tel. (212) 633-3750.

Abstracts/Contents Lists published in Analytical Abstracts, ASCA, Biochemical Abstracts, Biological Abstracts, Chemical Abstracts, Chemical Titles, Chromatography Abstracts, Clinical Chemistry Lookout, Current Contents/Life Sciences, Current Contents/Physical, Chemical & Earth Sciences, Deep-Sea Research/Part B: Oceanographic Literature Review, Excerpta Medica, Index Medicus, Mass Spectrometry Bulletin, PASCAL-CNRS, Pharmaceutical Abstracts, Referativnyi Zhurnal, Science Citation Index and Trends in Biotechnology.

See inside back cover for Publication Schedule, Information for Authors and information on Advertisements.

0021-9673/90/$03.50

Printed in The Netherlands

CONTENTS

(Abstracts/Contents Lists published in Analytical Abstracts, ASCA, Biochemical Abstracts, Biological Abstracts, Chemical Abstracts, Chemical Titles, Chromatography Abstracts, Current Contents/Life Sciences, Current Contents/Physical, Chemical & Earth Sciences, Deep-Sea Research/Part B: Oceanographic Literature Review, Excerpta Medica, Index Medicus, Mass Spectrometry Bulletin, PASCAL-CNRS, Referativnyi Zhurnal and Science Citation Index)

(Continued overleaf)

Contents (continued)

15 th International

Symposium

on Column Liquid

Chromatography

Convention Center

Basel, Switzerland

June 3–7, 1991

HPLC '91 Basel

Chairman

Dr. Fritz Erni

Secretariat

Swiss Industries Fair
Congress Department
P. O. Box
CH-4021 Basel
Switzerland

Telephone
++41 61/686 28 28
Telefax
++41 61/691 80 49

ANNOUNCEMENT AND CALL FOR PAPERS

12th INTERNATIONAL MASS SPECTROMETRY CONFERENCE

Amsterdam, The Netherlands

26–30 August 1991

The scientific programme will cover all aspects of mass spectrometry: theory, fundamental studies, applications, and instrumentation. An important aim of the Organizing Committee is to provide an atmosphere which will stimulate the exchange of information between the attending scientists.

Plenary lectures will be given by invited speakers who will review areas in mass spectrometry such as instrumentation, theory, multi-photon ionisation, gas phase ion chemistry, desorption and hyphenated methods and biochemical applications. Shorter keynote lectures, also to be presented by invited speakers, will consist of specialized reviews covering similar subjects, and topics such as high masses, clusters, organometallics, thermochemistry, isotope dilution and surface analysis, reaction dynamics, pyrolysis, geochemistry, environmental and forensic applications, biochemical and biomedical studies, and chemometrics.

Contributed papers will be accepted for poster sessions only. All those intending to contribute to the conference are invited to submit papers. All contributed papers will be refereed. The final date for submission of abstracts is **15 January 1991** and for revised/extended abstracts **1 June 1991**.

The proceedings of the Conference, comprising all plenary and keynote lectures in full, will be published by Elsevier Science Publishers as a hard-cover book, entitled "*Advances in Mass Spectrometry, Volume 12*" and as two consecutive volumes of the *International Journal of Mass Spectrometry and Ion Processes*. These will be published after the conference. A book containing the revised/extended abstracts of all contributed papers will be made available to registered participants at the conference. There will be an extensive exhibition of scientific equipment, including mass spectrometers in operation, and of the relevant literature.

The registration fee will be Dfl.500 if paid on or before **30 June 1991** and Dfl.550 if paid at a later date. The accompanying person's fee is Dfl.150. The registration fee for students working for a research degree will be Dfl.250 if paid on or before 30 June 1991. Students are encouraged to present a poster.

For further details, contact:

Conference Secretariat IMSC-XII
c/o RAI Organisatie Bureau Amsterdam bv
Europaplein 12
1078 GZ Amsterdam
The Netherlands

Experimental Design

A Chemometric Approach

S.N. Deming, *University of Houston, Houston, TX, USA, and* **S.L. Morgan,** *University of South Carolina, Columbia, SC, USA*

Now also available in a paperback edition!

"Deming and Morgan should be given high praise for bringing the principles of experimental design to the level of the practicing analytical chemist... an exceptionally lucid, easy-to-read presentation... an excellent addition to the collection of every analytical chemist. I recommend it with great enthusiasm." *(Analytical Chemistry)*

Unlike most current textbooks, this book approaches experimental design from the viewpoint of the experimenter rather than that of the statistician. It adopts a practical approach to experimental design and allows the reader to obtain the required information in the minimum number of experiments. It introduces the fundamentals of experimental design. Systems theory, response surface concepts, and basic statistics serve as a basis for the further development of matrix least squares and hypothesis testing. The effects of different experimental designs and models on the variance-covariance matrix and on the analysis of variance (ANOVA) are extensively discussed. Applications and advanced topics complete the text. Numerous worked examples are given.

The clear, practical approach adopted by the authors makes the book applicable to a wide audience. It will appeal particularly to those with a practical need (scientists, engineers, managers, research workers) who have completed their formal education but who still need to know efficient ways of carrying out experiments. It will also be an ideal text for advanced undergraduate and graduate students following courses in chemometrics, data acquisition and treatment, and design of experiments.

Contents: 1. System Theory. 2. Response Surfaces. 3. Basic Statistics. 4. One Experiment. 5. Two Experiments. 6. Hypothesis Testing. 7. The Variance-Covariance Matrix. 8. Three Experiments. 9. Analysis of Variance (ANOVA) for Linear Models. 10. A Ten-Experiment Example. 11. Approximating a Region of a Multi-factor Response Surface. 12. Additional Multifactor Concepts and Experimental Designs. Appendices: Matrix Algebra. Critical Values of t. Critical Values of F, {a} = 0.05. Index.

Data Handling in Science and Technology, 3
1987 1st repr. 1988 xiv + 286 pages
US$ 118.50 / Dfl. 225.00; 0-444-42734-1
Paperback: US$ 65.75 / Dfl. 125.00
Paperback ISBN: 0-444-43032-6

ELSEVIER

P.O. Box 211, 1000 AE Amsterdam, The Netherlands.

P.O. Box 882, Madison Square Station, New York, NY 10159, USA.

Comprehensive Analytical Chemistry

edited by **G. Svehla,** *Professor of Analytical Chemistry, University College, Cork, Ireland*

Vol. XXIV: Energy Dispersive X-Ray Fluorescence Analysis

by **B. Dziunikowski,** *Institute of Physics and Nuclear Techniques, Academy of Mining and Metallurgy, Warsaw, Poland*

In Volume IIC of the series, G.L. Macdonald contributed a chapter on X-Ray Spectrometry in which the principles of X-ray fluorescence analysis were presented with great clarity. Since that contribution appeared in 1971 tremendous developments have taken place with one of the most important new features being the appearance of energy-dispersive methods.

This new volume gives a detailed and up-to-date account of this important technique. It covers the various physical and technical problems associated with this analytical method, with emphasis on explaining the interferences due to matrix and particle size effects. Methods for overcoming these interferences are described and other sources of errors and the processing of measurement data are discussed. Also described are numerous applications of EDXRF analysis in a variety of fields including geological prospecting and mining, trace element analysis, biology, medicine, environmental pollution control, archaeology, forensic sciences, and others.

Contents: 1. Fundamentals. Energy quantization. Distribution of electrons in an atom. Atom excitation. Atom deexcitation. Photon scattering. Attenuation of X-ray beam. Mean and effective atomic number. 2. Sources of Primary (Exciting) Radiation. Properties of radioisotope sources. Production of radioisotope sources. Isotope X-ray sources. Influence of measuring conditions on the shape of X-ray spectrum. Low-power X-ray tubes. 3. Secondary Radiation of Sample. Intensity of fluorescence radiation. Intensity of scattered radiation. 4. Detection of X-Rays. Proportional counter. Scintillation counter. Solid-state detector. Detection efficiency. Energy resolution. Gas proportional-scintillation counters. 5. X-Ray Spectrometry. Electronic methods (pulse-height selection). Filter methods. Radiator methods. 6. Selection of Optimum Conditions for Analysis. Calibration. Sensitivity of analysis. Factors influencing sensitivity. 7. Disturbing Effects. Interelement radiation. Matrix effects. Particle-size effects. Mineralogical effects. Surface effects. 8. Methods for Eliminating Matrix Effects. Analysis of three-component materials. Analysis of multicomponent materials. Calculation correction methods. Methods requiring special preparation of samples. 9. Other Sources of Errors. Errors due to statistical fluctuations. Equipment effects. Background interference. Effects due to the physical state of the sample. 10. Processing of Measurement Data. Statistical distributions and their parameters. Precision. Accuracy. Rejecting an outlier. Decision limit, detection limit, and determination limit. 11. Applications of Energy-Dispersive X-Ray Fluorescence Analysis in Geological Prospecting and Mining. Field prospecting analyses. Analysis of drill cores and drillings. Analyses in boreholes (X-ray fluorescence logging). Laboratory analyses of geological materials. Analyses of lunar and Martian surfaces. 12. On-Stream Analyses. Introduction. Mineral processing control. Calciferous sludge analysis. Analysis of loose materials. 13. Trace Analysis. Introduction. Preconcentration methods. Analysis of water and effluent-waste pollutants. Analysis of air pollutants. X-ray fluorescence analysis in medical applications. 14. Miscellaneous Applications. Alloy analysis. Analysis of solutions. Analysis of gases. Analysis of petroleum products. Analysis of paints and lacquers. EDXRF analysis in archaeology. Coating thickness measurements. Other applications of EDXRF. References. Subject Index.

1989 xx + 432 pages
Price: US$ 215.50 / Dfl. 420.00
Subscr. Price: US$ 194.75 / Dfl. 380.00
ISBN 0-444-98897-1

ELSEVIER SCIENCE PUBLISHERS

P.O. Box 211, 1000 AE Amsterdam, The Netherlands
P.O. Box 882, Madison Square Station, New York, NY 10159, USA

Journal of Chromatography, 516 (1990) 301–312
Elsevier Science Publishers B.V., Amsterdam

CHROM. 22 537

Fabrication of columns for open-tubular liquid chromatography using photopolymerization of acrylates

S. EGUCHI[a], J. G. KLOOSTERBOER*, C. P. G. ZEGERS and P. J. SCHOENMAKERS
Philips Research Laboratories, P.O. Box 80 000, 5600 JA Eindhoven (The Netherlands)
and
P. P. H. TOCK, J. C. KRAAK and H. POPPE
Laboratory for Analytical Chemistry, University of Amsterdam, Nieuwe Achtergracht 166, 1018 WV Amsterdam (The Netherlands)
(First received April 3rd, 1990; revised manuscript received May 3rd, 1990)

ABSTRACT

In liquid chromatography, a significant improvement of separation can be achieved by using 5–10-μm I.D. open capillaries instead of packed columns. In these capillaries relatively thick (0.3–2 μm) films of stationary phases are required. These are difficult to prepare if polymer solutions are to be used. The fabrication of thick polymer films inside quartz-glass capillaries using chain cross-linking photopolymerization of monomers in liquid solution rather than cross-linking of polymers cast from solution is described. In a 9-μm capillary a film thickness of about 0.3 μm was readily prepared and plate numbers of $7 \cdot 10^4$ to $1.2 \cdot 10^5$ m^{-1} were obtained. The photopolymerization process can be carried out under either static or dynamic conditions. The latter method facilitates the manufacture of long columns with a length of several metres. The experimental conditions for making smooth coatings using a siloxane acrylate together with lauryl acrylate as a reactive diluent, and methods for inspection and testing of these columns, are described.

INTRODUCTION

Open-tubular liquid chromatography (OTLC) has the potential to become a useful method for very efficient separations of complex mixtures of thermally labile or non-volatile compounds. However, one of the major problems for the development of the technique is the necessity to combine a small inside diameter (I.D.) of the column with relatively thick stationary layers in order to combine a high efficiency with a sufficienct capacity for easy and accurate detection. Owing to the low diffusion rates

[a] On leave from Hitachi Research Laboratory, Hitachi Ltd., 4026 Kuji-cho, Hitachi-shi, Ibaraki-ken 319-12, Japan.

0021-9673/90/$03.50

of solutes in liquid mobile phases, the I.D. of the columns should be in the range 1–10 μm[1,2]. The use of such narrow columns implies very small peak volumes and, consequently, small injection and detection volumes. Therefore, special injection and detection devices have been developed. Nowadays it is possible to operate OTLC under optimum conditions, provided that suitable columns are available[3–9]. A particular drawback of small diameter columns is the difficulty of preparing suitable stationary phases with appropriate film thicknesses. In a 10-μm capillary the film thickness should be in the range 0.3–2 μm, depending on the diffusion coefficient of the solutes in the stationary phase[10,11].

Over the past few years considerable progress has been made in the preparation of stationary phases inside small I.D. capillaries[11–20]. Recently, a method was described for preparing a porous silica layer in 10-μm I.D. fused-silica capillaries[12–14]. The porous silica layer was prepared by coating the wall with poly(ethoxysilane) (PES), followed by conversion of PES into porous silica by treatment with ammonia. Columns prepared in this way showed good efficiency in liquid–liquid and reversed-phase chromatography. However, the phase ratios obtained by this procedure are insufficient as the thickness of the PES film is restricted by the coating procedures (the phase ratio is defined as the accessible surface area of the stationary phase divided by the volume of the mobile phase).

Apart from the preparation of porous layers, most progress has been made with the fabrication of columns coated with polysiloxanes using either static[11,12,17–19] or precipitation coating[20]. Very efficient columns have been prepared from 5- and 10-μm I.D. capillaries. However, just as with the porous silica layers, static evaporation coating procedures yielded only thin films, especially in the 5-μm I.D. capillaries. So far it has proved impossible to prepare films thicker than about 0.03 μm. The limitation of the thickness is caused by several factors. First, a very high concentration of polymer would be required. Second, the polymer solution should have a high viscosity in order to form a uniform and smooth film but Rayleigh instability should be avoided[21]. However, it is very difficult to filtrate concentrated, viscous solutions and to fill capillaries with them. Finally, the evaporation of the solvent from such solutions contained in a narrow capillary becomes prohibitively slow.

The precipitation coating procedure as introduced by Dluzneski and Jorgenson[20] has yielded thick films of polysiloxane phases. This procedure is very elegant and it has been demonstrated that coatings with suitable thicknesses in 5-μm I.D. columns with lengths of up to 3 m can be obtained in a relatively short time.

As an alternative to the techniques mentioned above, it was attempted to prepare thick stationary phases using *in situ* photopolymerization of a solution of a monomer and a photoinitiator, followed by evaporation of the solvent from the polymeric gel. This approach offers several advantages over the above-mentioned procedures:

(i) Low-viscosity monomers can be used to facilitate the filling of the narrow-bore capillary. A low viscosity also allows easy filtration of these monomers, which will prevent blockage of the column by impurities such as dust particles.

(ii) A wide choice of monomers is available. Within the class of highly reactive acrylates, for example, the polarities cover a wide range. This allows the manufacture of columns with, in principle, widely differing separation properties.

(iii) The polymer layers will have a higher stability if they are chemically bonded to the surface of a column. The surface of a column can be easily modified by silylation

with a compound containing acrylate groups. Copolymerization with the monomer then provides permanent adhesion.

The principles and use of photopolymerization in various manufacturing processes have been described, together with the relationship between monomer structure and some polymer properties[22].

This paper describes the preparation of a 0.5–1.0-μm thick polymer film inside 5–80-μm I.D. quartz-glass capillaries by means of *in situ* photopolymerization in solution using a siloxane acrylate as a cross-linking oligomer together with lauryl acrylate as a reactive diluent. The chromatographic properties of columns made in this way are described.

EXPERIMENTAL

Materials

Silica capillaries of 9–80 μm I.D. were made at Philips Research Laboratories in a similar way to optical fibres for telecommunication[23], but using a silica tube instead of a massive preform. Their outsides were coated with UV-cured acrylate polymers as are used for optical fibres (DS042 from DeSoto, DesPlaines, IL, U.S.A.). Commercially available capillaries, coated with a film of UV-absorbing polyimide, proved inadequate for *in situ* photopolymerization. Silica glass plates of 30–40-mm diameter were used as test disks for surface treatments.

Toluene (Merck, Darmstadt, F.R.G.) was dried over molecular sieves 4 A (Janssen, Beerse, Belgium). Chloroform, 2-propanol, tetrahydrofuran (THF), pentane and hexane (analytical-reagent grade, Merck) were used as supplied. Methanol (Merck) was used as a mobile phase for chromatographic testing. 3-(Methacryloxy)propyltrimethoxysilane (γ-MPS) (Petrarch Systems, Bristol, PA, U.S.A.) was distilled under reduced pressure. 3-(Acryloxy)propyltrimethoxysilane (γ-APS) (Petrarch Systems) and *n*-octyltriethoxysilane (n-OS) (Petrarch Systems) were used as supplied. Tetraethylene glycol diacrylate (TEGDA) (Polysciences, Warrington, PA, U.S.A.) and lauryl acrylate (LA) (Polysciences) were used without distillation. In addition to these monomers, a silicone acrylate (SiA; RC 710) (Goldschmidt, Essen, F.R.G.) was used. This acrylated dimethylsiloxane oligomer has a viscosity of 200 mPa s. Determination of unsaturation (by bromine addition) yielded a double bond content of 2.23 mmol g^{-1}, which corresponds to an acrylate equivalent weight of 450 g. α,α-Dimethoxy-α-phenylacetophenone (DMPA; Irgacure 651) (Ciba-Geigy, Basle, Switzerland) was used as a photoinitiator. Various anthracene derivatives were used as model compounds for testing the chromatographic properties.

Internal silylation of capillaries

Filling and washing of long capillaries (length 2–5 m, I.D. 80, 65, 10 and 9 μm) with solutions was carried out using a small reservoir pressurized with helium[14]. Silica capillaries were drawn at a temperature of 2000°C, which resulted in a very low density of surface silanol groups (SiOH). As in the silylation reaction the silane reacts with a silanol group, but not with a siloxane group, some of the siloxane groups must be converted into silanol groups. Therefore, the inner surfaces of the capillaries were etched with an alkaline solution using the method reported by Tock *et al.*[14]. A 1 *M* solution of potassium hydroxide was pumped through a silica capillary at room

temperature for about 2 h, using the pressurized vessel. After etching, the capillary was washed, first with water, then with 0.03 *M* hydrochloric acid for about 2 h, and finally with water until the effluent was neutral. Next, the capillary was dried at 125°C under a stream of helium for at least 4 h. The silylation was carried out by pumping a solution of silane in toluene (1–2%, v/v) through the etched capillary at 125°C for 1 h. The capillary was placed in an oven to control the temperature. Subsequently, it was washed with toluene and dried at room temperature under a stream of helium for at least 3 h.

Formation of polymer films inside capillaries

Two different means of UV irradiation were adopted, depending on the length of the capillaries. With test capillaries shorter than 60 cm UV irradiation was carried out statically, using one lamp (Philips, TLD 18W/08, length 60 cm). With capillaries longer than 60 cm dynamic irradiation was carried out by moving the capillary at a constant rate along the light source and using a longer lamp (Philips, TLD 36W/08, length 120 cm). This method is suitable for the preparation of columns of appreciable length. The light intensity distribution along the length of these long lamps was carefully checked with an International Light IL 745a UV-curing radiometer before use. After irradiation, the solvent was evaporated from one end of the capillary in a vacuum oven (pressure 15–20 kPa). The column was kept in the oven for at least 15 h. In view of the proposed mechanism of film formation (see below), it is obvious that the process has to be performed very carefully. Boiling of the solvent should be prevented at any time as this would promote irregular rupture of the gel. Finally, the capillary coating was thermally cured at 120°C, during at least one night.

Measurement of contact angles

In order to check whether surface treatments were effective or not, the wetting of the surface by a test liquid was observed before and after treatment[24]. On flat disks the contact angle θ between a sessile droplet of 3 μl and the surface was measured using a Raine–Hart goniometer. In capillaries the contact angles were obtained by measuring the rise of a test liquid inside the capillary. The filled capillary was left intact for at least 20 h until a constant reading of the rise of the test liquid was attained. Water was mainly used as a test liquid.

Chromatography

The chromatographic properties of 9-μm I.D. internally coatad capillaries were measured using the system for OTLC, shown in Fig. 1[14]. It consists of a thermostated solvent reservoir (volume 400 ml) which can be pressurized with helium, and serves as a constant-pressure pump. A 0.5-μl injection valve (Model 7520; Rheodyne, Berkeley, CA, U.S.A.) equipped with a splitting device is installed between the pump and the capillary column. A helium–cadmium laser (Model 356 XM; Omnichrome, Chino, CA, U.S.A.) is used as the light source for on-column fluorescence detection. The laser beam passes a 325-nm bandpass filter (Oriel, Stratford, CT, U.S.A.) and is focused with a quartz-glass lens (f = 50 mm) at the end of the capillary. The external protective coating of the capillary must be burned off at the end of the column over a length of 1 cm. The emitted light is collected at an angle of 90° by a Fresnel lens (f = 16 mm), then passes a 380-nm cut-off filter (Oriel). The intensity is measured with a photo-

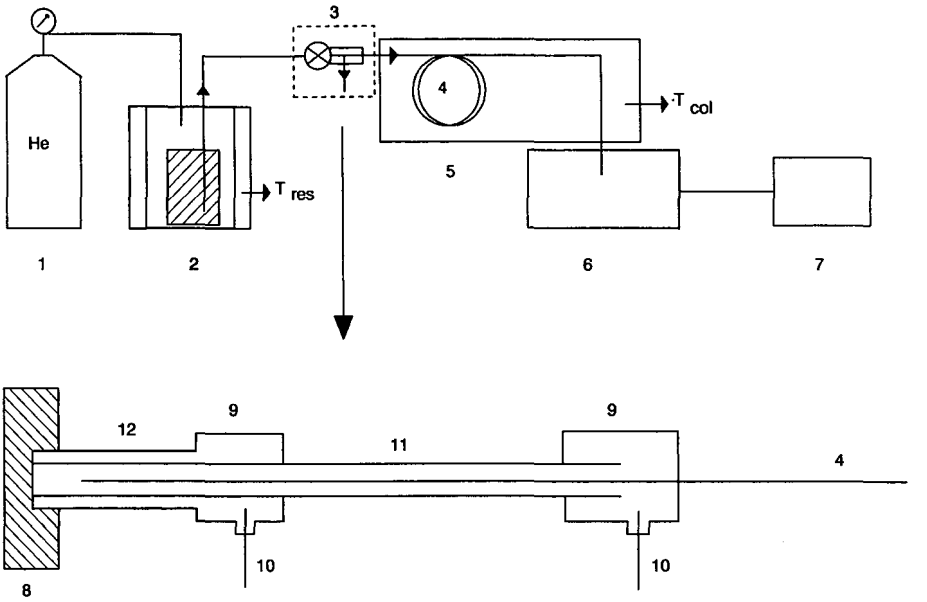

Fig. 1. Chromatographic set-up. 1 = Helium bomb; 2 = thermostated solvent reservoir; 3 = injector provided with a dual splitting device; 4 = capillary column; 5 = thermostated jacket; 6 = laser-induced fluorescence detector; 7 = strip-chart recorder; 8 = injector; 9 = 1/16-in. Swagelok union tee; 10 = waste capillary; 11 = fused-silica capillary, I.D = 300 μm; 12 = 1/16-in. stainless-steel tubing.

multiplier tube (Type 625 S; EMI, Hayes, U.K.). The photocurrent is amplified and converted into a voltage by means of an amplifier (Diomod 72-W; Knick, Berlin, F.R.G.). The signal is recorded with a potentiometric recorder (Siemens, Karlsruhe, F.R.G).

Methanol was used as the mobile phase throughout this study.

RESULTS AND DISCUSSION

Surface treatment of capillaries

In order to ensure proper adhesion of the polymer film to the wall of the capillary, the surface has to be reacted with a silane coupling agent possessing a copolymerizable (meth)acrylate group such as γ-MPS.

Treated capillaries were tested by determining contact angles from the capillary rise. Capillary rise measurements with water required a length of at least 50 cm in the case of a 80-μm I.D. capillary. Table I shows the change in contact angles in 80-μm I.D. capillaries observed after various surface treatments. Silylation causes a considerable increase in the contact angle. As in control experiments using flat disks even higher values were obtained, it was assumed that the capillary surface has a lower surface concentration of reactive SiOH groups than that of the disk. In order to achieve a maximum surface coverage, the capillaries were etched with dilute alkali solution. Etching reduces the contact angle of both capillaries and disks and subsequent silylation increases it again. The effect of etching on the ultimate contact angle is largest with the capillaries.

TABLE I

EFFECT OF VARIOUS SURFACE TREATMENTS ON CONTACT ANGLES OF WATER AT 20°C

No.	*Etching*	*Silylation (γ-MPS)*		*Contact angle, θ (°)*	
		Temperature (°C)	*Time (min)*	*Capillaries*	*Flat disks*
1	No	–	–	35–38	43
2	No	120	60	62	66
3	Yes	–	–	9	<5
4	Yes	120	60	74–82	67

Formation of polymer films inside silylated capillaries

Silicone resins have often been selected as stationary phases, as they show a very restricted swelling in polar solvents and as high diffusion coefficients of solutes have been reported[11,18,19]. A silicone acrylate resin (SiA) having the lowest viscosity available (0.2 Pa s) was selected. The silicone acrylate resin is basically a dimethylsiloxane, modified by substitution of acrylate groups. Polymer films could be obtained inside capillaries with an I.D. of 65 μm. However, filling with methanol not only caused a strong swelling of the gel but even complete blocking of the capillary occurred. A possible explanation of this unexpected behaviour is irregular rupture of the network, caused by too strong or inhomogeneous cross-linking[22] or by insufficient control of the rate of solvent evaporation. In order to obtain a more uniform polymer film, the cross-link density was reduced by the addition of LA [SiA/LA = 1:1 (w/w)]. The photoinitiator content was 2% (w/w) with respect to total monomer.

This mixture was applied to capillaries with a length of 1 m. The dynamic irradiation procedure was used in order to eliminate the effect of intensity variation along the fluorescent lamp. The capillaries were irradiated at a light intensity of 0.35 mW cm^{-2} and moved at a constant rate of 1.9–2.0 mm s^{-1}, so that the exposure time was 5 min. Next, THF was evaporated from one end of the capillary at 30°C under reduced pressure (15–20 kPa). Photographs of the cross-section and the outside of a capillary are shown in Fig. 2. In all sections almost the same cylindrical shape of the polymer film was observed. Next, the swelling behaviour of the polymer films was investigated in order to check whether blockage takes place inside the capillary. Fig. 3 shows a photograph of a polymer film after filling the capillary with methanol. From Figs. 2 and 3 it can be seen that there was no significant swelling of the polymer films, as could be expected from the large difference in solubility parameters of the polymer and methanol, respectively. Further, it has been reported that the degree of swelling of pure polydimethylsiloxane by methanol is very small[18]. The present polymer film appears to withstand methanol and other polar solvents, which prevents blockage of the capillary by swelling.

Finally, similar polymer films were made inside narrow-bore capillaries using the same procedure, except that the evaporation of THF was carried out at 60°C. In Fig. 4 scanning electron micrograph of a polymer film inside a 9-μm I.D. capillary (length 80 cm) is shown. The thickness of the film was estimated to be 0.3–0.4 μm. The uniformity of the film could not be assessed by microscopy.

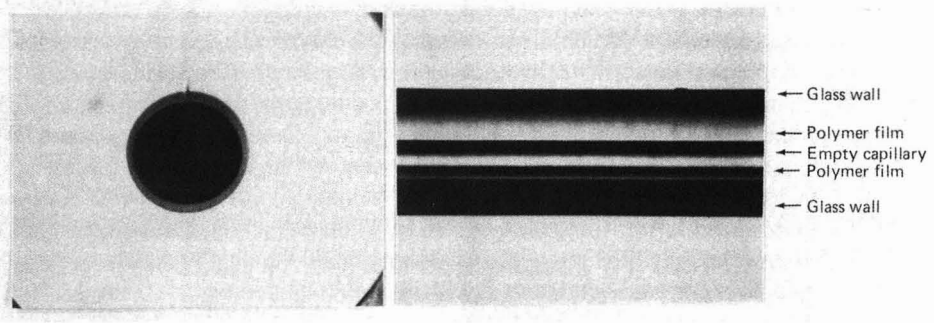

Fig. 2. Cross-section and side view of internally coated capillary with I.D. 65 μm and length 1 m. Viewed on its side, the bore of the capillary looks narrower than it is. This is due to refraction. Monomer: SiA–LA (1:1) with 2% (w/w) DMPA in THF. Monomer concentration: 30% (w/w). UV intensity: 0.35 mW cm^{-2}. Exposure time: 5 min.

The formation of cylindrical films is not always observed. When, for example, TEGDA was used as a monomer, with DMPA as the photoinitiator and THF as the solvent, a peculiar film shape was obtained (Fig. 5). The same characteristic "eye" shape was observed in a narrow-bore (9-μm I.D.) capillary. With increasing monomer concentration thicker films were formed but the "eye" shape of the film also became more prominent (Fig. 5b). At even higher concentrations films with a rough surface and numerous small plugs were formed. The typical "eye" shape is probably caused by rupture of the cylindrical gel on evaporation of the solvent. During polymerization in solution a strongly swollen gel is formed. On evaporation of the solvent the gel will tend to reduce its volume. As the gel is bonded to the wall, it can do so only by delamination or by rupture. Controlled rupture requires the control of cross-link density. Reduction of the cross-link density of the polymer network by adding a monoacrylate such as LA gave some improvement of the shape and the regularity of the polymer film but films of such compositions were unsuitable for chromatography

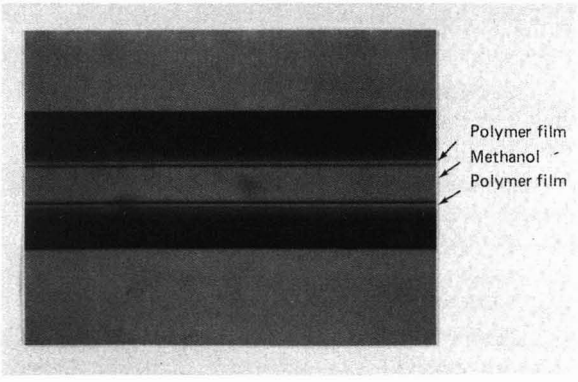

Fig. 3. Side view of a SiA–LA polymer film in a capillary with I.D. 65 μm after filling it with methanol. Preparation as in Fig. 2.

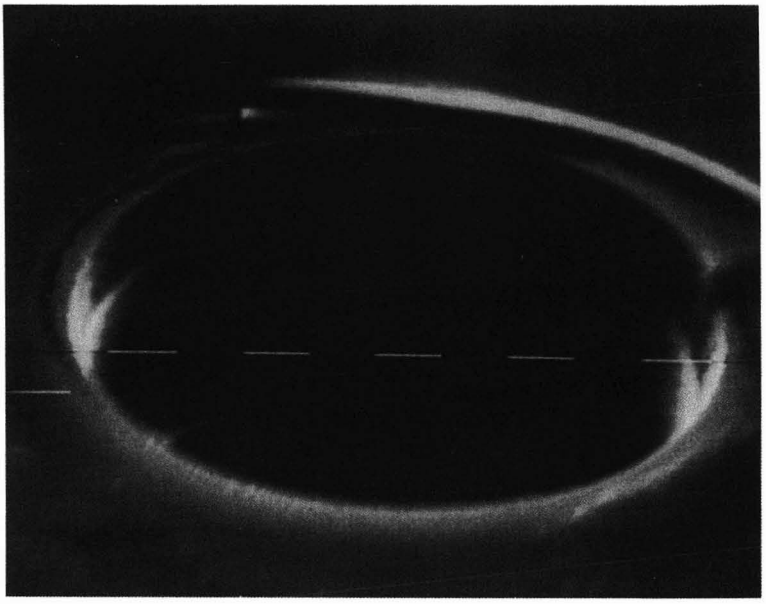

Fig. 4. Scanning electron micrograph of a polymer film inside a capillary with I.D. 9 μm. The film is just visible near the second and sixth white markers. Marker length, 1 μm. Preparation as in Fig. 2.

as swelling by the methanol eluent caused complete blocking of the column. Therefore, only the SiA–LA mixture was further investigated.

The proposed mechanism of film formation is further amplified by the observation that in capillaries which were treated with a non-copolymerizable silane such as n-OS a filament was formed instead of a film. This also emphasizes the necessity to use a coreactive silane coupling agent.

Chromatography

Fig. 6 shows a chromatogram of the separation of eight polycyclic aromatic hydrocarbons (PAHs) in an 8.5-μm I.D. capillary coated with the SiA–LA polymer, described above. Photopolymerization reduced the I.D. to 7.7 μm, as measured by the methods reported by Tock *et al.*[14]. The eight PAHs were well separated using pure methanol as the eluent. For 9-hydroxymethylanthracene and 9,10-diphenylanthracene capacity factors (k') of 0.18 and 2.05, respectively, were obtained. Compared with the separation on a conventional reversed-phase packing of C_{18}-modified silica particles in a packed column, using pure methanol as the eluent, the separation on the polyacrylate-coated capillary column is good. The column is very hydrophobic owing to the presence of the lauryl chains in the polymer and therefore the PAHs elute only with a solvent with a high eluting strength.

In Fig. 7 an H *vs.* u curve is shown for the PAHs. It can be seen that the measured plate height, H, of the solutes increases linearly with the linear velocity, u. The diffusion coefficients of the solutes in the stationary phase (D_s) were calculated from the slope of these lines by subtracting the calculated mobile phase diffusion (C_m) term.

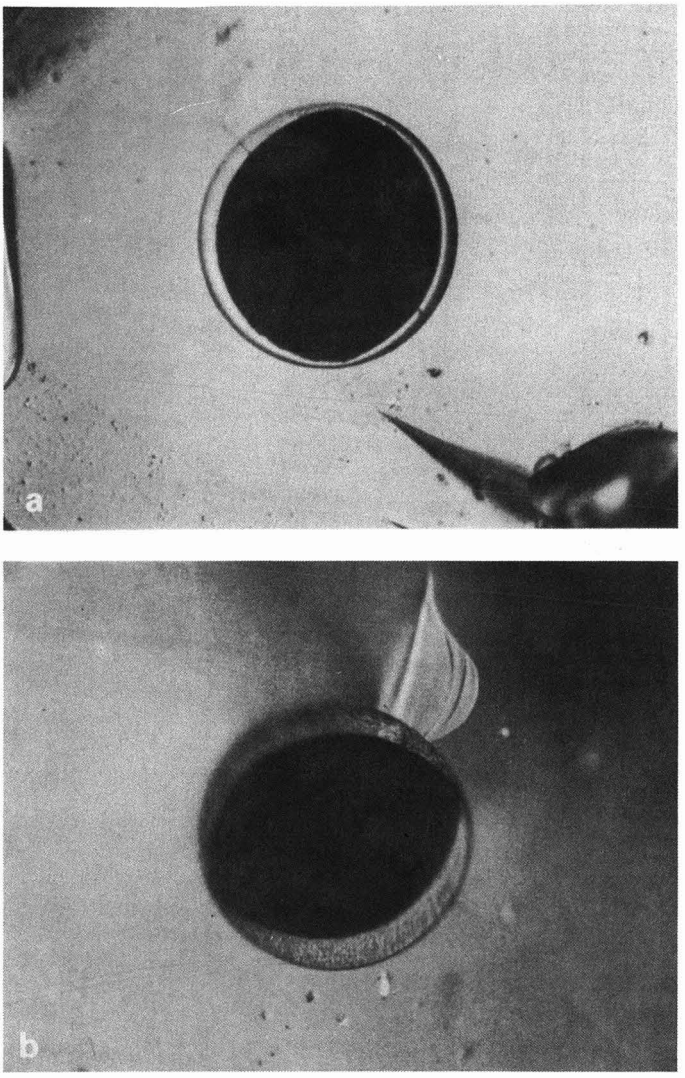

Fig. 5. Cross-section of internally coated capillaries with I.D. 65 μm. Monomer: TEGDA with 4% (w/w) DMPA in THF. Monomer concentration: (a) 20; (b) 30% (w/w). UV intensity: 0.52 mW cm^{-2}. Exposure time: 5 min.

In this calculation the value of the solute diffusion coefficient in the mobile phase (D_m) was taken to be 10^{-9} m^2 s^{-1}; k' and I.D. were determined experimentally. It was further assumed that no additional band broadening is introduced by irregularities of the film. The D_s values were found to be in the range $5 \cdot 10^{-12}$–$2 \cdot 10^{-11}$ m^2 s^{-1}; for anthracene $D_s = 2 \cdot 10^{-11}$ m^2 s^{-1}. If we compare this value with the reported value of $6 \cdot 10^{-12}$ m^2 s^{-1} for anthracene in a cross-linked silicone phase OV-101[11] it can be concluded that the present column material can be used at large thicknesses. Columns

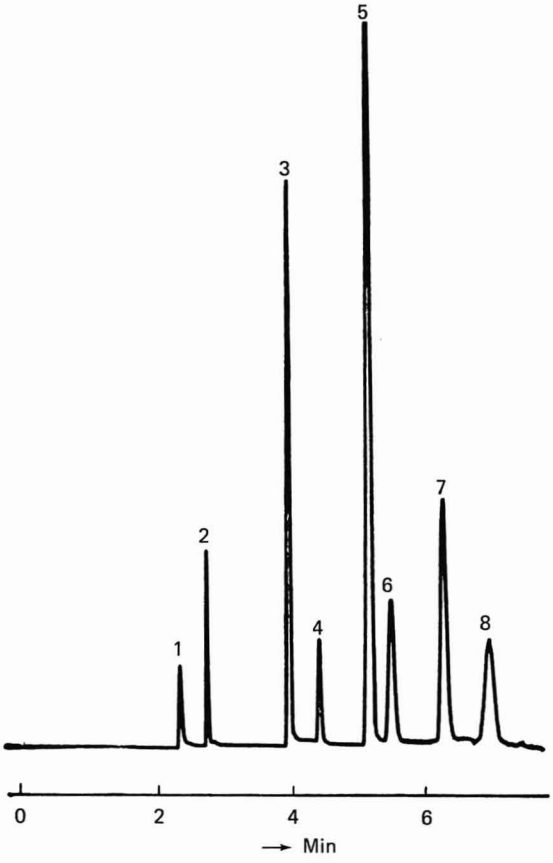

Fig. 6. Chromatogram obtained with the column shown in Fig. 4. Column dimensions: I.D. 7.7 μm, length 0.75 m. Mobile phase: methanol. Film thickness: 0.39 μm. Injection volume: 15 pl. Linear velocity: 5.5 mm s^{-1}. Pressure drop: 1.5 MPa. Solutes: 1 = fluorescein; 2 = 9-hydroxymethylanthracene; 3 = 9-cyano-anthracene; 4 = anthracene; 5 = fluoranthene; 6 = 9-phenylanthracene; 7 = 1,2-benzanthracene; 8 = 9,10-diphenylanthracene.

coated with layers 0.3–0.4 μm thick will support a considerably higher loading than the cross-linked OV-101 phase. Consequently, fewer detection problems are expected. As the D_s values of the solutes in the acrylate polymer are not known, it is not possible to compare the performance of the present column with theoretical plate-height estimates. To do so, it would be necessary to measure the diffusion coefficients of the solutes in the polymeric material used.

In Fig. 7 it can be seen that the efficiency obtained for anthracene is better than that for 9-hydroxymethylanthracene, although the k' value of the latter is smaller. The same observation was made with benzanthracene and phenylanthracene. This effect is not yet understood, it could perhaps be due to differences between the D_s values of the two pairs of solutes.

From the data shown in Fig. 7, plate numbers can also be calculated. These were found to be of the order of 10^5 m^{-1} for $u = 0.6$ mm s^{-1} and of the order of 10^4 m^{-1} for the highest linear velocities.

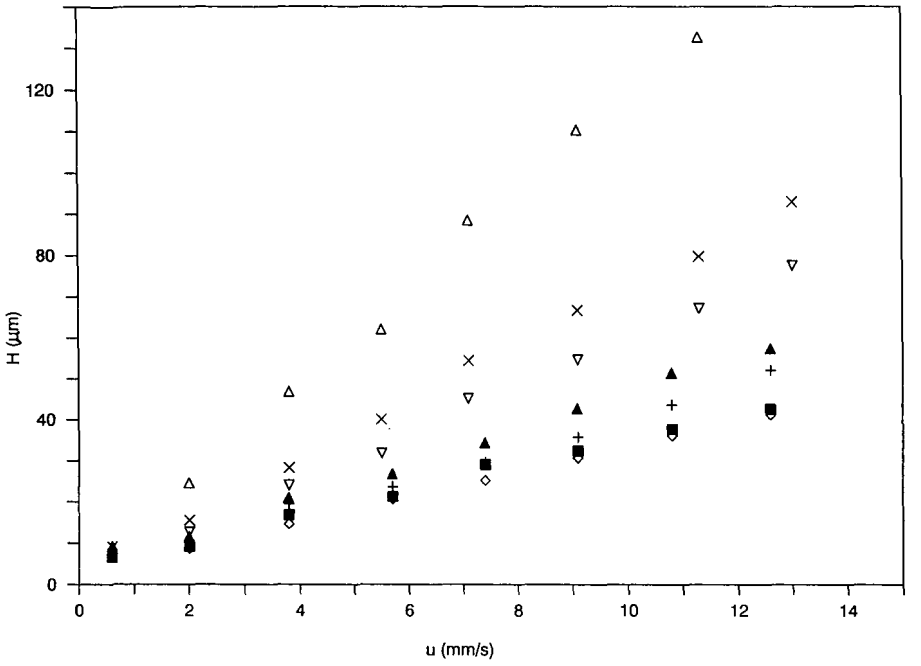

Fig. 7. Plate height H *vs.* linear velocity u for the column, eluent and solutes used in Fig. 6. Solutes ■ = 9-hydroxymethylanthracene, $k' = 0.18$; + = 9-cyanoanthracene, $k' = 0.71$; ◇ = anthracene, $k' = 0.91$; ▲ = fluoranthene, $k' = 1.25$; × = 9-phenylanthracene, $k' = 1.4$; ▽ = 1,2-benzanthracene, $k' = 1.75$; △ = 9,10-diphenylanthracene, $k' = 2.05$.

The performances of two other 8-μm I.D. columns, prepared in the same way as described above, were similar to that of the column described.

CONCLUSIONS

In situ photopolymerization of acrylic monomers in a 9-μm I.D. capillary has yielded a stable retentive layer with a suitable film thickness of about 0.4 μm. The chromatographic performance of the columns obtained sofar is very good, although a final evaluation would require a knowledge of the diffusion coefficients of test solutes in the acrylate photopolymer.

Filling of narrow-bore capillaries with a length of several metres with concentrated, dust-free solutions of monomers (as required for the formation of thick and smooth films) turned out to be easy.

Another feature of the reported method is that one can make columns of widely differing polarities, simply by changing the monomer. The swelling behaviour of the polymeric network can be controlled by variation of the cross-link density through the addition of non-cross-linking monomers.

ACKNOWLEDGEMENTS

Special thanks are due to C. M. G. Jochem for drawing the capillaries and to P. J.

Slikkerveer (both at Philips Research Laboratories) for explaining the gel rupture process.

REFERENCES

1 J. H. Knox and M. Saleem, *J. Chromatogr. Sci.*, 7 (1969) 614.
2 J. H. Knox and M. T. Gilbert, *J. Chromatogr.*, 186 (1979) 405.
3 J. B. Phillips, D. Luu, J. B. Pawliszyn and G. C. Carle, *Anal. Chem.*, 57 (1985) 2779.
4 H. P. M. van Vliet and H. Poppe, *J. Chromatogr.*, 346 (1985) 149.
5 L. A. Knecht, E. J. Guthrie and J. Jorgenson, *Anal. Chem.*, 56 (1984) 479.
6 R. T. Kennedy and J. W. Jorgenson, *Anal. Chem.*, 60 (1988) 1521.
7 J. de Wit and J. W. Jorgenson, *J. Chromatogr.*, 411 (1987) 201.
8 W. M. A. Niessen and H. Poppe, *J. Chromatogr.*, 394 (1987) 21.
9 A. Manz and W. Simon, *Microchim. Acta, Part I*, (1987) 147.
10 P. J. Schoenmakers, *J. High Resolut. Chromatogr. Chromatogr. Commun.*, 11 (1988) 278.
11 O. van Berkel, H. Poppe and J. C. Kraak, *Chromatographia*, 24 (1987) 739.
12 H. Poppe, J. C. Kraak, O. van Berkel-Geldof and P. P. H. Tock, in P. Sandra (Editor), *Proceedings of the Ninth Congress on Capillary Chromatography, Monterey, CA, 1988*, Hüthig, Heidelberg, 1989, pp. 345–354.
13 P. P. H. Tock, C. Boshoven, H. Poppe, J. C. Kraak and K. K. Unger, *J. Chromatogr.*, 477 (1989) 95.
14 P. P. H. Tock, G. Stegeman, R. Peerboom, H. Poppe, J. C. Kraak and K. K. Unger, *Chromatographia*, 24 (1987) 617.
15 J. Jorgenson and E. J. Guthrie, *J. Chromatogr.*, 255 (1983) 335.
16 M. J. Sepaniak, J. D. Vargo, C. N. Kettler and P. Maskarinec, *Anal. Chem.*, 56 (1984) 1252.
17 M. Farbrot, S. Folestad and M. Larsson, *J. High Resolut. Chromatogr. Chromatogr. Commun.*, 9 (1986) 117.
18 S. Folestad, B. Josefsson and M. Larsson, *J. Chromatogr.*, 391 (1987) 347.
19 S. Folestad and M. Larsson, *J. Chromatogr.*, 394 (1987) 455.
20 P. R. Dluzneski and J. W. Jorgenson, *J. High Resolut. Chromatogr. Chromatogr. Commun.*, 11 (1988) 332.
21 K. D. Bartle, C. L. Wooley, K. E. Markides, M. L. Lee and R. S. Hansen, *J. High Resolut. Chromatogr. Chromatogr. Commun.*, 10 (1987) 128.
22 J. G. Kloosterboer, *Adv. Polym. Sci.*, 84 (1988) 1.
23 A. G. Chynoweth and S. E. Miller (Editors), *Optical Fiber Telecommunications*, Academic Press, New York, 1979.
24 A. W. Adamson, *Physical Chemistry of Surfaces*, Interscience, New York, 2nd ed., 1967, ch. I and VII.

Journal of Chromatography, 516 (1990) 313–322
Elsevier Science Publishers B.V., Amsterdam

CHROM. 22 611

Enantiomeric resolution on molecularly imprinted polymers prepared with only non-covalent and non-ionic interactions

LARS I. ANDERSSON and KLAUS MOSBACH*
Department of Pure and Applied Biochemistry, University of Lund, Chemical Center, P.O. Box 124, S-221 00 Lund (Sweden)
(First received May 4th, 1990; revised manuscript received June 8th, 1990)

ABSTRACT

Molecular imprints were prepared utilizing only weak bonds between the print molecule and functional monomers; the bonding forces used in the imprinting process were only those weaker than covalent and ionic bonds. Methacrylate-based molecular imprints were prepared using a number of chiral compounds, including N-protected amino acid derivatives, as print molecules. Methacrylic acid was used as the functional monomer because the acid function of the monomer forms hydrogen bonds with a variety of polar functionalities, such as carboxylic acids, carbamates, heteroatoms and carboxylic esters, of the print molecule. Bulk polymers were prepared, ground and sieved to particles of size <25 μm, packed into high-performance liquid chromatographic (HPLC) columns and used for enantiomeric separations in the HPLC mode. The polymers were shown to effect efficient enantiomeric resolution of a racemate of the print molecule in addition to substrate selectivity for the print molecule in a mixture of substrates with very similar structures. For example, the enantiomers of Cbz-aspartic acid and Cbz-glutamic acid (Cbz = carbobenzoxy) were resolved with separation factors of 1.9 and 2.5, respectively, on polymers with molecular imprints of the L-form of the respective compounds. In addition, these polymers, prepared against Cbz-L-aspartic acid and Cbz-L-glutamic acid, respectively, had the ability to bind selectively the print molecule from a mixture of both racemates, although the two compounds differ only by one methylene group. The results presented represent a substantial widening of the scope of molecular imprinting in that it may now be possible to prepare molecular imprints against a very large number of compounds.

INTRODUCTION

The advances made recently in the field of molecular imprinting have been considerable, especially in the preparation of separation media for enantiomeric resolutions. The preparation of molecular imprints of amino acid derivatives and of other compounds by the non-covalent pre-arrangement approach has been described

0021-9673/90/$03.50

in a recent review[1]. Molecular imprints can be prepared against amino acid esters[2] and amino acid amides[3–7] using methacrylic acid as the functional monomer; this monomer interacts ionically with the amine of the print molecule, and its use is referred to below as the "ionic system". Such polymers can be used as stationary phases in the high-performance liquid chromatographic (HPLC) mode for enantiomeric separations of amino acid derivatives. A different approach to the preparation of molecular imprints involves the formation of reversible covalent bonds between monomers and a print molecule (for a review, see ref. 8), referred to below as the "covalent system". The reversible covalent bonds may be ketals[9], Schiff bases[10,11] or boronic esters[12,13]. However, the number of suitable reversible covalent bonds available for molecular imprinting is very limited; an adduct between the print molecule and suitable monomer(s) must be synthesized and the print molecule must be removed quantitatively from the polymer after the polymerization. Likewise, the number of compounds suitable for molecular imprinting utilizing ionic bonds is limited. In this paper this issue is addressed and we show that the limitations described can be overcome.

The role of hydrogen bonding in molecular recognition has been the focus of much attention recently[14]. It has long been known that carboxylic acids form hydrogen bonds with a great variety of polar functionalities, including carbamates, amides, carboxylic acids and carboxylic esters, and that the hydrogen bonds connecting one carboxylic acid with another are very strong[15]. By condensing Kemp triacid with various diamines, compounds were prepared that contained carboxylic acid functions arranged in a convergent molecular cleft for the selective binding of amines and neutral molecules[16]. Synthetic macrocyclic receptors in which the host–guest interactions are claimed to be based mainly on hydrogen bonds have also been reported[17,18]. These findings were applied to molecular imprinting, and in this paper we report for the first time the preparation of molecular imprints utilizing only bonds weaker than covalent and ionic between the print molecule and functional monomers. The interactions, during both the polymerization and the subsequent recognition event, are based solely on hydrogen bonds and other weak forces, such as hydrophobic interactions and dipole–dipole interactions. The resulting polymers were analysed for their ability to separate the enantiomers of print molecules and also for their ability to separate the original print molecule from a mixture of compounds similar in structure.

EXPERIMENTAL

Ethylene glycol dimethacrylate (EDMA) was obtained from Polysciences (Warrington, PA, U.S.A.) and methacrylic acid (MAA), 2,2′-azobis(2-methylpropionitrile) (AIBN) and *d*- and *l*-mandelic acids from Janssen Chimica (Beerse, Belgium). D- and L-Boc-tryptophans, D- and L-Boc-phenylalanines, D- and L-Boc-proline-N-hydroxysuccinimide esters and D- and L-Cbz-tryptophans were obtained from Nova Biochem (Läufelfingen, Switzerland) and D- and L-Cbz-aspartic acids and D- and L-Cbz-glutamic acids from Bachem (Bubendorf, Switzerland) (Boc = *tert.*-butoxycarbonyl; Cbz = carbobenzoxy, benzyloxycarbonyl). D- and L-Cbz-tryptophan methyl esters were prepared essentially as described in the literature[19]. Solvents were of either analytical-reagent or HPLC grade. HPLC analyses were performed with an LKB (Bromma, Sweden) system consisting of a Model 2152 HPLC controller, two Model 2150 HPLC pumps and a Model 2151 variable-wavelength monitor.

Polymer preparation

Polymers were prepared according to a standard method described previously[4,5] using methacrylic acid (MAA) as functional monomer and ethylene glycol dimethacrylate (EDMA) as cross-linker. The molar ratio of cross-linker to functional monomer to print molecule was 20:4:1, except for polymers prepared against Cbz-L-aspartic acid and Cbz-L-glutamic acid, where a molar ratio of 20:4:0.5 was used. MAA (10.48 mmol), EDMA (52.4 mmol), AIBN (0.76 mmol), chloroform (16 ml) and the appropriate amount of print molecule (2.62 or 1.31 mmol) were weighed into 50-ml borosilicate glass ampoules (Wheaton Scientific, Melvill, NJ, U.S.A.). The mixtures were cooled on ice, degassed under vacuum in a sonicating water bath and sparged with nitrogen for 5 min. The ampoules were then sealed with Parafilm and placed under a UV source (366 nm) at 4°C overnight (16 h). The bulk polymers were ground in a mechanical mortar (Retsch, Haan, F.R.G.) and sieved through a 25-μm sieve (Retsch). The fines were then removed by repeated sedimentation in acetonitrile and the particles were finally dried under vacuum.

High-performance liquid chromatography

Particles were suspended in chloroform–acetonitrile (17:3, v/v) by sonication and packed into 200 mm × 4.5 mm I.D. stainless-steel columns with acetonitrile as solvent at 300 bar using an air-driven fluid pump (Haskel Engineering Supply, Burbank, CA, U.S.A.). The columns were then washed on-line with methanol–acetic acid (9:1, v/v) until a stable baseline was obtained. The print molecule was almost quantitatively removed from the polymer by this treatment, as judged by Fourier transform IR measurements[7]. HPLC analyses were performed isocratically with the solvent compositions and flow-rates indicated for each polymer preparation in Tables I and II. Detection was at 250 nm. A mixture of 5 μg of each of the enantiomers of a given compound, prepared in the mobile phases, was injected for analysis in a total volume of 20 μl. Enantiomeric resolution was confirmed by separate injections of each of the enantiomers. The void volumes of the columns were determined by injection of acetone and chloroform. Capacity factors (k'), separation factors (α) and plate numbers (N) were calculated using standard chromatographic theory[20]. The resolution (R_s) was calculated according to Wulff *et al.*[12].

RESULTS AND DISCUSSION

The chromatographic performance of columns containing molecularly imprinted polymers has often been poor, as indicated by the broad peaks obtained. This has been attributed to mass transfer limitations, including both diffusion resistance and slow rates of binding and relase of the substrate. Previously, molecularly imprinted columns were run at elevated temperatures and low flow-rates[2,3,12]. A light-induced polymerization procedure was developed that could be performed at low temperatures (0°C)[4,5]. This method is easy to perform and the resulting polymer preparations display a significantly increased enantioselectivity in comparison with those prepared by previous methods. The resulting increase in resolving capacity allowed the preparation of columns that could be run at acceptable flow-rates at ambient temperature[4]. In addition, the peak shapes could be improved even further by applying gradient elution schemes[7]. The polymer preparations described here were all prepared using this improved polymerization procedure.

In the initial phase of this study we prepared molecular imprints against N-protected amino acids (see Fig. 1). The carboxylic acid function of the functional monomers was expected to form strong hydrogen bonds with the carboxylic acid function of the print molecules. Additionally, the methacrylic acid monomers may form hydrogen bonds with the carbamate function of the print molecules. The nitrogen in the pyrrole ring of the tryptophan derivatives may also form hydrogen bonds with the methacrylic acid monomers[15]. The polymer preparations were evaluated for their ability to resolve the enantiomers of print molecules in the chromatographic mode. In some instances the enantiomeric resolution of other substrates, similar in structure to the print molecule, was also analysed. Typical chromatograms of racemates of print molecules on polymers with molecular imprints against carboxylic acid derivatives are depicted in Fig. 2.

The results of the chromatographic evaluations of polymers with molecular imprints against the dicarboxylic acid derivatives Cbz-L-aspartic acid and Cbz-L-

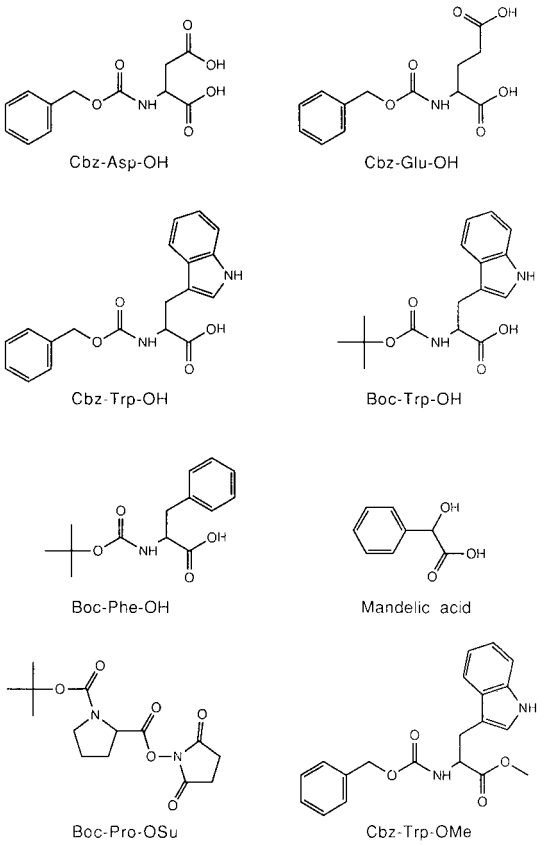

Fig. 1. Structures of the compounds used as print molecules. Abbreviations: Cbz-Asp-OH = N-benzyloxycarbonylaspartic acid; Cbz-Glu-OH = N-benzyloxycarbonylglutamic acid; Cbz-Trp-OH = N-benzyloxycarbonyltryptophan; Boc-Trp-OH = N-*tert.*-butoxycarbonyltryptophan; Boc-Phe-OH = N-*tert.*-butoxycarbonylphenylalanine; Boc-Pro-OSu = N-*tert.*-butoxycarbonylproline N-hydroxysuccinimide ester; Cbz-Trp-OMe = N-*tert.*-benzyloxycarbonyltryptophan methyl ester.

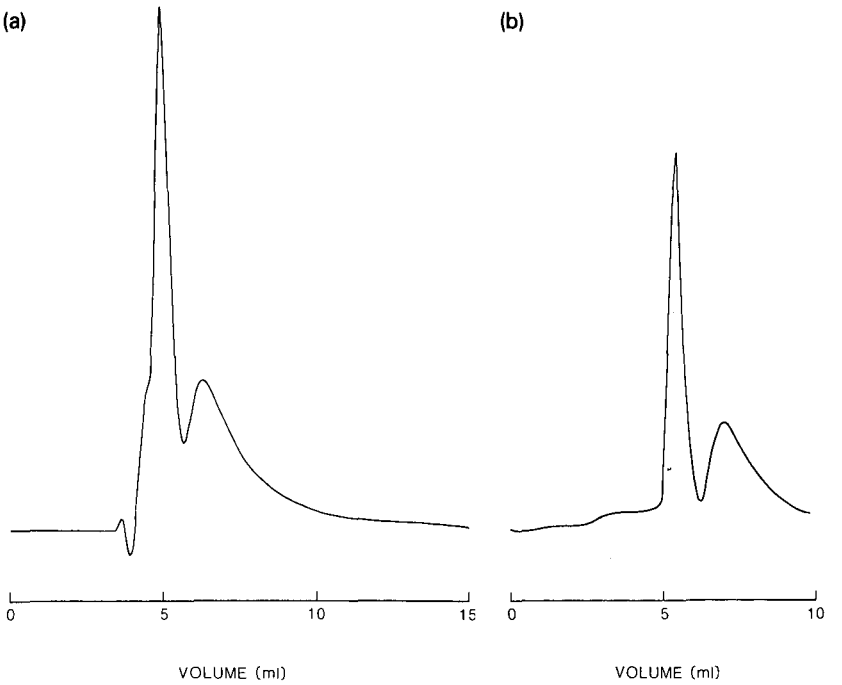

Fig. 2. Enantiomeric resolution of print molecule on polymers prepared with molecular imprints against Boc-L-tryptophan (Table II) and Boc-L-phenylalanine (Table II). Particles (<25 μm) were packed into 200 × 4.5 mm I.D. columns. Analyses were performed isocratically using (a) acetonitrile–chloroform–acetic acid (90:9.5:0.5, v/v/v) and (b) 0.25% (v/v) acetic acid in chloroform as the eluent at 1 ml/min at room temperature. Detection was at 250 nm. In all experiments, a mixture of 5 μg of each of the enantiomers of the compound was analysed. Plate numbers calculated for a non-retained, non-interacting void marker (acetone) were $N = 826$ for the column used in A and $N = 880$ for the column used in B. The analyses shown are (a) Boc-D,L-tryptophan on a polymer prepared against Boc-L-tryptophan and (b) Boc-D,L-phenylalanine on a polymer prepared against Boc-L-phenylalanine.

glutamic acid are presented in Table I. The enantiomers of the print molecule were resolved very efficiently on the respective polymer preparations. An interesting observation was that whereas analysis of a racemate of the "wrong" dicarboxylic acid gave no enantiomeric resolution with the present elution system (see Table I), injection of the pure enantiomers produced distinct peak maxima with separation factors in the range 1.05–1.08.

Analyses of a mixture of the two racemates, Cbz-aspartic acid and Cbz-glutamic acid, on these polymer preparations are shown in Fig. 3. The print molecule was the most retained compound on the respective polymer preparations, showing that efficient substrate selectivity between compounds very similar in structure was possible. For polymers molecularly imprinted against amino acid amides in the ionic system, the separation of the amino acid amide derivatives on a column with pre-defined specificity is highly dependent on the substitution of the amine moiety[7], whereas the side groups are of little importance[6]. In this respect, the extreme substrate selectivity of the dicarboxylic acid polymers is unexpected (Cbz-aspartic acid and Cbz-glutamic acid differ only by one methylene group, see Fig. 1).

TABLE I

ENANTIOMERIC RESOLUTION ON POLYMERS MOLECULARLY IMPRINTED WITH CBZ-L-ASPARTIC ACID AND CBZ-L-GLUTAMIC ACID

A mixture of 5 μg of each of the enantiomers of the amino acid derivatives was injected onto the column in a total volume of 20 μl of mobile phase. The elution was performed isocratically at room temperature using acetonitrile–chloroform–acetic acid (60:39.5:0.5, v/v/v) at a flow-rate of 1 ml/min (entries 1A and 2A) or 0.1 ml/min (entries 1B and 2B).

Entry	*Print molecule*	*N (acetone)*	*Cbz-aspartic acid*						*Cbz-glutamic acid*					
			k'_D	k'_L	N_D	N_L	α	R_s	k'_D	k'_L	N_D	N_L	α	R_s
1A	Cbz-L-Asp-OH	345	0.58	1.11	267	87	1.91	0.9	0.62	0.62	348[a]	281[a]	1.0	n.d.[b]
1B	Cbz-L-Asp-OH	820	0.58	1.25	500	142	2.16	1.7	0.61	0.61	564[a]	491[a]	1.0	n.d.
2A	Cbz-L-Glu-OH	538	0.49	0.49	458[a]	373[a]	1.0	n.d.	0.74	1.81	407	91	2.45	1.4
2B	Cbz-L-Glu-OH	995	0.51	0.51	n.d.	n.d.	1.0	n.d.	0.75	1.90	950	156	2.53	2.9

[a] Calculated on separate injections of the enantiomers, as injection of a racemate produced only a broad, partially resolved peak.
[b] n.d. = Not determined.

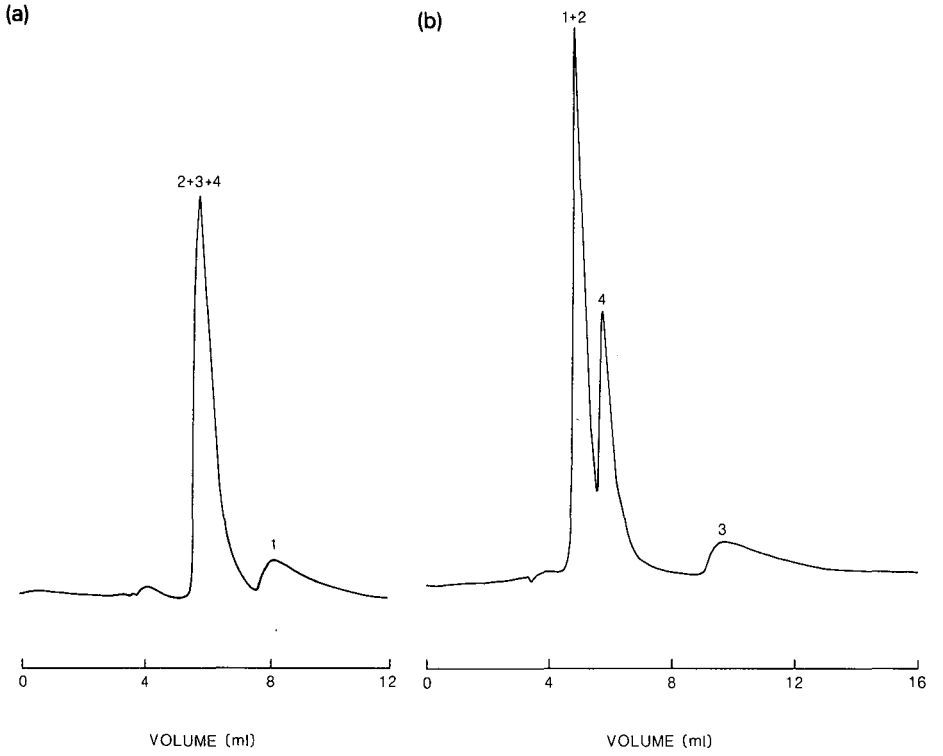

Fig. 3. Separation of (1) Cbz-L-aspartic acid, (2) Cbz-D-aspartic acid, (3) Cbz-L-glutamic acid and (4) Cbz-D-glutamic acid on polymers prepared against (a) Cbz-L-aspartic acid and (b) Cbz-L-glutamic acid. Particles (<25 μm) were packed into 200 × 4.5 mm I.D. columns. Analyses were performed isocratically using acetonitrile–chloroform–acetic acid (60:39.5:0.5, v/v/v) as the eluent at 0.1 ml/min at room temperature. Detection was at 250 nm. In both expriments, a mixture of 10 μg of each of the racemates of Cbz-aspartic acid and Cbz-glutamic acid was analysed.

The results of the molecular imprinting of the tryptophan derivatives Boc-L-tryptophan (see Fig. 2) and Cbz-L-tryptophan are presented in Table II. The enantiomers of the respective print molecules were resolved on both polymer preparations. In addition, the enantiomers of Cbz-tryptophan were resolved (α = 1.2) on the polymer preparation made against Boc-L-tryptophan and the enantiomers of Boc-tryptophan were resolved (α = 1.3) on the polymer preparation made against Cbz-L-tryptophan. This is analogous to previous findings with the ionic system[6,7]. Enantiomeric resolution of a racemate of the print molecule was also possible on polymers prepared with molecular imprints against other carboxylic acid derivatives, such as Boc-L-phenylalanine (see Fig. 2 and Table II) and *l*(−)-mandelic acid (see Table II).

After the successful preparation of polymers with molecular imprints of carboxylic acid derivatives, we examined print molecules with even weaker hydrogen bonding interactions with the functional monomers. Polymers were prepared against Boc-L-proline hydroxysuccinimide ester (Boc-L-Pro-OSu) and Cbz-L-tryptophan methyl ester (see Fig. 1) and analysed in the chromatographic mode. On both polymer

TABLE II

ENANTIOMERIC RESOLUTION OF THE ENANTIOMERS OF PRINT MOLECULES ON MOLECULARLY IMPRINTED POLYMERS

The eluents used were acetonitrile–chloroform–acetic acid (90:9.5:0.5, v/v/v) at a flow-rate of 1 ml/min (entries 1 and 2A) or 0.1 ml/min (entry 2B); 0.25% (v/v) acetic acid in chloroform at a flow-rate of 1 ml/min (entry 3); 0.5% (v/v) acetic acid in chloroform at a flow-rate of 0.5 ml/min (entry 4); chloroform–heptane (1:1, v/v) at a flow-rate of 1 ml/min (entry 5A) or 0.1 ml/min (entry 5B); and chloroform–heptane (3:1, v/v) at a flow-rate of 1 ml/min (entry 6A) or 0.1 ml/min (entry 6B). Other conditions as in Table I.

Entry	*Print molecule*	N_{void}[a]	k'_D	k'_L	N_D	N_L	α	R_s
1	Boc-L-Trp-OH	826	0.43	0.83	449	68	1.90	0.8
2A	Cbz-L-Trp-OH	449	0.56	0.94	147	25	1.67	0.1
2B	Cbz-L-Trp-OH	573	0.56	1.11	184	31	1.98	0.6
3	Boc-L-Phe-OH	825	0.68	1.21	783	143	1.77	1.4
4	*l*(−)-Mandelic acid	825	2.00	2.87	383	131	1.43	1.1
5A	Boc-L-Pro-OSu	771	1.10[b]	1.24[b]	435[b]	377[b]	1.1[b]	–
5B	Boc-L-Pro-OSu	825	1.10	1.38	537	403	1.25	0.8
6A	Cbz-L-Trp-OMe	463	1.41	1.80	345	78	1.28	0.2
6B	Cbz-L-Trp-OMe	771	1.41	2.05	776	213	1.46	1.5

[a] The void markers were acetone (entries 1–4) and chloroform (entries 5–6).

[b] Calculated on separate injections of the enantiomers, as injection of a racemate produced only a broad, partially resolved peak.

preparations the enantiomers of the print molecule were efficiently resolved (see Table II). The weaker hydrogen bonds between these substrates and the carboxylic acid functions of the polymers were recognized by the necessity to use less polar eluents to achieve suitable retardations in the successful chromatographic separations.

The mass transfer limitations in the HPLC separation are obvious, as shown by the observation that the enantiomeric separation increased and the resolution improved considerably when the flow-rate was decreased from 1 to 0.1 ml/min (Tables I and II). The observed increase in α is a result of the increase in k' for the L-form (the enantiomer used as the print molecule) at the low flow-rate, whereas the elution of the D-form was unchanged (see Tables I and II). As expected for columns packed with particles of the size used in this study (25 μm)[20], the plate numbers, N, for the D- and L-peaks and the void marker peak increased when the flow-rate was decreased, resulting in better resolution (see Tables I and II). A flow-rate of 0.1 ml/min is too low from a practical point of view; a flow-rate of 1 ml/min is routinely used in the studies of molecularly imprinted polymers. However, conducting parallel analyses at low flow-rates is justified in order to emphasize the potential for development of these chiral separation media. It is important to note that the chromatographic efficiency of these polymer preparations compared well with that reported for microcrystalline triacetylcellulose[21], a widely used chiral separation medium (Table I).

The results presented here clearly show that it is possible to prepare molecular imprints in synthetic polymers even if the coordination of functional monomers with the print molecule is not held together by strong covalent or ionic bonds. In the chromatographic separations it is a clear advantage if only weak forces between the substrate and the solid support operate, because the rates of binding and release are increased and the amount of competing ligand needed in the eluent is decreased. In this

context it should be mentioned that in the covalent system a catalyst was added to the eluent to speed up the binding reaction[12], and in the ionic system a high percentage of competing ligand (acetic acid) was added to the eluent[7]). The lower separation factors in the present system (α = 1.1–2.5 compared with 4–8 in the ionic system[7] are compensated for by the better chromatographic performance, resulting in resolutions which are as good as, and in some instances superior to, those with the previous ionic system.

CONCLUSIONS

Interest in molecular imprinting has grown in the last few years, as a means of producing stationary phases for column chromatography[1], as a model system for studying the recognition of a substrate by a macromolecule[1,8,22] and as a tool eventually to obtain enzyme-like catalysts[23–25]. Two basically similar approaches for the preparation of molecular imprints have been utilized in the past, involving either ionic[1] or covalent[8] bonds between the print molecule and the functional monomer(s). In this study we have shown that molecular imprinting is not limited to a small number of exclusive compounds which can form reversible covalent or ionic bonds with the functional monomer(s).

Enantiomeric resolution of print molecules was observed for all the stationary phases prepared; in the best cases the resolving capability was very good. The enantiomeric resolutions of substrates other than the print molecule were always less than that for the print molecule if they were resolved at all, at least with the eluent systems used. Substrate selectivity between compounds with very similar structures, as exemplified by the pair Cbz-aspartic acid and Cbz-glutamic acid, is efficient in the present system. The results presented here represent a substantial widening of the scope of molecular imprinting in that it may now be possible to prepare molecular imprints against a large number of substances.

The polymers used in this present study could be used in column chromatography both as a chiral stationary phase (pre-determined enantioselectivity) and as a normal phase (pre-determined substrate selectivity). The major shortcoming of these polymer preparations in column chromatography at present appears to be the sometimes pronounced broadening of peaks; however, as shown here, the potential exists for further improvements in column performance. Studies of the kinetics of binding and release are warranted and optimizations may include the preparation of beaded particles of defined size and shape.

ACKNOWLEDGEMENT

The authors thank the National Swedish Board for Technical Development for their generous support (Grant No. 712-87-03419).

REFERENCES

1 B. Ekberg and K. Mosbach, *Trends Biotechnol.*, 7 (1989) 92.
2 B. Sellergren, B. Ekberg and K. Mosbach, *J. Chromatogr.*, 347 (1985) 1.
3 B. Sellergren, M. Lepistö and K. Mosbach, *J. Am. Chem. Soc.*, 110 (1988) 5853.
4 D. J. O'Shannessy, B. Ekberg and K. Mosbach, *Anal. Biochem.*, 177 (1989) 144.

5 D. J. O'Shannessy, B. Ekberg, L. I. Andersson and K. Mosbach, *J. Chromatogr.*, 470 (1989) 391.
6 D. J. O'Shannessy, L. I. Andersson and K. Mosbach, *J. Mol. Recog.*, 2 (1989) 1.
7 L. I. Andersson, D. J. O'Shannessy and K. Mosbach, *J. Chromatogr.*, 513 (1990) 165.
8 G. Wulff, *Am. Chem. Soc. Symp. Ser.*, 308 (1986) 186.
9 K. J. Shea and T. K. Dougherty, *J. Am. Chem. Soc.*, 108 (1986) 1091.
10 G. Wulff, B. Heide and G. Helfmeier, *J. Am. Chem. Soc.*, 108 (1986) 1089.
11 Y. Fujuii, K. Matsusani and K. Kikuchi, *J. Chem. Soc., Chem. Commun.*, (1985) 415.
12 G. Wulff, H.-G. Poll and M. Minárik, *J. Liq. Chromatogr.*, 9 (1986) 385.
13 O. Norrlöw, M.-O. Månsson and K. Mosbach, *Swed. Pat. Appl.*, 8605372-5, 1986; *J. Chromatogr.*, 396 (1987) 374.
14 A. R. Fersht, *Trends Biochem. Sci.*, 12 (1987) 301.
15 D. Hadzi and S. Detoni, in S. Patai (Editor), *The Chemistry of Acid Derivatives*, Part 1, Wiley, Chichester, 1979, pp. 213–266.
16 J. Rebek, Jr., *Top. Curr. Chem.*, 149 (1988) 189.
17 S.-K. Chang and A. D. Hamilton, *J. Am. Chem. Soc.*, 110 (1988) 1318.
18 P. E. J. Sanderson, J. D. Kilburn and W. C. Still, *J. Am. Chem. Soc.*, 111 (1989) 8314.
19 A. Ito, R. Takahashi and Y. Baba, *Chem. Pharm. Bull.*, 23 (1975) 3081.
20 L. R. Snyder and J. J. Kirkland, *Introduction to Modern Liquid Chromatography*, Wiley, New York, 2nd ed., 1979.
21 R. Isaksson, P. Erlandsson, L. Hansson, A. Holmberg and S. Berner, *J. Chromatogr.*, 498 (1990) 257.
22 R. Arshady and K. Mosbach, *Makromol. Chem.*, 182 (1981) 687.
23 A. Leonhardt and K. Mosbach, *React. Polym.*, 6 (1987) 285.
24 D. Robinson and K. Mosbach, *J. Chem. Soc. Chem. Commun.*, (1989) 969.
25 L. I. Andersson and K. Mosbach, *Makromol. Chem., Rapid Commun.*, 10 (1989) 491.

Journal of Chromatography, 516 (1990) 323–331
Elsevier Science Publishers B.V., Amsterdam

CHROM. 22 567

Enantiomeric resolution of amino acid derivatives on molecularly imprinted polymers as monitored by potentiometric measurements

LARS I. ANDERSSON, AKIYOSHI MIYABAYASHI[a], DANIEL J. O'SHANNESSY[b] and KLAUS MOSBACH*

Department of Pure and Applied Biochemistry, Chemical Center, University of Lund, P.O. Box 124, S-221 00 Lund (Sweden)

(First received October 9th, 1989; revised manuscript received February 13th, 1990)

ABSTRACT

Potentiometric measurements have been applied to the detection of enantiomeric separations on molecularly imprinted polymers. A flow-through column electrode, based on the use of polymers imprinted against L-phenylalanine anilide, is described. The electrode consisted of a glass column in which the polymer was packed and where the end frits constituted the electrodes. The flow stream potential across the column can be continuously recorded as solvent is pumped through the system. The column resolved the enantiomers of phenylalanine anilide as detected by both UV absorption and potentiometric measurements and the recorded signals could be correlated with the concentration of phenylalanine anilide. The calibration graphs obtained for the UV absorption of phenylalanine anilide were linear over the concentration range investigated, whereas the potentiometric signal was shown to be exponentially linear with concentration. The application of molecular imprints to the preparation of supports suitable for chromatographic separations of enantiomers and for the preparation of specific electrodes is discussed.

INTRODUCTION

Molecular imprinting, which is a technique for preparing synthetic polymers containing specific recognition sites and is particularly useful for enantiomeric separations, is gaining increasing acceptance and has been reviewed recently [1,2]. In principle the method involves (a) mixing the print molecule with selected monomers, chosen for their ability to interact in a specific manner with the print molecule, (b)

[a] Present address: Department of Elementary Particle Physics, Physics Institute, University of Lund, Sölvegatan 14, 223 63 Lund, Sweden

[b] Present address: Smith Kline Beecham, Research and Development Division, L-47, Department of Macromolecular Sciences, 709 Swedeland Road, P.O. Box 1539, King of Prussia, PA 19406, U.S.A.

0021-9673/90/$03.50

polymerization in the presence of a suitable cross-linker and (c) removal of the print molecule from the resulting polymer. The result is a polymer possessing a "memory" for the print molecule. As molecularly imprinted polymers have the ability to bind the print molecule selectively in the presence of molecules of like structure, including the optical antipode, supports exhibiting excellent enantiomeric resolving capabilities have been reorted, especially for the separation of amino acid derivatives [2–4]. In many applications of chromatography, it is important not only to separate substances but also to determine them. In this paper, we demonstrate for the first time the use of molecularly imprinted polymers for quantitative analysis. In addition, potentiometry has been applied to molecular imprints.

Two detection systems were used: (i) UV absorption, which is the most common detection method in high-performance liquid chromatographic (HPLC) analyses, and (ii) potentiometric measurements. The latter detection technique is very interesting because it is a relatively new technique, simple to use and relies on a different mode of detection to UV absorption. Streaming potential measurements are based on recording the potential across a packed bed of, for example, a chromatographic material, placed in a continuous flow. The measurement of streaming potential can be regarded as a general method for recording binding reactions, as long as they involve a change in charge distribution on the surface at which they occur (see below). Several applications based on flow stream potential measurements have been reported, including quantification of the binding of proteins to ligands or antibodies on solid supports [5,6], flow-rate measurements [7] and in the construction of an HPLC detector [8].

We describe here the application of a flow-through column electrode for the separation and detection of small molecules in organic solvents. A polymer prepared against L-phenylalanine anilide, using methacrylic acid as the functional monomer, was used as this system has been well documented [3,4]. Polymer particles were packed into a glass column where the end frits were constructed as electrodes and connected directly to an electrometer. Solvent was pumped through the "electrode" and the flow stream potential was continuously recorded. The enantiomeric separation of a racemic mixture of phenylalanine anilide was detected by both UV absorption and potentiometric measurements and could be correlated with the concentration of solute.

THEORY

When a solid surface is brought into contact with a polar (most often aqueous) medium, an electric double layer is created. Ionization, ion adsorption and ion dissolution generate a net charge at the surface which attracts ions of the opposite charge from the bulk solvent. Also, the presence of a layer of oriented dipolar molecules at the surface may make a significant contribution to the electric double layer, especially in non-aqueous media. If the liquid phase surrounding the solid is forced to flow relative to the solid surface, a streaming potential will be developed. The flow of liquid carries a net charge, from the mobile portion of the electric double layer, which gives rise to a streaming current. A potential difference is thus created which causes a back flux of charge through ion migration, leak current. The measured streaming potential relates to an equilibrium condition when the streaming current and leak current cancel each other. When a liquid is forced through a porous "plug",

for example a column, the streaming potential measured between the ends of the plug, E_s, can be approximately described by the equation

$$E_s = \frac{\varepsilon p \zeta}{\eta \left(k_0 + \frac{2k_s}{a} \right)}$$

where ε is the permittivity, p is the pressure difference applied to force the flow of the liquid, η is the viscosity of the solvent, k_0 is the conductivity of the solvent, k_s is the surface conductivity and a is a geometrical parameter related to the average pore radius. By changing the solvent from aqueous to organic, thereby decreasing the conductivity, an increased streaming potential is expected. In aqueous media, k_s/a is in most instances considered to be negligible and the conductivity term is simplified to be equal to k_0. ζ is the zeta potential, whose electrokinetic behaviour depends on the potential at the surface of shear between the charged surface and the bulk solvent. Adsorption of solute on the solid surface may lead to a change in the potential ζ, therefore streaming potential measurements can be used to record affinity interactions between solute and solid support. A more detailed analysis of the described phenomena is given in ref. 9.

EXPERIMENTAL

Methacrylic acid (MAA) and ethylene glycol dimethacrylate (EDMA) were obtained from Aldrich Chemie (Steinheim, F.R.G.) and 2,2′-azobis(2-methylpropionitrile) (AIBN) from Janssen Chemica (Beerse, Belgium). D- and L-phenylalanine anilides were synthesized as described [3]. D- and L-leucine amides and D- and L-alanine amides were obtained from Nova Biochem (Läufelfingen, Switzerland). All solvents used were of the highest available grade. HPLC analyses were performed with an LKB (Bromma, Sweden) system consisting of a Model 2152 HPLC controller, two Model 2150 HPLC pumps and a Model 2151 variable-wavelength monitor.

Polymer preparation

The polymers were prepared as described [3] with EDMA as cross-linker and MAA as functional monomer. The crosslinker:monomer:print molecule molar ratio was 20:4:1. Polymerization in chloroform was initiated by AIBN and UV light at 0°C. The resulting bulk polymer was ground and sieved to particles of less than 25 μm.

Flow-through column electrode construction

The flow-through column electrode, shown schematically in Fig. 1, was constructed in a similar manner to one described previously [5,6]. The column consisted of a glass tube (50 mm × 5 mm I.D.) with PTFE adapters holding the nets of the electrodes in place. The electrodes were connected to a Keithley Instruments (Cleveland, OH, U.S.A.) Model 610 C solid-state electrometer. The nets (made of stainless steel) were welded to acid-proof stainless steel wires (diameter 0.3 mm) and the welding points were sealed with epoxy glue. All parts were carefully designed to be resistant to organic solvents. The solvent was pumped though the column at a constant flow-rate of 0.1 ml/min and a back-pressure of 15 bar.

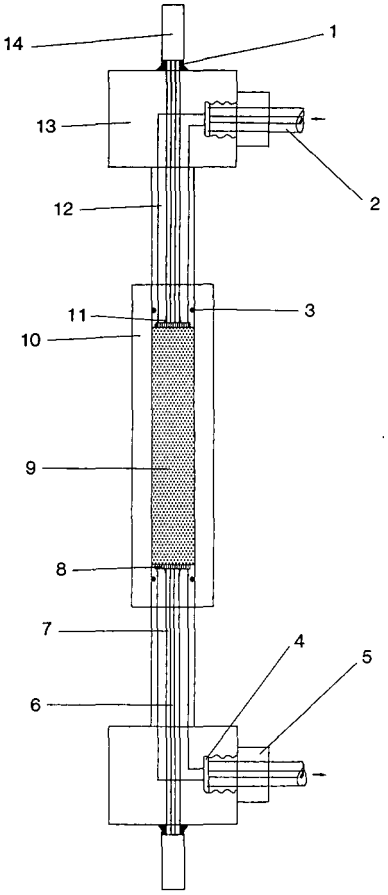

Fig. 1. Schematic diagram of the flow-through column electrode. 1 = Epoxy seal; 2 = PTFE tube; 3 = O-ring; 4 = rubber tube seal; 5 = PTFE tube support; 6 = stainless-steel wire (diameter 0.25 mm); 7 = PTFE tube; 8 = stainless-steel net electrode; 9 = imprinted polymer particles; 10 = glass tube 50 mm × 5 mm I.D., 3.5-mm thickness; 11 = epoxy seal; 12 = sample flow dome (diameter 3 mm); 13 = PTFE electrode support; 14 = lead wire contact.

Chromatography

The particles were dry-packed into the flow-through column electrode. The column was then washed on-line with acetonitrile–acetic acid (9:1, v/v) until a stable baseline was obtained. HPLC analyses were performed isocratically with acetonitrile–acetic acid (9:1, v/v) at a flow-rate of 0.1 ml/min and detection at 250 nm. Weighed samples were dissolved in the mobile phase and diluted to the appropriate concentration before injection in a total volume of 30 μl.

RESULTS AND DISCUSSION

The solvent was pumped at constant flow-rate using an HPLC pump via the injector into the column. The flow stream potential across the column, between the net

electrodes (see Fig. 1), was recorded continuously by the electrometer. The column effluent also passed through a UV detector. As the flow stream potential is linearely proportional to the flow-rate [7], it is extremely important to maintain as constant a flow as possible. Early attempts at potentiometric measurements using a peristaltic pump resulted in severe noise and baseline drift. Using a high quality HPLC pump it was possible to obtain a stable baseline, but the piston strokes of the pump were still detected at regular interval in the baseline.

A polymer imprinted against L-phenylalanine anilide was used as the performance of this polymer has been well described [3]. Racemic mixtures and also the pure enantiomers of phenylalanine anilide were applied to the column via the injection valve. Fig. 2 shows typical chromatograms obtained for this system and shows both UV recordings and the potentiometric recordings (note the different time scales). As potentiometric detection is performed across the column, and not post-column as in UV detection, the potentiometric signal appears earlier than the UV signal but the capacity factors (k') for the peaks obtained were the same for both detection methods (see Fig. 2C–F). The peaks obtained with the potentiometric detector were broader than those for the UV detector, owing to the longer residence time in the detector cell, *e.g.*, the column. There is a small shift in the capacity factor for the L-form in the mixture compared with the pure enantiomer (see Fig. 2A–D), the cause of which is unknown. Injection of solvent alone gave no peak in either mode of detection. In agreement with previous findings [3], the enantiomers of phenylalanine anilide were resolved on this column, as shown by both detection methods (see Fig. 2A and B). It must be stressed that as the potentiometric signal is exponentially proportional to the concentration (see below), the chromatograms recorded with the potentiometric detector become distorted (flattened), and the resolution may appear to be worse than it truly is. Earlier reports showed that a polymer prepared against L-phenylalanine anilide was able to resolve the enantiomers of a number of amino acid amides and

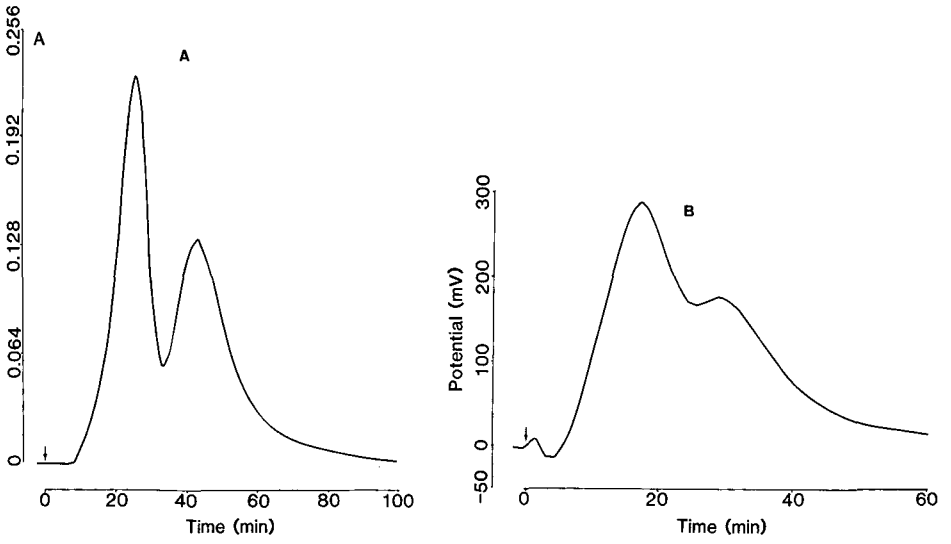

Fig. 2.

(Continued on p. 328)

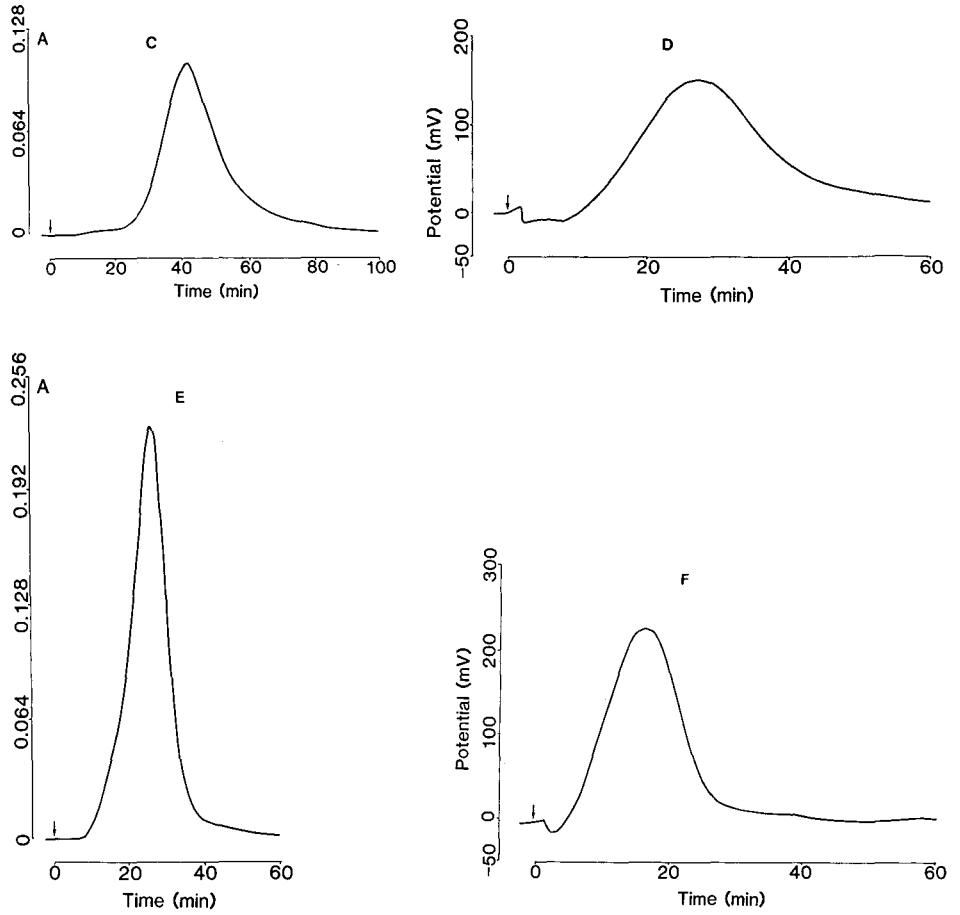

Fig. 2. Representative elution profiles of phenylalanine anilide in the flow-through column electrode. Note the different time scales. Particles of <25 μm, prepared from a polymer imprinted against L-phenylalanine anilide were dry-packed into a 50 mm $\times$ 5 mm I.D. glass column. Analyses were performed under isocratic conditons using acetonitrile–acetic acid (9:1, v/v) as the eluent at a flow-rate of 0.1 ml/min (15 bar). Samples consisted of a mixture of 15 μg of each of the enantiomers (A and B), 15 μg of the L-enantiomer (C and D) or 15 μg of the D-enantiomer (E and F). UV detection (A, C and E) was at 250 nm. The potentiometric recordings (B, D and F) were drawn by connecting the peaks of the noise, which were constant both in frequency and amplitude. The void volumes, calculated using acetic acid, were 1.11 ml on the UV recordings and 0.725 ml on the potentiometric recordings. Capacity factors, k', and peak widths at half peak height, $t_{1/2}$, were calculated to be (A) $k'_L = 2.86$ and $k'_D = 1.32$; (B) $k'_L = 2.93$ and $k'_D = 1.34$; (C) $k'_L = 2.73$, $t_{1/2} = 1.74$ ml (D) $k'_L = 2.79$, $t_{\frac{1}{2}} = 1.90$ ml; (E) $k'_D = 1.35$, $t_{\frac{1}{2}} = 1.02$ ml; (F) $k'_D = 1.31$, $t_{1/2} = 1.35$ ml. Separation factors, α, were calculated to be (A) 2.17 and (B) 2.19.

dipeptides [10] and a mechanism for the molecular recognition by these polymers was proposed based on the reported findings [10,11]. The detection of simple amino acid amides was not possible because of the absence of suitable UV absorbance. With the present potentiometric detection system, such analyses were possible. Racemic mixtures of leucine amide and alanine amide were therefore applied to the column and

followed potentiometrically. However, no enantiomeric resolution of these simple amides was observed. It is worth noting that separate injections of the pure enantiomers of these amides were clearly detectable and produced distinct peak maxima (leucine amide, $k'_L = 0.34$, $k'_D = 0.17$; alanine amide, $k'_L = 0.28$, $k'_D = 0.10$).

Known concentrations of the pure D- and L-enantiomers of phenylalanine anilide were applied to the column and UV and potentiometric signals were recorded. The calibration graphs obtained from these analyses are shown in Fig. 3. The UV signals were linear over the concentration range measured (1–100 μg) whereas the potentiometric signals were shown to be exponentially proportional to concentration. In potentiometric detection, irreversible "immobilization" or binding of the analyte to the solid support gives rise to a linear relationship between the signal obtained and the concentration applied. This relationship is exemplified by recording the change in streaming potential as protein is adsorbed on an affinity column [5,6]. The present system is in a state of dynamic equilibrium, where the binding of the analyte to the affinity support is reversible, in which case the potentiometric signal may not necessarily be linear with respect to concentration. Also, the effect(s) of the analyte in the moving liquid on the electric double layer, at the surface of the solid support, have to be considered. Consequently, the potentiometric signal will not bear a simple relationship to concentration but, as in the present instance, may be exponentially proportional to concentration. This is in agreement with other reports [8,12].

The signal response is also intimately related to the shape of the peaks observed in the present system, which indeed differ from those described previously for systems in which the analyte was irreversibly bound to the support. In the irreversible system, when analyte was applied to the column a stepwise change in the potential was recorded, which was constant until another aliquot of analyte was applied [5,6]. Introduction of analyte onto the column in the present system gave rise to a peak in the potentiometric signal (not a square peak as in the irreversible system), which then returned to the baseline. This may be attributed to a number of effects, of which only a few are well documented in the literature [9]. Further studies need to be performed before the characteristics of the potentiometric detector in organic media can be fully evaluated. As can be seen in Fig. 3B, the slope of the calibration graph for L-phenylalanine anilide is greater than that for D-phenylalanine anilide in potentiometric measurements. As the flow stream potential is a surface phenomenon, the concentration of the L-form will have a stronger influence on the signal than for the D-form, because the L-form has a higher affinity for the polymer. The lower limit of linearity of the potentiometric signal was calculated to be 10^{-5} g, but it must be stressed that as the system was not fully optimized this by no means reflects the true detection limit of this system.

The results presented above clearly show the utility of potentiometric detection in organic solvents, as applied to separations on molecularly imprinted polymers. Potentiometric detection systems should therefore be considered as an alternative or adjunct to the more common systems such as UV detectors, refractometers and polarimeters. The successful detection of phenylalanine anilide (and other compounds) in the flow-through column electrode suggests that molecularly imprinted polymers may be useful in the preparation of substrate-selective electrodes. By combining the general detection principle of potentiometric measurements and the selectivity achievable with molecular imprinting it may be possible to develop such an

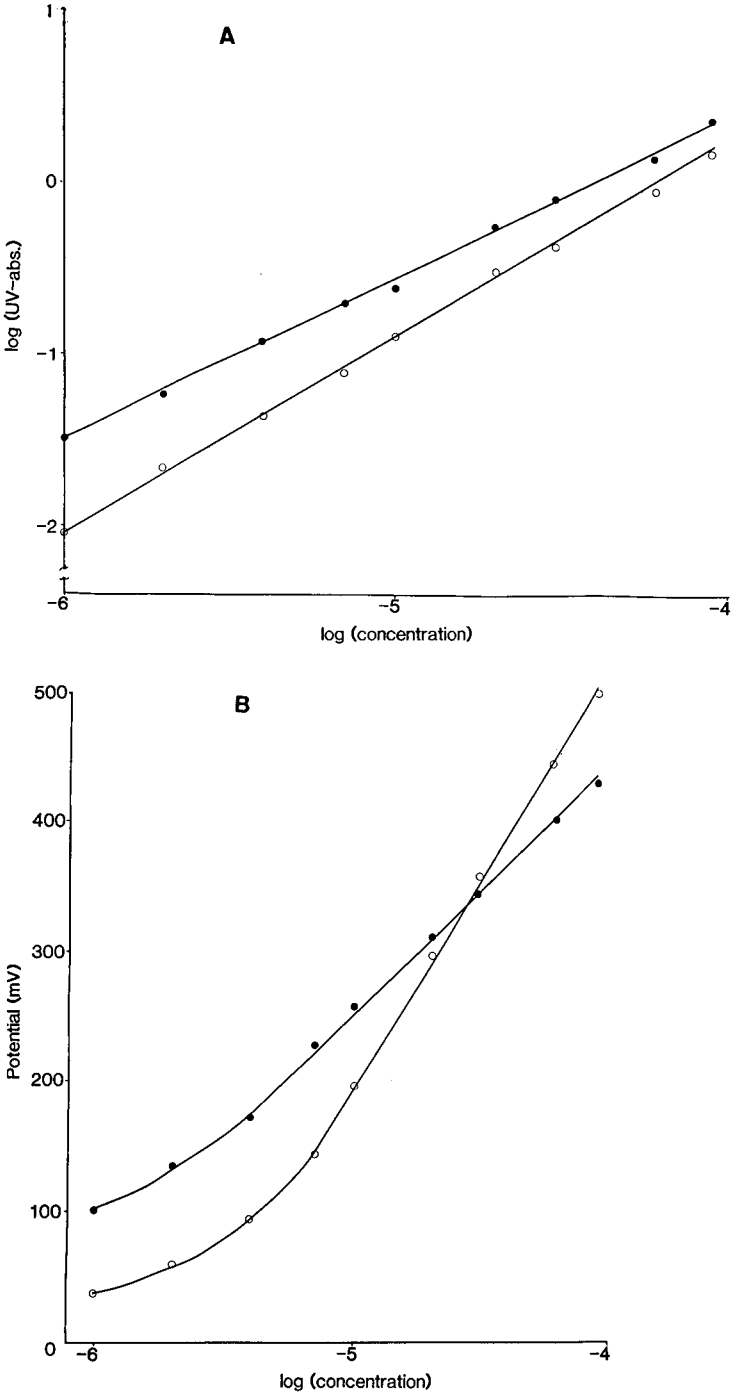

Fig. 3. Calibration graphs for (A) UV detection and (B) potentiometric detection. Analyses were performed with acetonitrile–acetic acid (9:1, v/v) as the eluent at 0.1 ml/min (15 bar). Weighed samples of (●) D- and (○) L-phenylalanine anilides were dissolved in the mobile phase and diluted to the appropriate concentration (1–100 μg) before injection in a total volume of 30 μl. UV detection was at 250 nm.

analytical device. Such electrodes may be prepared in the conventional format, as a miniature device or as an integrated system, where the active surface of the electrode is coated with the selective polymer.

It is apparent from the results presented that molecularly imprinted polymers can be used for the separation and quantification of amino acid derivatives. Although the resolution of the enantiomers of phenylalanine anilide was reasonable ($\alpha = 2.2$), peak broadening was evident. This has been described previously for molecular imprints and may result from the poor packing characteristics of the extremely irregular and poorly defined particles [10]. The preparation of beaded polymers, or more uniform particles, may improve the peak shapes obtained and therefore the resolution. Also, polymers obtained using print molecules allowing multiple interactions may lead to improved separations.

In conclusion, we have reported the use of potentiometric measurements in organic solvents as applied to enantiomeric separations of amino acid amides on molecularly imprinted polymers. Potentiometry measures changes in the charge distribution on the surface of the solid support and can therefore be used to show an affinity binding event, either reversible or irreversible in nature. The demonstration that the binding of compounds to these highly specific molecularly imprinted polymers can be followed by potentiometry, or UV analysis, suggests that it may be possible to prepare substrate-specific electrodes using the technique of molecular imprinting. Moreover, such polymers may be useful in the quantitative analysis of amino acid derivatives or other organic compounds.

ACKNOWLEDGEMENT

This project was supported in part by the National Swedish Board for Technical Development, grant 712-87-03419.

REFERENCES

1 G. Wulff, *ACS Symp. Ser.*, 308 (1986) 186.
2 B. Ekberg, K. Mosbach, *Trends Biotechnol.*, 7 (1989) 92.
3 D. J. O'Shannessy, B. Ekberg and K. Mosbach, *Anal. Biochem.*, 177 (1989) 144.
4 B. Sellergren, M. Lepistö and K. Mosbach, *J. Am. Chem. Soc.*, 110 (1988) 5853.
5 A. Miyabayashi, *Thesis*, Lund, 1989.
6 B. Mattiasson and A Miyabayashi, *Anal. Chim. Acta*, 213 (1988) 79.
7 K. D. Caldwell and M. N. Myers, *Anal. Chem.*, 58 (1986) 1583.
8 W. Kemula, B. K. Glód and W. Kutner, *J. Liq. Chromatogr.*, 6 (1983) 1823.
9 D. J. Shaw, *Introduction to Colloid and Surface Chemistry*, 3rd ed., Butterworths, London, 1985.
10 D. J. O'Shannessy, L. I. Andersson and K. Mosbach, *J. Mol. Rec.*, 2 (1989) 1.
11 L. I. Andersson, D. J. O'Shannessy and K. Mosbach, *J. Chromatogr.*, 513 (1990) 165.
12 V. A. DePalma, *Rev. Sci. Instrum.*, 51 (1980) 1390.

Journal of Chromatography, 516 (1990) 333–354
Elsevier Science Publishers B.V., Amsterdam

CHROM. 22 536

Immobilized metal ion affinity chromatography

Effect of solute structure, ligand density and salt concentration on the retention of peptides

MAKONNEN BELEW[a,*]
Institute of Biochemistry, Biomedical Centre, Uppsala University, Box 576, S-751 23 Uppsala (Sweden)
and
JERKER PORATH
Biochemical Separation Centre, Biomedical Centre, Uppsala University, Box 577, S-751 23 Uppsala (Sweden)
(First received February 27th, 1990; revised manuscript received May 4th, 1990)

ABSTRACT

The adsorption characteristics of a variety of synthetic peptide hormones and di-, tri- and tetrapeptides on Cu(II) immobilized on two commercially available high-performance chelating gels run under various experimental conditions are described. Methods for determining the concentration of immobilized Cu(II) *in situ* are also described. The Cu(II)-charged columns exhibit a net negative charge as judged from the significantly higher retention of some basic peptides in the absence of NaCl in the equilibration and elution buffers. At higher NaCl concentrations (2–4 *M*), aromatic interactions seem to be superimposed on the metal ion affinity characteristics of the peptides. The relationship between resolution of peptides and the concentration of immobilized Cu(II) ions has also been established for the Chelating Superose gel where 40 μmol Cu(II) ml^{-1} gel apparently gives the optimum resolution. The nature of the gel matrix also plays a role in the resolution of some peptides, the extent of which is difficult to predict. The results obtained also suggest that peptides containing aromatic and hydroxy amino acids are retarded more than those which lack them. Moreover, these same amino acids apparently strengthen the existing strong binding of peptides containing His, Trp or Cys to a Chelating Superose–Cu(II) column. Dipeptides with C-terminal His (*i.e.*, X-His) are neither bound nor retarded on a column of Chelating Superose–Cu(II) whereas those having the structure His-X are strongly bound. Some tri- and tetrapeptides containing His were also found not to bind to the column. The underlying cause of this anomalous adsorption behaviour is discussed

[a] Present address: Pharmacia LKB Biotechnology AB, Process Separation Division, S-751 82 Uppsala, Sweden.

0021-9673/90/$03.50

and is ascribed to "metal ion transfer" arising from the relatively higher affinity of such peptides towards immobilized Cu(II) ions than the chelator groups (iminodiacetate) which are covalently bound to the gel matrix.

INTRODUCTION

The introduction of commercial high-performance immobilized metal ion affinity (HP-IMA) adsorbents by Toyo Soda (Tokyo, Japan) and recently by Pharmacia LKB (Uppsala, Sweden) has made possible high-performance liquid chromatography (HPLC) applications of this versatile separation method to the high resolution of model proteins[1,2], the iso-forms of human platelet-derived growth factor[3] and synthetic peptide hormones and their analogues[4]. Whereas His, Cys and Trp residues in proteins are postulated to be the primary sites of interaction with immobilized transition metal ions, *i.e.*, 3d-block elements from Co to Zn[5,6], the results of Nakagawa *et al.*[4] suggest that the side-chains of amino acids other than these three can lead to a considerable retardation of some peptides. This might be due to the higher solvent accessibility of most or all of the constituent amino acids in the peptide hormones studied, suggesting that, at least with such low-molecular-weight solutes, their relative retentions might be predicted on the basis of their sequence (composition) and the published retention spectra[7] for α-amino acids on iminodiacetic acid (IDA)–Ni(II). In addition, the data published by Chothia[8] on the relative surface location of amino acid side-chains in a number of proteins might further contribute to the understanding of the relationship between structure and the experimentally found retention times of a series of peptides on an IMA adsorbent.

Preliminary studies on the effects of various salts, temperature and pH on the retention of amino acids[7] and oligopeptides[9] indicated that the coordination of these solutes with immobilized metal ions (IMI) can be significantly modulated by varying the experimental conditions. An extension of this work to proteins[10] indicated that high concentrations of anti-chaotropic salts (*e.g.*, sulphates) promote the retention of proteins on IMA adsorbents by a mechanism that is similar to that operating in hydrophobic interaction chromatography (HIC). However, a recent report by Sulkowski[11] showed that such an effect is variable and dependent on the nature of the sample solute in question, enhancing the retention of acidic proteins and markedly decreasing that of basic proteins. Thus, the chromatographic parameters which can have a bearing on the retention of biomolecules on IMA adsorbents is apparently complex but if the partial contributions of the various parameters could be established with certainty, the versatility of IMA methods could be further appreciated and fully exploited to solve a variety of separation problems. The results presented in this paper are a step in this direction with emphasis on structure–retention aspects in immobilized metal ion affinity chromatography (IMAC) of a series of amino acids and di- and oligopeptides run on Cu(II) ions immobilized on Chelating Superose or TSK gel chelate-5PW. Methods for the determination of the total ligand concentration in IMA adsorbents are outlined, in addition to the relationship between ligand concentration and the extent of retention of a series of peptides. We have also obtained some anomalous adsorption behaviour of His-containing peptides and plausible explanations for our observations are outlined. Finally, the effect of varying the salt

concentration in the eluent buffer on the retention of some selected peptides is reported and compared with previously reported findings.

EXPERIMENTAL

Chelating Superose (bead size *ca.* 10 μm), with a capacity for Zn(II) of 18, 26 and 31 μmol ml^{-1} gel, was kindly provided by Drs. L. Kågedal and M. Sparrman, and TSK gel chelate-5PW (bead size 10 μm and ligand concentration *ca.* 20 μmol ml^{-1} swollen gel) was a generous gift from Eng. Rolf Ehrnström (all of Pharmacia LKB). The chelating gels were provided ready packed in glass columns (75 × 8 mm I.D., bed volume 3.77 ml for the TSK chelate-5PW gel; 21 × 10 mm I.D., bed volume 1.65 ml and three other columns with I.D. 5 mm and lengths of 53, 56 and 60 mm for the Chelating Superose gel) and each is designed for HPLC applications. The chelating groups in Chelating Superose are IDA whereas those in TSK are not specified by the manufacturer but most likely are IDA also.

Individual amino acids and the dipeptide L-carnosine were obtained from Calbiochem (San Diego, CA, U.S.A.). The synthetic peptide hormones and di-, tri- and tetrapeptides were obtained from Bachem Feinchemikalien (Bubendorf, Switzerland). Gastrin-related peptide, Leu-enkephalin (sulphated) and neurotensin (residues 3–13) were a generous gift from Dr. Y. Nakagawa (Peptide Institute, Osaka, Japan). With few exceptions, the peptides were of the highest purity as judged from the chemical analysis data provided by the manufacturers. When deemed necessary, the composition of some peptides was checked by amino acid analysis. Analytical-reagent grade imidazole and EDTA (disodium salt) were obtained from E. Merck (Darmstadt, F.R.G.). All other chemicals were of analytical-reagent or reagent grade and were used as received.

The experiments were performed at room temperature (20°C) using a Pharmacia LKB HPLC system consisting of a pump (Model 2150), a variable-wavelength monitor (Model 2151), a controller (Model 2152), a two-channel recorder (Model 2210) and a Helirac fraction collector (Model 2212). Unless stated otherwise, the following buffers were used as eluents and will be referred to in abbreviated form throughout: buffer A (equilibration buffer), 20 m*M* sodium phosphate, 1.0 *M* in NaCl, pH 7.0; and buffer B (final gradient buffer), 0.1 *M* sodium phosphate, 1.0 *M* in NaCl, pH 3.8. Each buffer was filtered through a 0.45-μm membrane filter (Millipore, Bedford, MA, U.S.A.) and deaerated prior to use. However, in those experiments where the TSK gel chelate-5PW column was used, the concentration of NaCl in each of the buffers was reduced to 0.5 *M*.

Immobilization of Cu(II) ions[2,4,12]

Each column was regenerated by washing with three column volumes of a 50 m*M* solution of EDTA dissolved in buffer A (pH adjusted to 7.0) followed by washing with five column volumes of distilled water. Depending on the size of the column, 0.3–1.0 ml of a 0.2 *M* aqueous solution of $CuSO_4 \cdot 5H_2O$ (pH 3.9) was applied to the regenerated column followed by washing sequentially with five column volumes of distilled water, ten column volumes of buffer B [to elute weakly bound Cu(II) ions], five column volumes of distilled water and finally ten column volumes of buffer A for equilibration. The effluent was monitored by continuously recording the absorbance

at 220 nm with the detector set at 0.64 absorbance units full-scale (a.u.f.s.). This procedure resulted in a stable baseline absorbance of the effluent and the column was then ready for use.

Chromatography

Solutions of the individual amino acids or peptides (1 mg per 100 μl) were prepared in glass-distilled water, except in a few instances where small amounts of organic solvents or dilute NaOH were added to effect their dissolution. A mixture of the peptides was prepared by mixing together appropriate aliquots taken from the solutions of each peptide. Usually, about 5–10 μg of each amino acid or peptide (in 1 μl of solution), or an amount ranging from 2 to 12 μg of each peptide in the mixture (in 10 μl of solution), was applied to the equilibrated column for each chromatographic experiment. The flow-rate was maintained at 0.94 ml min^{-1} except for the Chelating Superose (CS) columns with an I.D. of 5 mm, where it was necessary to reduce it to 0.47 ml min^{-1}.

After sample application, the columns were eluted using one of two alternative procedures which are essentially similar to those developed by Nakagawa *et al.*[4]. The CS–Cu(II) columns were eluted for 15 min with buffer A followed by a programmed gradient elution from buffer A to buffer B as follows: 15–30 min, 15% B; 30–40 min, 80% B; and 40–70 min, 100% B. The TSK–Cu(II) column was eluted for 10 min with buffer A followed by a programmed gradient elution from buffer A to buffer B as follows: 10–20 min, 15% B; 20–35 min, 80% B; and 35–60 min, 100% B.

Determination of the concentration of immobilized ligand

Direct method. The Cu(II)-charged column, prepared as described above, is washed with sufficient EDTA solution (50 m*M* dissolved in buffer A, pH 7.0) to elute the immobilized Cu(II) ions. The effluent is collected in a 25- or 50-ml volumetric flask and diluted to the mark with the above EDTA solution. The total amount of Cu(II) ions in the eluate is then determined by atomic absorption spectrometry (AAS) using the EDTA solution as blank.

Frontal analysis[12,13]. Before connecting the column to the system, it is important that the buffer delivery lines and injection loop are filled with the stock solution of Cu(II) or imidazole. A 20 m*M* aqueous solution of $CuSO_4 \cdot 5H_2O$ (pH 3.9) is fed continuously to the regenerated column and the absorbance at 280 nm of the effluent is recorded until a constant plateau level equal to that of the stock solution being fed to the column is reached. The elution volume is then determined from the median bisector of the front of the elution profile. The internal volume of the column is determined from the elution volume of 1 *M* acetic acid (2 μl) injected onto the column. The amount of immobilized Cu(II) ions is calculated according to the empirical equation given under Results and Discussion.

Alternative frontal analysis. An alternative to the previous method is the frontal analysis of a solution of 20 m*M* imidazole dissolved in buffer A on a CS–Cu(II) or TSK–Cu(II) column following the previous procedure. The amount of imidazole bound to the immobilized Cu(II) ions is also calculated as above.

Amino acid analysis

Suitable aliquots of peptides were hydrolysed in evacuated and sealed tubes for

24 h at 110°C with 6.0 *M* HCl. The hydrolysates were analysed according to standard procedures.

Detection of peptides

This was routinely performed by continuously recording the absorbance at 220 nm of the chromatographic effluents or by the ninhydrin method after alkaline hydrolysis[14] of collected fractions. The latter procedure is used occasionally to distinguish peptide peaks from those generated by inorganic salts or impurities which absorb at 220 nm.

Analysis of data

Owing to the continuous development of the Chelating Superose columns during the course of this investigation, two different sizes (with I.D. 5 and 10 mm) were used. The retention of the peptides on the different columns is therefore expressed in terms of V_e/V_t as this treatment will facilitate comparisons of the results obtained on different columns.

RESULTS AND DISCUSSION

Concentration of immobilized ligand

There are four possible methods for determining the ligand concentration in such gels, *viz.*, by elemental nitrogen analysis and by the three procedures outlined under Experimental. The results obtained by the last three methods are presented here. Fig. 1 shows the frontal analysis curves of Cu(II) on CS and TSK columns where the elution fronts obtained are sharp, indicating uniformity of packing of the columns and an even distribution in the size of the small-particle gels. Based on the elution volumes obtained, the capacity of each column for Cu(II) was calculated using several alternative equations. Of these, the following gave results that agreed consistently with those determined by AAS (see Table I):

$$\text{Amount of Cu(II) immobilized } (\mu\text{mol ml}^{-1}) = \frac{(V_e - V_i)C}{V_t}$$

where

V_e = elution volume of the Cu(II) solution;
C = concentration of the Cu(II) solution fed to the column (μmol ml^{-1});
V_i = internal volume of the column [*i.e.*, void volume + gel volume that is available to acetic acid and presumably also to $Cu^{2+}(H_2O)_n$]; and
V_t = total volume of the column.

The values obtained by AAS and frontal analysis differ by about $\pm 10\%$ (Table I), except for the CS gel with the lowest ligand substitution where the variation is about 25%. This large variation might be due to the elution of a high percentage of the immobilized Cu(II) ions by buffer B from the latter gel prior to elution of the tightly bound Cu(II) ions by EDTA for the subsequent determination of its concentration by AAS.

The results obtained by frontal analysis of imidazole on CS–Cu(II) columns are in good agreement with those obtained above but not so on the TSK–Cu(II) column

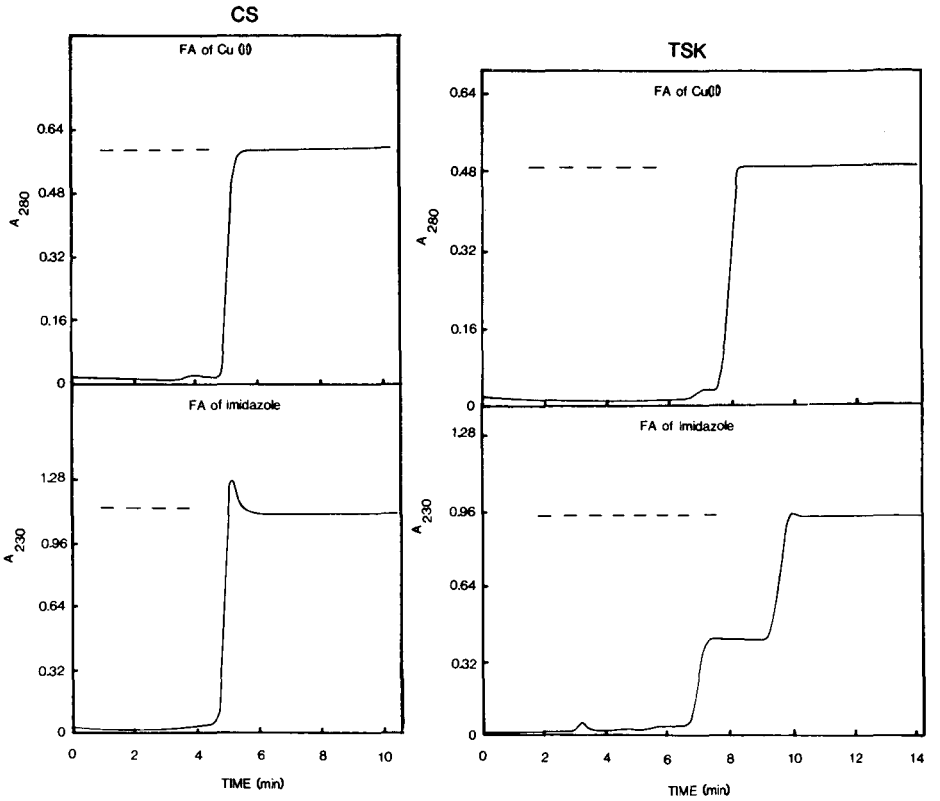

Fig. 1. Frontal analysis of Cu(II) on columns of Chelating Superose [21 × 10 mm I.D.; capacity for Zn(II) = 31 μmol ml^{-1}] and TSK gel chelate-5PW (75 × 8 mm I.D.) and of imidazole on each column after they have been fully charged with Cu(II) ions. The flow-rate in each instance was 0.94 ml min^{-1}. The internal volume (V_i) of the CS column was 1.32 ml and of the TSK column 3.00 ml. For further details, see *Frontal analysis* under Experimental.

(Fig. 1, Table I). In the latter, the imidazole elutes as a double front, indicating heterogeneity in the adsorption sites themselves [*i.e.*, immobilized Cu(II) ions]. Similar results were obtained when two other TSK–Cu(II) columns were tested, although in one of them the boundary between the first and second fronts was not as sharp as that shown in Fig. 1. These results cannot be ascribed to variations in the accessibility of the immobilized Cu(II) ions to such a small molecular sized solute as imidazole (which is also of analytical-reagent grade) but rather to variations in the manner in which the Cu(II) ions are immobilized to the chelator. This in turn implies that there are possibly two species of chelating ligands that are covalently attached to the matrix, one of which chelates the Cu(II) ions by three coordination sites (as in IDA) and the others not. Another plausible explanation can be ascribed to the matrix itself whose structure, whatever its nature, directly affects the uniform availability of the immobilized Cu(II) ions. In either instance, such heterogeneity in the adsorption sites might affect the separation of peptides and proteins and might account for some of the variations in the resolution of peptides we have obtained on the CS- and TSK-based IMA adsorbents.

TABLE I

CAPACITY FOR Zn(II) AND Cu(II) OF CHELATING SUPEROSE (WITH VARYING DEGREES OF LIGAND SUBSTITUTION) AND TSK GEL CHELATE-5PW AS DETERMINED BY SEVERAL ALTERNATIVE PROCEDURES

The Chelating Superose gels are divided into three groups on the basis of their capacity for Zn(II) ions as specified by the manufacturer. The data based on atomic absorption spectrometry and frontal analysis are averages calculated from three independent experiments performed on each gel according to the procedures outlined in detail in the text.

Chelating gel	*Capacity for M(II) (μmol ml^{-1} gel)*			
	Zn(II)[a]	*Cu(II)*[b]	*Cu(II)*[c]	*Imidazole*[c]
Chelating Superose (i)	18	15	19	20
Chelating Superose (ii)	26	30	32	34
Chelating Superose (iii)	31	42	39	41
TSK gel chelate-5PW[d]	–	23	23	20(32)[e]

[a] Determined by the manufacturer (Pharmacia LKB).

[b] Determined by atomic absorption spectrometry.

[c] Determined from frontal analysis data using the empirical equation given in the text.

[d] According to the manufacturer (Toyo Soda) the concentration of chelating groups is about 20 μmol ml^{-1} gel.

[e] Two different values are reported as a result of the two elution fronts obtained on this gel (see Fig. 1).

Of additional interest is the relatively lower capacity for Zn(II) compared with Cu(II) of all three CS gels examined. Smith *et al.*[15] also obtained similar results using Sephadex- and Sepharose-based chelating gels on the basis of which the capacities of the gels for metal ions can be arranged in the order Cu(II) > Ni(II) > Zn(II) > Co(II). These findings agree well with the reported stability constants for complex formation, in free solution, between these metal ions and diaminopropionic acid, amino acids, etc.[16]. The affinities of proteins for immobilized metal ions also follow the order given above, as show previously[2], suggesting that a good correlation exists between the affinities of IMI towards various solutes and their stability constants in free solutions.

Ion-exchange properties

Chelating Superose and TSK gel chelate-5PW behave as cation exchangers at or around neutral pH when free of metal ions. This is illustrated by the results in Fig. 2, where four basic peptide hormones are separated on the basis of their net charge by chromatography on a CS or TSK column equilibrated with 20 m*M* sodium phosphate buffer (pH 7.0). Three of the peptides are separated by isocratic elution whereas the most basic peptide (Met-Lys-bradykinin) can be eluted with 0.5 *M* NaCl in the equilibration buffer. Thus, the metal-free gels have a net negative charge at neutral pH. At lower pH, where the ionization of the two carboxyl groups is sufficiently suppressed, it is possible that the immobilized IDA groups will have a net positive charge and could thus exibit anion-exchange properties. In either instance, the low degree of substitution of these gels limits their use as ion exchangers for peptide separations. Inclusion of 0.5 *M* NaCl in the equilibration buffer abolished such ionic interactions and none of the peptides is bound by either of the gels.

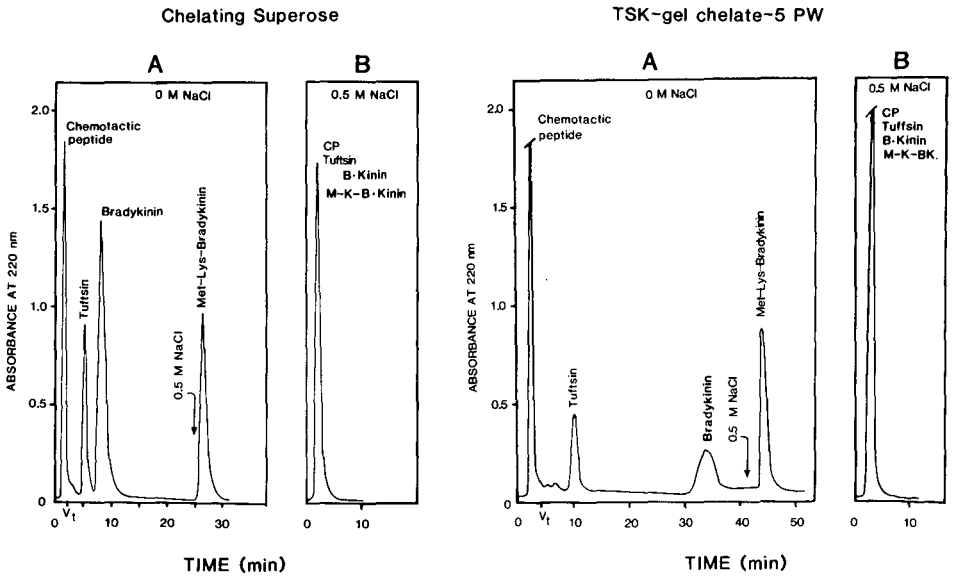

Fig. 2. (A) Cation-exchange characteristics of naked (metal ion-free) columns of Chelating Superose [54 × 5 mm I.D.; V_t = 1.06 ml; capacity for Zn(II) = 31 μmol ml^{-1}] and TSK gel chelate-5PW (75 × 8 mm I.D.; V_t = 3.77 ml). To each column (equilibrated with 20 m*M* sodium phosphate buffer, pH 7.0) were applied 20 μl of the sample solution, containing 100 μg of each of the four peptides, followed by isocratic elution with the equilibration buffer. The flow-rate was 0.47 ml min^{-1} for the CS column and 0.94 ml min^{-1} for the TSK column. The order of elution of the peptides from the two columns was established from individual runs with each peptide. Note that Met-Lys-bradykinin is strongly bound on each column, requiring the use of 0.5 *M* NaCl in the equilibration buffer to elute it. (B) Elution profile obtained when the same mixture of the four peptides was chromatographed on each of the above two columns equilibrated with 20 m*M* sodium phosphate buffer containing 0.5 *M* NaCl (pH 7.0). None of the peptides was bound by either column under these conditions.

Bradykinin is retarded much more on the TSK gel (V_e/V_t = 8.6) than on the CS gel (V_e/V_t = 3.5), which cannot be accounted for by differences in the concentrations of immobilized IDA groups which are, in fact, lower in the TSK gel than in the CS gel (see Table I). Considering the primary structure of bradykinin (see Table III), it is reasonable to propose that the two Phe residues participate in non-ionic interactions (probably of aromatic or hydrophobic character) with the TSK gel chelate-5PW matrix itself.

Effect of varying the salt concentration

Throughout this study, the equilibration and elution buffers contained 0.5 or 1.0 *M* NaCl. It was therefore appropriate to investigate the effects of varying the salt concentration on the resolution of peptides and proteins using the above four peptides as test solutes. Under the standard IMA chromatographic conditions adopted, these peptides are eluted isocratically from both the CS–Cu(II) and TSK–Cu(II) columns because none of them contains His, Trp or Cys residues for strong binding to the immobilized metal ions. Such a study can, of course, be extended to include neutral and acidic peptides and those containing His, Trp or Cys, but we feel that the results obtained here serve as a basis for future explorations in this area.

TABLE II

EFFECT OF VARYING THE CONCENTRATION OF NaCl (0–4.0 *M*) IN THE EQUILIBRATION BUFFER ON THE RELATIVE RETENTION VOLUMES (V_e/V_t) OF THE FOUR PEPTIDE HORMONES ON COLUMNS OF CS–Cu(II) OR TSK–Cu(II)

The data were calculated from the chromatograms shown in Fig. 3.

Peptide	*Chelator gel*	V_e/V_t				
		0 M	*0.5 M*	*1.0 M*	*2.0 M*	*4.0 M*
Chemotactic peptide	CS	0.6	0.7	0.7	0.8	1.5
	TSK	0.7	1.0	0.9	1.3	n.d.[a]
Tuftsin	CS	7.5	3.7	3.4	2.7	2.2
	TSK	n.e.[b]	2.2	1.8	1.6	n.d.
Met-Lys-bradykinin	CS	19.2	5.0	4.7	4.8	7.3
	TSK	n.e.	5.0	4.2	5.7	n.d.
Bradykinin	CS	15.5	6.9	6.9	8.2	13.6
	TSK	n.e.	6.4	5.7	8.3	n.d.

[a] n.d. = Not determined.
[b] n.e. = Not eluted after washing with 20 column volumes of the equilibration buffer.

In the absence of NaCl in the equilibration buffer, these peptides are much more retarded on CS–Cu(II) than on the corresponding metal-free gel but they can still be eluted under isocratic conditions (Fig. 3 and Table II). The order of elution of the peptides is also the same as in Fig. 2, indicating that the apparent anion-exchange characteristics of the CS gel are accentuated by the immobilized Cu(II) ions. A different situation arises on the TSK–Cu(II) column, where all except chemotactic peptide are so strongly adsorbed that they are not eluted by the equilibration buffer (Fig. 3 and Table II). Hence, the ion-exchange characteristics of the TSK gel are even more accentuated by the immobilized Cu(II) ions. Both of these results strengthen the hypothesis that the immobilized metal ions have a net negative charge[7,11] at neutral pH, suggesting that the basis for the adsorption of basic peptides and proteins to immobilized metal ions is of a bimodel character and can thus be manipulated by varying the NaCl concentration in the elution buffer to optimize the isolation of a particular solute in a mixture.

In the presence of 0.5 *M* and higher concentrations of NaCl in the equilibration buffer, the apparently predominant ionic interactions are suppressed or essentially eliminated. Thus, Met-Lys-bradykinin elutes before bradykinin from the CS–Cu(II) column, contrary to what was found above, and the separation of the peptides here appears to be governed primarily by their differential affinities towards the immobilized Cu(II) ions. Almost comparable resolutions of the peptides are also obtained on both the CS–Cu(II) and TSK–Cu(II) columns in the presence of 0.5 or 1 *M* NaCl in the elution buffers (see Fig. 3 and Table II). However, at even higher concentrations of NaCl [2 *M* for TSK–Cu(II) and 4 *M* for CS–Cu(II)] a different kind of interaction seems to prevail, leading to a stronger retention of all but one (tuftsin) of the four peptides (see Fig. 3 and Table II). As these three peptides have Phe as a common residue in their side-chains (see Table III for their structure), the additional

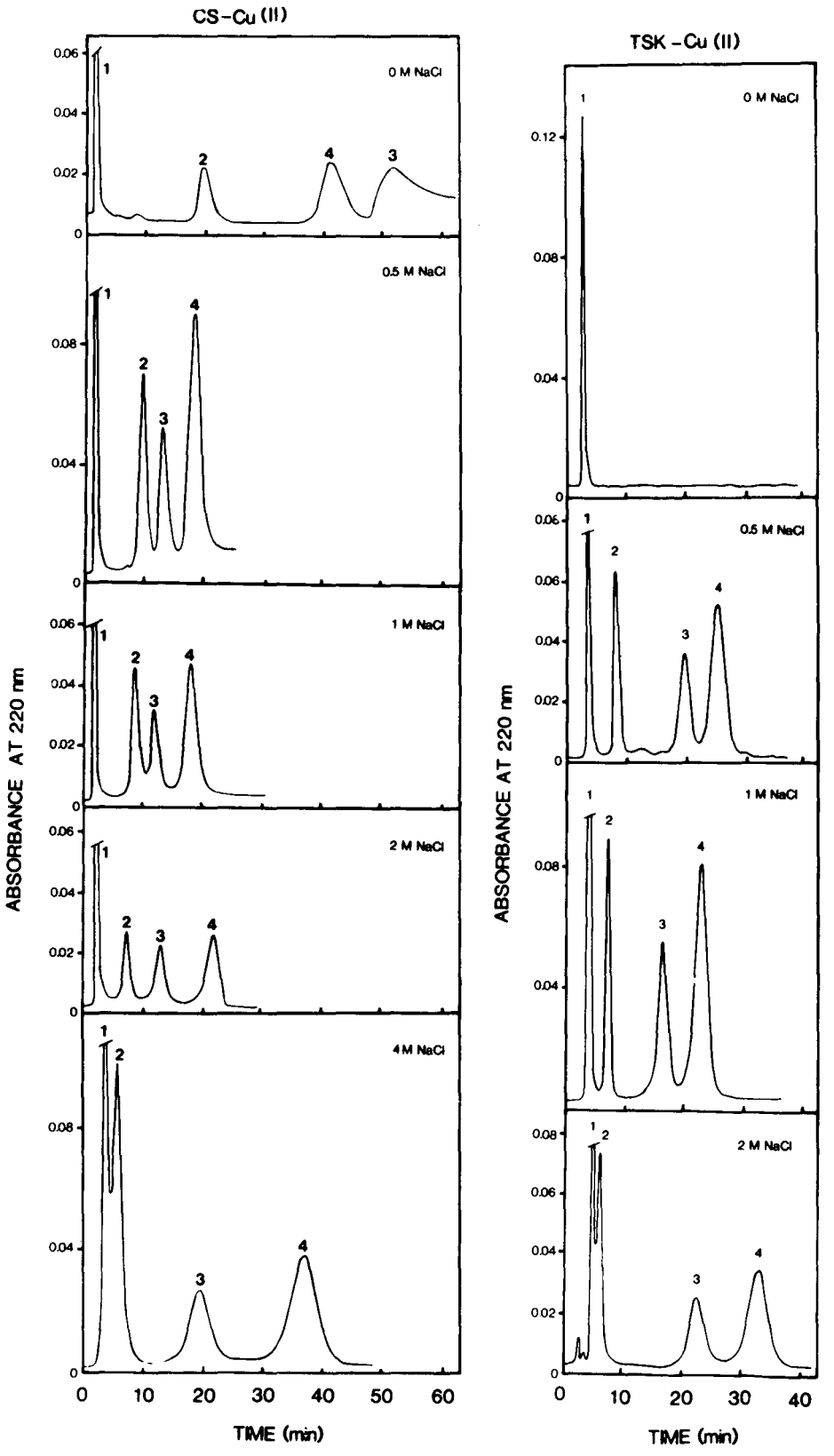
CS-Cu (II)
TSK-Cu (II)
0 M NaCl
0.5 M NaCl
1 M NaCl
2 M NaCl
4 M NaCl
ABSORBANCE AT 220 nm
TIME (min)
1
2
3
4

or secondary interactions seem to be of an aromatic/hydrophobic character. That bradykinin is retarded much more than Met-Lys-bradykinin suggests that lysine (a charged hydrophilic amino acid) has a modulating effect on the "hydrophobicity" of this peptide. This hypothesis is consistent with that suggested by Hemdan and Porath[9] based on the adsorption characteristics of di- and tripeptides on an IDA–Ni(II) column. A comparable result has also been obtained by Nakagawa *et al.*[4], where [Leu^5]-enkephalin is eluted much later than sulphated [Leu^5]-enkephalin from a TSK–Cu(II) column, lending further support to the proposed hypothesis.

Effect of ligand concentration

The elution profile of eleven synthetic peptide hormones from three CS–Cu(II) adsorbents with various ligand concentrations is shown in Fig. 4A. The best resolution of the peptides is obtained on the column with the relatively highest ligand concentration [capacity for Zn(II) = 31 μmol ml^{-1} gel], irrespective of whether the peptides are tightly bound or not. With decreasing ligand concentration, the resolution also decreases and in the case of peptides 8 and 9 (angiotensin III and II, respectively) they coelute from the column with the lowest ligand concentration. The pH profiles obtained on the three columns are identical and thus cannot account for the variations in the resolution obtained here. Moreover, it has also been observed[17] that the resolution of proteins was markedly decreased as the capacity of the gel for Zn(II) was increased from 31 to about 40 μmol ml^{-1}. It seems, therefore, that the optimum resolution of peptides and proteins is obtained on the CS–Cu(II) adsorbent with a capacity for Zn(II) of about 31 μmol ml^{-1} [or about 40 μmol ml^{-1} for Cu(II)], as is also evident from the family of curves shown in Fig. 4B. The effect of the column dimensions on the resolution of the peptides was also investigated using two columns with dimensions of 54 × 5 mm I.D. and 21 × 10 mm I.D. The results indicated that the longer the column, the better is the resolution of peptides that elute under isocratic conditions. However, those peptides which are eluted in the gradient are not markedly affected.

For comparison, the same mixture of peptides was chromatographed on a TSK–Cu(II) column (Fig. 5). The resolution of the peptides obtained here is essentially comparable to that obtained on the CS–Cu(II) column [capacity for Zn(II) = 31 μmol ml^{-1}] with the exception that peptides 4, 5, 6 and 9 are markedly

Fig. 3. Effect of varying the concentration of NaCl in the equilibration buffer on the retention times of the four peptide hormones shown in Fig. 2 on a column of CS–Cu(II) (54 × 5 mm I.D.; V_t = 1.06 ml) or TSK–Cu(II) (75 × 8 mm I.D.; V_t = 3.77 ml). In each instance, 2 μl of a solution of the four peptides in distilled water (containing 5 μg of each peptide) were applied to the columns equilibrated with 20 m*M* sodium phosphate buffer containing the indicated concentrations of NaCl (pH 7.0). For the CS–Cu(II) column the flow-rate was 0.47 ml min^{-1}, except when the equilibration buffer contained 4 *M* NaCl, when it was necessary to reduce it to 0.37 ml min^{-1} owing to increased back-pressure. For the TSK–Cu(II) column, the flow-rate was 0.94 ml min^{-1} throughout. The ligand concentration [based on Cu(II)] of the Chelating Superose gel was 42 μmol ml^{-1} and of the TSK gel chelate-5PW 23 μmol ml^{-1}. The peptide mixture was chromatographed under isocratic conditions throughout. 1, Chemotactic peptide; 2, tuftsin; 3, Met-Lys-bradykinin; 4, bradykinin. Note that Met-Lys-bradykinin is much more retarded than bradykinin in the absence of NaCl in the equilibration buffer. Inclusion of 0.5–4 *M* NaCl in the equilibration buffer reverses their elution positions.

TABLE III

RELATIVE RETENTION VOLUMES (V_e/V_t) AND ELUTION pH FOR A SERIES OF SYNTHETIC PEPTIDE HORMONES AFTER HP-IMAC ON CS–Cu(II) (21 × 10 mm I.D.; V_t = 1.65 ml) AND TSK–Cu(II) (75 × 8 mm I.D.; V_t = 3.77 ml) COLUMNS

For experimental details see text. In calculating the V_e/V_t ratios, appropriate corrections were made for the "dead volume" in the connecting tubes. With few exceptions, the purity of each peptide is given as 95% or better by the manufacturers. The elution profile of peptides 1–11 are shown in Figs. 4A and 5.

No.	*Peptide*	*Primary structure*[a]	*CS–Cu(II)*		*TSK–Cu(II)*	
			V_e/V_t	*pH*	V_e/V_t	*pH*
1	Chemotactic peptide	For-Met-Leu-Phe	0.9	7.0	0.8	7.0
2	Tuftsin	Thr-Lys-Pro-Arg	3.5	7.0	1.8	7.0
3	Met-Lys-bradykinin	Met-Lys-Arg-Pro-Pro-Gly-Phe-Ser-Pro-Phe-Arg	4.4	7.0	4.7	6.9
4	Bradykinin	Arg-Pro-Pro-Gly-Phe-Ser-Pro-Phe-Arg	6.8	7.0	5.5	6.5
5	Substance P	Arg-Pro-Lys-Pro-Gln-Gln-Phe-Phe-Gly-Leu-Met-NH_2	11.7	6.8	7.3	6.0
6	Somatostatin	Ala-Gly-Cys-Lys-Asn-Phe-Phe-Trp-Lys-Thr-Phe-Thr-Ser-Cys	14.4	6.5	8.3	5.6
7	Thyrotropin-releasing hormone (TRH)	PyroGlu-His-Pro-NH_2 · H_2O	25.2	5.0	10.8	4.9
8	Angiotensin III (human)	Arg-Val-Tyr-Ile-His-Pro-Phe-Ac-OH · $4H_2O$	29.3	4.7	12.1	4.8
9	Angiotensin II	Asp-Arg-Val-Tyr-Ile-His-Pro-Phe	30.4	4.7	14.4	4.3
10	Luteinizing hormone-releasing hormone (LH-RH)	PyroGlu-His-Trp-Ser-Tyr-Gly-Leu-Arg-Pro-Gly-NH_2	35.1	4.4	14.7	4.3
11	Angiotensin I	Asp-Arg-Val-Tyr-Ile-His-Pro-Phe-His-Leu	38.9	4.2	17.2	3.8
12	[Tyr^8]-substance P	Arg-Pro-Lys-Pro-Gln-Gln-Phe-Tyr-Gly-Leu-Met-NH_2	11.7	6.8		
13	Physaelamine	PyroGlu-Ala-Asp-Pro-Asn-Lys-Phe-Tyr-Gly-Leu-Met-NH_2	0.9	7.0		
14	Neurotensin (bovine)	PyroGlu-Leu-Tyr-Glu-Asn-Lys-Pro-Arg-Arg-Pro-Tyr-Ile-Leu	0.9	7.0		
15	Neurotensin (residues 3–13)	Tyr-Glu-Asn-Lys-Pro-Arg-Arg-Pro-Tyr-Ile-Leu	2.5	7.0		
16	Liver cel growth factor	Gly-His-Lys	1.5	7.0		
17	Eledoisine-related peptide	Lys-Phe-Ile-Gly-Leu-Met-NH_2	4.5, 6.5	7.0		
18	Gastrin-related peptide	AoC-Trp-Met-Asp-Phe-NH_2	3.0, 7.0	7.0		
19	MSH-release inhibiting factor (MIF)[b]	Pro-Leu-Gly-NH_2 · $\frac{1}{2}H_2O$	5.3			
20	Delta sleep-inducing peptide (DSIP)	Trp-Ala-Gly-Gly-Asp-Ala-Ser-Gly-Glu	2.7, 3.8, 6.2	7.0		
21	Oxytocin	Cys-Tyr-Ile-Gln-Asn-Cys-Pro-Leu-Gly-NH_2	5.3	7.0		
22	[Leu^5]-enkephalin	Tyr-Gly-Gly-Phe-Leu	6.4	7.0		
23	Tyr-bradykinin	Tyr-Arg-Pro-Pro-Gly-Phe-Ser-Pro-Phe-Arg	8.2	7.0		
24	Des-Arg^9-bradykinin	Arg-Pro-Pro-Gly-Phe-Ser-Pro-Phe	7.3	7.0		

[a] For = Formyl; PyroGlu = pyroglutamic acid; AoC = *tert.*-amyloxy-carbonyl; Ac = acetyl.
[b] MSH = melanocyte-stimulating hormone.

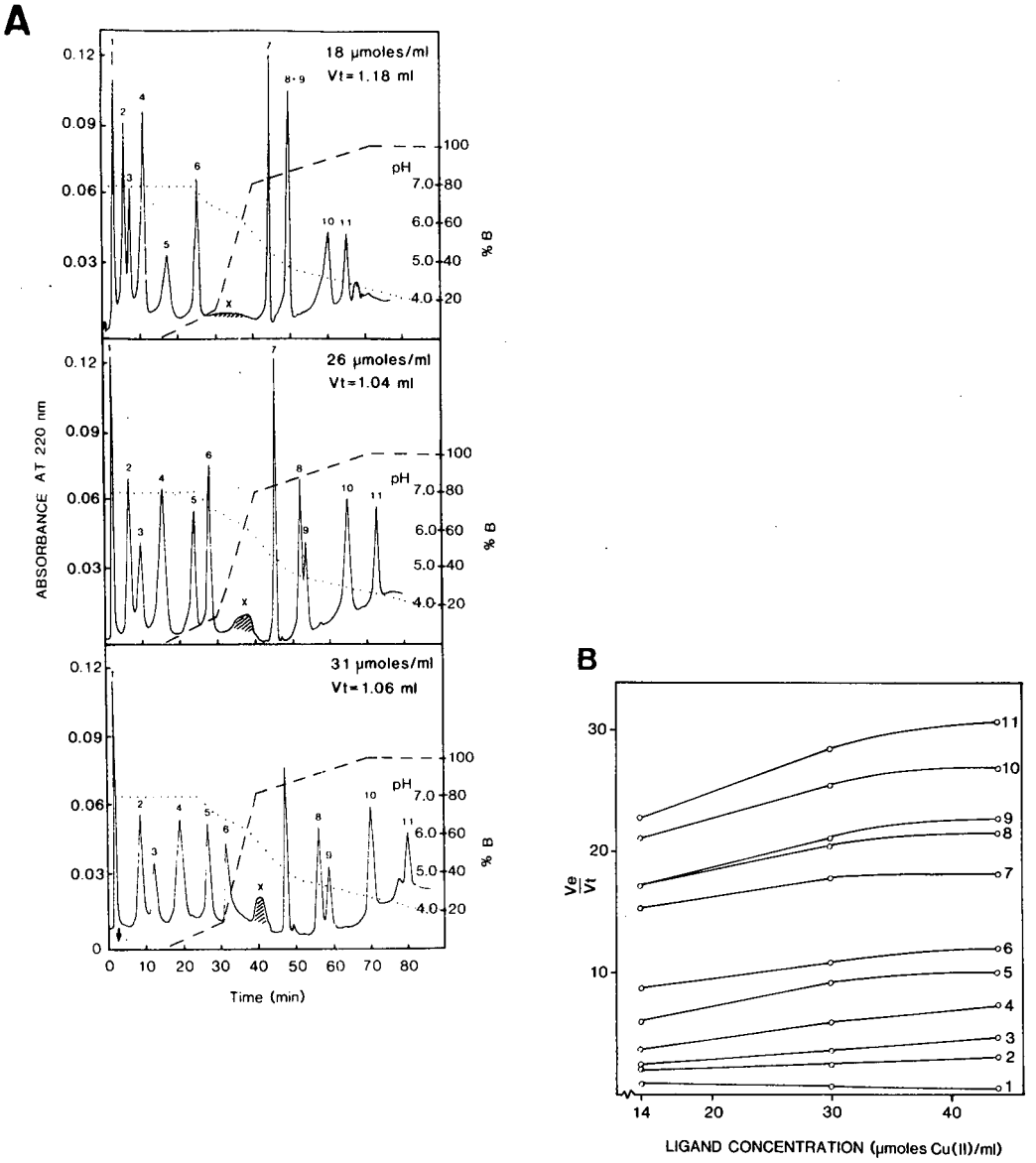

Fig. 4. (A) Effect of varying the concentration of immobilized ligand [Cu(II)] on the resolution of a mixture of eleven synthetic peptide hormones on columns of CS–Cu(II). The total volume and capacities for Zn(II) of each column (I.D. 5 mm) are shown. The actual concentration of immobilized Cu(II) ions on each of the columns is given in Table I and the names and structures of the peptides are given in Table III. The flow-rate was maintained at 0.47 ml min^{-1} and the chromatogram was developed by a programmed gradient elution procedure as described. (B) Effect of varying the concentration of immobilized ligand [Cu(II)] on the retention (expressed as V_e/V_t) of the eleven peptides shown in (A). Note that the retention volumes and the resolution of the peptides increase with increase in the concentration of immobilized ligand.

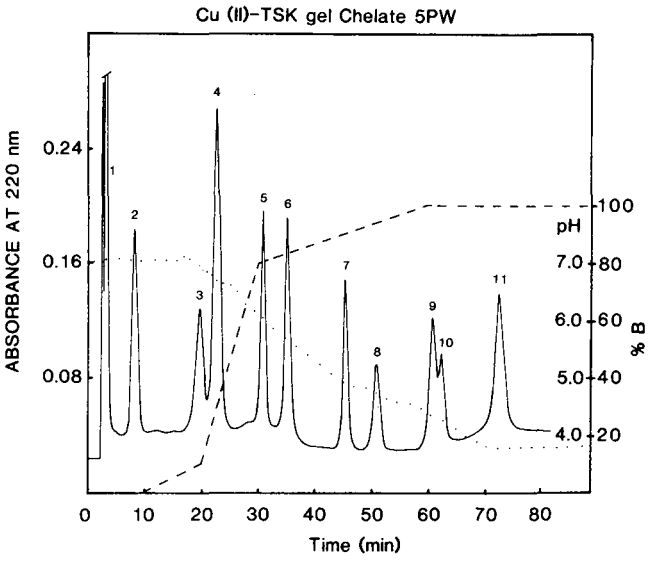

Fig. 5. Chromatography of the eleven peptide hormones shown in Table III and Fig. 4A on a column (75 × 8 mm I.D.; V_t = 3.77 ml) of TSK–Cu(II). The chromatogram was developed by a programmed gradient elution procedure as described at a flow-rate of 0.94 ml min^{-1}. Note that (i) the order of elution of the peptides is the same as on the CS–Cu(II) column shown in Fig. 4A; (ii) peptides 4, 5, 6 and 9 are more retarded on this column than on the corresponding CS–Cu(II) column (*cf.*, Fig. 4A and Table III), reflecting the influence of the polymer matrix; and (iii) peptides 9 and 10 elute close to each other, in contrast to the situation in Fig. 4A.

retarded on this column as judged from a comparison of the pH at which they elute from the two columns (see Table III). This might be due to a significant contribution from secondary interactions between the TSK–Cu(II) adsorbent and these solutes, probably arising from their higher content of aromatic amino acids.

Retention spectra of amino acids

The results obtained are compiled in Table IV, and show that all the amino acids are strongly retarded or bound by CS–Cu(II), although there are large variations in the strength of their binding. Of particular interest is the non-binding of β-alanine to CS–Cu(II) (Table V), indicating that the α-amino nitrogen of amino acids is of primary importance for their binding to IMAC adsorbents. It is therefore apparent that, for all the amino acids, their α-NH_2 nitrogens and their carboxyl groups participate to form a bidentate coordination bond with IDA–Cu(II) whereas His, Cys and Trp are bound by an extra coordination bond to form a stronger tridentate complex. The aliphatic basic and acidic amino acids including Pro and Ser are significantly retarded on the column but elute at the beginning of the pH gradient (in the pH range 7.0–6.5). The remaining amino acids are more strongly bound and elute in the pH range 6.5–4.5. Of these, the hydroxy-containing (Thr, Pro-OH) and aromatic (Phe, Tyr) amino acids and also Asn and Met are eluted earlier than the most strongly bound amino acids of all, *viz.*, Trp, Cys and His. These results differ markedly from those reported for IDA–Ni(II)[7], where all except Trp, Cys and His had V_e/V_t values less than 10. Of

TABLE IV

RELATIVE RETENTION VOLUMES OF THE NATURALLY OCCURRING AMINO ACIDS OBTAINED AFTER HP-IMAC ON A CHELATING SUPEROSE–Cu(II) COLUMN

About 5–10 μg of each amino acid in 1 μl of buffer were applied to the equilibrated column (21 × 10 mm I.D.; V_t = 1.65 ml) and elution was performed as described under Experimental. After application of each amino acid, they were eluted by a decreasing pH gradient identical with that shown in Fig. 4A. The flow-rate was maintained at 0.94 ml min^{-1} and the effluent was continuously monitored at 220 nm with the detector output set at 0.16–0.64 a.u.f.s. The Chelating Superose gel has a capacity for Zn(II) of 31 μmol ml^{-1} gel (according to the manufacturer) and for Cu(II) of 42 μmol ml^{-1} gel as determined by us (see Table I).

Amino acid	V_e/V_t	*Amino acid*	V_e/V_t
Gly	12	Cys-Cys	26
Ala	11	Phe	17
Ser	14	Tyr	19
Thr	17	Trp	24
Val	11	His	31
Leu	13	Arg	15
Ile	12	Lys	13
Pro	14	Asp	14
Pro-OH	20	Glu	11
Met	16	Asn	17
Cys	26	Gln	14

TABLE V

RELATIVE RETENTION VOLUMES OF SOME SELECTED DI- AND TRIPEPTIDES, CONTAINING Phe, Tyr, Cys AND His RESIDUES OBTAINED AFTER HP-IMAC OF EACH ON A CHELATING SUPEROSE–Cu(II) COLUMN (21 × 10 mm I.D.; V_t = 1.65 ml).

For experimental details, see text and Table IV.

No.	*Amino acid or peptide*	V_e/V_t	*No.*	*Amino acid or peptide*	V_e/V_t
1	Phe	17.0	21	Histamine	30.2
2	Phe-Phe	2.6	22	His-His	39.0, 41.0
3	Phe-Phe-Phe	7.4	23	His-Leu	27.0
4	Pre-Asp	1.1	24	His-Pro	26.0
5	Tyr	19.0	25	Pro-His-Asp	24.0
6	Tyramine	1.4	26	Asp-His	3.1
7	Tyr-Tyr	4.3	27	His-Phe	29.6
8	Tyr-Tyr-Tyr	14.5	28	His-Trp	36.5
9	Trp	24.0	29	His-Tyr	31.3
10	Trp-Trp	24.5	30	Tyr-His	1.5
11	Trp-Asp	2.0	31	His-Gly-Gly	28.0
12	Arg-Trp	3.7	32	Gly-Gly-His	1.5
13	Gly-Trp	7.1	33	Cyclo(Gly)-His	26.8
14	Trp-Tyr	10.3	34	L-Carnosine (β-Ala-L-His)	23.0
15	Tyr-Trp	10.8	35	L-Anserine (β-Ala-L-1-methyl-His)	23.4
16	Cys	26.0	36	β-Ala	1.5
17	Cys-Cys	26.0	37	Gly-His-Lys	1.5
18	Cys-bis-Phe	9.4		(liver cell growth factor)	
19	Cys-bis-His	8.3	38	Asp-Ala-His-Lys	1.5
20	His	31.0	39	ACTH (residues 3–10) (Tyr-Met-Glu-His-Phe-Arg-Trp-Gly)	1.5

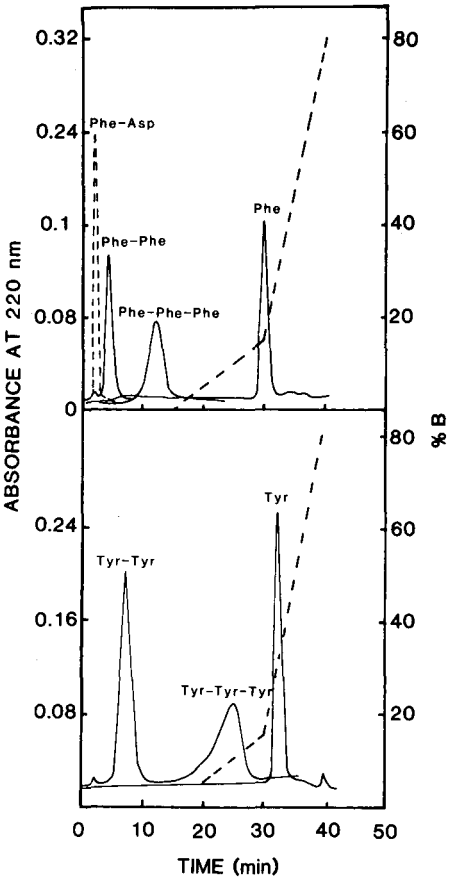

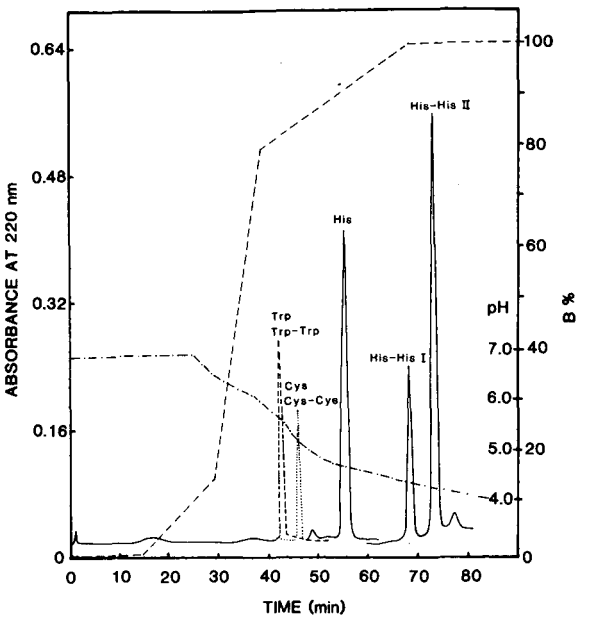

Fig. 6. Composite chromatograms showing the elution profiles of Phe, Tyr and their respective di- and tripeptides on a column (21 × 10 mm I.D.; V_t = 1.65 ml) of CS–Cu(II) with a capacity for Cu(II) of 42 μmol ml^{-1} [31 μmol ml^{-1} for Zn(II)]. Each amino acid or peptide was run separately on the column at a flow-rate of 0.94 ml min^{-1}. The adsorbed solutes (Phe, Tyr and Tyr-Tyr-Tyr) were eluted by a programmed gradient elution procedure as described. The quantitative elution data are compiled in Table V.

Fig. 7. Composite chromatogram showing the elution profiles of His, Trp, Cys and their respective dipeptides on a column (21 × 10 mm I.D.; V_t = 1.65 ml) of CS–Cu(II). See the legend to Fig. 6 for further details and Table V for the quantitative elution data. His-His gives rise to two distinct fractions reflecting the presence of a closely related impurity in the commercial dipeptide used.

interest in the present connection is the relatively high V_e/V_t values obtained for Asn, Met and the aromatic and hydroxy-containing amino acids, indicating that peptides containing these amino acids but no His, Trp or Cys residues would be retarded to varying extents on a CS–Cu(II) column provided that the amino-terminal residue is not blocked. With some exceptions, the results in Table III support this hypothesis.

Effect of solute structure

The foregoing results indicate that there is an apparent relationship between the retention of the peptides and their primary structures. Accordingly, the peptides

shown in Figs. 4A and 5 and Table III can be grouped into three categories, *viz.*, peptides 1–4, which elute isocratically, peptides 5 and 6 (containing Trp and Cys), which are bound moderately, and peptides 7–11 (containing His), which are bound tightly. On the basis of an extended series of experiments using a variety of peptides other than those shown in Fig. 4A or 5 and the retention spectra of some selected amino acids and di- or tripeptides (see Table V and Figs. 6 and 7), an attempt will be made here to rationalize the differential retentions of peptides on CS–Cu(II) adsorbent. By virtue of the relatively small molecular size of the peptides used here, it is assumed that most or all of their constituent amino acids are exposed to the solvent and are thus available for interaction with the immobilized Cu(II) ions.

Role of the α-amino and carboxyl groups

Peptides that lack His, Trp or Cys and whose amino terminal residues are blocked do not bind to CS–Cu(II) (Table III, peptides 1, 13 and 14). Removal of the blocked amino terminal residue results in a noticeable increase in retention, *e.g.*, neurotensin (residues 3–13) and neurotensin (Table III). The α-amino group of peptides is thus of primary importance for coordination with immobilized Cu(II) ions. However, this is not the case for the carboxyl terminal group, as peptides with blocked C-terminals are significantly retarded on the CS–Cu(II) column (Table III, peptides 5, 12, 17 and 19). These findings are in agreement with, and give support to, the recent proposal by Porath[18] that transition metal ions preferentially coordinate with nitrogen atoms. They also indicate that IMAC could be useful for separating blocked peptides from the mixture obtained after peptide synthesis. The ε-amino group of lysine and the guanidino group of arginine do not seem to coordinate with CS–Cu(II) since their V_e/V_t values are not markedly different from those of the aliphatic amino acids (Table IV). A comparable result has also been reported by Brookes and Pettit[16] for the interaction of these basic amino acids with Cu(II) ions in free solution.

Role of the aromatic amino acids and His, Cys and Trp

The significantly high retention on CS–Cu(II) of Phe and Tyr (Table V and Fig. 6) or of peptides containing these two residues, *e.g.*, angiotensin II and III (1 His, 1 Phe, and 1 Tyr) compared with TRH (1 His), indiates that they strengthen the binding of peptides, and possibly even proteins, to such adsorbents. However, the presence of charged amino acids in the immediate vicinity of Phe or Tyr markedly decreases the retention of the peptides, *e.g.*, Phe-Asp (Table V) and Met-Lys-bradykinin (Table III). Moreover, the spacing out of these residues in the peptide chain should also be taken into account, as our results show that the V_e/V_t of Phe-Phe or Tyr-Tyr is much lower than for the corresponding tripeptides or single amino acids. It is thus apparent that secondary and higher structures of peptides and proteins should be considered in order to assess with certainty the partial contributions of the aromatic amino acids to their overall retention on IDA–Cu(II) adsorbents.

His, Cys and Trp are by far the most important amino acids involved in strong coordination with metal ions of Groups IB, IIB and VIII. The results in this paper provide ample support as far as immobilized Cu(II) ions are concerned, where the strength of their binding follows the order: His-His > Cys = Cys-Cys > Trp = Trp-Trp (Table V). This relationship is also reflected in the retention of peptides containing these residues, *e.g.*, TRH (1 His and a blocked α-amino group) is bound

more strongly than somatostatin (1 Trp, 2 Cys, involved in a disulphide and 3 Phe). Likewise, angiotensin I (2 His) is bound more strongly than LH-RH (1 His and 1 Trp). The spacing out of these three residues in a peptide chain also influences their strength of binding. Our data thus support and extend the proposal by Sulkowski[6] in this respect. The conformation of the peptide must also be taken into consideration as it has a direct bearing on the availability of these residues for interaction. A case in point is somatostatin, whose structure is reminiscent of the "zinc fingers" in DNA-binding proteins[19,20], where its Trp residue is exposed to the surface and thus accessible for binding to immobilized Cu(II) ions.

Anomalous adsorption behaviour

In the course of this study, we came across some His-containing peptides that did not bind to CS–Cu(II), *viz.* Gly-His-Lys (GHK[a]) and Tyr-His (Table V, peptides 37 and 30, respectively). Smith *et al.*[15] also obtained such unexpected adsorption behaviour. Their results showed, with few exceptions, that peptides having the structure X-His did not bind to (Sephadex G-25)–IDA–Cu(II) whereas those with the structure His-X were bound irrespective of the nature of the amino acids represented by X. Despite the high affinity constants in solution for GHK, which they quoted (log K = 19.95), their explanation for its apparent inability to bind to immobilized IDA–Cu(II) was ascribed to the formation of different kinds of metal–solute complexes in solution and on the matrix-bound metal ion. We differ in this last interpretation and instead outline below an alternative hypothesis which is consistent with solution or column data obtained by others and with our own results on columns.

GHK is a so-called "liver cell growth factor"[21] normally found in human plasma in association with human serum albumin (HSA) and α-globulin fractions. The GHK–Cu(II) complex is also reported to have diverse biological action such as wound healing and tissue repair as well as significant superoxide dismutase activity[22]. GHK is able to remove Cu(II) from the HSA–Cu(II) complex very effectively at neutral pH[23,24], indicating that its affinity for Cu(II) (pK = 16.2, see refs. 24 and 25) is equal to or higher than that of HSA. The X-ray structure of the GHK–Cu(II) complex shows that the Cu(II) ion is coordinated to three nitrogens of GHK, *viz.*, the α-amino, imidazole and one peptide nitrogen as well as two oxygens of water[22]. Although GHK is postulated to form a ternary complex with Cu(II) that is already bound to HSA to form [HSA–Cu(II)–GHK] *in solution*, a similar situation, *i.e.*, the formation of [CS–Cu(II)–GHK], does not seem to occur on a CS–Cu(II) column, probably as a result of steric hindrances or the instability of such a ternary complex on the column. Its lack of binding to CS–Cu(II) can thus be ascribed to the removal of Cu(II) ions from the column to form a GHK–Cu(II) complex which, of necessity, will not be retarded on or bound by the CS–Cu(II) column. We have also considered an alternative explanation for the non-binding of GHK to CS–Cu(II), *i.e.*, the C-terminal Lys affects the pK of its adjacent His residue[26] to such an extent that the peptide as a whole does not bind to the CS–Cu(II) column. However, as its neutral analogue (Gly-His-Gly) also does not bind[15], this proposal was rejected in favour of that outlined above.

---

[a] GHK is erroneously abbreviated as GHL[22] in the literature. As K, and not L, is the one-letter code for lysine we have used it consistently in this paper.

To our knowledge, only two such events are unequivocally documented in the IMAC literature[26,27]. Thus Muszyńska *et al.*[26] have shown that Zn(II)-depleted and inactive carboxypeptidase A strips off Zn(II) ions from an IDA–Zn(II) column and elutes from it in its enzymatically active form, fully loaded with Zn(II) ions. Likewise, Andersson *et al.*[27] have shown that HSA strips off Ni(II) ions from an IDA–Ni(II) column, eluting from it in the form of an HSA–Ni(II) complex. Clearly, these results illustrate the occurrence of "metal ion transfer"[29] on IMAC of some specific proteins and peptides. For such an event to take place, the following conditions seem to be necessary: (i) the association constant solute–M(II) > C–M(II), where C = chelator and M(II) = metal ion, and (ii) the ternary complex C–M(II)–solute is unstable and dissociates in favour of a solute–M(II) complex, leading to a "metal ion transfer" event. If, on the other hand, the association constant C–M(II) > S–M(II), then a stable, ternary complex can be formed and the solute could be bound by or, retarded on, the IMA adsorbent.

The question thus arises: can this hypothesis explain the other results we obtained in Table V? We believe it does, for reasons outlined below.

Of the His-containing dipeptides shown in Table V, those having the structure X-His do not bind to CS–Cu(II) whereas those having the structure His-X are bound strongly with V_e/V_t values in excess of 25. The only exception is His-His, which is the most strongly bound dipeptide to CS–Cu(II) that we have found during this investigation. The underlying principle for the results obtained is apparently "metal ion transfer" from the CS–Cu(II) to those dipeptides having X-His as their structure simply because such dipeptides form a strong tridentate coordination bond with the immobilized Cu(II) ions via the free α-amino group of the amino terminal residue X, the intervening peptide nitrogen and the imidazole of His, as in the case of GHK. Owing to such strong binding, their affinity towards the immobilized Cu(II) ions is apparently much stronger than that of Cu(II) ions to the IDA of Chelating Superose, with the result that such dipeptides strip off the Cu(II) ions from the CS–Cu(II) and subsequently pass through the column unretarded. When the order is reversed, as in His-X, the α-amino nitrogen of the X residue is blocked and will in effect not coordinate with the immobilized Cu(II) ions. Under such circumstances, the overall interaction is weakened as the peptide nitrogen does not form such a strong coordination bond with CS–Cu(II) as does the α-amino nitrogen. Consequently, such peptides will bind to CS–Cu(II) through their His residues and their overall retention will be about the same as that of a single His residue. The carboxyl group does not contribute significantly to the overall binding of His-containing di- or tripeptides, as can be deduced from the finding that histamine binds as strongly as His to CS–Cu(II) (see Table V).

Further support for the above hypothesis is provided by the retention of L-carnosine and L-anserine (peptides 34 and 35, respectively, in Table V). These two peptides are strongly bound to CS–Cu(II) despite the fact that they also have X-His as their general structure. However, in β-Ala its NH_2 group is not in the α-position and apparently does not form a coordination bond with immobilized Cu(II) ions as does the α-amino group of the common amino acids (see Table V, peptide 36). These two

peptides are thus bound to immobilized Cu(II) ions entirely through their His residues. The same holds for cyclo-Gly-His:

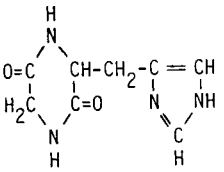

where the α-amino group of Gly is blocked, showing that this dipeptide is bound to CS–Cu(II) entirely through its His residue. These results are consistent with the proposition that a free α-amino group in combination with a His residue at the carboxyl terminus of dipeptides results in "metal ion transfer" from CS–Cu(II) to the dipeptide in question.

The discussion outlined above also applies to the His-containing tripeptides shown in Table V. As would be expected, His-Gly-Gly is bound but not Gly-Gly-His. The latter tripeptide is a well studied synthetic molecule which mimics the Cu(II) transport site of human serum albumin[23]. It binds Cu(II) in free solution as a 1:1 complex in the pH range 6.5–11 and the dissociation constant of the peptide–Cu(II) complex is $1.18 \cdot 10^{-16}$, compared with $6.61 \cdot 10^{-17}$ for albumin–Cu(II)[23]. The Cu(II)-binding site of human serum albumin is attributed entirely to the tetrapeptide Asp-Ala-His-Lys situated at the amino terminus of the molecule[30]. Despite its very high affinity towards Cu(II), it does not bind to immobilized Cu(II) either (Table V, peptide 38). In view of what has been discussed earlier, it is both consistent and reasonable to propose that the lack of binding of these peptides to CS–Cu(II) is also due to "metal ion transfer" from CS–Cu(II) to these peptides. On the basis of these findings we can postulate that the corresponding Cu(II)-binding sites of bovine (Asp-Thr-His-Lys) and rat (Glu-Ala-His-Lys) serum albumins[25] would also strip off Cu(II) from a CS–Cu(II) column and thus not bind either. The corresponding site for dog serum albumin (Glu-Ala-Tyr-Lys)[25] would not be expected to bind to CS–Cu(II), nor would it strip off Cu(II) ions from the column owing to replacement of the important His residue by Tyr at position 3 of its sequence.

Direct proof to the proposed hypothesis would be metal ion analysis of those peptides [X-His, GHK and the Cu(II)–binding tetrapeptides of the various serum albumins] after their passage through a CS–Cu(II) column. Unfortunately, these peptides were not available for such experiments. However, some orienting experiments are in progress aimed at adapting modern mass spectrometric methods to establish the Cu(II) content in small amounts of such peptides. Moreover, our results suggest that the passage of such peptides through a CS–Cu(II) column would be a very elegant and simple method for optimally loading them with Cu(II) ions for further analysis, *e.g*, to load Gly-His-Lys in order to use it as a therapeutic agent for wound-healing purposes[22].

Practical implications

The results presented here serve as guidelines when one is investigating the optimum conditions necessary for the separation of peptides and proteins on IMA adsorbents through a systematic variation of the relevant chromatographic param-

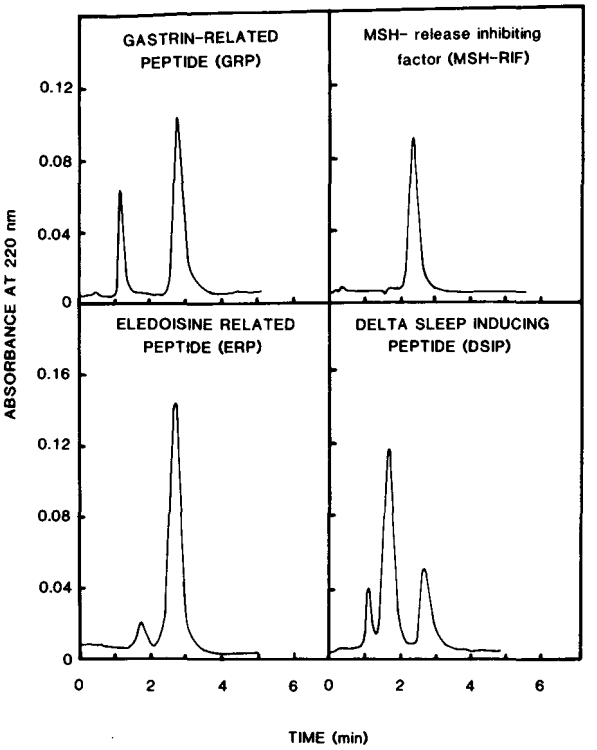

Fig. 8. Test of the purity of some commercially available synthetic peptide hormones by IMAC on a column (21 × 10 mm I.D.; bed volume 1.65 ml) of CS–Cu(II) equilibrated with buffer A. Each peptide was eluted under isocratic conditions at a flow-rate of 0.94 ml min^{-1}. The primary structures of the peptides are shown in Table III.

eters. It is envisaged that IMAC will be of special interest for researchers in the area of peptide synthesis as concerns both the purification of a specific peptide or an independent check of its purity by a separation mechanism which is different from that of the commonly used reversed-phase chromatography (RPC). An example of this is presented in Fig. 8, where the purity of four commercially available synthetic peptide hormones was determined by HP-IMAC on a CS–Cu(II) column. With one exception, the preparations contained one or more impurities.

A distinct advantage of IMA-based adsorbents over RPC is the use of entirely aqueous buffers as eluents in the former, a consideration which is important for safety in the laboratory working environment. IMAC is also a versatile method in that a range of different metal ions can be immobilized on the same chelating gel, making it possible to choose the most suitable immobilized metal ion for a particular application. An additional parameter that can be varied is the salt concentration in the equilibration buffer. Our results indicate that at low concentrations of salt in the equilibration buffer, ionic interactions are superimposed on metal ion recognition, which could be exploited to magnify small differences in the surface properties of peptides or proteins and thus lead to their optimum separation. We are convinced that this point will receive increasing attention in the future use of IMAC. We would also

like to point out that, as far as we know, denaturation of proteins or peptides on IMA adsorbents is a rare phenomenon.

ACKNOWLEDGEMENTS

We thank Drs. L. Kågedal and M. Sparrman and Eng. R. Ehrnström of Pharmacia LKB Biotechnology for generously providing the chelating gels and Dr. Y. Nakagawa of the Peptide Institute, Osaka, Japan, for his generous gift of gastrin-related peptide, Leu-enkephalin (sulphated) and neurotensin (residues 3–13). Financial support was provided by the Swedish Natural Science Research Council.

REFERENCES

1 Y. Kato, K. Nakamura and T. Hashimoto, *J. Chromatogr.*, 354 (1986) 511.
2 M. Belew, T. T. Yip, L. Andersson and R. Ehrnström, *Anal. Biochem.*, 164 (1987) 457.
3 A. Hammacher, U. Hellman, A. Johnsson, A. Östman, K. Gunnarsson, B. Westermark, Å. Wasteson and C. H. Heldin, *J. Biol. Chem.*, 263 (1988) 16493.
4 Y. Nakagawa, T. T. Yip, M. Belew and J. Porath, *Anal. Biochem.*, 168 (1988) 75.
5 J. Porath, J. Carlsson, I. Olsson and G. Belfrage, *Nature (London)*, 258 (1975) 598.
6 E. Sulkowski, *Trends Biotechnol.*, 3 (1985) 1.
7 E. S. Hemdan and J. Porath, *J. Chromatogr.*, 323 (1985) 255.
8 C. J. Chothia, *J. Mol. Biol.*, 105 (1976) 1.
9 E. S. Hemdan and J. Porath, *J. Chromatogr.*, 323 (1985) 265.
10 J. Porath and B. Olin, *Biochemistry*, 22 (1983) 1621.
11 E. Sulkowski, in R. Burgess (Editor), *Protein Purification: Micro to Macro*, Alan R. Liss, New York, 1987, p. 149.
12 M. Belew, T. T. Yip, L. Andersson and J. Porath, *J. Chromatogr.*, 403 (1987) 197.
13 A. Tiselius, *Ark. Kem. Min. Geol.*, 14B (1940) 1.
14 C. H. W. Hirs, S. Moore and W. H. Stein, *J. Biol. Chem.*, 219 (1956) 623.
15 M. C. Smith, T. C. Furman and C. Pidgeon, *Inorg. Chem.*, 26 (1987) 1965.
16 G. Brookes and L. D. Pettit, *J. Chem. Soc., Dalton Trans.*, (1976) 42.
17 L. Kågedal, in J.-C. Janson and L. Rydén (Editors), *Protein Purification; Principles, High Resolution Methods, and Applications*, VCH, New York, 1989, p. 227.
18 J. Porath, *Trends Anal. Chem.*, 7 (1988) 254.
19 J. M. Berg, *Proc. Natl. Acad. Sci. U.S.A.*, 85 (1988) 99.
20 A. Klug and D. Rhodes, *Trends Biochem. Sci.*, 12 (1987) 464.
21 L. Pickart and M. M. Thaler, *Nature New Biol.*, 243 (1973) 85.
22 L. Pickart and S. Lovejoy, *Methods Enzymol.*, 147 (1987) 314.
23 S. Lau, T. P. A. Kruck and B. Sarkar, *J. Biol. Chem.*, 249 (1974) 5878.
24 S. Lau and B. Sarkar, *Biochem. J.*, 199 (1981) 649.
25 J. W. Dixon and B. Sarkar, *J. Biol. Chem.*, 249 (1974) 5872.
26 G. Muszyńska, Y.-J. Zhao and J. Porath, *J. Inorg. Biochem.*, 26 (1986) 127.
27 L. Andersson, E. Sulkowski and J. Porath, *J. Chromatogr.*, 421 (1987) 141.
28 E. Sulkowski, *BioEssays*, 10 (1989) 170.
29 T. Peters and F. A. Blumenstock, *J. Biol. Chem.*, 242 (1967) 1574.
30 B. Sarkar, J.-P. Laussac and S.-J. Lau, in B. Sarkar (Editor), *Biological Aspects of Metals and Metal-Related Diseases*, Raven Pres, New York, 1983, p. 23.

Journal of Chromatography, 516 (1990) 355–364
Elsevier Science Publishers B.V., Amsterdam

CHROM. 22 620

Retention of benzo[*a*]pyrene on cyclodextrin-bonded phases

PETER R. FIELDEN* and ANDREW J. PACKHAM
Department of Instrumentation and Analytical Science, UMIST, P.O. Box 88, Manchester M60 1QD (U.K.)
(First received August 2nd, 1989; revised manuscript received June 14th, 1990)

ABSTRACT

The retention of polynuclear aromatic hydrocarbons by cyclodextrin-bonded phases is complex. It consists of inclusion formation, the mechanism which confers the unique retention properties to this phase, an ionic component due to the external hydroxyl groups and a reversed-phase like component. This complex retention mechanism allows the resolution of compounds that would otherwise prove difficult to resolve on conventional normal or reversed phases.

The relative effect of each of these mechanisms on retention is determined by the column temperature and by the type and percentage of the mobile phase organic modifier. In this study the effect that the alteration of these parameters has on the retention of benzo[*a*]pyrene is reported. The multi-mode retention mechanism is clearly shown to be in effect.

INTRODUCTION

Cyclodextrins are polymers consisting of helical 1,4-α-glucoside monomers. The molecule is shaped as a torus with major and minor openings. The minor opening is surrounded by primary hydroxyl groups which are bound to the silica support by a hydrocarbon linkage. The larger major opening is surrounded by secondary hydroxyl groups which are responsible for the external hydrophilic environment. In contrast, the internal environment is hydrophobic and responsible for the formation of cyclodextrin–analyte inclusion complexes. This occurs if the analyte is of the correct size and charge distribution[1].

Three cyclodextrins have been successfully bound to a 5-μm spherical silica base. These have been named α-, β- and γ-cyclodextrins and consist of six, seven and eight glucose monomers, respectively. The internal diameters are 0.57, 0.78 and 0.95 nm and in all three cases the torus depth is around 0.78 nm (ref. 2). Both the α- and β-cyclodextrins are available in an acetylated form to reduce possible ionic interactions. The size of benzo[*a*]pyrene has been calculated as 0.88 nm across the long axis suggesting that while the α-cyclodextrin will not form an inclusion complex, both the β and γ will. This has been confirmed by Woodberry *et al.*[2], where benzo[*a*]pyrene was

0021-9673/90/$03.50

shown not to form an inclusion complex with the α-cyclodextrin, a 1:1 host–analyte ratio was obtained with the β-cyclodextrin and a 1:2 host–analyte ratio with the γ-cyclodextrin. It was proposed that in the γ-cyclodextrin benzo[*a*]pyrene was able to stack allowing two molecules to enter the cavity simultaneously.

The cyclodextrins are a relatively new bonded phase and have been successfully used for the separation of a number of chiral compounds such as benzo[*a*]- and benzo[*e*]pyrene[3], dansyl-D- and -L-leucine[1], and *ortho-*, *para-* and *meta*-nitro-anilines[1]. Mycotoxins, polynuclear aromatic hydrocarbons, quinones and heterocyclic compounds have all been resolved on these phases highlighting the resolving power of these columns[4]. These separations have been achieved due to the ability of the phase to form a stable inclusion complex with the analyte. The stability of the complex depends on the charge distribution, and the shape and size of the molecule forming the complex. There must be a hydrophobic region within the molecule that is the correct size to enter the cavity, the complex stability may be enhanced by the presence of external polar groups that can interact with secondary hydroxyls. If the analyte is too large it will be unable to enter the cavity and no inclusion derived retention will occur, although retention may still occur by an ionic interaction mechanism. In this mode the column acts as a high-density diol column. In the β-cyclodextrin (acetylated) column the secondary hydroxyls have been acetylated thus reducing the possibility of ionic interactions. If the analyte is too small it will enter the cavity but the stability of the complex is poor and the retention will be low. It is also possible to use non-polar solvents such as hexane with these phases, in this case no inclusion occurs and retention is due purely to external adsorption.

In this paper we have investigated the effect of temperature and the type and concentration of mobile phase modifier on the retention of the probe molecule benzo[*a*]pyrene. Benzo[*a*]pyrene has been used in this study as it is known to enter, and thus be retained, by both the β- and γ-cyclodextrins and also due to its environmental importance. In a recent study by Olsson *et al.*[5] the retention of a range of polynuclear aromatic hydrocarbons by monomeric and polymeric C_{18}-bonded phases was not found to be as high as that of conventional reversed phases, the authors did suggest that the cyclodextrin-bonded phases may offer significant advantages where the separation of polynuclear aromatic hydrocarbons of different molecular weights is required. The authors of this paper have reported a multidimensional high-performance liquid chromatographic (HPLC) configuration with both C_{18} and cyclodextrin columns that was used to realise the determination of low levels of benzo[*a*]pyrene in aviation and diesel fuel after direct injection of the fuel[6]. Three different mechanisms of retention have been identified, inclusion derived retention, normal-phase type retention and a novel retention mechanism limited to a number of solvents.

EXPERIMENTAL

Materials

Benzo[*a*]pyrene was obtained from BDH (Poole, U.K.). Chromatographic solvents were also obtained from BDH and were of HiPerSolv grade except for the propan-1-ol which was of Aristar grade. The propan-2-ol was obtained from May and Baker (Dagenham, U.K.). The water used in this study was distilled and stored in glass. The α-cyclodextrin, β-cyclodextrin (acetylated) and γ-cyclodextrin columns (250 ×

4.6 mm I.D.) were packed by Astec (U.S.A.) supplied by Technicol (Stockport, U.K.) Standard benzo[*a*]pyrene solutions were made up in acetonitrile and stored in the dark to avoid photo-induced degradation. A concentration of 400 ng ml^{-1} benzo[*a*]pyrene was used, equivalent to an injection of 8 ng.

Equipment

All chromatography was carried out using either system A (retention measurement of benzo[*a*]pyrene) or system B (determination of the retention time of an unretained compound (t_0).

System A. A Waters series 6000 HPLC pump was used, the mobile phase being generated by a modified Micrometeritic gradient former. The flow-rate used was 1.0 ml min^{-1} for all solvents except for propan-1-ol and propan-2-ol containing mixtures, when, due to pressure limitations, a flow-rate of 0.5 ml min^{-1} was selected. All solvents were filtered through a 2-μm Millipore filter under negative pressure and continuously degassed with helium. A Rheodyne, Model 7125 syringe loading injection valve with a 20-μl sample loop was used to introduce the sample. A Perkin-Elmer series 3000 fluorescence detector was used to monitor the eluent. The excitation and emission wavelengths were 254 nm and 420 nm, respectively. Excitation and emission slits were 5 nm. The columns were maintained at the desired temperature using a Grant Instruments (Cambridge, U.K.), Model SE10 water bath.

System B. A Kontron Instruments 420 LC pump was used for this study, with the mobile phases continuously degassed with helium. The columns under investigation were thermostated in a Perkin-Elmer LC-65T column oven. A house-built conductivity cell, consisting of a 1/16 × 0.043 in. through-hole cross-coupler which had been drilled to allow the positioning of a pair of 1-mm diameter gold disc electrodes in the flow stream, was also maintained at constant temperature in the oven. The conductivity of the column effluent was monitored using an Orion Research 101 conductivity meter. The procedure described by Hinze *et al.*[7] was adapted to estimate t_0. In order to promote a significant change in conductivity due to the probe alcohols, potassium chloride was added to the methanol–water (50:50, v/v) and pure water phases to a concentration of 0.05 *M*. In this way, a decrease in conductivity was measured. For the acetonitrile phase, no electrolyte was added and the probe peaks gave an increase in conductivity. Determinations were made at column temperatures of 25 and 50°C.

During the study both a Hewlett-Packard 3390A integrator and a Midas Chromatographic Data Station, Comus Instruments (Hull, U.K.) were used to determine the retention times and a Goerz BBC SE 120 chart recorder was used to record the chromatograms. When not in use the columns were equilibrated with 100% methanol.

RESULTS AND DISCUSSION

In this study five commonly used reversed-phase solvents and one normal-phase solvent were used to study the retention of the polynuclear aromatic benzo[*a*]pyrene on the β-, β-(acetylated) and γ-cyclodextrin-bonded phases.

When studying the retention of species on stationary phases under different mobile phase conditions, it is beneficial to utilise the parameter of phase capacity ratio,

k', in the description. This relies on obtaining an accurate estimate of the retention time of an unretained spcies, t_0. For most stationary phases, there are recommended probes that yield this information. For cyclodextrin-bonded phases, however, it is not so straightforward.

The method reported by Hinze *et al.*[7] was used in this study in order to obtain an estimate of t_0. Plots of retention times of the probe alcohols *vs.* their formation binding constants for β-cyclodextrin complexation are extrapolated to zero binding constant to yield the retention time equivalent to the column void volume. Table I gives a summary of estimates of t_0 in terms of column void volume for a selection of mobile phases at the two temperatures studied, using the probes methanol, ethanol and propanol. It is interesting to note that in methanol and water mobile phases, the elution order at both temperatures is methanol, ethanol and propanol; whilst in 100% acetonitrile, the elution order is completely reversed. This indicates the complexity of the cyclodextrin retention mechanism and stresses the difficulty in obtaining a realistic value for t_0. Also, for mobile phases consisting of either 100% water or 100% acetonitrile, the data are not linear, such that an exponential rather than a linear curve fit was more appropriate for the extrapolation. In view of these results, it was decided to quote the actual retention time of benzo[*a*]pyrene for a given mobile phase and temperature rather than the preferred parameter of phase capacity ratio.

Fig. 1 shows a three dimensional surface plot of the retention time on a β-cyclodextrin column in response to changes in the temperature and percentage of methanol. The steep peak between 40 and 60% methanol and 20 and 40°C (shaded) corresponds to the region in which inclusion is promoted. At higher temperatures and methanol concentrations a plateau is seen which corresponds to very low levels of retention. The temperature dependence of the inclusion complex is shown with little retention occurring above 60°C.

Similar surface plots have been obtained with both the β-cyclodextrin (acetylated) and γ-cyclodextrin columns. In contrast Fig. 2 shows the surface plot for the β-cyclodextrin column in response to changes in acetonitrile concentration and temperature. The steep inclusion peak is clearly present as is a ridge seen at high acetonitrile concentrations between 80 and 100% (shaded). The ridge shows only slight temperature dependence. Again, similar results are obtained with the other two bonded phases when using acetonitrile as the organic phase modifier. Tetrahydrofuran

TABLE I

ESTIMATED VOID VOLUME RETENTION TIME (t_0) FOR THE β-CYCLODEXTRIN COLUMN OBTAINED AT DIFFERENT OPERATING CONDITIONS

All flow-rates 1.0 ml min^{-1}.

Mobile phase	*Temperature (°C)*	*Estimated t_0 (min)*
Water (0.05 *M* potassium chloride)	25	3.23
Methanol–water (50:50) (0.05 M Potassium chloride)	25	2.95
100% acetonitrile	25	3.58
Water (0.05 *M* potassium chloride)	50	3.28
Methanol–water (50:50) (0.05 M Potassium chloride)	50	3.02

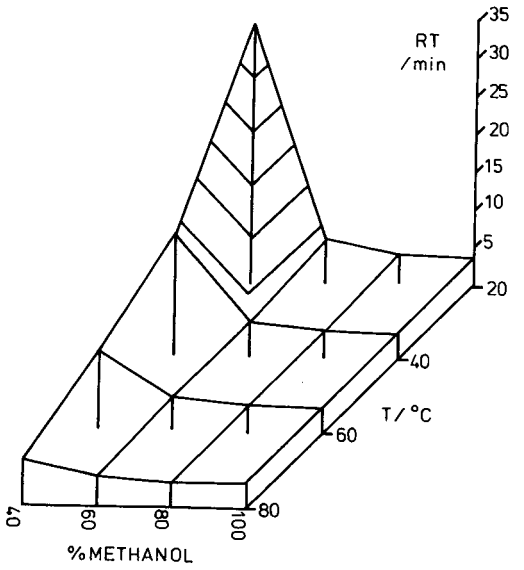

Fig. 1. Three-dimensional surface plot showing the retention time (RT) response with alterations in the column temperature and the percentage methanol in the mobile phase. Column: β-cyclodextrin; flow-rate: 1 ml min^{-1}; 8 ng benzo[*a*]pyrene injected.

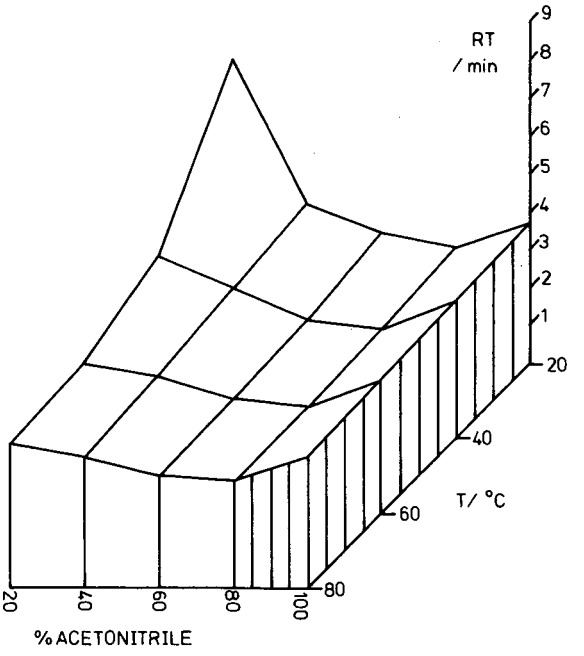

Fig. 2. Three-dimensional surface plot showing the retention time (RT) response with alterations in the column temperature and the percentage acetonitrile in the mobile phase. Column: β-cyclodextrin; flow-rate: 1 ml min^{-1}; 8 ng benzo[*a*]pyrene injected.

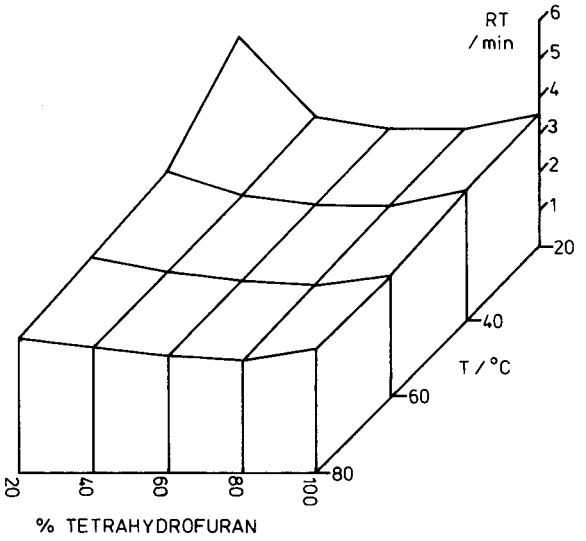

Fig. 3. Three-dimensional surface plot showing the retention time (RT) response with alterations in column temperature and the percentage of tetrahydrofuran in the mobile phase. Column: β-cyclodextrin; flow-rate: 1 ml min^{-1}; 8 ng benzo[*a*]pyrene injected.

(Fig. 3) gave similar results to those obtained using acetonitrile although the size of both the inclusion peak and retention ridge were reduced. In Figs. 4 and 5 the retention times with varying acetonitrile concentrations at 20°C and 80°C, respectively, are compared, all three bonded phases respond in a similar way. From these figures it is possible to isolate three regions on the graph; a steep portion on the left, shown to be temperature dependent, and correspond to inclusion complex formation, a shallow

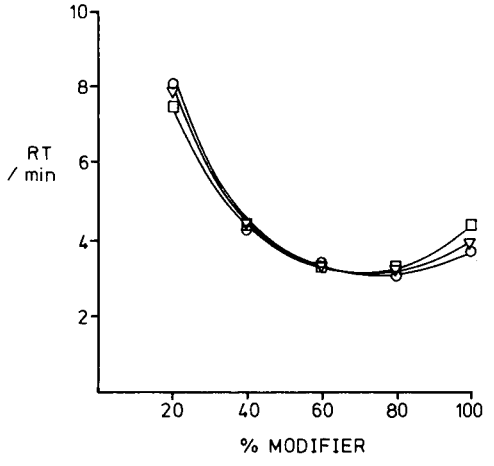

Fig. 4. Comparison of the retention time (RT) of benzo[*a*]pyrene on the three different bonded phases at 20°C with variations in the percentage of acetonitrile in the mobile phase; flow-rate: 1 ml min^{-1}. □ = β-cyclodextrin; ▽ = β-cyclodextrin (acetylated); and ○ = γ-cyclodextrin.

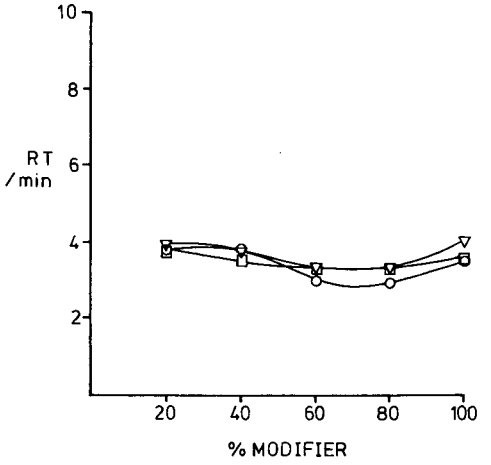

Fig. 5. Comparison of the retention time (RT) of benzo[*a*]pyrene on the three different bonded phases at 80°C with variations in the percentage of acetonitrile in the mobile phase; flow-rate: 1 ml min^{-1}. □ = β-cyclodextrin; ▽ = β-cyclodextrin (acetylated); and ○ = γ-cyclodextrin.

plateau with minimum retention times, and a high percentage organic modifier derived retention increase that is temperature independent. The occurance of a minimum, as seen in Fig. 4 (and also Fig. 6), is similar to that described by Han and Armstrong[8], who studied the influence of percentage acetonitrile on the capacity factor of some dansyl amino acids separated using a β-cyclodextrin phase.

Fig. 6 shows the variation in retention time for benzo[*a*]pyrene at 20°C, when

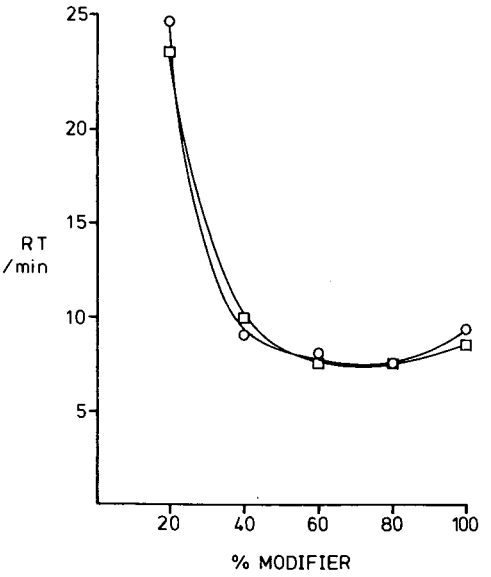

Fig. 6. Retention time (RT) of benzo[*a*]pyrene on the β-cyclodextrin (acetylated) column at 20°C with propan-1-ol (□) and propan-2-ol (○) as the organic modifiers; flow-rate: 0.5 ml min^{-1}.

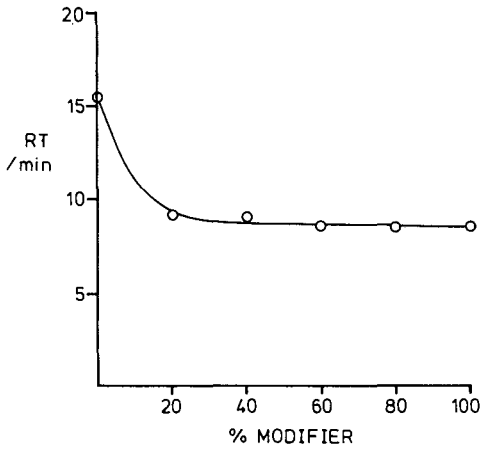

Fig. 7. Retention time (RT) of benzo[*a*]pyrene on the β-cyclodextrin (acetylated) column in the normal phase. From 100% hexane to 100% propan-2-ol (modifier); flow-rate: 0.5 ml min^{-1}.

propan-1-ol or propan-2-ol is used as the organic phase modifier. The effect obtained is more similar to acetonitrile than to methanol. In the final figure (Fig. 7) the retention of benzo[*a*]pyrene in the normal-phase mode is shown. In the normal-phase hexane was used as the bulk solvent with propan-2-ol as the modifier. The flow-rate used to obtain the data reported in Figs. 6 and 7 was 0.5 ml min^{-1} due to pressure limitations caused by the high viscosity of propan-1-ol and propan-2-ol. It is clear from these figures that retention can occur in both the normal and reversed phases, highlighting the complex retention mechanism of the bonded phases.

The results have clearly outlined the dual retention mechanism of the β-, β-(acetylated) and γ-cyclodextrin bonded phases. In the reversed phase mode the retention is achieved by two separate mechanisms that can be classified as temperature dependent and temperature independent. The temperature dependent retention occurs due to the formation of an inclusion complex between the cyclodextrin torus and the analyte. This is the normal retention mode for this type of bonded phase, and is affected by temperature. At higher temperatures due to increased molecular vibration the formation of the complex is suppressed, complete dissociation occurs at between 60 and 70°C. This mechanism is responsible for the stereo selectivity of the bonded phase. At low polarities the mobile phase organic modifier forms a more stable complex in the cavity than can be formed by the analyte and so little retention, by this mechanism, occurs.

The temperature independent mechanism is more complex. The following explanation, based on our data has been proposed. In polar organic phases (*i.e.* up to 60% acetonitrile) the cyclodextrin cavity is open and analyte inclusion, and so retention, can occur if the shape and charge requirements are met. In addition, the tori form a tight coat over the silica base as the hydrocarbon linkage between the torus and the silica particle will be constricted due to the high polarity. A similar effect occurs in bonded reversed phases such as octadecyl silanol and octa silanol and is responsible for the alteration in retention with mobile phase polarity. At higher organic modifier percentages (between 60 and 80% acetonitrile) the formation of the inclusion complex

is almost totally suppressed. The tori coat, although slightly relaxed does not significantly alter the retention. This is reflected in the plateau in retention seen between these percentages; over this range the retention time is not affected by the mobile phase polarity. At lower polarities, (*i.e.* above 80% acetonitrile) the formation of the inclusion complex is fully suppressed as the cyclodextrin cavity is completely occupied by the mobile phase. Therefore the inclusion complex formation cannot lead to the increased retention at these polarities. This is confirmed as the effect is temperature independent. It is proposed that further relaxation of the silica support–cyclodextrin linkage leads to a reduction in the coat density so allowing the analyte to pass around and behind the torus and so be retained by a reversed phase, or ionic interaction type of mechanism. Ionic interactions with the cyclodextrin, leading to increased retention have been ruled out as the β-cyclodextrin (acetylated) column gives an almost identical surface plot to that of the β-cyclodextrin column. The phenomenon is seen most clearly with acetonitrile, and to a lesser extent with tetrahydrofuran, propan-1-ol and propan-2-ol. The temperature independent retention increase is not present when methanol is used as the organic modifier. This can be explained when the relative polarities of the solvents are taken into account. Methanol has a greater polarity than either acetonitrile or tetrahydrofuran and so at even 100% methanol the polarity has not fallen to a value capable of promoting linkage relaxation. Tetrahydrofuran, although capable of forming solutions with a similar polarity to 100% acetonitrile, does not produce the effect to a similar degree. This is probably due to the higher dipole moment of acetonitrile producing a more profound relaxation induced retention. Propan-1-ol and propan-2-ol, although in the same solvent group as methanol have significantly lower polarities, closer to acetonitrile than to methanol, and so are likely to cause the relaxation induced retention in high concentration organic mobile phases.

In this study only benzo[*a*]pyrene has been closely studied although similar results have been noted with pyrene and benzo[*a*]anthracene suggesting that this phenomenon may been seen with a wide range of compounds. benzo[*a*]pyrene and other polynuclear aromatic hydrocarbons have been shown to form stable inclusion complexes with both the β- and γ-cyclodextrin-bonded phases[4].

While the increase in retention by the temperature independent process reported here is small, when compared to that achieved by complexation, it is believed that this phenomenon should be closely studied. The production of packing materials, processing "reversed-phase like" retention mechanisms in organic mobile phases could be coupled, without difficulty, to normal and size-exclusion columns without any solvent incompatibility problems. Such a ability would signicantly aid the analyst attempting the separation of complex matrices within a multicolumn separation scheme. Further studies are to be undertaken to probe more closely the nature of this novel and useful bonded phase. It is planned to study the relaxation induced effect more closely, this will include the synthesis of bonded phases with structural characteristics similar to those of the cyclodextrin molecule but without the ability to form the inclusion complexes. Other compound groups are also to be studied to determine how widespread this effect is.

CONCLUSIONS

The retention mechanism of benzo[*a*]pyrene on β-cyclodextrin-, β-cyclodextrin-(acetylated) and γ-cyclodextrin-bonded-phase columns is complex consisting of at least three distinct retention mechanisms. Certain solvents such as acetonitrile may cause some relaxation in the link binding the cyclodextrin to the silica support. This effect results in a broad minimum retention time at acetonitrile concentrations between 60 and 80%. At lower concentrations retention due to inclusion occurs, while at higher concentrations, and thus lower polarities, retention, possibly due to tori coat relaxation occurs. Although the degree of relaxation induced retention is small when compared to inclusion related retention, it is still significant and may possibly be used to finely adjust the retention of a specific analyte with respect to interferences; thus allowing the specific analysis of an analyte in a complex mixture. Because of the problems associated with the estimation of the t_0 the k' values should be treated with caution when referring to cyclodextrin stationary phases and the conditions under which they were obtained must be explicitly reported.

ACKNOWLEDGEMENTS

The authors gratefully acknowledge the support of A. J. Packham who is in receipt of a Science and Engineering Research Council CASE award, co-sponsored by ESSO Petroleum Company (ESSO Research Centre, Abingdon, U.K.). We are also indebted to Technicol (Stockport, U.K.) for the supply of columns used in this study and to Comus Instruments (Hull, U.K.) for the Midas Chromatographic Data Station.

REFERENCES

1 D. W. Armstrong and W. DeMond, *J. Chromatogr. Sci.*, 22 (1984) 411.
2 R. Woodberry, S. Ransom and C. Fu-Ming, *Anal. Chem.*, 60 (1988) 2621.
3 D. W. Armstrong, D. Wade, A. Alak, W. L. Hinze, T. E. Riehl and K. H. Bui, *Anal. Chem.*, 57 (1985) 234.
4 D. W. Armstrong, A. Alak, D. Wade, W. L. Hinze and T. E. Riehl, *J. Liquid Chromatogr.*, 8 (1985) 261.
5 M. Olsson, L. C. Sander and S. A. Wise, *J. Chromatogr.*, 477 (1989) 277.
6 P. R. Fielden and A. J. Packham, *J. Chromatogr.*, 497 (1989) 222.
7 W. L. Hinze, T. E. Riehl, D. W. Armstrong, W. DeMond, A. Alak and T. Ward, *Anal. Chem.*, 57 (1985) 237.
8 S. M. Han and D. W. Armstrong, *J. Chromatogr.*, 389 (1987) 256.

Journal of Chromatography, 516 (1990) 365–373
Elsevier Science Publishers B.V., Amsterdam

CHROM. 22 583

Direct stereochemical resolution of aspartame stereoisomers and their degradation products by high-performance liquid chromatography on a chiral crown ether based stationary phase

SYLVIE MOTELLIER and IRVING W. WAINER*
Pharmaceutical Division, St. Jude Children's Research Hospital, Memphis, TN 38105 (U.S.A.)
(First received March 27th, 1990; revised manuscript received May 22nd, 1990)

ABSTRACT

The direct stereochemical resolution of the four stereoisomers of aspartame (N-DL-α-aspartyl-DL-phenylalanine methyl ester) and their degradation products was achieved on a high-performance liquid chromatography chiral stationary phase based upon a chiral crown ether. The chromatographic conditions included a mobile phase composed of aqueous perchloric acid adjusted to a pH of 2.8 and modified with 1.5% of 2-propanol and a temperature gradient. The active L,L-isomer (sold under the brand name NutraSweet) was measured in a diet cola and coffee sweetened with NutraSweet. Degradation products of NutraSweet were also detected but no racemization of stereochemical contamination was observed.

INTRODUCTION

Aspartame (N-DL-α-aspartyl-DL-phenylalanine methyl ester, or APM, Fig. 1) is a dipeptide derivative which can exist in four possible stereoisomeric forms: L,L-APM, D,D-APM, D,L-APM and L,D-APM. The L,L-isomer (NutraSweet) is a low-calorie sweetener widely used as a sugar substitute in diet soft drinks and other food products.

Various high-performance liquid chromatographic (HPLC) methods have been developed for the analysis of L,L-APM in food products including isocratic[1–3] and gradient[4] approaches. These assays were able to separate L,L-APM from other ingredients such as caffeine, benzoic acid, colorants and flavors. However, these methods did not measure L,L-APM degradation products which may also be present.

L,L-APM is unstable over time and the degradation of the compound is accelerated by elevated temperature and pH[5–9]. For example, in diet soft drinks, only 30 to 40% of the sweetener remained after 6 months of storage at ambient temperature[6]. The major degradation pathway in acidic media involves initial cyclization to a diketopiperazine (DKP) followed by hydrolysis which yields the

0021-9673/90/$03.50

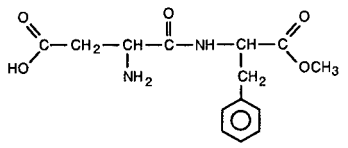

Aspartame (APM)

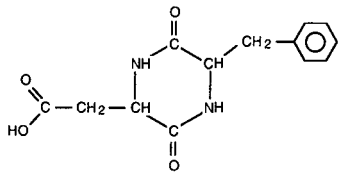

Diketopiperazine (DKP)

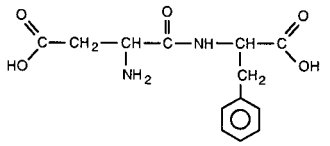

Aspartyl-phenylalanine (Asp-Phe)

Fig. 1. APM and its breakdown products.

aspartyl-phenylalanine dipeptide, Asp-Phe, which is eventually cleaved to the free amino acids, aspartic acid (Asp) and phenylalanine (Phe)[9]. A second pathway in basic media involves the production of the Asp-Phe through direct hydrolysis of the APM[9]. The structures of the DKP and dipeptide are presented in Fig. 1. The breakdown of APM also results in the release of methanol.

While a number of methods have been developed to measure the decomposition products of L,L-APM[5–7], they do not take into account any possible racemization during the synthesis or degradation processes of L,L-APM which could generate one or more of the three other stereoisomers. To our knowledge, only three articles deal with this problem[8–10].

Gaines and Bada[9] observed racemization at high temperature of L,L-APM degradation products, specifically L,L-DKP. However, the analytical method utilized an achiral reversed-phase HPLC system and only diastereomeric pairs could be separated; an accurate measurement of each stereoisomer could not be obtained[8].

Jadaud and Wainer[10] were able to resolve the enantiomeric pairs L,L-/D,D-APM and L,D-/D,L-APM using a column based upon α-chymotrypsin. However, the resolutions of the diastereomeric pairs L,D-/D,D-APM and D,L-/L,L-APM were poor, which led to overlapping when the four stereoisomers were chromatographed together.

In this paper, we report the chromatographic resolution of the four stereoisomers of APM on an HPLC chiral stationary phase based upon a chiral crown ether (CR-CSP). The system was also able to resolve the diastereomeric pairs of DKP and the four corresponding dipeptides. The method was used to analyze the composition of a diet cola and coffee sweetened with NutraSweet. Degradation products of

NutraSweet were detected but no racemization or stereochemical contamination was observed.

EXPERIMENTAL

Chemical

The four stereoisomers of APM were kindly provided by NutraSweet (Mt. Prospect, IL, U.S.A.). L-Asp-L-Phe, β-L,L-APM, DL-Asp and DL-Phe were purchased from Sigma (St. Louis, MO, U.S.A.). The perchloric acid was from Aldrich (Milwaukee, WI, U.S.A.) and the 2-propanol was from Burdick & Jackson (Muskegon, MI, U.S.A.). The diet cola and Equal (the commercially available packet form of NutraSweet) were purchased at the local market.

Apparatus

The chromatographic system consisted of a Beckman 110B solvent delivery module (Beckman, Houston, TX, U.S.A.), a Rheodyne 7125 injector equipped with a 20-μl loop (Alltech Assoc., Deerfield, IL, U.S.A.), a Spectra-Physics SP8773XR UV detector set at 210 nm (Spectra-Physics, San Jose, CA, U.S.A.) and a Shimadzu C-R6A integrator (Shimadzu, Columbia, MD, U.S.A.). The column temperature was controlled by a Forma Scientific module 2006 circulating water bath (Forma Scientific, Marietta, OH, U.S.A.) equipped with an Alltech HPLC column jacket. The column used for this study consisted of a 150 × 4 mm I.D. stainless-steel column packed with a chiral stationary phase composed of a chiral crown ether coated on a polymeric support (Crownpack CR(+), Daicel, Los Angeles, CA, U.S.A.).

Chromatographic conditions

The mobile phase was prepared by addition of perchloric acid to HPLC grade water until a pH of 2.8 was obtained. The aqueous perchloric acid was modified with 1.5% of 2-propanol. The flow-rate was 0.6 ml/min. To prevent corrosion and decomposition of the stationary phase, the column was washed every night with HPLC grade water.

Temperature gradient

The chromatography was carried out using the following temperature gradient: 0–26 min, T = 10°C; 26–70 min, T = 10–40°C (linear gradient); 70–80 min, T = 40°C.

Samples

The chromatographic standards were prepared in distilled water (100 μM) and directly injected onto the column. The diet cola was degassed in an ultrasonic bath, diluted to 1/5 with distilled water and filtered through a 0.45-μm Millipore filter (Millipore, Bedford, MA, U.S.A.) before injection. One packet of Equal (1 g NutraSweet) was added to 150 ml of warm coffee. The solution was heated to a temperature of 70°C on a hotplate and held at that temperature for 10 min, diluted while hot to 1/40 with distilled water, filtered through a 0.45-μm Millipore filter and immediately injected onto the column.

RESULTS AND DISCUSSION

The results from the chromatography of the stereoisomers of APM and the major degradation products are presented in Table I and Fig. 2. For APM, the D,L- and D,D-isomers eluted first with capacity factors of 9.94 and 11.03, respectively, and were separated from each other with a resolution factor (R_s) of 1.20. The two other isomers (L,D-APM and L,L-APM) were only slowly eluted from the column under the isocratic and isothermal conditions used for the separation of D,L-APM and D,D-APM, *i.e.*, at a constant temperature of 10°C.

TABLE I

RESULTS FROM THE CHROMATOGRAPHY OF THE STEREOISOMERS OF APM AND THEIR MAJOR DEGRADATION PRODUCTS ON A CR-CSP

See Fig. 2 for experimental conditions.

Peak	*Compound*	*k'*	α^a	R_s^b
1	L,L-APM	33.52		
2	L,D-APM	23.62	1.42	7.32
3	D,D-APM	11.03	2.14	11.08
4	D,L-APM	9.94	1.11	1.20
5	L-Asp-D-Phe	8.92		
6	D,D + L,L-DKP	7.24		
7	D,L + L,D-DKP	5.12		
8	D-Asp-D-Phe	4.74		
9	D-Asp-L-Phe	3.67		
10	L-Asp-L-Phe	24.34		

[a] Selectivity between two adjacent peaks.
[b] Resolution between two adjacent peaks.

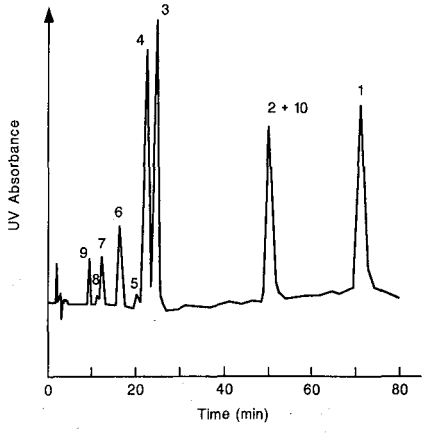

Fig. 2. Chromatogram of a 1-day-old synthetic mixture of the four stereoisomers of APM (0.1 m*M* of each isomer). Peaks: **1** = L,L-APM; **2** = L,D-APM; **3** = D,D-APM; **4** = D,L-APM; **5** = L-Asp-D-Phe; **6** = D,D-DKP + L,L-DKP; **7** = D,L-DKP + L,D-DKP; **8** = D-Asp-D-Phe; **9** = D-Asp-L-Phe; **10** = L-Asp-L-Phe. Chromatographic conditions: column: Crownpack CR(+), Daicel, 150 × 4 mm I.D. Injection loop: 20 µl. Mobile phase: aqueous $HClO_4$ (pH = 2.8)–2-PrOH (98.5:1.5, v/v). Flow-rate: 0.6 ml/min. Temperature gradient: 0–26 min: T = 10°C; 26–70 min: linear gradient from T = 10–40°C. Detector: 210 nm, sensitivity = 0.02 a.u.f.s., attenuation = 2^5.

The use of larger concentrations of organic modifiers to improve the chromatography of the late eluting peaks was not attempted due to the characteristics of the stationary phase and the recommendations of the manufacturer. Therefore, standard solvent gradient techniques were not explored and, instead, a temperature gradient was used. In this approach, the temperature was raised from 10–40°C, starting after the elution of the first two isomers. Under these conditions, both L,D- and L,L-APM were eluted within 80 min, $k' = 23.62$ and 33.52, respectively, with significant peak compression. The L,D- and L,L-isomers were separated from each other with a resolution factor (R_s) of 7.32. The enantiomeric pairs were resolved with stereoselectivities (α) of 2.38 (D,L/L,D) and 3.04 (D,D/L,L).

These data indicate that the elution order of the APM isomers was determined by the configuration of the aspartyl moiety. The results are consistent with the proposed chiral recognition mechanism in which inclusion complexes are formed between a protonated primary amino group in the vicinity of the chiral center of the solute and the polyether rings of the chiral stationary phase (CSP). The difference in the stabilities of the diastereomeric solute–CSP complexes is due to additional π–π and steric interactions[11,12]. The APM and dipeptide solutes chromatographed in this study contain a primary amino function in the aspartyl moiety of the molecule and it is the configuration of this moiety which should, and in fact does, control the enantiomeric elution order, *i.e.*, the compounds which contain D-Asp, D,L- and D,D-APM, elute before those which contain L-Asp, L,D- and L,L-APM. It is of interest to note that the diastereomeric elution order is also affected by the configuration of the Asp moiety. When Asp is in the D-configuration, the APM containing L-Phe elutes before the one containing D-Phe. On the contrary, when Asp is in the L-configuration, the APM containing D-Phe elutes before the one containing L-Phe.

According to the scheme proposed by Gaines and Bada[9], under slightly acidic conditions, *e.g.*, distilled water, the primary amino group of APM rapidly reacts with the methylester moiety to give a cyclised compound, the 5-benzyl-3,6-dioxo-2-piperazine acetic acid (DKP, Fig. 1). The ring reopens to give the corresponding dipeptide, aspartyl-phenylalanine (Asp-Phe), which can thereafter by hydrolysed to the free amino acids, Asp and Phe. At acidic pH values, DKP is the major decomposition product.

Although authentic samples of the four possible DKPs were not available, they were synthesized following the procedure described by Gaines and Bada[8,9]. Each isomer of APM was dissolved in distilled water and stored at ambient temperature. The composition of the solution was followed during a 14-day period. The results of this study are illustrated by the experiment involving L,L-APM which is presented in Fig. 3. The predominant component of the fresh solution was L,L-APM; a second minor peak, **6**, was also present, Fig. 3a. After 2 days, **6** had significantly increased, and a third peak, **10**, had appeared, Fig. 3b. By day 14, both L,L-APM and **10** had disappeared from the chromatogram leaving only **6**, Fig. 3c. Peak **10** was identified as L-Asp-L-Phe by injection of a standard solution of the dipeptide. Under the chromatographic conditions used in this study, the free amino acids DL-Asp and DL-Phe were eluted at the solvent front and could not be detected. It is assumed that the disappearance of **10** was due to hydrolytic cleavage of the dipeptide[9].

Similar results were obtained with D,D-APM. After 14 days, peak **6** was also the predominant peak in the chromatogram of the D,D-APM solution. These results

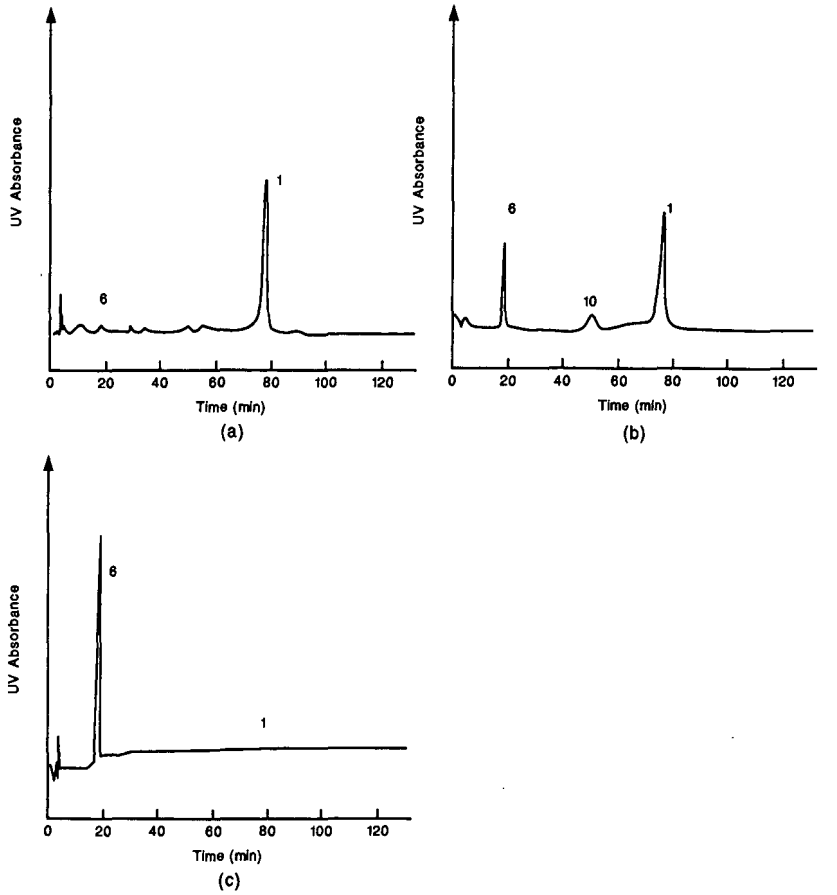

Fig. 3. Degradation of L,L-APM in distilled water as a function of time, where (a) fresh solution; (b) 2-day-old solution; (c) 14-day-old solution and **1** = L,L-APM; **6** = L,L-DKP; **10** = L-Asp-L-Phe. Chromatographic conditions: see Fig. 2.

support the identification of **6** as the DKP arising from D,D- and L,L-APM. Since DKP does not contain a primary amino group, it is unable to form an inclusion complex with the chiral stationary phase and enantioselective separations cannot occur. Thus, the pair of enantiomers, D,D- and L,L-DKP, gives rise to only one peak.

When D,L- and L,D-APM were studied, a common predominant peak, **7**, was found in the chromatograms of the two solutions at day 14. Using the same approach employed for the identification of peak **6**, these results allowed us to identify **7** as the enantiomeric D,L-/L,D-DKP. In addition, since **7** was not detected in any of the chromatograms run during the degradation studies of L,L- and D,D-APM and since **6** was not found in similar studies carried out with L,D- and D,L-APM, it appears that racemization did not occur. It is of interest to note that although the CR-CSP was unable to resolve the enantiomeric DKPs, the separation of the diastereomeric D,D-/L,L-DKP and L,D-/D,L-DKP was achieved under these conditions.

A third peak was also detected in each of the chromatograms from the aqueous

solutions of D,L-, D,D- and L,D-APM with capacity factors of $k' = 3.67$ (**9**), 4.74 (**8**) and 8.92 (**5**), respectively. The magnitudes of the peaks and the time courses of their appearances were similar to the appearance of L-Asp-L-Phe in the aqueous solution of L,L-APM (Fig. 3). The three peaks were, accordingly, assumed to be D-Asp-L-Phe (**9**), D-Asp-D-Phe (**8**) and L-Asp-D-Phe (**5**). The chromatograms of the aqueous solutions of each of the four APM stereoisomers contained only a single peak which could be assumed to be Asp-Phe. This is further evidence that racemization did not occur under the experimental conditions used in this study.

This method was applied to the analysis of L,L-APM in a diet cola and in coffee sweetened with the commercially available packet form of L,L-APM (Equal). The results of the assay of the diet cola are presented in Fig. 4. The chromatogram demonstrates that L,L-APM (**1**) is the predominant form of the sweetener and that L,L-DKP (**6**) is only a minor contamination.

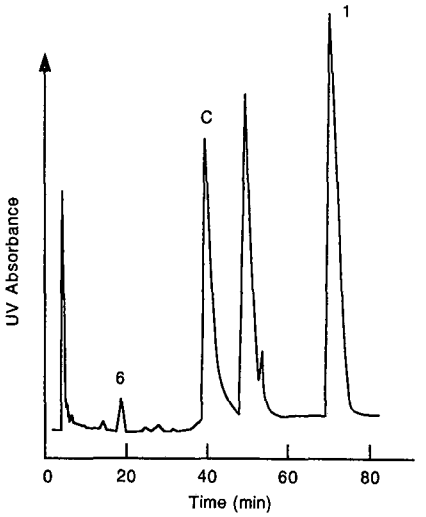

Fig. 4. Determination of L,L-APM and its decomposition products in a diet cola, where **1** = L,L-APM; **6** = L,L-DKP; C = caffeine. Chromatographic conditions: see Fig. 2.

Peak C was identified as caffeine by injection of a standard solution of this compound. Peak C was absent from a caffeine-free form of the diet cola. The peak next to peak C in the chromatogram was not present in a sugar-sweetened form of the cola and was present in both the caffeinated and decaffeinated diet colas. The peak does not co-elute with L-Asp-L-Phe, which was added to the analytical samples, and therefore does not represent this dipeptide. The compound was not identified. The small peak at 26 min is eluted at the retention time of the β form of L,L-APM and could, therefore, indicate that this compound is a minor contaminant. Trace amounts of β-L,L-APM have been found previously in a diet cola by Lawrence and Iyengar[13]. In this study, further identification of this component was also not pursued.

If we consider L,L-DKP as the only degradation compound, the degree of degradation can be estimated using the ratio between the areas of the L,L-DKP and

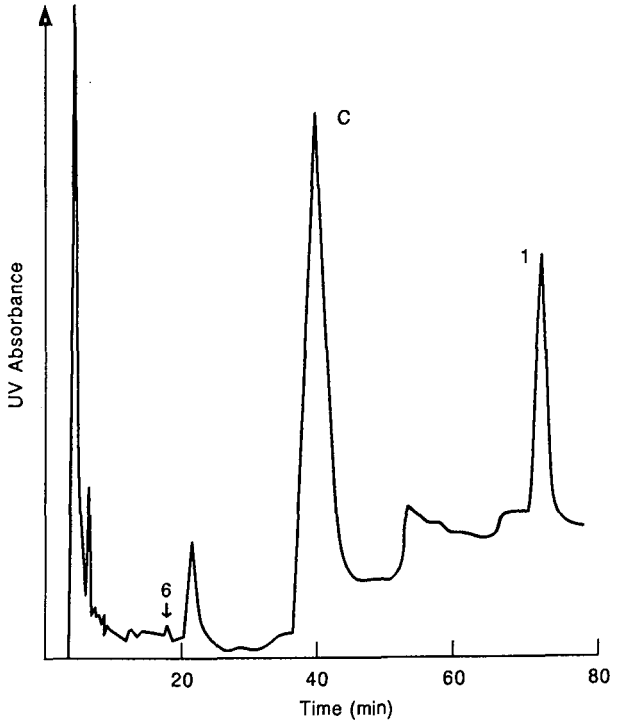

Fig. 5. Determination of L,L-APM and its decomposition products in coffee sweetened with Equal, where **1** = L,L-APM; **6** = L,L-DKP; C = caffeine. Chromatographic conditions: see Fig. 2.

L,L-APM peaks. For this sample of diet cola, the calculated degree of degradation of L,L-APM was 1.3%.

The results of the experiment involving the addition of Equal to hot coffee followed by heating at 70°C for 10 min are presented in Fig. 5. Peaks corresponding to L,L-APM (**1**), L,L-DKP (**6**) and caffeine (C) were identified. The other peaks in the chromatogram and caffeine were present in a sample of unsweetened coffee. In this experiment, the degradation of L,L-APM to L,L-DKP was less than 1%. The same experiment, carried out with a heating time of 20 min instead of 10 min, gave similar results. In contrast, when water is used instead of coffee, after 10 min of heating at 70°C, 21% of the L,L-APM was degraded to L,L-DKP. These observations indicate that L,L-APM is more thermally stable in coffee than in water.

Racemization of the L,L-APM was not observed in either the diet cola or the sweetened coffee.

CONCLUSION

The results of this study indicate that the isomers of aspartame and their degradation products can be chromatographically separated on the CR-CSP. The analytical method can be used to rapidly determine the isomeric composition of

aspartame and the degree of its degradation in food products. The CR-CSP appears to be quite stable under the conditions used in this study. The column has been in constant use for over two months without significant deterioration in its chromatographic performance.

REFERENCES

1 C. J. Argoudelis, *J. Chromatogr.*, 303 (1984) 256.
2 N. G. Webb and D. D. Beckman, *J. Assoc. Off. Anal. Chem.*, 67 (1984) 510.
3 H. J. Issaq, D. Weiss, C. Ridlon, S. D. Fox and G. M. Muschik, *J. Liq. Chromatogr.*, 9 (1986) 1791.
4 J. T. Hann and I. S. Gilkison, *J. Chromatogr.*, 395 (1987) 317.
5 R. Cross and B. Cunico, *LC, Mag. Liq. Chromatogr. HPLC*, 2 (1984) 678.
6 W. S. Tsang, M. A. Clarke and F. W. Parrish, *J. Agric. Food Chem.*, 33 (1985) 734.
7 W. Neirynck and L. Nollet, *Belg. J. Food Chem. Biotechnol.*, 43 (1988) 83.
8 S. M. Gaines and J. L. Bada, *J. Chromatogr.*, 389 (1987) 219.
9 S. M. Gaines and J. L. Bada, *J. Org. Chem.*, 53 (1988) 2757.
10 P. Jadaud and I. W. Wainer, *Chirality*, (1990), in press.
11 L. R. Souse, G. D. Y. Sogah, D. H. Hoffman and D. J. Cram, *J. Am. Chem. Soc.*, 100 (1978) 4569.
12 T. Shinbo, T. Yamaguchi, K. Nishimura and M. Sugiura, *J. Chromatogr.*, 405 (1987) 145.
13 J. F. Lawrence and J. R. Iyengar, *J. Chromatogr.*, 404 (1987) 261.

Journal of Chromatography, 516 (1990) 375–382
Elsevier Science Publishers B.V., Amsterdam

CHROM. 22 550

Simultaneous liquid chromatographic determination of methionine hydroxy analogue and DL-methionine in feed formulations

D. WAUTERS, J. DE MOL and L. DE TEMMERMAN*
Monsanto Technical Centre Europe, Science and Technology Development, Rue Laid Burniat, B-1348 Louvain-La-Neuve (Belgium)
(First received December 27th, 1989; revised manuscript received May 9th, 1990)

ABSTRACT

A liquid chromatographic method for the simultaneous determination of methionine hydroxy analogue and DL-methionine in compounded feed samples is described. Samples are subjected to a simple extraction procedure followed by quantification on a LiChrospher reversed-phase column with ultraviolet detection at 214 nm. The reproducibility and recovery were determined for a range of typical European feed formulations. An excellent correlation was found between the data obtained by this method and by conventional methods.

INTRODUCTION

The use of synthetic amino acids as supplements in compounded feeds is essential in today's feed industry and intensive animal husbandry to formulate diets which meet the animal's nutrient requirements at the minimum cost. These additives allow the biological value of the proteins fed to be improved and the level of proteins in the feed to be reduced.

Considering the economic importance of the essential amino acid levels of feed formulations on animal performance, an accurate method for the determination of synthetic methionine, lysine and threonine sources is a key factor in feed quality control.

Synthetic methionine is added either as DL-methionine or its methionine hydroxy analogue (Alimet[a], MHA[a]). The presence of these feed additives can be determined by several methods. Methods for determining DL-methionine include high-performance ion-exchange chromatography in combination with pre- or postcolumn derivatization or an amino acid analyser[1–5]. These methods are not applicable to the

[a] Alimet and MHA are registered trade marks of Monsanto Co., St. Louis, MO, U.S.A.

0021-9673/90/$03.50

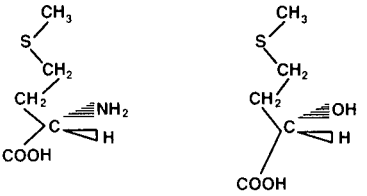

Fig. 1. Structures of DL-methionine and methionine hydroxy analogue (Alimet).

analysis of methionine hydroxy analogue because it contains an α-hydroxy instead of an α-amino group, as shown in Fig. 1.

A gas chromatographic method for the determination of the methionine hydroxy analogue was reported by Day *et al.*[6] and modified by Feit *et al.*[7]. A capillary isotachophoresis technique was utilized by Vinjamoori and Schisla[8]. The development of high-performance liquid chromatographic (HPLC) methods, allowing substantial simplification of the preparative steps, was reported by Baudichau *et al.*[a], Balschukat *et al.*[10] and Gerstl and Ranfft[11].

Because the above-mentioned feed supplements are both used to correct methionine deficiencies in animal feeds, a technique allowing for both compounds to be determined in a single analysis is much needed. The existing methods for the determination of methionine on one hand and methionine hydroxy analogue on the other are different in terms of both sample preparation and the actual determination itself. Consequently, none of them allows an accurate simultaneous determination of both compounds.

An HPLC technique has been developed for the simultaneous determination of both synthetic methionine sources. The method has been tested for its recovery and accuracy on a range of typical European feed formulation samples. The results obtained have been compared with those obtained by conventional methods.

EXPERIMENTAL

Apparatus and reagents

A Waters Assoc. HPLC system was used, consisting of two Model 510 pumps, a Model 712 WISP automatic sample injector, a Model 481 LC spectrophotometer and a workstation running Baseline 810 software. The column was a 250 × 4 mm I.D. Merck LiChrospher 100 RP-18 (5 μm) reversed-phase column.

For eluent preparation, water and methanol of HPLC grade (Baker, Deventer, The Netherlands), 85% orthophosphoric acid (analytical-reagent grade) (Merck, Darmstadt, F.R.G.) and sodium hydroxide pellets (analytical-reagent grade) (Baker) were used.

The apparatus included a centrifuge, an automatic shaker and a feed grinder to facilitate sample preparation.

Sample preparation

A sample of feed is ground to a mean particle size of 600 μm and 6.0 ± 0.1 g are accurately weighed into a vial. To this are added 30 ml of distilled water at *ca.* 90°C.

The sample is then shaken on an automatic shaking machine (Z 620 Vortex Station; Zymark, Hopkinton, MA, U.S.A.) for 10 min in order to extract both sources of methionine. After the sample has been shaken as prescribed, a minimum of 30 min are allowed for settling. The sample is then centrifuged for ca. 10 min at 2000 g (Heraeus Christ Labofuge 6L; Heraeus, Osterode, F.R.G.) to clear the solution. A portion of the supernatant is placed in an HPLC sample vial and 15 μl are injected onto the HPLC column.

Chromatographic conditions

The separation is carried out using a linear gradient programme with the following eluents: solvent A, 0.03 *M* H_3PO_4, adjusted to pH 3 with 0.1 *M* NaOH; solvent B, 0.03 *M* H_3PO_4–methanol (9:1), adjusted to pH 3 with 0.1 *M* NaOH. The programme is as follows: 0–8 min, 100% A; 8–9 min, linear change to 100% B; 9–44 min, 100% B; 44–45 min, linear change to 100% A; 45–60 min, 100% A.

The flow-rate used is 0.6 ml/min, detection wavelength 214 nm and detector attenuation 0.2 a.u.f.s.

Calibration and calculation

Standard solutions containing both methionine sources are prepared by weighing *ca.* 20.0, 40.0 and 60.0 mg of DL-methionine and Alimet (accurate to 0.1 mg) into a 100-ml volumetric flask, diluting with distilled water to the mark and agitating. The shelf-life of the standards is 1 month.

A 15-μl volume of each standard solution is injected onto the HPLC column and peak heights and areas are calculated. Two calibration graphs can be generated by plotting either peak-area counts or peak height against the amount of DL-methionine or the amount of Alimet injected. The standards need to be injected just before each series of feed samples to be analysed. At the end of a series of analysis the standards are reinjected and if the results obtained differ more than 5% from the initial values the whole analysis is rejected.

Good linear relationships exist for peak-area counts *versus* the amount of DL-methionine at levels of 0.01–0.40% (w/w) (r = 0.9967) and for Alimet at levels of 0.05–0.40% (w/w) (r = 0.99952). These ranges cover the normal ranges of concentrations applied in supplemented feeds.

RESULTS AND DISCUSSION

The modification of the preparative steps and the actual HPLC analysis in comparison with conventional methods is obvious.

The conventional extraction procedure shows marked differences for both sources: Alimet undergoes an aqueous extraction, and the extraction of DL-methionine from feeds is done with hydrochloric acid. Experiments have shown the latter reagent to be unsuitable for Alimet extraction.

Kabwe wa Mupenda[12] demonstrated that DL-methionine extraction recoveries obtained with hydrochloric acid and with distilled water at ambient temperature are not statistically different. Further, the solubility of DL-methionine in aqueous solutions increases 5-fold (176.0 *vs.* 33.8 g/l) when the water temperature is increased from 25 to 100°C[13,14]. For these reasons the extraction of both sources was conducted with distilled water at *ca.* 90°C.

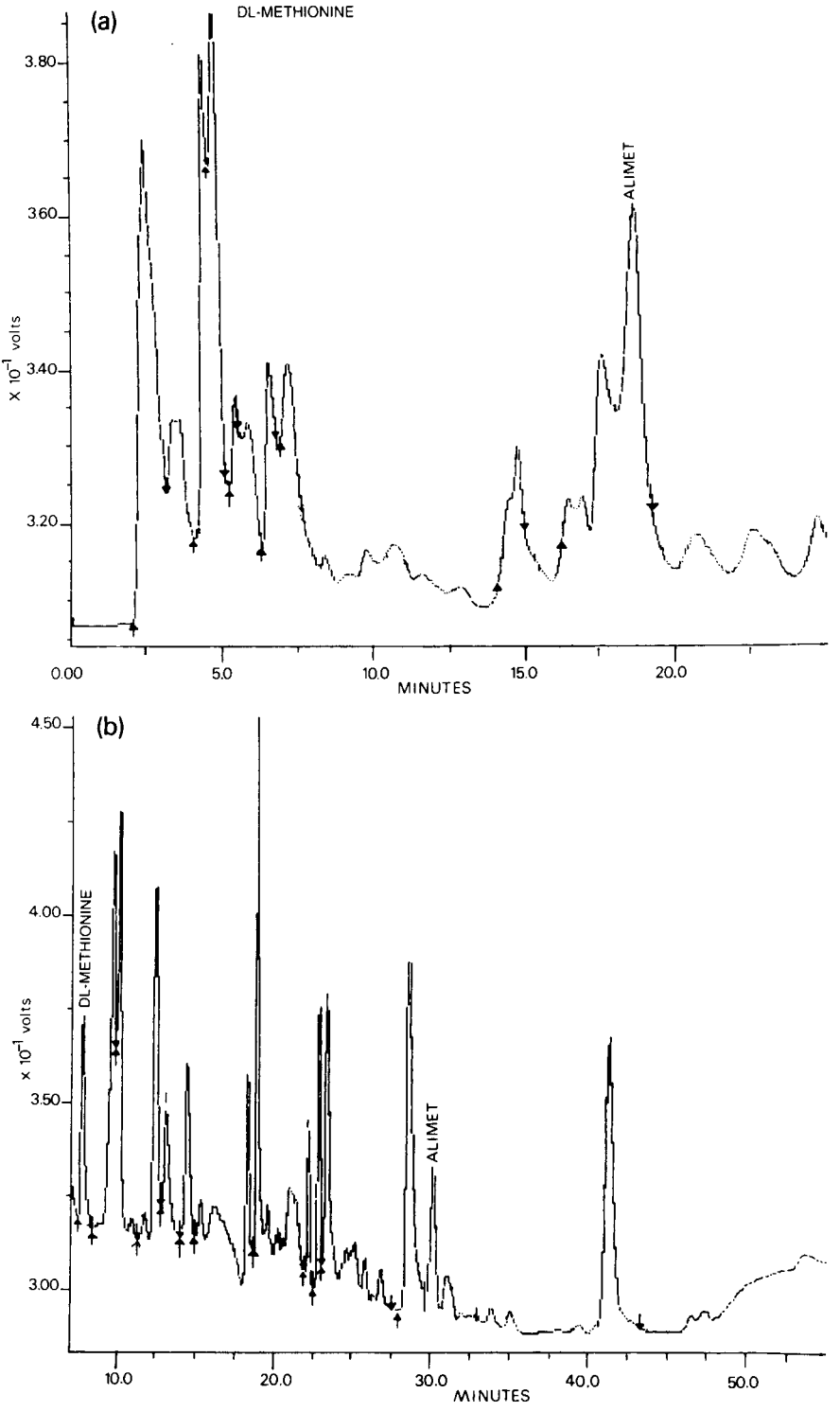

Fig. 2. Comparison of HPLC separation with different reversed-phase columns: (a) LiChrosorb; (b) LiChrospher. Both chromatograms were recorded on the same feed sample extract at 0.068% Alimet and 0.060% DL-methionine supplementation levels.

Ultraviolet scans of both compounds showed high UV absorbance at wavelengths between 200 and 220 nm. The detection wavelength was chosen as 214 nm, which yields good sensitivity and interference-free Alimet and DL-methionine detection.

The HPLC separation was carried out on a LiChrospher reversed-phase column. This type of column was selected because of its large number of theoretical plates and its specific characteristics towards polar compounds, *i.e.*, more retentive than other reversed-phase columns and avoiding poor peak shapes of these compounds[15,16]. Fig. 2 clearly demonstrates the improvement obtained by using a LiChrospher *versus* a LiChrosorb reversed-phase column.

For the eluents it must be stressed that careful control of the pH is required to ensure a good separation of the different compounds showing UV absorbance at 214 nm. Fig. 3 shows some typical chromatograms of standard solutions and feed samples separated on the LiChrospher reversed-phase column. DL-Methionine and Alimet are clearly separated, allowing their detection and determination in compounded feeds in the presence of other constituents.

Method validation

The percentage recovery and reproducibility of the method were determined by analysing spiked feeds at several supplementation levels. In addition, a wide variety of compounded feed samples representing formules commonly used in European mar-

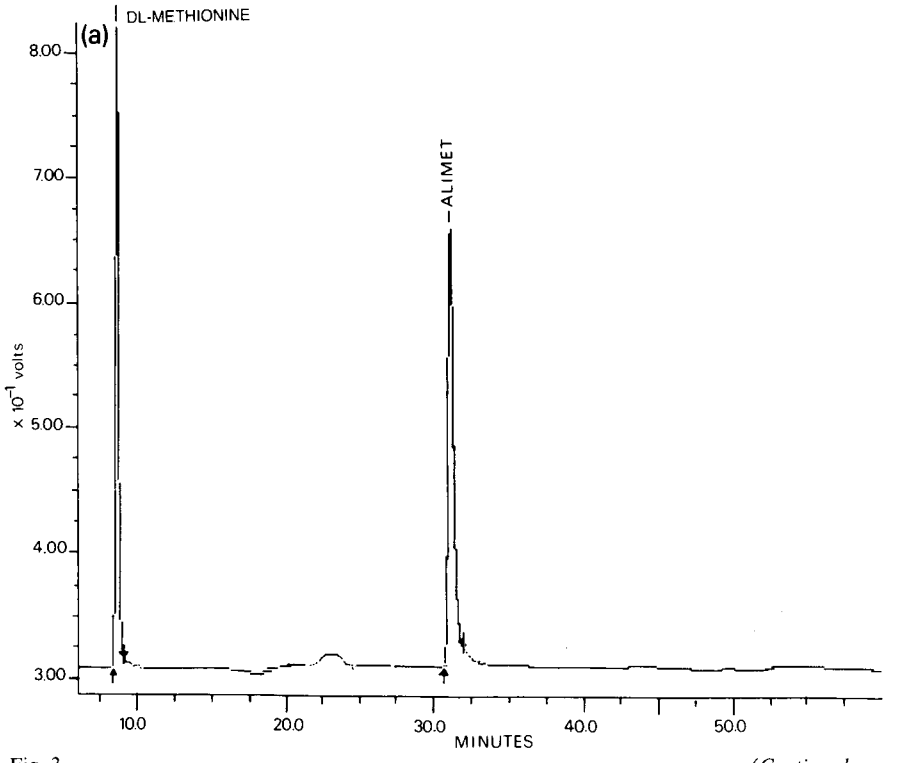

Fig. 3.

(Continued on p. 380)

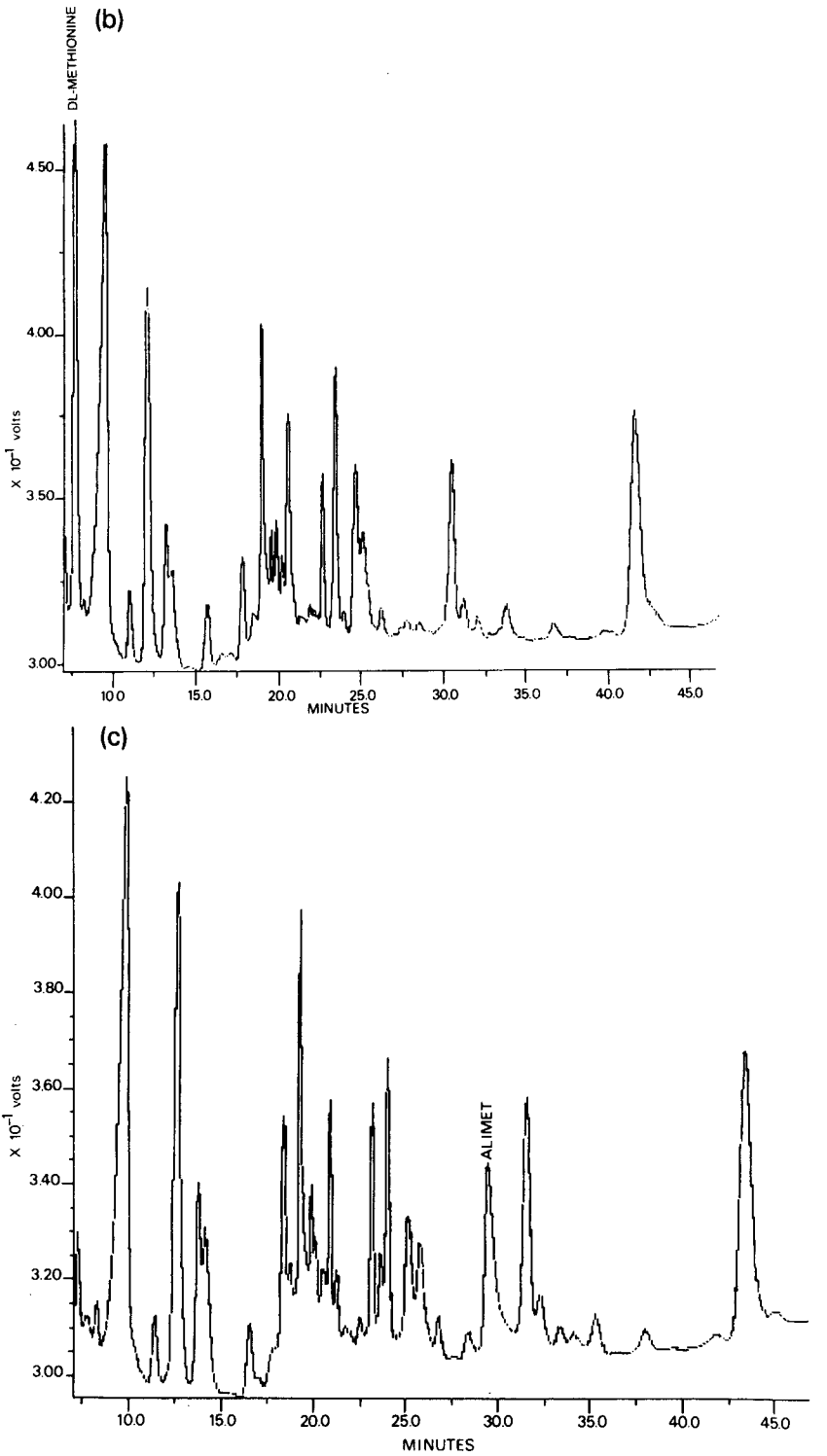

Fig. 3. Typical chromatograms of (a) DL-methionine-Alimet standard solution; (b) feed sample extract at 0.120% DL-methionine supplementation level; (c) feed sample extract at 0.092% Alimet supplementation level.

TABLE I

RECOVERY AND PRECISION OF ANALYSES ON SUPPLEMENTED TEST FEED SAMPLES BASED ON FIVE INDEPENDENT ANALYSES AT EACH SUPPLEMENTATION LEVEL

Alimet added (%)	*DL-Methionine added (%)*	*Recovery (%)*	*R.S.D. (%)*
0.07	–	96.7	2.8
0.35	–	98.6	4.2
–	0.06	95.0	3.0
–	0.40	97.4	1.6

TABLE II

RECOVERIES FOR COMMERCIAL FEED SAMPLES

Origin	*Theoretical Alimet applied (%, w/w)*	*Theoretical DL-methionine applied (%, w/w)*	*Recovery (%)*	*Recovery conv.[a] (%)*
F.R.G.	–	0.010	90.0	
	–	0.040	86.3	
	–	0.060	98.3	
	–	0.080	101.3	
	–	0.100	89.0	
Spain	0.125	–	90.4	97.6
	0.193	–	99.0	114.5
	–	0.170	101.7	94.1
	–	0.230	115.3	108.6
France	0.068	–	94.1	101.4
	0.068	–	100.0	101.4
	0.140	–	110.0	100.0
	–	0.060	95.0	110.0
	–	0.140	110.7	
Portugal	0.0092	–	90.2	85.9
	–	0.129	100.0	
	–	0.177	94.9	
Netherlands	0.120	–	106.6	100.8
	0.129	–	103.8	100.0
	0.129	–	94.5	107.7
	–	0.125	105.8	
	–	0.312	111.2	

[a] Recovery obtained by conventional methods, *i.e.*, HPLC determination for Alimet and DL-methionine separately[1,5,9,11].

keting areas were examined for potential interferences and recoveries.

Recovery tests. Recovery tests were performed by adding known amounts of Alimet and DL-methionine to a compounded feed. A between-day reproducibility of the assay was obtained by executing five repeated determinations on feed sample extracts. The precision was determined by calculating the relative standard deviations (R.S.D.) for each set of five analyses (Table I). The R.S.D.s obtained are comparable to those reported for the determination of both substances by conventional methods[9,17,18].

Validation on commercial feed samples. In order to evaluate the effect of a typical sample matrix in terms of potential interferences, numerous feed samples

originating from Belgium, The Netherlands, Spain, Italy, France, F.R.G., U.K., Portugal, Poland and Israel were qualitatively examined. None of these samples exhibited a peak eluting at or near the retention time of either DL-methionine or its hydroxy analogue.

A quantitative evaluation of commercial poultry and pig feeds ranging in supplementation levels from 0.010 to 0.312% (w/w) and originating from different countries was made using the proposed method. The results in Table II demonstrate that in each instance the amount of Alimet or DL-methionine is within a range of 85–115% of the theoretically expected levels. Moreover, excellent agreement between the results obtained by the proposed simultaneous analysis method and the conventional methods[1,5,9,11] was recorded.

CONCLUSION

A reliable method for the simultaneous determination of Alimet and DL-methionine in compounded feed samples has been developed. It involves a simple extraction procedure followed by a gradient HPLC analysis on a LiChrospher reversed-phase column. The separation is excellent for a wide variety of samples, and the procedure yields accurate results and shows excellent correlation with conventional methods.

REFERENCES

1 D. H. Spackman, W. H. Stein and S. Moore, *Anal. Chem.*, 30 (1958), 1190–1206.
2 A. Beck, H. Schmidtborn, M. Spindler and H. Tanner, *Kraftfutter*, 3 (1982) 118–124.
3 D. Matesic, *J. Assoc. Off. Anal. Chem.*, 65 (1982) 62–65.
4 C. W. Gehrke, L. L. Wall, J. S. Absheer, F. E. Kaiser and R. W. Zumwalt, *J. Assoc. Off. Anal. Chem.*, 68 (1985) 811–821.
5 M. Foulon, *Internal Report*, University of Louvain-la-Neuve, September 1989.
6 R. J. Day, D. E. Borowy and R. M. Schisla, *J. Agric. Food Chem.*, 31 (1983) 889–891.
7 M. J. Feit, R. I. Daun, M. H. Model and D. C. Zietlow, *Poult. Sci.*, 63 (1984) 100.
8 D. V. Vinjamoori and R. M. Schisla, *J. Assoc. Off. Anal Chem.*, 69 (1986) 474–477.
9 A. Baudichau, D. C. Bruyer, R. Ontiveros and W. D. Shermer, *J. Sci. Food Agric.*, 38 (1987) 1–8.
10 D. Balschukat, E. Kress and H. Tanner, *Landwirtsch. Forsch.*, 41 (1988) 120–130.
11 R. Gerstl and K. Ranfft, *Landwirtsch. Forsch.*, 42 (1989) 6–11.
12 M. Kabwe wa Mupenda, *M. S. Thesis*, University of Louvain-la-Neuve, June 1988.
13 R. C. Weast (Editor), *CRC Handbook of Chemistry and Physics*, CRC Press, Boca Raton, FL, 69th ed. (1988).
14 *Merck Index*, Merck , Rahway, NJ, 10th ed. 1983.
15 J. W. Dolan, L. R. Snyder and M. A. Quarry, *Int. Lab.* 17, No. 8 (1987) 66–71.
16 M. J. Walters, *J. Assoc. Off. Anal. Chem.*, 70 (1987) 465–469.
17 R. Laffi, S. Marchetti, A. Baudichau and M. Marchetti, *Doc. Vet.*, 9, No. 4 (1988) 53–57.
18 G. Viroben, *Journee Association Française des Techniciens de l'Alimentation Animale: Quoi de Neuf en Matière d'Acides Aminés Industriels, Paris, May 1986.*

Journal of Chromatography, 516 (1990) 383–393
Elsevier Science Publishers B.V., Amsterdam

CHROM. 22 535

Simultaneous ion chromatography of inorganic anions together with some organic anions and alkaline earth metal cations using chelating agents as eluents

DAREN YAN[a]
Department of Chemistry, Central-South University of Technology, Changsha, Hunan 410012 (China)
and
GEORG SCHWEDT*
Institut für Anorganische und Analytische Chemie, Technische Universität Clausthal, Paul-Ernst Strasse 4, D-3392 Clausthal-Zellerfeld (F.R.G.)
(First received January 17th, 1990; revised manuscript received May 4th, 1990)

ABSTRACT

The possibility of the simultaneous separation of inorganic and some organic anions and alkaline earth metal cations was investigated on two silica gel-based anion exchangers with the chelating agents ethylenediaminetetraacetic acid (EDTA), 1,2-diaminocyclohexanetetraacetic acid (DCTA), ethylene glycol bis(2-aminoethyl ether) tetraacetic acid (EGTA) and diethylenetriamionepentaacetic acid (DTPA) as eluents. The retention times (t_R) of all the inorganic and organic anions decreased with increasing pH and concentration of the eluents, whereas for the alkaline earths the t_R *vs.* pH plots were "bell-shaped", which indicated that alkaline earths could be separated either as metal cations or as chelating anions, depending on the pH and concentration of the eluent, but with almost the same sequence Ba^{2+}, Sr^{2+}, Ca^{2+}, Mg^{2+}.

Under the experimental conditions EDTA and DCTA were usually applicable for the simultaneous separation of inorganic and some organic anions and alkaline earth metal ions, whereas EGTA and DTPA were more suitable for inorganic and organic anions but not good for alkaline earth metal ions.

The proposed method was used for the simultaneous determination of some inorganic and organic anions and alkaline earth metal ions in natural samples such as drinking water, mineral water, brine and spinach juice, with satisfactory results.

INTRODUCTION

For the simultaneous determination of inorganic anions and cations[1–11], particular attention has been focused on single-column ion chromatography with

[a] Present address: Institut für Anorganische und Analytische Chemie, Technische Universität Clausthal, D-3392, Clausthal-Zellerfeld, F.R.G.

0021-9673/90/$03.50

chelating agents as eluents. Yamamoto *et al.*[9] effected the separation of inorganic anions and Ca and Mg cations on an anion-exchange column with EDTA (see *Reagents and solutions* for full names) as eluent and conductivity detection. Matsushita[10] separated inorganic anions and some divalent metal ions by using DCTA as eluent and UV detection. An ion-chromatographic method using chelating agents and selctive UV detection for the same purpose was recently described[11].

With regard to the simultaneous determination of organic and inorganic anions, only a few publications have considered non-suppressed single-column ion chromatography. Cortes[12] separated some inorganic and organic anions by using an "amino column" and UV detection, Skelly[13] separated glycolic acid, NO_2^- and NO_3^- by a reversed-phase system and Haddad and Croft[14] separated acetate, lactate, chloride and phosphate on a polymeric anion column with UV detection.

In this study, an attempt has been made to separate simultaneously some inorganic and organic anions and all the alkaline earth metal cations, for which the chelating agents EDTA, DCTA, EGTA and DTPA were systematically investigated as eluents on the silica gel-based anion-exchange columns Nucleosil SB and Nucleosil Anion II with both conductivity and UV detection.

EXPERIMENTAL

Apparatus

The instrumentation consisted of an a high-performance liquid chromatographic pump (Model 2200, Bischoff, Leonberg, F.R.G.), an Ion Chromatograph 690 conductivity detector (Metrohm, Herisau, Switzerland), a UV detector (Biotronik, Maintal, F.R.G.) and a Chromato-Integrator (Merck/Hitachi, Darmstadt, F.R.G.).

The separation columns used were Nucleosil 10 SB (250 × 4 mm I.D.) and Nucleosil 10 Anion II (250 × 4 mm I.D.) (Macherey, Nagel & Co., Düren, F.R.G.).

Reagents and solutions

The eluents were prepared by dissolving 1–3 mmol of EDTA (ethylenediaminetetraacetic acid; Titriplex II), DCTA (1,2-diaminocyclohexanetetraacetic acid; Titriplex IV), EGTA (ethylene glycol bis(2-aminoethyl ether)tetraacetic acid; Titriplex VI) and DTPA (diethylenetriaminepentaacetic acid; Titriplex V) in 1 l of deionized, distilled water followed by adjusting the pH to a certain value between 4 and 8 with lithium hydroxide solution. Before use all eluents were filtered through a 0.2-μm membrane filter. Stock solutions of inorganic and organic anions and alkaline earths were prepared from the salts at concentrations of 1 mg/l, then diluted to the desired concentrations.

All reagents were of analytical-reagent grade and used without further purification.

Chromatographic conditions

Unless stated otherwise, the chromatographic experiments were performed at a flow-rate of 2 ml/min and the sample volume used was 100 μl. The sensitivity of the conductivity detector was set at 2 μS/cm and the integrator attenuation was set at 5. The sensitivity of the UV detector was 0.16–0.08 a.u.f.s. and the detection wavelength length was 205 nm. The separation systems, including the separation columns, the concentrations, pH values and flow-rates of the eluents are summarized in Table I.

TABLE I

THE SEPARATION SYSTEMS

Column	*Eluent*	*Concentration (mmol/l)*	*pH*	*Flow-rate (ml/min)*
Nucleosil SB	EDTA	1, 2, 3	4.2–8.0	2
	DCTA	1, 2, 3	4.5–7.5	2
	EGTA	1–5	4.4–8.0	2
	DTPA	1, 2	4.5–7.5	2
Nucleosil Anion II	EDTA	1	4.0–6.0	2
	DCTA	1.5	4.5–7.0	1

RESULTS AND DISCUSSION

Effect of pH and concentration of the eluent

The active species of EDTA and aminopolycarbonic acids as eluents are their anions, which are dependent directly on the pH and concentration of the eluent. The effects of pH and concentration eluents were therefore systematically investigated.

Considerating the stability of the silica-based exchangers and the solubility of the aminopolycarbonic acids, the pH of the eluents was adjusted to a certain value between 8 and 4. Plots of retention times *vs.* pH of EDTA and DCTA eluents on both

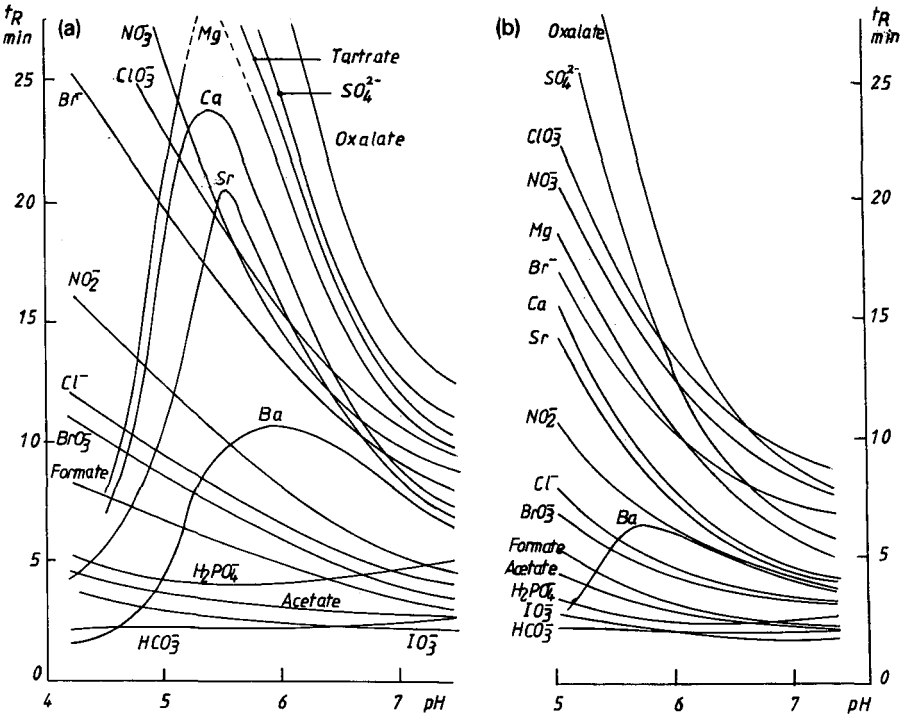

Fig. 1. Effects of pH and concentration of eluents. Column: Nucleosil SB (250 × 4 mm I.D.). Eluent, EDTA, (a) 1 mmol/l and (b) 3 mmol/l; flow-rate, 2 ml/min; conductivity detection. t_R = Retention time.

TABLE II

RETENTION TIME OF SOME INORGANIC AND ORGANIC ANIONS AND ALKALINE EARTH METAL CATIONS ON THE NUCLEOSIL SB COLUMN

Conditions: Nucleosil 10 SB column (250 × 4 mm I.D.); flow-rate, 2 ml/min; conductivity detection.

Ion	*Retention time (min)*									
	EDTA			*DCTA*			*EGTA*		*DTPA*	
	1 mM, pH 6.0	*1 mM, pH 7.0*	*3 mM, pH 6.0*	*2 mM, pH 5.0*	*2 mM, pH 6.0*	*2 mM, pH 7.0*	*2 mM, pH 7.7*	*3 mM, pH 7.7*	*2 mM, pH 4.5*	*2 mM, pH 6.0*
F^-			2.90	4.80	2.50	2.40	3.90	3.30		
HCO_3^-	2.80	2.80	2.42	2.41	2.42	2.40	4.90	4.22		
IO_3^-	3.02	2.63	2.50	2.90	2.32	2.24	5.33	4.60		
$H_2PO_4^-$	4.21	5.00	2.94	3.33	3.30	3.20	16.4	14.8	3.90	4.73
BrO_3^-	5.80	4.80	5.02	5.90	4.32	3.63	8.52	7.60	5.21	
Cl^-	6.11	4.54	5.12	6.22	4.33	3.80	8.65	7.32	5.12	3.70
NO_2^-	8.22	6.01	7.05	8.32	5.80	4.75	11.2	8.90	7.40	4.80
Br^-	12.5	9.80	11.0	12.2	8.40	7.11	18.4	14.9	9.40	7.03
ClO_3^-	15.9	10.9	14.5	15.3	9.70	9.20	23.5	19.0	10.3	8.80
NO_3^-	14.6	10.1	13.2	14.7	10.0	8.50	20.8	16.5	12.0	6.94
SO_4^{2-}	25.5	12.9	13.2	23.3	10.2	7.10	18.9	18.0	16.1	8.50
Acetate	4.20	3.00	3.30	3.90	3.11	2.52	4.62	4.03	3.22	2.71
Formate	4.80	3.32	3.63	4.80	3.42	3.01	5.21	4.70	4.90	2.90
Propionate	4.40	3.90	3.93	4.60	3.30	2.90	5.40	4.60	3.50	2.91
Pyruvate	6.50	3.50	3.75	5.60	4.30	3.2	6.90	5.90	4.10	3.20
Tartrate	25.0	13.9	13.2	25.5	11.6	7.20	21.0	20.0	12.9	9.5
Oxalate	32.4	15.5	17.0	29.0	14.2	8.30	25.0	23.0	13.7	12.0
Ba^{2+}	5.5	8.8		2.2	3.0	4.3				
Sr^{2+}	15.5	9.20		13.2	13.7	8.80				
Ca^{2+}	16.5	8.40	7.70	28.3	15.3	9.02	13.4			
Mg^{2+}	23.0	12.0	11.4			12.7	4.5			

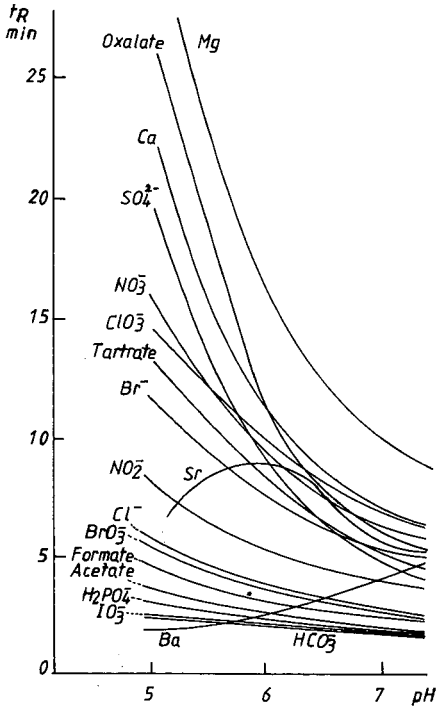

Fig. 2. Influence of pH of DCTA. Column: Nucleosil SB (250 × 4 mm I.D.). Eluent, DCTA (3 mmol/l); flow-rate, 2 ml/min; conductivity detection.

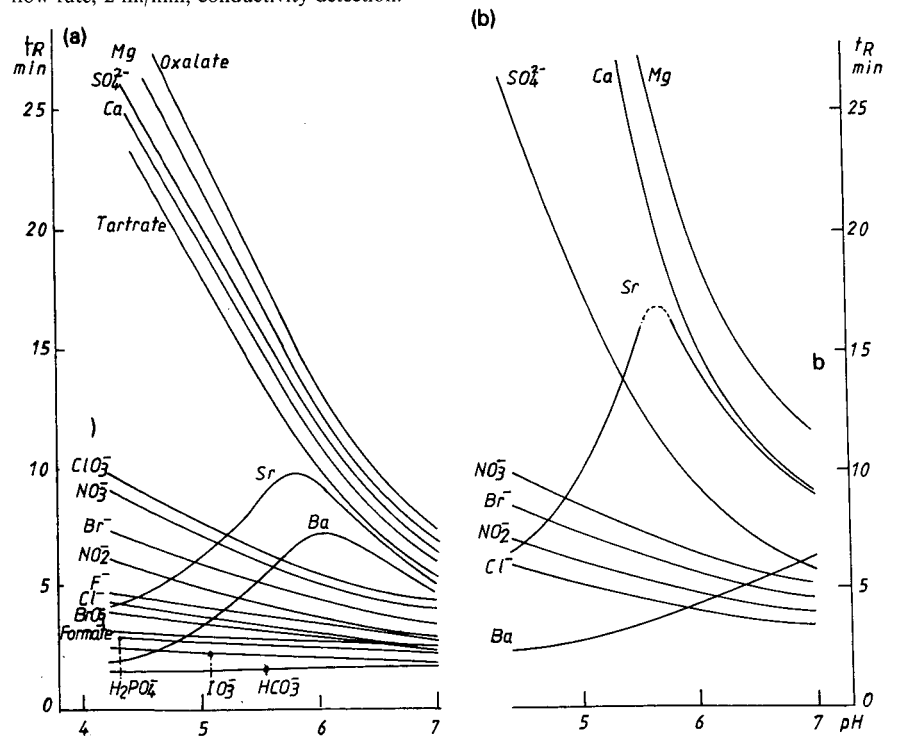

Fig. 3. Influence of pH of eluents. Column: Nucleosil Anion II (250 × 4 mm I.D.). Eluent: (a) 1 mmol/l EDTA at 2 ml/min; (b) 1.5 mmol/l DCTA at 1 ml/min. Conductivity detection.

TABLE III

COMPARISON OF RETENTION TIMES OF VARIOUS IONS ON THE NUCLEOSIL ANION II AND NUCLEOSIL SB COLUMNS WITH EDTA AS ELUENT

Elution conditions: 1 mmol/l EDTA, pH 6.0, flow-rate 2 ml/min.

Column	*Retention time (min)*									
	Acetate	*Formate*	Cl^-	NO_2^-	Br^-	NO_3^-	SO_4^{2-}	*Oxalate*	Ca^{2+}	Mg^{2+}
Nucleosil Anion II	2.1	2.9	3.2	4.0	4.8	5.7	12.0	14.1	11.0	12.5
Nucleosil SB	3.1	4.8	6.1	8.0	12.2	14.5	25.0	30.0	18.1	22.5

columns are shown in Figs. 1, 2 and 3. The retention times of some inorganic and organic anions and alkaline earth metal ions on the Nucleosil SB column with EDTA, DCTA, EGTA and DTPA as eluents are partly summarized in Table II. For inorganic and organic anions the retention times decreased regularly with increase in the pH of the eluent, characterized by a negative slope of the plots, whereas for the alkaline earth metal ions the retention time *vs.* pH plots were "bell-shaped", which indicated that the alkaline earths should be separated either as metal cations before the top of the diagram with a positive slope or as chelating anions after the top characterized by the negative slope when the pH and the concentration of the eluents become high enough.

Fig. 1 also shows the dependences of the retention times on the concentration of EDTA. For the elution of inorganic and organic anions and also alkaline earth metal ions all the retention times decreased regularly with the increasing EDTA concentration. However, among the alkaline earths only Ba^{2+} showed "bell-shaped" plots at all EDTA concentrations in the range 1–3 mmol/l. Near the top of the diagram the alkaline earths should exist partly as cations and partly as anions, thus causing weak conductivity signals which cannot be used for the quantitative detection. The conductimetric detection of the alkaline earths was therefore possible only within the limits of the range just after or before the top of the diagram.

Comparison between Nucleosil Anion II and Nucleosil SB

The Nucleosil Anion II separation column had a lower capacity than that of the Nucleosil SB column and was suitable for the rapid separation of various anions and Ca^{2+} and Mg^{2+}. In addition, Nucleosil Anion II permitted lower eluent concentrations to be used for the separation and was favourable for trace analysis. However, on this column the elution sequence could not be reversed by changing the pH or eluent concentration. Fig. 3, shows the plots of retention times *vs.* pH on this column and Table III compares the retention times for various ions on the Nucleosil Anion II and Nucleosil SB columns with EDTA as eluent.

Because of its greater capacity, the Nucleosil SB column could be suitable for the separation of more ions. Moreover, on this column it is possible to change the elution sequence of some ions. For example, by using EDTA as eluent SO_4^{2-} was eluted after Ca^{2+} and Mg^{2+} (see Fig. 4). However, SO_4^{2-} could be eluted before Ca^{2+} and Mg^{2+} if DCTA was used instead of EDTA as the eluent on the same column (see Fig. 5). The elution sequence of some ions could be reversed by changing the pH and eluent concentration. For example, the elution sequence of NO_3^- could be changed step by step from NO_3^-, Ca^{2+}, Mg^{2+}, SO_4^{2-} (eluent 1 mmol/l EDTA, $5.3 < pH < 6.6$) through Ca^{2+}, NO_3^-, Mg^{2+}, SO_4^{2-} ($pH > 6.6$) and Ca^{2+}, Mg^{2+}, NO_3^-, SO_4^{2-} (2 mmol/l EDTA, $pH < 6.3$) to Ca^{2+}, Mg^{2+}, SO_4^{2-}, NO_3^- (3 mmol/l EDTA, $pH > 6$) by increasing the concentration and pH of EDTA as shown in Fig. 1.

It is of interest that the elution sequence of the alkaline earths in all these separation systems generally remained Ba^{2+}, Sr^{2+}, Ca^{2+}, Mg^{2+} (except when using EGTA as eluent, when Mg^{2+} was always eluted before Ca^{2+}), which is the opposite of that in separation systems involving cation exchangers[15–17].

On the Nucleosil SB column with EDTA or DCTA as eluent, $H_2PO_4^-$ was generally eluted before Cl^-, but with EGTA as eluent $H_2PO_4^-$ was far behind Cl^- (see Fig. 6). A separation of acetate, formate, pyruvate, Cl^-, NO_2^-, $H_2PO_4^-$, SO_4^{2-} and NO_3^- was thereby achieved (Fig. 6). However, EGTA was not suitable for the elution

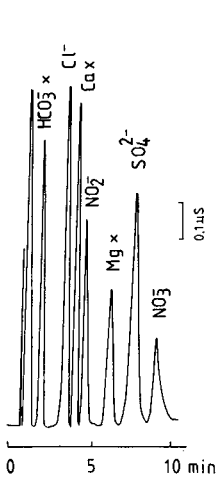

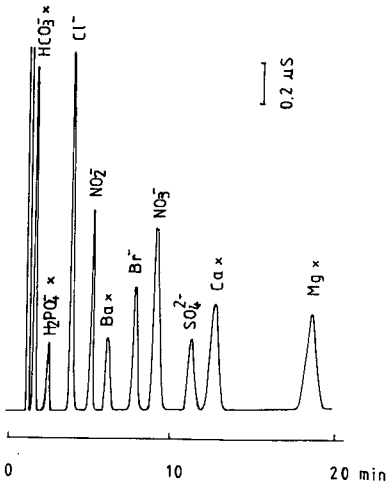

Fig. 4. Rapid separation of main inorganic anions, Ca^{2+} and Mg^{2+} with EDTA as eluent. Column: Nucleosil SB. Eluent: 2 mmol/l EDTA, pH 7.5, flow-rate 2 ml/min. Conductivity detection, sensitivity = 1 µS/cm. Concentrations: HCO_3^- 40, Cl^- 35, Ca^{2+} 20, NO_2^- 20, Mg^{2+} 8, SO_4^{2-} 30, NO_3^- 20 mg/l. × = Reversed negative signal.

Fig. 5. Simultaneous IC of inorganic anions and alkaline earth metal ions with DCTA as eluent. Column: Nucleosil SB. Eluent: 1 mmol/l DCTA, pH 7, flow-rate 2 ml/min. Conductivity detection. × = Reversed negative signal.

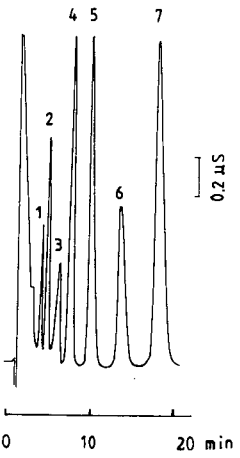

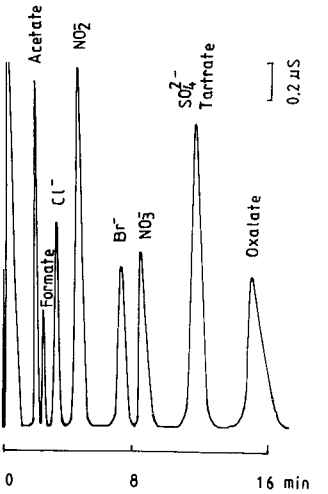

Fig. 6. Chromatographic separation of inorganic and organic anions with EGTA as eluent. Column: Nucleosil SB. Eluent: 4 mmol/l EGTA, pH 7.0, flow-rate 2 ml/min. Conductivity detection. 1 = Acetate; 2 = formate; 3 = pyruvate; 4 = Cl^-; 5 = NO_2^-; 6 = $H_2PO_4^-$; 7 = SO_4^{2-}.

Fig. 7. Chromatographic separation of inorganic and organic anions with DTPA as eluent. Column: Nucleosil SB. Eluent: 1 mmol/l DTPA, pH 7.5, flow-rate 2 ml/min. Conductivity detection.

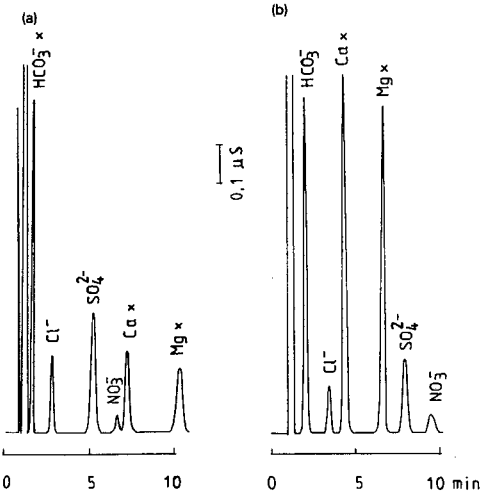

Fig. 8. IC analysis of mineral water with DCTA and EDTA as eluents. Column: Nucleosil SB. Eluent: (a) 3 mmol/l DCTA, pH 6.75, flow-rate 2 ml/min; (b) 2 mmol/l EDTA, pH 7.5, flow-rate 2 ml/min. Conductivity detection, sensitivity = 1 μS/cm, attenuation = 5. Concentrations found: HCO_3^- 180, Cl^- 4.2, NO_3^- 2.0, SO_4^{2-} 7.8, Ca^{2+} 40.2, Mg^{2+} 19.0 mg/l. × = Reversed negative signal.

of the alkaline earths because of peak broadening owing to the slow chelating reaction.

With DTPA as eluent, NO_3^-, SO_4^{2-}, tartrate and oxalate could be better separated than with other eluents, but DTPA was not suitable for the separation of the alkaline earths for the same reasons as given above for EGTA. A chromatogram for the separation of acetate, formate, Cl^-, NO_2^-, Br^-, NO_3^-, SO_4^{2-}, tartrate and oxalate is shown in Fig. 7.

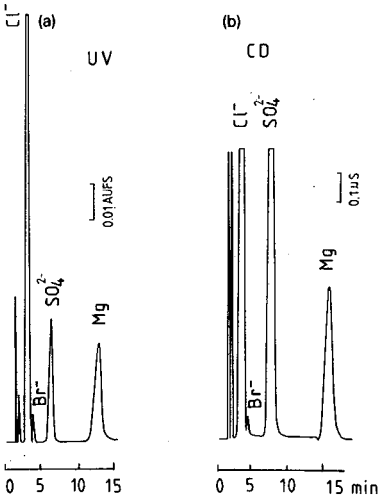

Fig. 9. IC analysis of brine with UV and conductivity detection. Column: Nucleosil Anion II. Eluent: (a) 1 mmol/l DCTA, pH 6.6, flow-rate 1.5 ml/min; (b) 1 mmol/l DCTA, pH 6.0, flow-rate 1.5 ml/min. Detection: (a) UV detector, 205 nm, Range = 0.16 a.u.f.s., attenuation = 4; (b) conductivity detector, sensitivity = 1 μS/cm, attenuation = 5. Concentrations found: Br^- 0.8, Cl^- 220, SO_4^{2-} 80, Mg^{2+} 72 mg/l. × = Reversed negative signal.

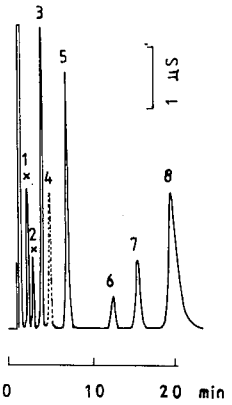

Fig. 10. IC analysis of spinach juice. Column: Nucleosil Anion II (from a batch with higher capacity). Eluent: 3 mmol/l EDTA, pH 5.4, flow-rate 2.5 ml/min. Conductivity detection, sensitivity = 5 μS/cm, attenuation = 4. Concentrations found: 1 = $H_2PO_4^-$ 40; 2 = acetate 20; 3 = Cl^- 45; 4 = NO_2^- 33 (dashed line, reduced from NO_3^- overnight); 5 = NO_3^- 33; 6 = Mg 35; 7 = SO_4^{2-} 32; 8 = oxalate 126. × = Reversed negative signal.

Application

The proposed method was applied to for the simultaneous determination of some inorganic and organic anions and alkaline earths metal ions in natural samples.

Fig. 8 shows the IC analysis of a mineral water with the Nucleosil SB column and a conductivity detector using EDTA and DCTA as eluents, giving different elution sequence for Ca^{2+}, Mg^{2+}, NO_3^- and SO_4^{2-} and different signal strengths for Ca^{2+} and Mg^{2+}.

Fig. 9 shows the IC analysis of a brine sample in which the trace amount of Br^- present could be successfully separated from the large amounts of Cl^-, SO_4^{2-} and Mg^{2+}. It can be seen that the UV detector was more suitable than the conductivity detector for the detection of trace Br^-.

Fig. 10 shows the chromatogram of freshly squeezed spinach juice which was diluted and filtered first through double-folded filter-papers and then through a 0.2-μm membrane filter. An unexpectedly complete separation and simultaneous determination of oxalate, acetate, Cl^-, NO_3^-, SO_4^{2-} and alkaline earths in this spinach sample was achieved. The sample solution of the spinach juice was not stable and the NO_3^- was enzymatically reduced to NO_2^- if the solution was allowed to stand overnight.

In conclusion, this IC method is a simple, versatile and practical technique for the simultaneous determination of various inorganic and organic anions and metal cations, and may find new applications in the analysis of environmental, food, drink and biomedical samples. An IC determination of urate, oxalate, SO_4^{2-}, Cl^-, Ca^{2+}, Na^+, NH_4^+, K^+, etc., in renal calculi has been achieved and will be reported separately.

ACKNOWLEDGEMENT

This work was supported by the Stiftung Volkswagenwerk, Hannover, F.R.G.

REFERENCES

1 H. Small and T. E. Miller, *Anal. Chem.*, 54 (1982) 462.
2 V. Cheam and A. S. Chau, *Analyst (London)*, 112 (1987) 993.
3 Z. Iskanolarani and T. E. Miller, *Anal. Chem.*, 57 (1985) 1591.
4 D. J. Pietrzyk and D. M. Brown, *Anal. Chem.*, 58 (1986) 2554.
5 V. K. Jones and J. G. Tarter, *J. Chromatogr.*, 312 (1984) 456.
6 V. K. Jones, S. A. Frost and J. G. Tarter, *J. Chromatogr. Sci.*, 23 (1985) 442.
7 V. K. Jones and J. G. Tarter, *Analyst (London)*, 113 (1988) 183.
8 G. Schwedt and B. Kondratjonok, *Labor Praxis*, 12 (1988) 540.
9 M. Yamamoto, H. Yamamoto, Y. Yamamoto, S. Matsushita, N. Baba and T. Ikushige, *Anal. Chem.*, 56 (1984) 832.
10 S. Matsushita, *J. Chromatogr.*, 312 (1984) 327.
11 B. Kondratjonok and G. Schwedt, *Fresenius' Z. Anal. Chem.*, 332 (1989) 855.
12 H. J. Cortes, *J. Chromatogr.*, 234 (1982) 517.
13 N. E. Skelly, *Anal. Chem.*, 54 (1982) 712.
14 P. R. Haddad and M. Y. Croft, *Chromatographia*, 21 (1986) 11.
15 D. R. Yan and G. Schwedt, *Fresenius' Z. Anal. Chem.*, 320 (1985) 325.
16 D. R. Yan DR, J. A. Zhang and G. Schwedt, *Fresenius' Z. Anal. Chem.*, 335 (1989) 687.
17 D. R. Yan and G. Schwedt, *Fresenius' Z. Anal. Chem.*, (1990) in press.

Journal of Chromatography, 516 (1990) 395–404
Elsevier Science Publishers B.V., Amsterdam

CHROM. 22 589

Analysis of *n*-octyl(phenyl)-N,N-diisobutylcarbamoylmethylphosphine oxide and TRUEX process solvent by gas and liquid chromatography

RALPH C. GATRONE*, PAUL G. RICKERT and E. PHILIP HORWITZ
Chemistry Division, Argonne National Laboratory, Argonne, IL 60439 (U.S.A.)
and
BARBARA F. SMITH, CATHERINE S. BARTHOLDI and AARON M. MARTINEZ
Chemistry and Laser Sciences Division, Los Alamos National Laboratory, Los Alamos, NM 87545 (U.S.A.)
(Received March 23rd, 1990)

ABSTRACT

Complementary analytical procedures using capillary gas chromatography (GC) and high-performance liquid chromatography (HPLC) have been developed for the analysis of the TRUEX process solvents (CMPO–TBP–tetrachloroethylene or normal paraffinic hydrocarbons) and the extractant CMPO. GC analyses are accomplished in 20 min using a 15 m × 0.25 μm I.D. DB-5 capillary column with flame ionization detection. The analysis requires derivatization with diazomethane. HPLC analyses are performed in 10 min using a C_{18} reversed-phase column and a mobile phase consisting of acetonitrile–water–triethylamine (79:29.5:0.5) with refractive index and ultraviolet detection. The methods provide information regarding the presence of acidic and neutral impurities in stock extractant, fresh process solvent, and recovered TRUEX solvent.

INTRODUCTION

The TRUEX process[1] is an actinide extraction/recovery process designed to reduce the concentration of the transuranic elements in nuclear waste solutions. The process ultilizes the extractant *n*-octyl(phenyl)-N,N-diisobutylcarbamoylmethylphosphine oxide (CMPO, **1**, iBu = isobutyl; Ph = phenyl] with tributylphosphate (TBP, **2**) in either a chlorocarbon diluent (tetrachloroethylene) or a normal paraffinic hydrocarbon (dodecane)[2].

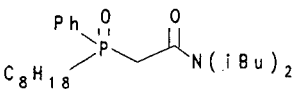

1

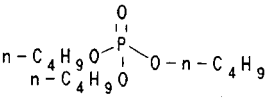

2

Before the process can be successfully implemented in the reduction of nuclear waste solutions two major technical problems have to be overcome: (1) the commercial production of solvent extraction (SX) grade CMPO and (2) the development of satisfactory analytical methods for determining the purity of extractant and process solvent before and after processing.

A number of impurities are present in CMPO when the extractant is prepared by the Grignard method as developed at Argonne. Horwitz and Gatrone[3] have established a set of criteria for an acceptable purity of the now commercially available extractant. The specifications determined for the SX-grade CMPO are based upon a knowledge of the chemistry of americium(III), the most difficult transuranic metal ion to extract from nuclear waste, in the TRUEX process and the impurities present in the extractant[4,5] which adversely affect this chemistry. The presence of even trace amounts of acidic impurities hampers the back extraction of Am(III) by dilute nitric acid. Because of the complexity of the TRUEX chemistry, a two-tier set of specifications have been developed[a]. The first set of specifications are based on the chromatographic details described in this paper: $> 95\%$ (w/w) CMPO, $< 2\%$ (w/w) additional neutral organophosphorus compounds and $< 3\%$ (w/w) hexadecane. The second set of specifications are based on the performance of the process solvent and will not be described in this paper.

Several acidic and neutral degradation products have been observed due to hydrolysis and radiolysis of the process solvent[6–8]. Any satisfactory analytical technique developed for the analysis of the extractant or fresh process solvent should ideally be applicable to the determination of the continued usefulness of spent solvent and should allow the facile analysis of the process solvent during waste processing. To date, no entirely satisfactory method for the analysis of the TRUEX process solvent or of the extractant has been reported. The development of a capillary gas chromatographic (GC) method for the determination of the concentration of CMPO and TBP in the process solvent has been reported[9], but no attempt to examine the process solvent or commercially available CMPO for the presence of acidic or neutral impurities was made.

The objective of this paper is to report the experimental details of a capillary GC method and a complementary high-performance liquid chromatographic (HPLC) method for the analysis of the TRUEX process solvent. The methods are applicable to fresh and spent solvent and may be applied during the processing of nuclear waste by TRUEX.

EXPERIMENTAL

Technical-grade (95%) CMPO was obtained from M & T Chemical Co. (Rahway, NJ, U.S.A.) and was purified as previously reported[4]. TBP was obtained from Eastman and was distilled from calcium hybride at reduced pressure. Tetrachloroethylene (Gold Label, TCE), Diazald®, anhydrous ethyl ether and triethylamine were obtained from Aldrich and used as received. Methylene chloride (Aldrich) was

[a] Performance specifications and the data that established these criteria are available from E. P. Horwitz, Chemistry Division, Argonne National Laboratory, Argonne, IL 60439, U.S.A.

made acid free prior to use by filtering through a column of alumina. High-purity acetonitrile and water were obtained from Burdick and Jackson and was used after Millipore (0.45 μm) filtration. The potential acidic and neutral impurities: diphenylphosphinic acid (DΦP), *n*-octyl(phenyl)phosphinic acid [OΦP], di-*n*-octylphosphinic acid (DOP), diphenylphosphine oxide (DΦPO), *n*-octyl(phenyl)phosphine oxide [O(Φ)PO], di-*n*-octylphosphine oxide (DOPO), diphenyl-N,N-diisobutylcarbamoylmethylphosphine oxide [DΦD(iB)CMPO] and di-*n*-octyl-N,N-diisobutylcarbamoylmethylphosphine oxide [DOD(iB)CMPO] were prepared as previously described[4,5]. The neutral degradation product from the radiolysis of CMPO, methyl(octyl)-(phenyl)phosphine oxide [M(O)(Φ)PO], was prepared according to the method of Kaplan as described in ref. 6.

GC analyses

GC analyses were performed on a Hewlett-Packard 5890 (Palo Alto, CA, U.S.A.) equipped with a flame ionization detector, a split–splitless injector and a Hewlett-Packard 3393A computing integrator. A fused-silica bonded-phase capillary column, DB-5 (J&W Scientific, Rancho-Cordova, CA, U.S.A.), 15 m × 0.25 mm I.D. (0.25 μm film thickness) was employed. The temperature profile was 100°C for 1 min, increased to 260°C at 10°C/min and held for 9 min. The detector and injector temperatures were held at 300°C. Injections of 1 μl were made using a split ratio of 35:1.

Samples were derivatized with diazomethane (CH_2N_2) to convert any acidic impurities to the respective methyl esters for GC analysis by reaction of an ether solution of the analyte with a freshly distilled ethereal solution of diazomethane at room temperature. The ethereal solution was slowly introduced until the yellow color indicative of excess diazomethane persists. Diazomethane was prepared by the base decomposition of Diazald[10]. The excess diazomethane and ether solvent are removed by gently warming in a water bath until a sample of constant weight is obtained TRUEX samples were prepared by diluting 1 ml of the process solvent (0.25 *M* CMPO, 0.75 *M* TBP in TCE) after derivatization to 20 ml with acid-free methylene chloride. Samples of CMPO were prepared by derivatizing 100 mg of CMPO in ether, followed by the addition of 1 ml of methylene chloride and further dilution to 10 ml.

HPLC analyses

HPLC analyses were performed on a Waters Associates (Milford, MA, U.S.A.) liquid chromatograph equipped with a multisolvent delivery pump (Model 600) and a differential refractive index (RI) detector (Model 410) with a sensitivity setting of 64. Helium sparging of the mobile phase reservoir reduced baseline drift. A programmable multi-wavelength UV–VIS detector (Model 490) set to 262 nm (0.05 a.u.f.s.) was coupled to the system.

A Waters reversed-phase μBondapak stainless-steel column (30 cm × 3.9 mm I.D.) was maintained at 32°C. A Waters Model UK6 injector system was used to introduce samples.

RESULTS AND DISCUSSION

GC Analyses

Fig. 1 displays sequential injections of the TRUEX process solvent formulated from purified CMPO and TBP in TCE. Fig. 2 displays the capillary gas chromatogram for a synthetic mixture of potential impurities as well as several structurally similar extractants. The retention times and detectability limits are summarized in Table I.

Previous studies of the GC behavior of CMPO and TBP samples have indicated that these compounds demonstrate linear behavior with respect to a flame ionization detector over the concentration ranges 0.08–0.48 mg and 0.2–1.2 mg[7–9]. The relative behavior of CMPO and TBP are similar such that no internal standard is necessary for the quantitative analysis of the TRUEX process solvent.

However, we are also concerned with the analysis of degraded TRUEX process solvent. Therefore, dibutylphosphoric acid and *n*-octyl(phenyl)phosphinic acid, acidic degradation products from TBP and CMPO, respectively, were selected to calibrate the flame ionization detector for acidic components. The methyl esters of the acidic compounds were prepared by reaction with excess diazomethane. The calibration curves were obtained in triplicate and displayed linear behavior over the range 25–500 ng, the expected range for the impurities to be present based upon the earlier degradation studies[7]. Capillary GC provides a relatively rapid (20 min), reliable method for the analysis of samples of the TRUEX process solvent and its component parts. We have been able to reproducibly detect trace quantities (*ca.* 20 μg) of a variety of structurally similar compounds in the presence of large quantities of the substrates (CMPO and TBP). The data obtained from this method are extremely useful for the analysis of commercial preparations of CMPO for partial specification compliance as well as for the investigation into the hydrolytic and radiolytic stability of the process solvent.

A major limitation of the capillary GC method is the necessity to derivatize the acidic components in order to detect their presence. The free acid forms of the impurities are retained by the column indefinitely and lead to the significant degradation of column performance.

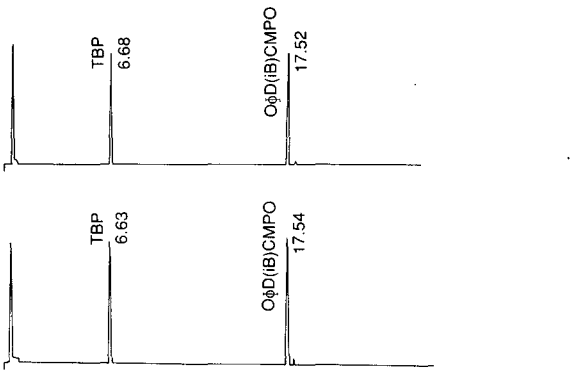

Fig. 1. Replicate injections of TRUEX process solvent. Numbers at peaks indicate retention times in min.

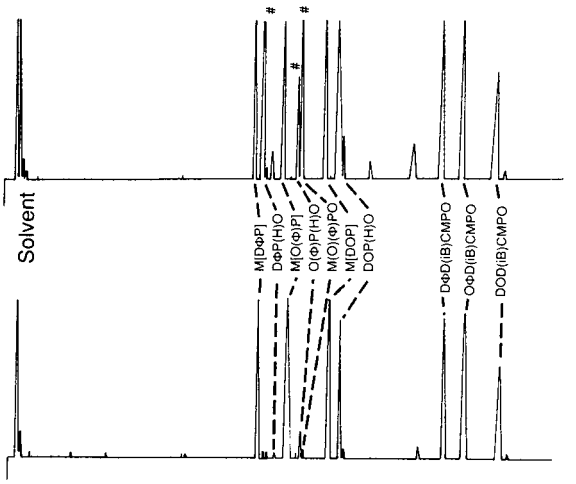

Fig. 2. Injection of the synthetic mixture of impurities and structurally related derivatives. Peaks marked with # were added to the initial mixture after derivatization with diazomethane.

TABLE I

RETENTION TIME AND DETECTION LIMITS FOR POTENTIAL IMPURITIES IN CMPO PREPARATIONS OR TRUEX SOLVENT

Compound		*Gas chromatography*		*Liquid chromatography*[a]		
No.	*Abbreviation*	t_R *(min)*	*Detection limit (μg)*	t_R *(min)*	*RI detection limit (μg)*	*UV detection limit (μg)*
1	CMPO	17.54 ± 0.02	–	9.20	0.038	0.031
2	TBP[b]	6.63 ± 0.05	–	6.81	0.51	–
3	(DΦP)[c]	9.84 ± 0.03	18.5	1.98	0.28	0.12
4	(OΦP)[c]	11.03 ± 0.05	21.3	1.99	0.32	0.28
5	(DOP)[c]	12.65 ± 0.02	23.2	2.02	0.31	20.7
6	DΦPO	10.12 ± 0.03	19.3	3.60	0.88	0.15
7	DOPO	13.12 ± 0.05	18.5	–	–	–
8	OΦPO	11.52 ± 0.02	22.3	5.68	0.36	0.22
9	DΦD(iB)CMPO	17.12 ± 0.02	–	–	–	–
10	DOD(iB)CMPO	19.46 ± 0.03	–	–	–	–
11	MOΦPO	11.72 ± 0.03	21.5	5.50	0.30	0.20
12	DBP[c]	4.01	19.8	–	–	–
13	Dodecane[b]	–	–	4.89	–	–
14	CIBA	–	–	4.78	0.08	0.34
15	TCE[b]	–	–	5.93	0.08	0.34
16	Isopar[b]	–	–	4.27	–	–

[a] Retention times are reported for the RI detector; the UV detector retension times are shorter by 0.2 min.

[b] Can be added to form TRUEX process solvent.

[c] Detected as methyl ester by GC.

A second limitation of the GC method is the presence of the tertiary phosphine oxide, M(O)(Φ)PO (**11**), at a retention time (t_R) of 11.72 min in Fig. 2. This phosphine oxide arises because of the thermolysis of CMPO in the injector port. Identification of the peak at this retention time as the tertiary phosphine oxide was confirmed by the synthesis of an authentic sample. Furthermore, the thermolysis of CMPO at 179°C provided significant amounts (>30%) of M(O)(Φ)PO.

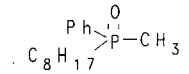

11

An additional limitation of the GC method is indicated in Fig. 2. It should be noted that only traces of the DΦPO (t_R = 10.12 min) and O(Φ)PO (t_R = 11.52 min) are observed in the lower chromatogram despite the introduction of equal amounts of all impurities prior to derivatization with diazomethane. The retention times of the phenyl-substituted phosphine oxides was confirmed by introducing samples after the derivatization reaction was complete and the excess diazomethane was evaporated. Furthermore, we have observed that DΦPO and O(Φ)PO react with diazomethane to yield the respective methyl esters of the phosphinic acids, *i.e.* diphenylphosphinic acid methyl ester and octyl(phenyl)-phosphinic acid methyl ester (Fig. 3). Secondary phosphine oxides, *i.e.* bis-substituted phosphine oxides with a single P–H bond are tautomeric with the phosphinous acid structure. It is conceivable that the electron-withdrawing phenyl substituent would stabilize the phosphinous acid structure to a degree where a sufficient quantity was present to react with diazomethane yielding the methyl ester of the phosphinous acid. It is well known that the methyl esters of phosphinous acids are very susceptible towards oxidation and rapidly yield the respective phosphinic acid methyl ester upon exposure to air. The hypothesis is further supported by the data in Fig. 2 which indicate that more electron-rich secondary phosphine oxides, such as the dialkylphosphine oxides (*e.g.* DOPO) do not react with diazomethane in this manner.

Another disadvantage of the developed GC method is that repeated injections of underivatized samples of the TRUEX process solvent or of CMPO leads to significant injector contamination, resulting in increased amounts of M(O)(Φ)PO with concomitant loss of quantification. This disadvantage is significantly reduced by derivatizing all samples with diazomethane prior to analysis and a periodic replacement of the injector insert.

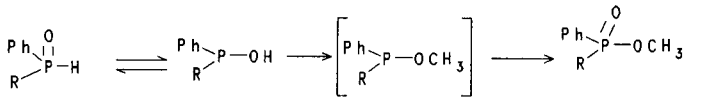

6 R = Ph

8 R = C_8H_{17}

3 R = Ph

4 R = C_8H_{17}

Fig. 3. The reaction of a phenyl-substituted secondary phosphine oxide with diazomethane.

HPLC analyses

The aforementioned difficulties with the GC method suggested that an alternative, non-destructive analytical technique might have some advantages. HPLC was selected for further evaluation.

Because of the polar nature of the acidic impurities, a reversed-phase column was selected to shorten the analysis time. Various acetonitrile–water mobile phases were investigated for separating CMPO and TBP. The mobile phase ratios were varied from 15 to 30% water, which increased the retention time of CMPO (11 min) and provided baseline separation of the two components. However, the CMPO peak was unsymmetrical with considerable tailing. We were able to resolve these problems by introducing 0.5% triethylamine, which shortened the analysis time to 9 min.

The effect of flow-rate on the separation of CMPO and TBP using acetonitrile–water (70:30) was investigated. Constant flow-rates of 1 and 1.5 ml/min were compared with a programmed flow-rate varied between the two flow-rates. The programmed flow-rate did not significantly enhance the chromatogram with respect to peak shape or tailing reduction compared to the higher flow-rate and also caused baseline drift problems. A flow-rate of 1.5 ml/min decreased the peak width at half-height relative to the 1 ml/min flow-rate, but not enough to justify the extra solvent required. Therefore, the conditions utilized are as indicated in the Experimental.

Two calibration curves were obtained in triplicate for CMPO in the ranges 100–800 mg and 0.1–10 mg or the RI detector. The curves are linear over both ranges with a least squares regression fit of 0.999 for both. A calibration curve for CMPO was obtained in the range 0.1–10 mg for the UV detector with a linear regression fit of 0.999. A calibration curve for TBP in the range 2.72–13.6 mg was likewise obtained for the RI detector and was linear with a fit of 0.994. TBP does not absorb sufficiently for the UV detector to be useful.

The most deleterious impurities to the TRUEX process are the acidic compounds (see above). We investigated the HPLC behavior of DΦP, O(Φ)P and DOP using the optimized analytical conditions. The results are summarized in Table I. The three phosphinic acids elute in appproximately 2 min (Fig. 4) and are unresolved. DOP has a slightly longer retention time but is not baseline resolved. All three compounds were detected using the RI detector. Solvent intereference occurred with the RI detector in the acidic-component retention-time region. To determine if sample volume affected peak height, 0.8 mg of each phosphinic acid was dissolved in 2 and 4 ml of mobile phase and injected. The peak heights were reproducible to within 7% for all compounds and responses were linear over the 0.8–1.6 mg range studied. Despite the lack of peak resolution we were able to obtain a total acidic content for a sample using the RI detector, which was in good agreement with the GC results. For process evaluation, where the exact concentrations of each identifiable acidic component is unnecessary, an analysis of total acidic interference should be sufficient. If further resolution were necessary, a capillary GC analysis could be used.

Only DΦP and O(Φ)P, which contain a chromophore, are detectable using the UV detector. The observed response is linear over the range studied, which is at least twice the detection limit. However, the response factors are quite different, as expected. The stronger chromophore of (DΦP) allows for better UV detection.

Minimum detection limits (signal-to-noise ratio 2) were determined for the three acids and are reported in Table I. For the conditions and instrument settings

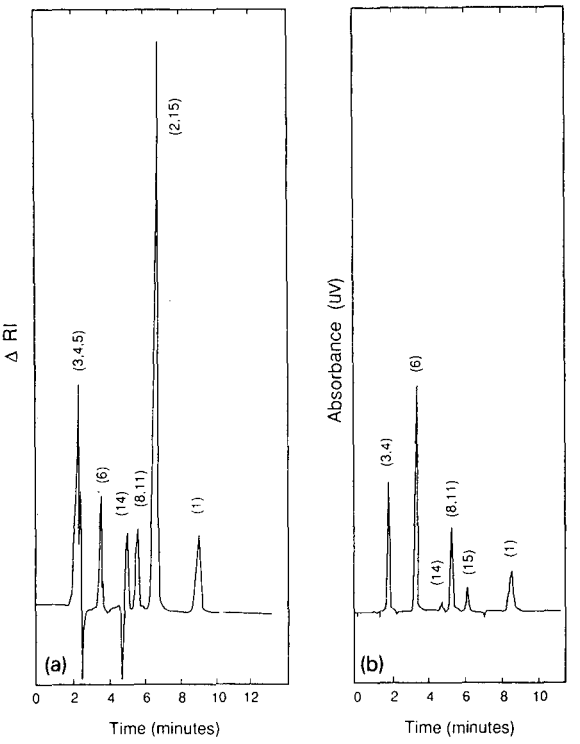

Fig. 4. Detection of a mixture of CMPO (1), TPB (2), (DΦP) (3), [O(Φ)P] (4), DOPO (5), DΦPO (6), O(Φ)PO (8), M(O)(Φ)PO (11), CIBA (14) TCE (15), using RI (a) and UV (b).

indicated, the limits of detection are in a similar range for both detectors. Under these conditions with a 10-μl injection of a 0.2 *M* solution of CMPO (solubility in the mobile phase is limited to 0.25 *M*), 0.3 mg (0.04%) of acid impurities could be detected with the RI detector. In the UV detector, a.u.f.s. settings < 0.05 resulted in a noise increase proportional to the signal of the sample. Therefore, to obtain lower detection limits (0.005–0.01 a.u.f.s. working range), an additional noise-reducing filter would need to be installed in the UV–VIS detector.

The UV detector only detected the phenyl-substituted species, whereas the RI detector can detect all compounds potentially present. The RI detector had solvent interference peaks in the acid region, which reduced the detection limits, and the UV detector did not. The detection limits for the UV detector were greater than the RI detector under certain conditions. Using the two detectors in tandem allows one to glean the advantages of both and some speciation may be accomplished.

The neutral impurites or degradation products usually observed in samples of TRUEX process solvent are not generally deleterious to the performance of the process. However, their presence reduces the concentration of the CMPO in the process solvent. In addition, the phosphorus-containing neutral species can degrade or oxidize to acidic impurities.

The neutral secondary phosphine oxide impurities DΦPO, O(Φ)PO, and DOPO have not been observed in degraded process solvent[6] nor are they generally encoun-

tered in commercially available samples of CMPO that we have analyzed. However, M(O)(Φ)PO is formed during the degradation of CMPO by hydrolytic and radiolytic mechanisms[6–8]. It has been suggested that this tertiary phosphine oxide is not significantly deleterious to the process in minor concentrations and may to some extent be able to replace CMPO in the extraction of Am(III) as the CMPO is consumed[6]. However, significant concentrations of M(O)(Φ)PO in the process solvent reduce the overall effectiveness of the process solvent to extract/strip transuranic metal ions and necessitate the replacement of the solvent. Degraded solvent also contains traces of N,N-diisobutylacetamide[7,8]. Commercial samples of CMPO have been observed to contain minor concentrations of 2-chloro-N,N-diisobutylacetamide (CIBA), a starting material used in the preparation of the extractant. Because of the thermal instability of CMPO, which generates M(O)(Φ)PO, and the reaction of phenyl-substituted secondary phosphine oxides with diazomethane (see above), the application of an HPLC method to the neutral impurities also was warranted.

Fig. 4 displays the chromatogram of the acidic impurities [DΦP, O(Φ)P and DOP] and the neutral impurities [DΦPO, O(Φ)PO, M(O)(Φ)PO, CIBA]. The detection limits and retention times are summarized in Table I for both the RI and UV detectors. The compounds fall into three rough regions of the chromatogram with the acidic impurities eluting first, the neutral impurities with TBP and TCE eluting second, and CMPO eluting last. The neutral impurities provide a linear response in the range studied to at least twice their detection limit and provice baseline resolution. The impurities O(Φ)PO and M(O)(Φ)PO are detected by both detectors and could not be discriminated using the HPLC conditions developed herein. Fortunately, these compounds are readily detected by the previously developed GC method. TBP and TCE do not provide baseline resolution under these conditions. However, TCE is detectable by the UV detector and TBP is not, which allows discrimination between the two compounds by use of both detectors. As both compounds are used to formulate the TRUEX process solvent, both would be present in large concentrations and would not interfere with the analysis for CMPO or the impurities.

CONCLUSIONS

The development of a capillary GC and an HPLC procedure for the analysis of TRUEX process solvent provides complementary procedures for the identification and quantification of neutral and acidic impurities in addition to the solvent components. Analyses using the GC method require derivatization before analysis but give reliable identification and quantification data for a diverse number of structurally similar compounds. The development of the complementary HPLC process overcomes some of the difficulties encountered with the GC method. HPLC obviates the need for derivatization, eliminates thermal decomposition during analysis, and readily allows the direct analysis of radioactive process samples. Reliable quantification of total acidic and/or neutral components has been accomplished despite the inability to identify individual acidic or neutral components.

ACKNOWLEDGEMENTS

The Argonne group would like to thank the Westinghouse Hanford Company, Richland, WA, U.S.A., for providing the funding for this research. The Los Alamos group would like to thank Fred Marsh and Steve Yarbo of Los Alamos (Group MST.12) for supplying the need for and support of analytical method development.

REFERENCES

1 W. W. Schulz and E. P. Horwitz, *Sep. Sci. Technol.*, 23 (1988) 1191.
2 W. W. Schulz and E. P. Horwitz, *J. Less-Common Metals*, 122 (1986) 125.
3 E. P. Horwitz and R. C. Gatrone, unpublished results.
4 R. C. Gatrone, L. Kaplan and E. P. Horwitz, *Solvent Extr. Ion Exch.*, 5 (1986) 1075.
5 E. P. Horwitz, R. Chiarizia and R. C. Gatrone, *Solvent Extr. Ion Exch.*, 6 (1988) 93.
6 R. Chiarizia and E. P. Horwitz, *Solvent Extr. Ion Exch.*, 4 (1986) 677.
7 K. L. Nash, R. C. Gatrone, G. A. Clark and P. G. Rickert, *Sep. Sci. Technol.*, 23 (1988) 1355.
8 K. L. Nash, P. G. Rickert and E. P. Horwitz, *Solvent Extr. Ion Exch.*, 7 (1989) 655.
9 A. S. Boparai, *J. Chromatographic Sci.*, 24 (1986) 434.
10 T. H. Black, *Aldrichimica Acta*, 1 (1983) 3.

Journal of Chromatography, 516 (1990) 405–413
Elsevier Science Publishers B.V., Amsterdam

CHROM. 22 551

Chromatographic determination of amines in biological fluids with special reference to the biological monitoring of isocyanates and amines

IV. Determination of 1,6-hexamethylenediamine in human urine using capillary gas chromatography and selective ion monitoring

MARIANNE DALENE, GUNNAR SKARPING* and TORBJÖRN BRORSON
Department of Occupational and Environmental Medicine, University Hospital, 221 85 Lund (Sweden)
(First received January 8th, 1990; revised manuscript received May 9th, 1990)

ABSTRACT

A capillary gas chromatographic (GC) method was developed for the determination of 1,6-hexamethylenediamine (HDA) in hydrolysed human urine. The method was based on a derivatization procedure with heptafluorobutyric anhydride. The amides formed were determined using capillary GC with selected ion monitoring in the chemical ionization mode with ammonia as reagent gas. The overall recovery was 34% for a concentration of 100 μg/l of HDA in urine. The minimum detectable concentration in urine was below 0.5 μg/l. The precision of the method was 5% (n = 9). Deuterium-labelled HDA [$H_2NC^2H_2(CH_2)_4C^2H_2NH_2$] was used as the internal standard. A male subject was exposed to hexamethylene diisocyanate (HDI) for 7.5 h in a test chamber. The average air concentration of HDI was *ca.* 30 μg/m^3, which corresponds to *ca.* 85% of the threshold limit value in Sweden (35 μg/m^3). The half time of urinary levels of HDA was *ca.* 1.4 h and more than 90% of the urinary elimination was completed within 4 h after the exposure. The amount of HDA excreted in urine was *ca.* 10 μg, corresponding to *ca.* 10% of the estimated inhaled dose of HDI.

INTRODUCTION

1,6-Hexamethylenediamine (HDA) is an aliphatic diamine of industrial importance. HDA is used as raw material for nylon 66, and in the manufacture of urethane coatings and polyamides. The compound is also used in paints and as a curing agent for epoxy resins[1]. HDA is moderately toxic[2–4], but has been associated with health

0021-9673/90/$03.50

hazards in the work environment[5]. In addition, HDA has been determined in air after pyrolysis of lacquered metal parts with a lacquer-resin based on 1,6-hexamethylene diisocyanate (HDI)[6].

Measurements of the concentrations of chemicals in the air in the breathing zone give only fragmentary information about the absorbed dose, and do not ensure that the worker is totally protected from adverse health effects. Biological monitoring integrates exposure by all routes (*e.g.*, pulmonary, oral and skin) and from all sources. It also consider individual factors such, as work load habits and genetic differences in biotransformation.

The possibility of using urine analyses for diamines as a test for occupational diisocyanate exposure was proposed by Rosenberg and Savolainen[7] and Brorson *et al.*[8].

Methods for the determination of 2,4- and 2,6-diaminotoluene and 4,4′-methylenedianiline (MDA) in human urine using gas chromatography–mass spectrometry (GC–MS) were described in Parts II and III in this series[9,10]. Deuterium-labelled internal standards were used. The biological monitoring of inhalation exposure to 2,4- and 2,6-toluenediisocyanate and skin exposure to MDA, respectively, were the purposes of those studies.

Methods for the determination of HDA, at mg/l levels in plasma, have been described by Egorin *et al.*[11]. Recently, a method based on a two-phase derivatization procedure with ethyl chloroformate was developed in our laboratory[12]. Capillary GC with thermionic specific detection (GC–TSD) made it possible to determine low concentrations (10–1000 μg/l) of HDA in urine after oral administration of the compound.

However, the potential use of HDA as a marker of HDI exposure made it necessary to develop an even more sensitive method. The aim of this study was to develop a method for the determination of HDA in trace amounts (μg/l) in complex matrixes such as biological fluids.

EXPERIMENTAL

Apparatus

A Shimadzu (Kyoto, Japan) GCMS-QP 1000 EI/CI quadrupole mass spectrometer connected to a Shimadzu GC-9A gas chromatograph equipped with a split/splitless injection system SPL-G9 and a Shimadzu autosampler (AOC-9) was used.

The starting temperature of the column oven was set near to the boiling point of the solvent, and for toluene it was 100°C isothermal for 2 min. The split exit valve was kept closed for 1 min after injection. After elution of the solvent, the column was programmed at 30°C/min to 280°C, where it was maintained for 1 min. The capillary column outlet was mounted directly in the ion source. The gas chromatograph–mass spectrometer interface and the ion source were held at 250°C. Chemical ionization was utilized with ammonia and isobutane as reagent gases. Samples were introduced into the chromatographic system with an autosampler using a splitless technique at 250°C. The carrier gas was helium and the inlet pressure was 1 kg/cm^2. The amount injected was typically 4 μl, using a Hamilton 701RN syringe with a point style 5 needle with a conical point and a side-hole to minimize septum coring.

For enrichment and evaporation of solvent a vacuum desiccator connected to an aspirating pump was used. The apparatus was equipped with an electrically heated oven, designed and manufactured at our laboratory. A Sigma 3E-1 centrifuge (Sigma, Harz, F.R.G.) was employed for phase separation.

Columns

A fused-silica capillary column (30 m × 0.247 mm I.D.) coated with DB-5 bonded stationary phase (J & W Scientific, Folsom, CA, U.S.A.) with a film thickness of 0.25 μm was used.

Chemicals

Chemicals used were 1,6-hexamethylenediamine (HDA) and toluene from Janssen (Beerse, Belgium), heptafluorobutyric anhydride (HFBA) from Pierce (Rockford, IL, U.S.A.), deuterium-labelled HDA [$H_2NC^2H_2(CH_2)_4C^2H_2NH_2$] from MSD Isotopes (Merck Frosst Canada, Montreal, Canada), HCl, NaOH and K_2HPO_4 from Merck (Darmstadt, F.R.G.)

Synthesis of 1,6-hexamethylenediheptafluorobutyramide

After recrystallization of HDA from toluene, 0.2 g (1.6 mmol) of the amine and 1.6 g (4 mmol) of HFBA were dissolved in ethyl acetate and the solution was heated at 50°C for 10 min. After cooling to room temperature, the excess of reagent and liberated acids were extracted with a 1 *M* phosphate buffer solution (pH 7.0) and the organic phase was eluted through a silica column with ethyl acetate. Evaporation of the ethyl acetate to dryness gave a *ca.* 500 mg (80%) yield of the amide (HDA–HFBA).

Preparation of standard solutions

Standard solutions of the HDA–HFBA derivatives was prepared by dissolving accurately weighed amounts in toluene. The solutions were then further diluted with toluene to the appropriate concentrations. Standard solutions of HDA and deuterium-labelled HDA were prepared and stored as 6 *M* HCl solutions.

Sampling and storage of urine samples

Urine samples were acidified by the addition of 5 ml of 6 *M* HCl per *ca.* 100 ml of urine. The urine samples were stored in a refrigerator at 4°C until analysis.

Work-up procedure

A 1.5-ml volume of 6 *M* HCl and 1.5 ml of 6 *M* HCl containing the internal standard (*ca.* 6 μg/l), were added to a 2-ml urine sample. The mixture was heated at 100°C overnight for hydrolysis. After cooling to room temperature, a 2-ml aliquot was transferred to a test-tube and 4 ml of saturated NaOH and 3 ml of toluene was added. HDA was extracted into the organic phase by shaking the mixture for 5 min. The sample was then centrifuged at 1500 *g* for 10 min. A 2-ml volume of the organic layer was transferred into a 10-ml test-tube and 20 μl of HFBA were added. The mixture was immediately shaken vigorously for 5 min on a Vortex mixer. The excess of reagent and the acid formed were extracted for 10 min with 2 ml of 1 *M* phosphate buffer solution (pH 7.5). The toluene layer, containing the amide formed, was then transferred into a test-tube. The toluene phase was evaporated in a vacuum desiccator at 30°C and the

dry residue was dissolved in 50 μl of toluene. A volume of 4 μl was then injected into the GC–MS system. Duplicate analyses and injections were made.

RESULTS AND DISCUSSION

Standard

The identity of the HDA–HFBA derivative was confirmed by GC–MS, and the purity was determined using capillary GC–TSD and GC with flame ionization detection. The purity was further examined by elemental analysis, and was found to be higher than 99%.

Internal standard

The determinations by GC–MS were performed using tetradeuterated HDA as the internal standard. The hydrogen atoms in the α-positions to the amine groups were exchanged with deuterium atoms. Several advantages of using the deuterium-labelled compound as internal standard were found. The chromatographic and chemical properties were found to be similar to those of HDA, which was very important owing to the low overall recovery. No interferences were found for the mass fragments monitored using chemical ionization and the similar ionization patterns of HDA and tetradeuterated HDA were favourable for easy calibration of the mass spectrometer. Finally, tetradeuterated HDA was not expected to occur as an interferent in the sample.

Work-up procedure

Storage and treatment of samples. HDA-spiked urine samples were found to be stable after acidification. No noticeable change in the sample composition was observed when stored in darkness at room temperature for several weeks.

Hydrolysis. No losses were found in the hydrolysis step for HDA-spiked urine. The sum of free HDA and hydrolysable HDA conjugates was determined.

Derivatization. A two-phase derivatization of aliphatic diamines with HFBA has earlier been developed for aqueous solutions. For urine samples the recoveries were very low, and not reproducible[13]. In this study, the derivatization procedure was therefore performed in toluene, after extraction of aqueous urine hydrolysates. The excess of reagent and liberated acid were removed by extraction with a 1 *M* phosphate buffer solution (pH 7.5), without any measurable loss of the HDA amide derivative.

Enrichment. A 1-ml volume of the organic phase containing the amide derivative was evaporated to dryness and the residue dissolved in 50 μl of toluene, giving a 50-fold enrichment. The recovery for the evaporation and enrichment step was *ca.* 100%.

Choice of reagent

Derivatization reagents such as trifluoroacetic anhydride (TFAA), pentafluoropropionic anhydride (PFPA), heptafluorobutyric anhydride (HFBA), acetic anhydride (AA), ethyl chloroformate and isobutyl chloroformate were tested, giving *ca.* 100% recovery. All the reagents tested could be used for a single-phase derivatization. With the exception of the AA derivatives, all the tested derivatives were found to have satisfactory chromatographic behaviour. However, the sensitivity of the GC–selected ion monitoring (SIM) system was much better for the perfluoro fatty acid

derivatives. The HDA–HFBA derivative showed a slightly better sensitivity and better resolution relative the matrix, and the HDA–HFBA derivative was therefore chosen.

Mass spectrometry

Electron impact (EI) with ionization potential 70 eV and chemical ionization (CI) with ammonia or isobutane were investigated (Fig. 1). It was established that several components in the sample were derivatized with the acylating reagent. Selective detection was therefore necessary. The sensitivity in the EI mode was relatively low, and *ca.* 50 ng were needed to give an acceptable spectrum when injecting 1 μl of standard solution. The relative abundance of the molecular ion was only *ca.* 1%. Owing to the relative abundance, the fragment ions of *m/z* 339 and 343 ($M^+ - C_3F_7$) were chosen for the SIM of HDA–HFBA and tetradeuterated HDA–HFBA. When analysing spiked urine samples, baseline separation of the investigated compounds relative to the matrix could not be achieved.

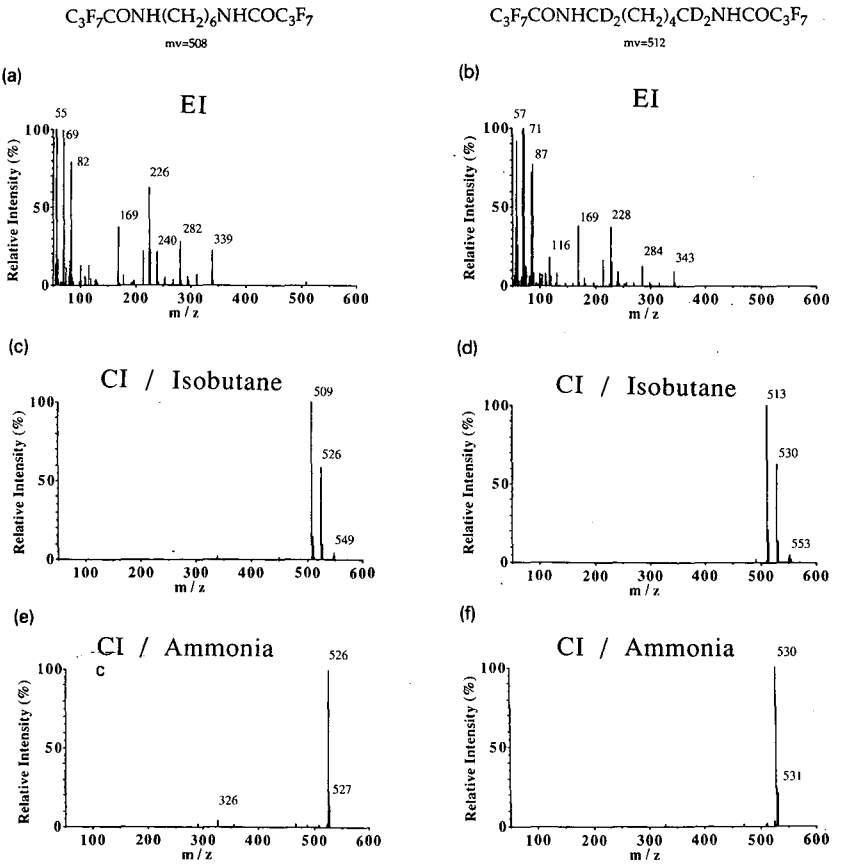

Fig. 1. Mass spectra obtained with electron impact (70 eV) for (a) HDA–HFBA derivative and (b) deuterium-labelled HDA–HFBA derivative, chemical ionization using isobutane for (c) HDA–HFBA derivative and (d) deuterium-labelled HDA–HFBA derivative and chemical ionization using ammonia for (e) HDA–HFBA derivative and (f) deuterium-labelled HDA–HFBA derivative. The amount injected was *ca.* 70 ng. mv = Molecular weight.

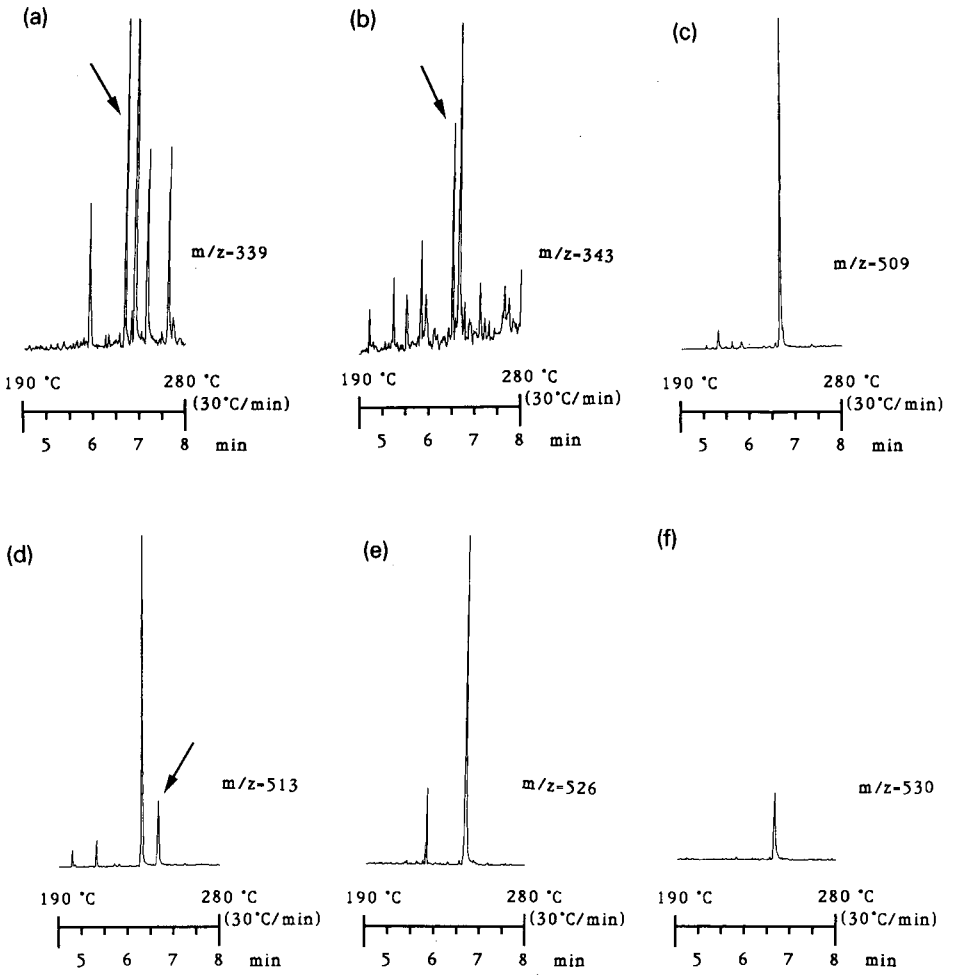

Fig. 2. Selected ion monitoring of HDA in hydrolysed urine samples using electron impact and chemical ionization. Chromatogram (a) shows EI and m/z = 339, (c) shows CI using isobutane and m/z = 509 (M + 1) and (e) shows CI using ammonia and m/z = 526 (M + 18) for a urine sample from a subject exposed for 7.5 h to HDI (the HDI air concentration was *ca.* 30 $\mu g/m^3$). The peaks in the chromatograms correspond to a concentration of *ca.* 20 μg of HDA per litre of hydrolysed urine. Chromatogram (b) shows EI and SIM, m/z = 343, (d) shows CI using isobutane, m/z = 513 (M + 1), and (f) shows CI using ammonia, m/z = 530 (M + 18), for deuterium-labelled HDA–HFBA derivative used as the internal standard. Column: J & W Scientific fused-silica column coated with DB-5 bonded stationary phase (30 m × 0.247 mm I.D.), film thickness 0.25 μm. Inlet pressure of the carrier gas (helium): 1.0 kg/cm^2. Splitless injection (1 min) of 4 μl of toluene. Temperature programming: isothermal at 100°C (2 min), increased at 30°C/min to a final temperature of 280°C, which was maintained for 1 min.

However, when using CI with ammonia as the reagent gas, the M + 18 ions of HDA–HFBA and tetradeuterated HDA–HFBA (*m/z* 526 and 530, respectively) were the most abundant. The abundance of the M + 1 ions (*m/z* = 509 and 513, respectively) was less than 2%. Using isobutane as the reagent gas, the M + 1 ions were the most abundant (*m/z* 509 and 513, respectively). The relative abundances of the M + 18 ions were *ca.* 60%.

SIM with ammonia as reagent gas (monitoring the ions of *m/z* 526 and 530, respectively) showed a *ca.* ten times higher sensitivity than that with isobutane (*m/z* = 509 and 513, respectively). Also, the selectivity when analysing urine samples was improved. The contamination of the ion source was much lower when ammonia was used. The analysis of several hundred of samples without cleaning the ion source were therefore possible. Baseline separation of the investigated compounds relatively the urine matrix was also found. The use of ammonia as reagent gas was therfore concluded to be the best choice for the determination of HDA in hydrolysed urine.

Chromatography

The chromatographic behaviour of the amide derivatives was excellent. The use of a column with an apolar stationary phase with relatively low film thickness was preferred owing to the lower temperature and column bleeding. Chromatograms of urine samples originating from HDI-exposed subjects are shown in Fig. 2. No interfering peaks disturb the evaluation of the chromatogram using SIM and CI.

Quantitative analysis

Recovery. On extracting HDA from aqueous solutions by the addition of saturated NaOH to an organic phase, no losses were found. However, on extracting urine hydrolysates by the same procedure, considerable losses were found. On spiking human urine and performing the work-up procedure, the overall recovery was found to be 34 ± 4% (n = 12) for a concentration of 100 μg of HDA per litre of urine.

Calibration graphs. Human urine was spiked by adding different amounts of HDA and performing the work-up procedure as described above. For each HDA concentration two determinations, with duplicate injections, were made. No significant difference between plotted peak heights or peak-areas ratios, relative to the internal standard, was observed. The investigated concentration range of 1–30 μg/l in urine gave a correlation coefficient of 0.985 for the peak-area ratio measurements (n = 7).

Precision. The overall precision was found to be 5% (n = 9) for human urine spiked with 22 μg/l of HDA.

Detection limit. The detection limit using SIM and EI was set by the matrix and was found to be more than 100 μg/l of HDA in urine.

The detection limit using SIM and CI with ammonia as reagent gas was *ca* 0.5 μg/l of HDA in urine. No interfering peaks appeared when urine samples from five unexpected subject were examined. As the detection limit is set by the instrument, it would be possible to lower the detection limits by using a more sensitive instrument and by further enrichment of the sample.

Application

A male subject was exposed to HDI for 7.5 h in a test chamber. The average

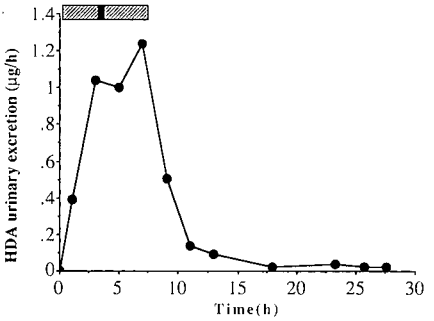

Fig. 3. Urinary excretion of HDA and hydrolysable HDA conjugates for a subject exposed to HDI for 7.5 h in a test chamber. The HDI air concentration was *ca.* 30 $\mu g/m^3$ and the estimated inhaled dose of HDI was *ca.* 100 μg. Urinary excretion is shown at the mid-time of each observation period. Bar: shaded area, HDI exposure; black area, exposure-free period.

concentration of HDI was *ca.* 30 $\mu g/m^3$, which corresponds to *ca.* 85% of the threshold limit value (TLV) in Sweden (35 $\mu g/m^3$). The estimated dose of inhaled HDI was *ca.* 100 μg. All urine was sampled before, during and after the exposure, and the related amine HDA was determined in hydrolysed urine. The half-time of urinary levels of HDA was short ($t_{1/2} \approx 1.4$ h) and >90% of the urinary elimination was completed within *ca.* 4 h after termination of the exposure (Fig. 3). The detection limit of the method was sufficient for the determination of HDA in urine, thus offering the possibility of biological monitoring of occupational HDI exposure.

CONCLUSIONS

A method has been developed for assessing occupational exposure to HDI and HDA. Selective and sensitive determination of HDA in hydrolysed urine, at low $\mu g/l$ levels, was possible using GC–MS. The use of tetradeuterated HDA as internal standard was demonstrated to give accurate and precise determinations. The method makes it possible to determine HDA in urine of subjects exposed to HDI at the Swedish TLV level.

ACKNOWLEDGEMENTS

The authors thank Professor Staffan Skerfving, Head of the Department of Occupational and Environmental Medicine, for his interest in this work. Dr. Carsten Sangö is thanked for his interest and valuable discussions. Åsa Amilon performed skilful technical assistance. We also gratefully acknowledge the Swedish Work Environment Fund (AMFO 88-0161) for financial support.

REFERENCES

1 M. Sittig, *Handbook of Toxic and Hazardous Chemicals and Carcinogens*, Noyes, Park Ridge, NJ, 2nd ed., 1985.
2 O. L. Dashiell and G. L. Kennedy, *J. Appl. Toxicol.*, 4 (1984) 320.
3 F. R. Johannsen, G. J. Levinskas, R. Ben-Dyke and G. K. Hogan, *Fundam. Appl. Toxicol.*, 9 (1987) 504.
4 C. A. Manen, R. D. Hood and J. Farina, *Teratology*, 28 (1983) 237.

5 R. R. Beard and J. T. Noe, *Patty's Industrial Hygiene and Toxicology*, Wiley-Interscience, New York, 1981, p. 3135.
6 G. Skarping, M. Dalene and L. Mathiasson, *J. Chromatogr.*, 435 (1988) 453.
7 C. Rosenberg and H. Savolainen, *Analyst (London)*, 111 (1986) 1069.
8 T. Brorson, G. Skarping, J. F. Sandström and M. Stenberg, *Int. Arch. Occup. Environ. Health*, 62 (1990) 79.
9 J. F. Sandström, G. Skarping and M. Dalene, *J. Chromatogr.*, 479 (1989) 135.
10 A. Tiljander, G. Skarping and M. Dalene, *J. Chromatogr.*, 479 (1989) 145.
11 M. J. Egorin, E. G. Zuhowski, M. S. B. Nayar and P. S. Callery, *J. Chromatogr.*, 415 (1987) 148.
12 G. Skarping, M. Dalene, T. Brorson, J. F. Sandström, C. Sangö and A. Tiljander, *J. Chromatogr.*, 479 (1989) 125.
13 L. Renman, *Doctoral Thesis*, Lund University, 1987.

Journal of Chromatography, 516 (1990) 415–426
Elsevier Science Publishers B.V., Amsterdam

CHROM. 22 547

Capillary supercritical fluid chromatography of aliphatic amines

Studies on the selectivity and symmetry with three different columns using carbon dioxide or nitrous oxide as mobile phase[a]

OLLE GYLLENHAAL* and JÖRGEN VESSMAN
Department of Analytical Chemistry, Pharmaceutical R & D, AB Hässle, S-431 83 Mölndal (Sweden)
(First received January 17th, 1990; revised manuscript received May 8th, 1990)

ABSTRACT

The supercritical fluid chromatography of intact aliphatic amines with different columns is described. One group of amines was based on N,N-dimethyl-*n*-octylamine and related primary and secondary amines, and the other on the amino alcohol metoprolol and several of its analogues. Columns with three different phases were investigated, one non-polar coated with 5% phenyl methyl polysiloxane and two more polar with 25% cyanopropyl methylphenyl polysiloxane and Carbowax 20M. Generally, equal molar amounts were injected under splitless conditions and the peak symmetry was recorded.

The system with the non-polar silicone phase was more inert, followed by the wax-phase column. The cyanopropyl column gave severe peak tailing although it was loaded with five times more of the amines than the other columns. The selectivity was investigated and was found higher with the two polar columns. Both showed a marked increase in the retention of amines with free hydrogens. With nitrous oxide the selectivity was almost the same as that with carbon dioxide as mobile phase. The nature of the flame ionization detector changed, however, giving a negative baseline drift on pressure programming. An interesting conclusion is that the amines are chromatographed as such with carbon dioxide as the mobile phase.

INTRODUCTION

Many drugs contain aliphatic nitrogens. Primary amines do not occur so widely, although many tertiary amines are metabolized by dealkylation to primary amines

[a] Parts of this paper were presented at the *Symposium on Supercritical Fluid Chromatography, Snowbird, UT, U.S.A., June 1989.*

0021-9673/90/$03.50

or may contain trace amounts of the latter as impurities in drug substances. Today the method of choice for the monitoring of impurities is liquid chromatography with UV-detection. Accurate quantification requires a knowledge of the molar absorptivity, ε, which is not always the case with unknown impurities. Here, gas chromatography with flame ionization detection would be attractive, but the necessity to derivatize in order to prevent adsorption in the gas chromatographic system in principle precludes the use of this technique. The adsorption is often less pronounced with apolar stationary phases as in this instance the column walls can be highly deactivated in comparison with more polar phases, as these require some activity in order to be wetted before forming stable films. Still, the high boiling point of many amines often makes gas chromatography unattractive.

In supercritical fluid chromatography (SFC) there is a widespread conception that carbon dioxide can react with primary and secondary aliphatic amines. Few reports exist on the SFC of primary amines with carbon dioxide. Most chromatograms of tertiary amines have been recorded after split injection followed by density programming of the fluid, the actual amount introduced being virtually unknown. As with temperature programming in capillary gas chromatography, this mode of elution improves the peak shape. Under SFC conditions there are widely different opinions about the feasability of chromatographing primary amines without complications using carbon dioxide as the fluid. Except for several papers by Fields and co-workers[1–4], there are few publications that deal with the SFC of free amines in any detail. It has been suggested that a relationship between the basicity of an amine and its compatibility with carbon dioxide exists[5]. It was concluded that amines with pK_b below 9 would react[5], but these constants refer to aqueous solutions[2]. Fields and Grolimund[2] were able to show that this rule does not apply to tertiary alkylamines but for most secondary alkylamines except where the amine is sterically hindered. The presence of water may play a role but even under anhydrous conditions carbon dioxide reacted with diglycolamine and bis-2-propanolamine, as indicated by pressure measurements[6]. The use of alternative fluids such as dichlorodifluoromethane and sulphur hexafluoride has also been demonstrated[3,4].

David and Sandra[7] were not able to elute long-chain fatty acid amines by capillary SFC with nitrogen-selective detection. The column was ruled out as the cause as the amines could be gas chromatographed[7]. It is difficult to evaluate these observations as the amounts of the amines injected and the column temperatures were not given. As a conclusion the authors advocated derivatization of the amines with trifluoroacetic anhydride[7]. For the study of impurities derivatization will always be a drawback, the main reason being the possibility of different reaction kinetics of the components which might induce discrimination.

In a study on capillary and micropacked columns for SFC, Schomburg *et al.*[8] were unable to elute unspecified primary and secondary amines with carbon dioxide with several different supports. They suspected that if the amines do not react with carbon dioxide in the column itself to give insoluble carbamates, they might react at the elevated temperature in the restrictor zone. In this case the problem seems more likely to be due to the nature of the support materials investigated than to the mobile phase itself.

Nitrous oxide was selected as the mobile phase for basic compounds to eliminate the risk of reaction with analytes containing primary and secondary amine

functions, although mainly aromatic amines were studied[9]. A nitrogen-selective detector was chosen for its high selectivity and low detection limits, although it was found that the selectivity towards hydrocarbons was only *ca.* 200. Some adsorption in the column was also observed when free amines were analysed at 100 ppm or lower.

In capillary SFC the flame ionization detector is the most widely used. This detector offers good detectability and compatibility with some of the fluids most often used as mobile phases. Another important advantage is that equal amounts of hydrocarbons give the same signal independent of molecular weight. The signal is reduced when heteroatoms are introduced, but still the peak area can be used to calculate amounts with good accuracy.

The aim of this work was to investigate the selectivity for aliphatic amines using three capillary columns with different stationary phases available for SFC. We were also interested in observing the peak symmetry of the amines in the chromatographic system, as few data exist on this aspect in SFC. As discussed above, primary amines may react with carbon dioxide. Therefore, nitrous oxide was also studied in order to eliminate any artefacts with carbon dioxide and to see whether there were any significant selectivity changes.

EXPERIMENTAL

Apparatus

SFC was performed with an instrument constructed in our laboratories from an ISCO (Lincoln, NE, U.S.A.) μ-LC 500 syringe pump for fluid delivery, a Hewlett-Packard 5710A gas chromatograph as column oven and for detection and a Perkin-Elmer 56 recorder. The pump head was cooled to -15°C, when the pump was filled with liquid carbon dioxide or nitrous oxide, with an EK 12 cooling bath (Freon) from Hake (Karlsruhe, F.R.G.).

In all experiments the oven temperature was 100°C and the detector temperature 300°C. The inlet pressures of hydrogen and air to the flame ionization detector were 20 and 25 p.s.i., respectively. With nitrous oxide as the fluid it was necessary to lower the hydrogen pressure to 15 p.s.i. in order to reduce the detector noise.

The injection valve was a Valco (Houston, TX, U.S.A.) C14W.06 and all injections were made in the splitless mode. The column was attached to the bottom of this valve through a 5-cm piece of precut stainless-steel tubing of 0.01 in. I.D. and 1/16 in. O.D. (0.02 in. for the the DB-Wax column). The column extended *ca.* 0.2 mm from the stainless-steel tubing towards the rotor of the valve. At the other end of the tubing the column was sealed with a 15% graphite Vespel ferrule on a 1/16-in. stainless-steel Swagelock union. Ten seconds after injection the valve was returned to the load position. Frit restrictor (in 100 μm I.D. fused-silica tubing) (Lee Scientific, Salt Lake City, UT, U.S.A.) were shortened to *ca.* 8 mm, giving a linear velocity of 15 cm/s at 1500 p.s.i. carbon dioxide, the oven at 100°C and the detector at 300°C.

Columns

All capillary columns were 20 m $\times$ 100 μm I.D. fused-silica columns for SFC. They were SB-Phenyl-5, film thickness $d_f = 0.5$ μm, and SB-Cyanopropyl-25, $d_f = 0.25$ μm (both from Lee Scientific) and DB-Wax, $d_f = 0.10$ μm, from J&W (Folsom, CA, U.S.A.).

Fluids

The cylinder with carbon dioxide 3.5 (99.95% purity) and dipper tube was from AGA (Lidingö, Sweden), as was the nitrous oxide 2.0 (99.0% purity).

Chemicals

The simple aliphatic amines used are listed in Table I. They are available from Eastman Kodak (Rochester, NY, U.S.A.) and Fluka (Buchs, Switzerland). Metoprolol tartrate and analogues were from the Department of Organic Chemistry, AB Hässle.

TABLE I

ALIPHATIC AMINES STUDIED

Name	*Abbreviation*	*Structure*[a]
Simple aliphatic amines		
N,N-Dimethyl-*n*-octylamine	DMOA	$C_8H_{17}N(CH_3)_2$
N-Methyl-*n*-octylamine	MOA	$C_8H_{17}NHCH_3$
n-Octylamine	OA	$C_8H_{17}NH_2$
Tri-*n*-Butylamine	TBA	$N(C_4H_9)_3$
Di-*n*-Hexylamine	DiHxA	$NH(n\text{-}C_6H_{13})_2$
Metoprolol and analogues		
Metoprolol	Meto	$ArCH(OH)CH_2NHCH(CH_3)_2$
H 105/29	tButyl	$ArCH(OH)CH_2NHC(CH_3)_3$
H 173/09	Ethyl	$ArCH(OH)CH_2NHC_2H_5$
H 98/52	PrimAmine	$ArCH(OH)CH_2NH_2$
H 170/64	Alcohol	$ArCH(OH)(CH_2)_3CH_3$
H 170/69	Amine	$ArCH_2CH_2NHCH(CH_3)_2$
Oxazolidone of metoprolol	Oxaz	$ArCH(O)CH_2N(CO)CH(CH_3)_2$

[a] Ar = 4-(2-methoxyethyl)phenoxy.

Sample solutions

The amines were dissolved in ethyl acetate and diluted to $2 \cdot 10^{-4}M$. In some instances a small volume of phosphate buffer (pH 12) was added to convert salts into free bases. This ethyl acetate stock solution was further diluted 1:5 (to $4 \cdot 10^{-5}M$). Owing to adsorption in the chromatographic system some amines were not diluted. The amounts loaded into the valve are given in the tables.

Calculations

After isobaric (isoconfertic) chromatography the capacity factor, k', was calculated. Ethyl acetate was assumed to be unretained. The asymmetry factor was calculated 10% up from the baseline and at as high a chart speed of the recorder as possible.

RESULTS AND DISCUSSION

Chromatographic system

As our aim was to study the SFC of aliphatic amines, maximization of the number of theoretical plates was not attempted. By using split or timed split injections, the column efficiency can be utilized better, but this injection mode is not practical when known, or reproducible, amounts are to be injected. In this work the molar amount injected was the same with a few exceptions. The amount is based on the nominal volume of the injection valve. This, however, can vary by as much as 30%[10]. With each column we studied the retention of the amines under constant conditions. The peak symmetry was also recorded and is given as the asymmetry factor. The three columns will be discussed in some detail under separate headings and then in comparison with their competitors. Thus the hold-up time in the chromatographic system will be different for the individual amines. Another approach would have been to obtain the same retention (capacity factor) for each amine, but then the actual density of the mobile phase would have been different. Representative chromatograms are given in Fig. 1 for (a) a neutral compound and (b) a secondary amine.

Capillary chromatography of amines

Chromatography of underivatized aliphatic amines is hampered by their polar nature, which causes interactions with polar and acidic sites in the chromatographic system. Generally the free silanol groups of the fused-silica column wall are responsible. In this study we chose one group of simple aliphatic amines as test compounds (Table I) and also one group based on the β-adrenoreceptor blocking agent metoprolol, which in addition to a secondary amine function has a secondary alcohol group in the molecule. Here compounds lacking either the amine or the alcohol were also available for comparison (Table I).

SB-Phenyl-5 column

This column was coated with methyl phenyl polysiloxane (substitution degree 5:95) and cross-linked for SFC use. In the group of simple aliphatic amines, with carbon dioxide as mobile phase, the symmetry is best for the two tertiary amines tributylamine and dimethyloctylamine (Table II). For the other amines in this group, with free hydrogens, the asymmetry factor is almost 2. The poor, and varying, symmetry for octylamine is not surprising. The superior symmetry of the dihexylamine peak can be explained by better shielding of the nitrogen of the *n*-hexyl group compared with the methyl group of N-methyloctylamine.

The retention as shown by the capacity factors are of the same magnitude for the octylamines. The dihexylamine is retained almost twice as much as tributylamine, both having the same number of carbon atoms. This is more likely to be a solubility effect than interaction of the free hydrogen with any silanol groups. The poor selectivity, and thus differentiating power, is even more evident with the metoprolol group. Here most capacity factors are about 0.5–0.6 and there is little difference if the alcohol is removed, 0.53 *vs.* 0.58. The symmetry improves with increased bulkyness of the alkyl substituent on the nitrogen atom. The *tert.*-butyl peak is symmetrical whereas the ethyl analogue has a marked asymmetry. The analogous compound without the nitrogen, the secondary alcohol, has a pronounced tendency to give leading peaks

TABLE II

RESULTS WITH SB-PHENYL-5 COLUMN AND CARBON DIOXIDE

Compound[a]	*Pressure (p.s.i.)*	*Capacity factor, k'*	*Separation factor, α (=k'/k')*	*Asymmetry factor*	*Amount injected on-column (in 60 nl) (ng)*
DMOA	1500	0.73	1.00	1.21	38
MOA		0.80	1.10	1.52	34
OA		0.65	0.89	1.80, 1.62	31
TBA		1.00	1.37	1.18	44
DiHxA		1.89	2.59	1.35	44
Meto	2500	0.58	1.00	1.17	64
tButyl		0.62	1.07	1.04	67
Ethyl		0.58	1.00	1.54	62
PrimAmine		0.55	0.95	n.m.[b]	56
Alcohol		0.53	0.91	0.88	67
Alcohol				0.82	22
Amine		0.52	0.90	1.16	60
Oxaz		0.93	1.60	0.98	23

[a] See Table I.
[b] Not measured.

with the amounts injected. It is also interesting that the oxazolidone derivative of metoprolol is strongly retained on this non-polar phase.

With nitrous oxide virtually the same observations can be made. The pressure was adjusted so that the capacity factors of tributylamine and metoprolol were almost the same as those with carbon dioxide. The data are listed in Table III. The

TABLE III

RESULTS WITH SB-PHENYL-5-COLUMN AND NITROUS OXIDE

Compound[a]	*Pressure (p.s.i.)*	*Capacity factor, k'*	*Separation factor, α*	*Asymmetry factor*	*Amount injected on-column (in 60 nl) (ng)*
DMOA	1250	0.74	1.00	1.21	38
MOA		0.77	1.04	1.83	34
OA		0.63	0.85	1.88	31
DiHxA		1.80	2.43	1.97	44
TBA		0.98	1.32	1.07	44
Meto	2150	0.55	1.00	0.99	64
tButyl		0.56	1.02	0.91	67
Ethyl		0.54	0.98	1.04	62
PrimAmine		0.53	0.96	1.53	63
Alcohol		0.47	0.85	0.65	67
Alcohol				0.61	22
Amine		0.48	0.87	1.07	60
Oxaz		0.95	1.73	0.67	69
Oxaz				0.74	23

[a] See Table I.

symmetry is perhaps slightly better for some of the compounds. This is more evident in the metoprolol group of compounds. The fact that the separation factor hardly changes on going from carbon dioxide to nitrous oxide means that nitrous oxide as fluid offers little from a selectivity point of view. This observation has also been reported by others[11,12].

The main interest here with nitrous oxide is that this fluid strongly suggests that the octylamine peak with carbon dioxide as the fluid is no artefact, *e.g.*, a carbaminic acid product. As the conditions of the flame ionization detector were not identical, comparison of peak areas may be misleading. A possible way to circumvent this problem would be to include markers with nitrogen atoms in the molecules.

The octylamines were also gas chromatographed at 100°C on an SE-54 capillary column (d_f = 0.25 μm). The capacity factors recorded were, in order of increasing molecular weight and substitution, 1.33, 1.85 and 1.91.

SB-Cyanopropyl-25 column

This column is coated with cyanopropyl phenyl methyl polysiloxane (substitution degree 25:25:50). For the chromatography of amines this column required five times more concentrated solutions to give any peaks that were useful for calculation of asymmetry and capacity factors. Polar compounds devoid of aliphatic amine groups posed no problem. With the simple aliphatic amines the symmetry is better for the tertiary than the secondary compounds but is still poor. The selectivity is more marked here than with the SB-Phenyl-5 column discussed above. The secondary amines are retained 4–5 times more strongly than the tertiary amines (Table IV). However, even in this system it is not possible to differentiate between metoprolol and its *tert.*-butyl analogue.

When nitrous oxide was available this column was not capable of giving any meaningful chromatograms of amines. The reason for the poor performance of this column with aliphatic amines is not clear. It may be related to incomplete deactivation and the acidic nature of the column wall silica. Another possible cause is the

TABLE IV

RESULTS WITH SB-CYANOPROPYL-25 COLUMN AND CARBON DIOXIDE

Compound[a]	*Pressure (p.s.i.)*	*Capacity factor, k'*	*Separation factor, α*	*Asymmetry factor*	*Amount injected on-column (in 60 nl) (ng)*
DMOA	1500	0.12	1.00	9	194
MOA		0.51	4.25	21	172
TBA		0.11	0.92	12.5	222
DiHxA		0.64	5.33	>28	222
Meto	3000	0.46	1.00	9.3	320
tButyl		0.45	0.98	20	335
Alcohol		0.22	0.48	0.78 0.83	67
Amine		0.22	0.48	30	300
Oxaz		1.77	3.85	1.12	68

[a] See Table I. OA, PrimAmine and Ethyl were not attempted.

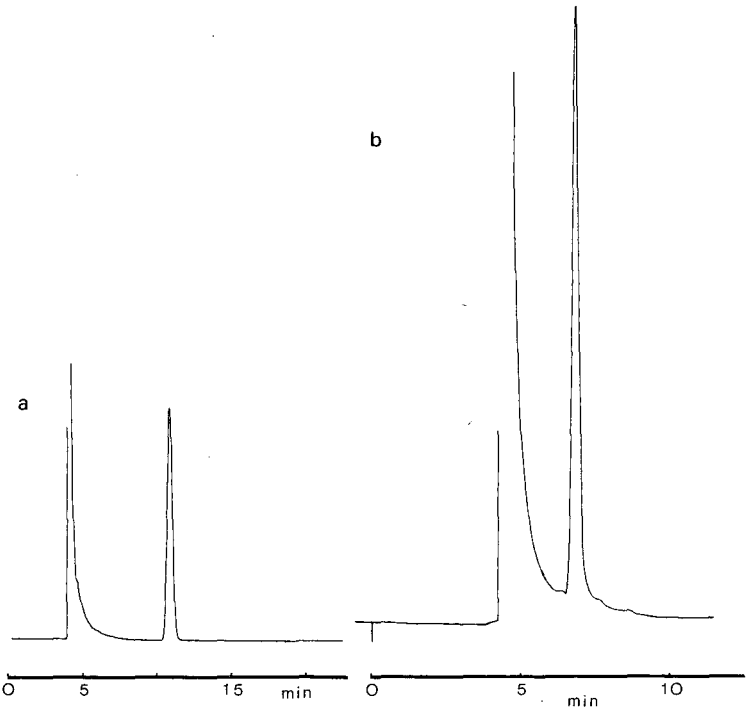

Fig. 1. (a) Chromatogram of metoprolol oxazolidone using carbon dioxide as mobile phase with an inlet pressure of 3000 p.s.i. The cyanopropyl column was kept at 100°C and 68 ng were injected. (b) Chromatogram of N-ethyl analogue of metoprolol using carbon dioxide as mobile phase with an inlet pressure of 2500 p.s.i. The 5% phenyl methyl column was kept at 100°C and 62 ng were injected.

phase itself. The cyanopropyl groups might have been oxidized to carboxylic groups to some extent. If so, the reasons why and how are unknown. Fields and Grolimund[4] described a poor performance of an old column as compared with a new column when analysing polar compounds with sulphur hexafluoride as mobile phase.

DB-Wax column

This column has a very thin film, only 0.10 μm thick. With the simple aliphatic amines the pressure used is below the critical pressure (P_c) of both carbon dioxide and nitrous oxide. The tertiary amines give symmetrical peaks whereas the secondary amines give severe tailing (Table V). Octylamine was difficult to chromatograph and it was necessary to increase the amount injected in order to obtain a peak. The capacity factors of the tertiary amines are low compared with those of the secondary amines, just as with the cyanopropyl phase, showing the interaction of the free hydrogens of the amines with the ether groups of the stationary phase. In the metoprolol group there is little difference in the symmetry between the three homologues. The retention differs considerably and from the pair with amine or alcohol only it is evident that the alcohol is more important for a high retention than the amine. It is perhaps not surprising that the oxazolidone requires a 400 p.s.i. higher inlet pressure for an acceptable elution time (Table V).

TABLE V

RESULTS WITH DB-WAX COLUMN

Compound[a]	*Pressure (p.s.i.)*	*Capacity factor, k'*	*Separation factor, α*	*Asymmetry factor*	*Amount injected on-column (in 60 nl) (ng)*
With carbon dioxide					
DMOA	950 (sub-P_c)	0.14	1.00	1.02	39
MOA		0.46	3.28	4.3	35
OA		0.74 ca	5.3	n.m.	104
TBA		0.14	1.00	0.81	44
DiHxA		0.78	5.57	5.0	44
Meto	2300	1.69	1.00	1.63	64
tButyl		1.42	0.84	1.58	67
Ethyl		2.48	1.47	1.78	62
PrimAmine		–			125
Amine		0.43	0.25	1.36	60
Alcohol		1.23	0.73	1.09	67
Oxaz	2700	1.99		0.85	68
With nitrous oxide					
DMOA	(800 sub-P_c)	0.14	1.00		
MOA		0.25	1.79		
TBA		0.11	0.79		
DiHxA		0.50	3.57		
OA		0.3	2.1		
Meto	1920	1.66	1.00		
tButyl		1.37	0.83		
Alcohol		1.2	0.73		
Amine		0.43	0.26		

[a] See Table I.

This column bled more than the silicone phase columns. The bleeding increased when the ethyl acetate solvent front had passed. Later this phenomenon was shown to be related to the nature of the solvent. On injecting ethyl acetate or toluene the bleeding and baseline instability were pronounced whereas this was not observed with hexane.

With nitrous oxide there was a marked difference in capacity factor for some of the simple aliphatic amines. Whether this is due to the nitrous oxide itself or to it being a liquid is not certain. In the metoprolol group the differences were small.

Choice of column

In this work only three columns were investigated. The most important criterion for selecting a certain column must be inertness. The support surfaces in capillary columns are not as inert as is usually presumed under SFC conditions[8]. The column surface deactivation is critical[4]. Owing to the poor peak symmetry of most amines and the large amounts required, the cyano column is out of the question for practical work. The second criterion is the selectivity. Although a large number of

TABLE VI

COMPARISON OF THE SELECTIVITIES WITH CARBON DIOXIDE AND NITROUS OXIDE AS THE MOBILE PHASE FOR AMINO ALCOHOLS

Compound[a]	*Column*			
	SB-Phenyl-5		*DB-Wax*	
	CO_2, 2500 p.s.i.	*N_2O, 2500 p.s.i.*	*CO_2, 2300 p.s.i.*	*N_2O, 1920 p.s.i.*
Meto	1.00	1.00	1.00	1.00
tButyl	1.07	1.02	0.84	0.83
Ethyl	1.00	0.98	1.47	–
PrimAmine	0.95	0.96	–	–
Alcohol	0.91	0.85	0.73	0.72
Amine	0.90	0.87	0.25	0.26

[a] See Table I.

plates can be achieved in SFC, this is at the expense of time. Therefore, the selectivity is of great importance. With this in mind, the Carbowax type of column might be of interest (*cf.*, Table VI). However, owing to the thin film this column will be of little practical value when looking for impurities at levels below 1% in, *e.g.*, drug substances, as the main component will easily overload and any separation of minor peaks in the close vicinity of the parent peak will be destroyed.

The capacity factors obtained with the SB-Phenyl-5 and the SB-Cyanopropyl-25 columns, using carbon dioxide as the fluid, are presented in Table VII. Although the film thickness differs it is striking how little hydrocarbons are retained on the polar column. Octanoic acid gave a good peak on the cyanopropyl column, which is as expected from the poor results with amines.

TABLE VII

COMPARISON OF CAPACITY FACTORS

Compound	*Column*	
	SB-Phenyl-5 (d_f = 0.5 μm)	*SB-Cyanopropyl-25 (d_f = 0.25 μm)*
Octanol	0.49	0.30
Octanoic acid	0.76	0.99
Undecane	0.57	–
Dodecane	0.72	–
Tetradecane	1.55	0.15
Octylamine	0.65	–
N-Methyloctylamine	0.80	0.51
N,N-Dimethyloctylamine	0.73	0.12

Carbon dioxide and amines

The results do not confirm the suggestion that carbon dioxide reacts with secondary and primary amines during capillary SFC. As the capacity factor of octylamine is the same with both carbon dioxide and nitrous oxide, and the peak areas are of the same order of magnitude, this suggests that the amines are chromatographed as such.

Changing the time in the system, with constant temperature and pressure, would give a change in peak area of the amine if it reacted to some extent during chromatography. Owing to the poor peak shape of octylamine this was studied with N-methyloctylamine. The detector temperature was varied between 150 and 350°C, as stopping the flow by keeping the valve in between inject and load gave broad peaks that were impossible to integrate properly. Although successful under certain circumstances[13], this mode would require a second valve in order to maintain a constant pressure in the column. The dead time thus varied between 8 and 13.4 min. The peak-area ratio *vs.* an inert marker was constant over the temperature range studied (1.21 ± 3.1%) and the area/height ratio changed only slighty. The last observation indicates that there is no significant peak broadening due to a low detector temperature and hence poor volatilization of the analyte in the frit restrictor used.

Nitrous oxide and flame ionization detector

With nitrous oxide as mobile phase, the noise of the flame ionization detector increased when the hydrogen and air flow-rates were as recommended by the manufacturer. The colour of the flame was distinctly white instead of faintly blue. The noise decreased when the hydrogen inlet pressure was reduced. On pressure programming the baseline decreased with increasing pressure. With carbon dioxide as the fluid it is normally the reverse and due to impurities. The difference in peak area for metoprolol oxazolidone was 20% between 2600 and 3200 p.s.i. in the isobaric mode (Fig. 2).

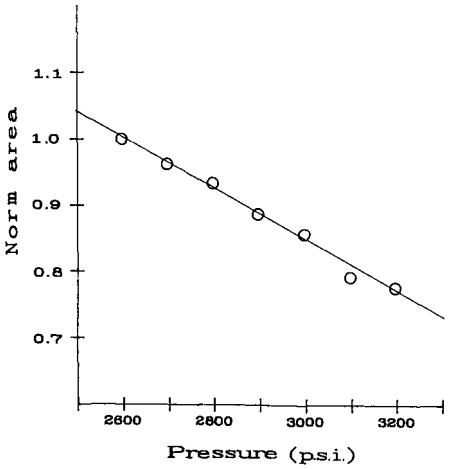

Fig. 2. Peak area *versus* pressure: SFC of metoprolol oxazolidone with nitrous oxide as mobile phase and flame ionization detection. Amount injected, 68 ng. Column: SB-Cyanopropyl-25. Each point is the average of three injections. For other conditions, see Experimental.

Apparently the flame is more oxidizing in nature and should perhaps be reoptimized for use with nitrous oxide as the mobile phase. A higher baseline level has been reported[12,14] and the detection limit was three orders of magnitude lower for hydrocarbons. Impurities have also been suggested to be involved[15]. The flame ionization detector response also changes with the density of carbon dioxide[16]. Hence, care should be taken when examining polymers where the individual oligomers elute at widely different densities, or erroneous results will be obtained.

REFERENCES

1 S. M. Fields, K. Grolimund and H. M. Widmer, in M. Perrut (Editor), *Proceedings of International Symposium on Supercritical Fluids, October 17–19, 1988, Nice*, Institut National Polytechnique de Lorraine, Nancy, 1988, p. 457.
2 S. M. Fields and K. Grolimund, *J. High Resolut. Chromatogr. Chromatogr. Commun.*, 11 (1988) 727.
3 S. M. Fields and K. Grolimund, paper presented at *Symposium on Supercritical Fluid Chromatography, Snowbird, UT, June 13–16, 1989.*
4 S. M. Fields and K. Grolimund, *J. Chromatogr.*, 472 (1989) 197.
5 D. K. Dandge, J. P. Heller and K. V. Wilson, *Ind. Eng. Chem., Prod. Res. Dev.*, 24 (1985) 162.
6 R. N. Maddox, G. J. Mains and M. A. Rahman, *Ind. Eng. Chem. Res.*, 26 (1987) 27.
7 F. David and P. Sandra, *J. High Resolut. Chromatogr. Chromatogr. Commun.*, 11 (1988) 897.
8 G. Schomburg, A. Deege, G. Breitenbruch and W. Roeder in P. Sandra and G. Redant (Editors), *10th International Symposium on Capillary Chromatography, Riva del Garda, Italy, May 22–25, 1989*, Hüthig, Heidelberg, 1989, p. 1194.
9 L. Mathiasson, J. Å. Jönsson and L. Karlsson, *J. Chromatogr.*, 467 (1989) 61.
10 T. Greibokk, B. E. Berg and H. Johansen, in M. Perrut (Editor), *Proceedings of International Symposium on Supercritical Fluids, October 17–19, 1988, Nice, Institut National Polytechnique de Lorraine, Nancy*, 1988, p. 425.
11 B. W. Wright, H. T. Kalinoski and R. D. Smith, *Anal. Chem.*, 57 (1985) 2823.
12 E. Lundanes, B. Iversen and T. Greibrokk, *J. Chromatogr.*, 366 (1986) 391.
13 M. B. Evans, M. S. Smith and J. M. Oxford, *J. Chromatogr.*, 479 (1989) 170.
14 T. Greibrokk, J. Døhl, A. Farbrot and B. Iversen, *J. Chromatogr.*, 371 (1986) 145.
15 S. Olesik, unpublished work.
16 C. Borra, G. P. Mapelli and S. Trestianu, in M. Perrut (Editor), *Proceedings of International Symposium on Supercritical Fluids, October 17–19, 1988, Nice, Institut National Polytechnique de Lorraine, Nancy*, 1988, p. 431.

Journal of Chromatography, 516 (1990) 427–432
Elsevier Science Publishers B.V., Amsterdam

CHROM. 22 624

Note

Rapid method for esterification of trace levels of carboxylic acids for analysis by gas chromatography–electron-capture detection

R. D. MORTIMER

Food Research Division, Bureau of Chemical Safety, Food Directorate, Health Protection Branch, Health and Welfare Canada, Ottawa, Ontario K1A 0L2 (Canada)

(First received March 2nd, 1990; revised manuscript received June 18th, 1990)

Pyrethroid insecticides are widely used because of their effectiveness, short lifetime in the field and relatively low mammalian toxicity. The principal reason for the short lifetime and low toxicity is the ease with which these esters are hydrolyzed on exposure to sunlight or in contact with esterase enzymes[1]. Cypermethrin (**I**), for example, yields permethrin acid (**II**) and the cyanohydrin of 3-phenoxybenzaldehyde on hydrolysis. The latter product is subsequently oxidized to phenoxybenzoic acid

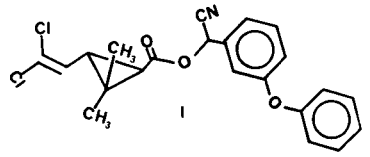

I

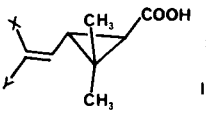

II: X = Y = Cl

III: X = Cl, Y = CF_3

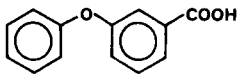

IV

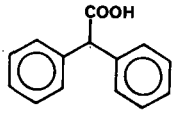

V

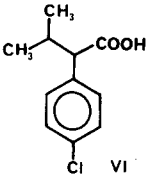

VI

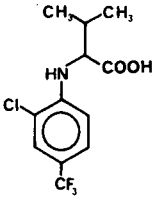

VII

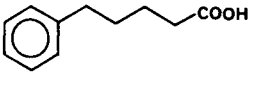

VIII

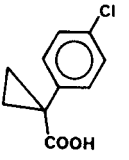

IX

0021-9673/90/$03.50

(**IV**). Because of the halogen atoms present in acid **II**, methylation yields a volatile ester which is readily analyzed by gas chromatography (GC) with electron-capture detection (ECD). In order to detect acid **IV** by ECD, however, it is necessary to employ a derivatization agent which itself contains the detectable function. There are a number of these reagents available, such as pentafluorobenzyl bromide[2–6], halogen-containing silylating agents[7] or halogenated alcohols[8,9], but the conditions of derivatization typically require long reaction times or elevated temperatures. In some instances, the need to remove excess reagent in order to minimize background interference can also be problematic. For example, esterification of carboxylic acids with trichloroethanol (100°C for 10 min) left an excess of high-boiling trichloroethanol that required separation on a silica column[9].

The carbodiimide-coupled esterification of carboxylic acids is a well known reaction which has been done under a variety of conditions[10]. Although hexafluoroisopropanol and dicyclohexylcarbodiimide have been used to esterify amino acids on a synthetic scale for peptide synthesis[11], there appears to be no reference to the use of these two reagents for the purpose of trace analysis. Poole and Schuette[8] do refer, however, to esterification with a number of halogenated alcohols via mixed anhydrides, including hexafluoroisopropanol. For example, hydroxyphenylacetic acids were esterified with hexafluoroisopropanol and pentafluoropropionic anhydride at 65°C for 90 min[12].

Inspite of its limited use, hexafluoroisopropanol should be an excellent derivatization reagent for carboxylic acids: its volatility (b.p. 59°C) and water solubility would facilitate removal, it is commercially available at reasonable cost and in high purity, and the six fluorine atoms would make its derivatives ECD sensitive. While attempting to circumvent the limitations of present derivatization methods, it was observed that the carbodiimide coupled esterification of 3-phenoxybenzoic acid (**IV**) occurred very rapidly at room temperature when the alcohol was hexafluoroisopropanol. This report concerns carbodiimide-coupled esterification with hexafluoroisopropanol as a simple and rapid means of preparing volatile derivatives of low concentrations of carboxylic acids for analysis by GC–ECD.

EXPERIMENTAL

Instrumentation

GC was carried out on a Varian 3700 instrument equipped with a ^{63}Ni electron-capture detector an a flame-ionization detector, a SGE on-column injector, a 30 m × 0.32 mm DB-1701 column (unless otherwise stated) with a 0.25 μm film thickness, and a HP3300A integrator. Helium carrier gas flow was 1.9 ml/min and the nitrogen make-up gas was set at 25 ml/min. The detector was maintained at 250°C. Typical GC conditions were: initial oven temperature of 120°C was maintained for 10 min then raised at 60°C/min to 145°C and held there for 10 min.

In this way, the more volatile esters were eluted within the first ten minute period and the less volatile esters were eluted within the second ten minute period. All the hexafluoroisopropyl esters eluted as sharp, symmetrical peaks with half-height widths of 2–5 s depending on their retention times.

Reagents and standards

Distilled-in-glass grade solvents were purchased from Caledon Labs. (Georgetown, Canada). Diisopropylcarbodiimide (DIC), dicyclohexylcarbodiimide (DCC), 1-(3-dimethylaminopropyl)-3-ethylcarbodiimide hydrochloride (EDI), 3-phenoxybenzoic acid (3-PBA), diphenylacetic acid, 1-(4-chlorophenyl)cyclopropanecarboxylic acid, oxalyl chloride and hexafluoroisopropanol (HFIP) were purchased from Aldrich (Milwaukee, WI, U.S.A.). Fenvalerate acid [**VI**, 2-(4-chlorophenyl)-3-methylbutyric acid] was purchased from Chemical Dynamics (South Plainfield, NJ, U.S.A.). Permethrin acid [**II**, 3-(2,2-dichlorovinyl)-2,2-dimethylcyclopropanecarboxylic acid], as a 56:44 mixture of *cis–trans* isomers, and cyhalothrin acid [**III**, *cis*-3-(*Z*-2-chloro-2-trifluoromethylvinyl)-2,2-dimethylcyclopropanecarboxylic acid] were kindly donated (>98.4% purity) by ICI Americas (Goldsboro, NC, U.S.A.). Fluvalinate acid [**VII**, 2-(2-chloro-4-trifluoromethylanilino)-3-methylbutyric acid] was prepared by saponification of fluvalinate donated by Sandoz (Des Plaines, IL, U.S.A.) and recrystallization of the crude acid in cyclohexane to a constant melting point, m.p. 133–134°C.

HFIP ester standards of acids **II–VI**, **VIII** and **IX** were prepared by gently warming the acid on a hotplate set at 75°C (typically 100–200 mg in a 5-ml vial) with excess oxalyl chloride until effervescence ceased, evaporation of the residual oxalyl chloride with a stream of nitrogen, and mixing the acid chloride with a 3-fold excess of HFIP and pyridine in methylene chloride. The esters were purified by silica column chromatography followed by bulb-to-bulb distillation at 0.5 Torr except for acid **IX** the ester of which was a waxy solid, m.p. 47–48°C. Acid **VII** was condensed with HFIP by carbodiimide (EDI) coupling in methylene chloride and the resulting ester purified as above. Methyl and ethyl esters were made by the Brook–Chan method (alcohol plus trimethylsilyl chloride)[13]. Structures were verified by mass spectrometric fragmentation patterns, precise mass determinations and proton magnetic resonance spectra.

Derivatization procedure

A 1.0-ml volume of a stock solution of carboxylic acid (1–2 ppm in a non-polar solvent such as methylene chloride, hexane or toluene) was added to a 10-ml volumetric flask and diluted to roughly 9 ml with hexane. A 10-μl volume of HFIP was added, swirled into solution, then 15 μl of DIC was added. The flask was filled to the mark with hexane and shaken briefly to mix. After 1 min, an aliquot of the reaction mixture was transferred to a small vial and shaken vigorously with an equal volume of 5% potassium carbonate. The bulk of the top layer was then removed by Pasteur pipette and dried over anhydrous sodium sulphate prior to GC analysis of a 1-μl aliquot.

RESULTS AND DISCUSSION

Initial experiments with 3-phenoxybenzoic acid (**IV**) (0.8 mg/ml in methylene chloride) using a 1.5-fold excess of EDI and a 25-fold excess of HFIP showed that the yield of ester, as determined by GC–FID, was independent of reaction time (15 min to 4 hr). Subsequent work with permethrin acid (**II**) at 0.12 μg/ml (2 mg DCC and 5 μl HFIP in 1 ml cyclohexane) measured the yield of ester after 1, 2, 5, 12 and 25 min. After 1 min, the yield was 98.9% and the mean value of the five samples was

96.0 ± 3.3% (S.D.). In addition, the *cis–trans* ratio was maintained on esterification (by comparison with the ratio determined from NMR of the original acid sample) indicating no rate discrimination due to steric effects.

Further reactions showed that the ester yield was independent of the type of carbodiimide used (DCC, DIC or EDI) or whether a 5-, 10- or 25-fold excess of HFIP was used. Subsequent reactions used an equimolar amount of carbodiimide and alcohol and both in large excess (10 mmolar). The reagents may be mixed up to 90 min before use but background peaks increase with postmix time. In cyclohexane, HFIP was only soluble to approximately 1% but, if a larger percentage was used, the second phase rapidly disappeared once carbodiimide was added. DIC became the carbodiimide of choice because it is a liquid, easily handled by syringe, and readily soluble in all the non-polar solvents used. EDI is non-volatile but insoluble in hydrocarbon solvents, such as cyclohexane.

Choice of solvent is critical[10]. At 1 mg/ml, **IV** gave 107 ± 4, 105, 88, 35, 25 and 14% yield of ester in cyclohexane, 2,4,4-trimethylpentane, toluene, ethyl acetate, ethyl ether and acetonitrile, respectively, after 60 min. Esterification of **II** showed a similar solvent dependence; reaction in cyclohexane, acetonitrile, acetone, or THF gave 103, 3, 0 and 0% yields, respectively, after 10 min. If 5% acetone was added to the cyclohexane, the yield fell to 28%.

Dimethylaminopyridine catalyzes some carbodiimide-coupled reactions and produces higher yields[10]. In the present study, however, at 1 ppm carboxylic acid concentrations and with a large excess of reagents, DMAP had no effect on the yields.

To demonstrate the generality of the reaction, a series of carboxylic acids representing a variety of structures were esterified at trace concentrations (0.1 to 0.2 ppm) using the conditions described in the experimental section. The reactions were done in duplicate and analyzed by GC–ECD in duplicate. The yields of esters were determined by comparison of the integrated area counts to those of standard ester calibration curves. The mean value and the standard deviation of the four results for each acid are tabulated in Table I. The acids include primary, secondary and tertiary structures as well as an amino acid and various pyrethroid metabolites. Maximum

TABLE I

YIELDS OF HFIP ESTERS FROM REPRESENTATIVE ACIDS[a]

Acid	*Yield ± S.D.*[c] *(%)*
Permethrin acid (**II**)	106 ± 3
Cyhalothrin acid (**III**)	101 ± 3
3-Phenoxybenzoic acid (**IV**)	89 ± 4
Diphenylacetic acid (**V**)	96 ± 7
Fenvalerate acid (**VI**)	82 ± 3
Fluvalinate acid (**VII**)	77 ± 2 (101 ± 3)[b]
5-Phenylvaleric acid (**VIII**)	63 ± 7
Cyclopropane acid (**IX**)	78 ± 6

[a] After 1 min at room temperature; acid concentration 0.1–0.2 ppm.
[b] After 25 min.
[c] S.D. = Standard deviation.

yields were reached within 1 min at room temperature except for fluvalinate acid (**VII**) which required 25 minutes to reach quantitative yield. Acid **VII** has a free amino group which may slow the reaction of the carboxylic acid with the carbodiimide as a result of intramolecular hydrogen bonding between the acid proton and the amino group.

The yields from the 0.1–0.2 ppm concentration range in Table I were similar to those from an experiment in the 0.6–1.2 ppm concentration range (data not shown). Limited data at 0.01–0.02 ppm suggests the yields are similar at this concentration also. The lowest detectable levels of the HFIP esters for **II** and **IV** were 0.07 pg (each isomer) and 0.8 pg, respectively, at a signal-to-noise ratio of 2.5.

The rate of esterification with HFIP is exceptionally fast: when **II** was reacted with methanol or ethanol (less sterically hindered alcohols!) under the same conditions, no product peaks were observed even after 30 min. A 1% yield of the methyl ester would have been readily detectable. A competitive experiment in which an equimolar mixture of HFIP and methanol were used gave only the HFIP ester product on GC. The selectivity of the reaction for HFIP should ensure a cleaner product when the derivatization is applied to plant extracts containing co-extractive alcohols as the reaction with these alcohols will be much slower. The greater reaction rate of HFIP is presumably due its much lower pK_a value in comparison to other alcohols. For example, the pK_a values of isopropanol and hexafluoroisopropanol are 17 and 9.3, respectively[14]. Hexafluoroisopropanol has the acidity of a phenol and, indeed, preliminary work shows that phenols also rapidly generate esters under these conditions. It has long been recognized that the rate of the initial reaction of carboxylic acid with carbodiimide to form a 1-O-acyl isourea is dependent on the pK_a of the acid[10]. Only recently, however, did Balcom and Petersen[15] conclude that the further reaction of the intermediate 1-O-acyl isourea with a second molecule of acid to form an anhydride was also pK_a dependent. The observed faster rate of esterification with HFIP over normal alcohols; *i.e.*, non-acidic, is consistent with their conclusion.

The HFIP esters are stable to column chromatography and vacuum distillation and have a number of advantages over other esters (*e.g.*, methyl esters): rapid rate of formation, earlier elution on GC, elution at a lower GC column temperature, faster elution on silica chromatography, and in the case of permethrin acid isomers, complete separation on silica thin-layer chromatography (*RF* values of 0.39 and 0.29 when eluted with cyclohexane).

The solvent restriction and the lower yields in some cases are disadvantages whose significance must be judged on an individual basis. Once the 1-O-acyl isourea is formed, there is a competition between the bimolecular reaction with alcohol and the unimolecular 1,3-shift which produces an unreactive N-acyl urea. Balcom and Peterson[15] showed that the rate of the former reaction declined with increasing solvent polarity whereas that of the latter reaction remained unchanged. As a result, as the solvent polarity increases, the 1,3-shift becomes dominant and the yield of the ester declines. If the 1,3-shift could be suppressed, the reaction developed herein would be more generally useful.

Nevertheless, in spite of these limitations, the present method is simple, rapid and clean, and generates ECD-sensitive derivatives in good to quantitative yield. The application of this method of esterification to the analysis of pyrethroid metabolites in food products is currently being investigated.

REFERENCES

1 J. P. Leahey, *The pyrethroid Insecticides*, Taylor & Francis, London, Philadelphia, PA, 1985.
2 T. Tsukioka and T. Murakami, *J. Chromatogr.*, 469 (1989) 351.
3 R. F. Arrendale, J. T. Stewart, R. Manning and B. Vitayavirasuk, *J. Agric. Food Chem.*, 37 (1989) 1130.
4 H. B. Lee and A. S. Y. Chau, *J. Assoc. Off. Anal. Chem.*, 66 (1983) 1023.
5 E. Fogelqvist, B. Josefsson and C. Roos, *J. High Resolut. Chromatogr. Chromatogr. Commun.*, 3 (1980) 568.
6 R. J. Strife and R. C. Murphy, *J. Chromatogr.*, 305 (1984) 3.
7 A. Zlatkis and C. F. Poole, *Anal. Chem.*, 52 (1980) 1002A.
8 C. F. Poole and S. A. Schuette, *Contemporary Practice of Chromatography*, Elsevier, Amsterdam, New York, 1984, p. 499; and references cited therein.
9 K. Blau and G. S. King, *Handbook of Derivatives for Chromatography*, Heyden, Philadelphia, PA, 1978, pp. 39–103.
10 M. Mikolajczyk and P. Kielbasinski, *Tetrahedron*, 37 (1981) 233; and references cited therein.
11 L. S. Trzupek, A. Go and K. D. Kopple, *J. Org. Chem.*, 44 (1979) 4577.
12 B. A. Davis, D. A. Durden, P. Pun-Li and A. A. Boulton, *J. Chromatogr.*, 142 (1977) 517.
13 M. A. Brook and T. H. Chan, *Synthesis*, (1983) 201.
14 B. Carre and J. Devynck, *Anal. Chim. Acta.*, 131 (1981) 141.
15 B. J. Balcom and N. O. Petersen, *J. Org. Chem.*, 54 (1989) 1922.

Journal of Chromatography, 516 (1990) 433–441
Elsevier Science Publishers B.V., Amsterdam

CHROM. 22 623

Note

Purification of anti-paraquat monoclonal antibodies by affinity chromatography on immobilised hapten

B. J. HORSTMANN*, H. A. CHASE and C. N. KENNEY
University of Cambridge, Department of Chemical Engineering, Pembroke St, Cambridge (U.K.)
(First received September 15th, 1989; revised manuscript received June 14th, 1990)

Monoclonal antibodies are currently of great commercial interest for their applications in the areas of both in vitro and in vivo diagnostic and therapeutic agents[1–3]. Many purification methods have been successfully applied. Initial enrichment steps such as ultrafiltration are used to concentrate the product. Purification, however, is generally carried out by a chromatographic technique[4]. Many such techniques have been used; ion exchange[5], affinity chromatography using immobilised Protein A[6], and hydroxyapatite[7]. None of these methods has a truly general application, however, due to the heterogeneity in isoelectric point, hydrophobicity and biological activity of different monoclonal antibodies[8].

Purification of monoclonal antibodies by affinity chromatography on the immobilised antigen is possible in situations where the antigen is cheap, in ready supply, and capable of being immobilised on an inert support in a stable form. Often in such cases the antigen is a small molecule or "hapten", rather than a complex protein. Affinity purification is particularly advantageous when it exploits the variable region of the antibody, as it enables antigen-specific antibody to be separated from other antibodies. Affinity purification utilising the interaction at the antigen binding site also allows active antibody to be separated from antibody in which the binding site has been denatured.

In this paper, a paraquat derivative (Fig. 1) immobilised on AH-Sepharose 4B is employed for the purification of antiparaquat monoclonal antibodies from ascites fluid. The purified antibody was required for the preparation of immobilised antibody affinity adsorbents, part of a larger research program studying the characteristics of such adsorbents[9], so it was particularly important that the antigen-specific antibody was selected by the purification procedure. Successful affinity purification relies on the absence of any non-specific interactions, or at least their reduction to an insignificant level. Non-specific binding is a particular problem in the case of the

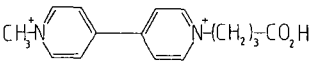

Fig. 1. The chemical structure of paraquat propionate.

0021-9673/90/$03.50

paraquat ligand as it is positively charged and therefore has ion-exchange properties. In the presence of salt, however, such ion-exchange interactions are reduced to an insignificant level and two different protocols for carrying out the chromatography were investigated.

(i) The ascites fluid is applied to the column, the column is washed briefly with buffer, and then more extensively with 1 *M* NaCl. After further washing with buffer the antibody is eluted at low pH.

(ii) The ascites fluid is applied to the column in the presence of 1 *M* NaCl. After washing with buffer the antibody is eluted at low pH.

The advantage of the second strategy over the first is that material that would bind to the column via ion exchange interactions never gets the chance to bind, so it is probable that the capacity of the column for the specifically bound antibody would be greater. It is also much faster, as the need for a separate salt wash and subsequent washing step is removed. On a larger scale difficulties might arise with the addition of large quantities of salt to the crude starting material as this would involve an extra process step.

In order to produce monoclonal antibodies hybrid cells are prepared by fusing lymphocyte (antibody producing) cells with myeloma cells to give hybridoma cells. The hybridoma cells secrete not only heavy and light chains of the required antibody, but may secrete heavy and light chains from the myeloma. The anti-paraquat monoclonal antibodies were prepared by fusion with the NS-1 mouse myeloma cell line[6,10], which secretes only light chains. Once cloned, cell lines were selected for antibody activity. In the selected cell line, however, some light chain from the parent NS-1 myeloma was secreted, so that as the heavy and light chains combine to form the antibody molecules, there will be some antibody with two light chains from the NS-1 myeloma, which will not bind antigen, some mono-valent antibody which contains one light chain from the NS-1 myeloma, but will bind antigen, using the other light chain, and the required antibody with two antigen-binding light chains. The purification procedure must therefore be capable of separating the mono- and bi-valent antibody.

EXPERIMENTAL

Materials

Paraquat propionate and mouse ascites fluid containing antiparaquat monoclonal antibody were a kind gift of ICI Corporate Bioscience Group. AH-Sepharose 4B was obtained from Pharmacia Biotechnology International, Uppsala, Sweden. 1-Ethyl-3-(3 dimethylaminopropyl)carbodiimide and papain immobilised on carboxymethyl cellulose beads were obtained from Sigma (U.K.).

Methods

Preparation of paraquat–Sepharose. In order to attach paraquat covalently to the Sepharose matrix, a derivative of paraquat, paraquat propionate (Fig. 1), which contains a carboxyl groups, and AH-Sepharose 4B which contains free primary amino groups on 6-carbon spacer arms were used. The spacer arm was employed to reduce the possible steric hindrance to the access of antibody from the surface of the support. Steric hindrance often results if a small antigen is bound too closely to the surface of the support[11].

A carbodiimide coupling procedure was employed. A 1-g amount of dry AH-Sepharose 4 was allowed to swell then washed with 200 ml of 0.5 *M* NaCl according to the manufacturers instructions, then washed with distilled water at pH 4.5, and added to a solution of 50 mg paraquat propionate in 3 ml water at pH 4.5. A solution of 100 mg 1-ethyl-3-(3 dimethylaminopropyl)carbodiimide was added dropwise to the suspension whilst the pH was maintained between 4.5 and 6. The suspension was left gently shaking overnight. Non-coupled material was removed by five alternate washings with 0.1 *M* sodium acetate buffer, pH 4 and 0.1 *M* buffer, pH 8.3 each containing 0.5 *M* NaCl.

Purification of antibody from ascites fluid. The purification runs were carried out using an automated chromatography system as described previously[12]. Micro-computer controlled valves allow buffer, sample, salt and eluent in turn to be pumped through the column. The effluent from the column passes through a UV spectrophotometer, which measures the optical density at 280 nm, and is then collected in a fraction collector.

In each case a 1-cm diameter column containing 3 ml of adsorbent was used and run at a flow-rate of 0.5 ml/min.

For the method in which a separate salt wash step was used, ascites fluid was diluted × 5 with 10 m*M* sodium phosphate buffer containing 0.65% sodium chloride, pH 7.5 (phosphate-buffered saline, PBS) and applied to the column. The column was washed briefly with PBS, and then more extensively with 1 *M* NaCl buffered with 10 m*M* sodium phosphate, pH 7.5. After a further PBS wash, the antibody was eluted with 0.2 *M* glycine, pH 2.5 (the optimum pH was determined by lowering the pH in steps until no further antibody was removed). The eluted fractions were neutralised immediately, and dialysed into a suitable buffer.

For the adsorption method carried out in the presence of salt, the ascites fluid was diluted × 5 with 10 m*M* sodium phosphate buffered salt solution, pH 7.5, and NaCl added to a final concentration of 1 *M* NaCl, before being applied to the column. After the application, the column was washed with PBS, and then eluted as above.

In each case the collected fractions were reduced with 2-mercaptoethanol and run on 10% polyacrylamide gels in the presence of sodium dodecyl sulphate (SDS). The method used was that published by Chase[12]. The quantity of pure antibody in the eluted peaks was determined from optical density measurements of the pooled fractions. An extinction coefficient of 1.4 was assumed[13].

The purity of the eluted material was also assessed by using a fast protein liquid chromatography system (FPLC; Pharmacia). A total of approximately 1 mg of protein was applied to a 1 ml Mono Q column in 0.1 *M* sodium acetate, pH 5, and then eluted with a 0–1 *M* NaCl gradient.

Papain digestion of antibody. The digestion was carried out following the method of Kaye and Janeway[14]. 10 U of papain immobilised on carboxymethyl cellulose beads was added to approximately 18 mg of antibody in 25 ml PBS containing 0.1% sodium azide, 4 m*M* EDTA and 0.01 *M* 2-mercaptoethanol. The solution was stoppered to exclude air, and incubated at 37°C for 18 h. The immobilised papain was then removed by centrifugation.

Separation of papain-digested fragments. A 10-ml volume of the digested antibody was applied at 0.25 ml/min to the immobilised paraquat column described

above. Buffer, separate salt wash, and elution were carried out as for the purification runs.

RESULTS AND DISCUSSION

The results of the two purification runs are shown in Figs. 2 and 3. Figs. 2a and 3a show the spectrophotometer signal as a function of time, which is an indication of the protein content of the column outlet. For a mixture of proteins the optical density cannot be readily converted into a protein concentration, so the signal is left in arbitrary units for convenience. From this trace, the adsorption, washing and elution phases of the purification run can be seen. The SDS–polyacryl amide gel electrophoretic (PAGE) analysis (Figs. 2b and 3b) shows that the starting material contains a number of different proteins.

For the purification using a separate salt wash step (Fig. 3), some proteins start to appear in the outlet stream as the adsorption phase progresses. During the salt wash, many proteins are eluted. The eluted peak, however, contains only three bands. The SDS-PAGE analysis is carried out in the presence of 2-mercaptoethanol, under which conditions, the antibody is broken down into two heavy chains with a molecular weight of 50 000, and two light chains with a molecular weight of approximately 25 000. The track on the gel corresponding to the eluted peak shows one band in the heavy chain region, and, somewhat unexpectedly, two in the light chain region.

For the run in the presence of salt (Fig. 2), breakthrough of unbound proteins is immediate and a great number of components pass straight through the column. It can be seen from the optical density trace that there is a rise near the end of the application stage, suggesting that the antibody is beginning to break through. This is confirmed by the corresponding gel tracks (7 and 8), where bands corresponding to the eluted peak appear (it is the appearance of the light chain that is observed; the appearance of the heavy chains is masked by the albumin (molecular weight 66 000) passing through the column). So, the effective capacity of the adsorbent under these conditions has been reached, and was estimated to be about 6 mg/ml of adsorbent. The amount of antibody recovered was greater for the run in which the adsorption was carried out in the presence of salt (6 mg/ml adsorbent as opposed to 4,3 mg/ml adsorbent).

The gels from both purification protocols show that although all the contaminating material has been removed, the eluted peak shows not just one antibody light chain, but two different ones. Only one of these can be due to the bi-valent paraquat-specific antibody. The other one is present due to the existence of antibody molecules which in addition to the heavy chains contain one paraquat specific light chain and one light chain from the myeloma parent. These "monovalent" molecules contain one paraquat specific "arm", and therefore bind to the affinity column, but their presence in the affinity product may be undesirable. If the antibody is itself to be used as an affinity ligand, then the presence of antibody with only one specific site may reduce the potential capacity of the immunoadsorbent.

To determine which of the two light chains corresponds to the paraquat-specific arm, papain digestion of the eluted antibody was carried out. The action of papain on immunoglobulin G is highly specific. It divides the antibody into three sections, two fragments, known as Fab fragments, and one Fc fragment, with the latter having no

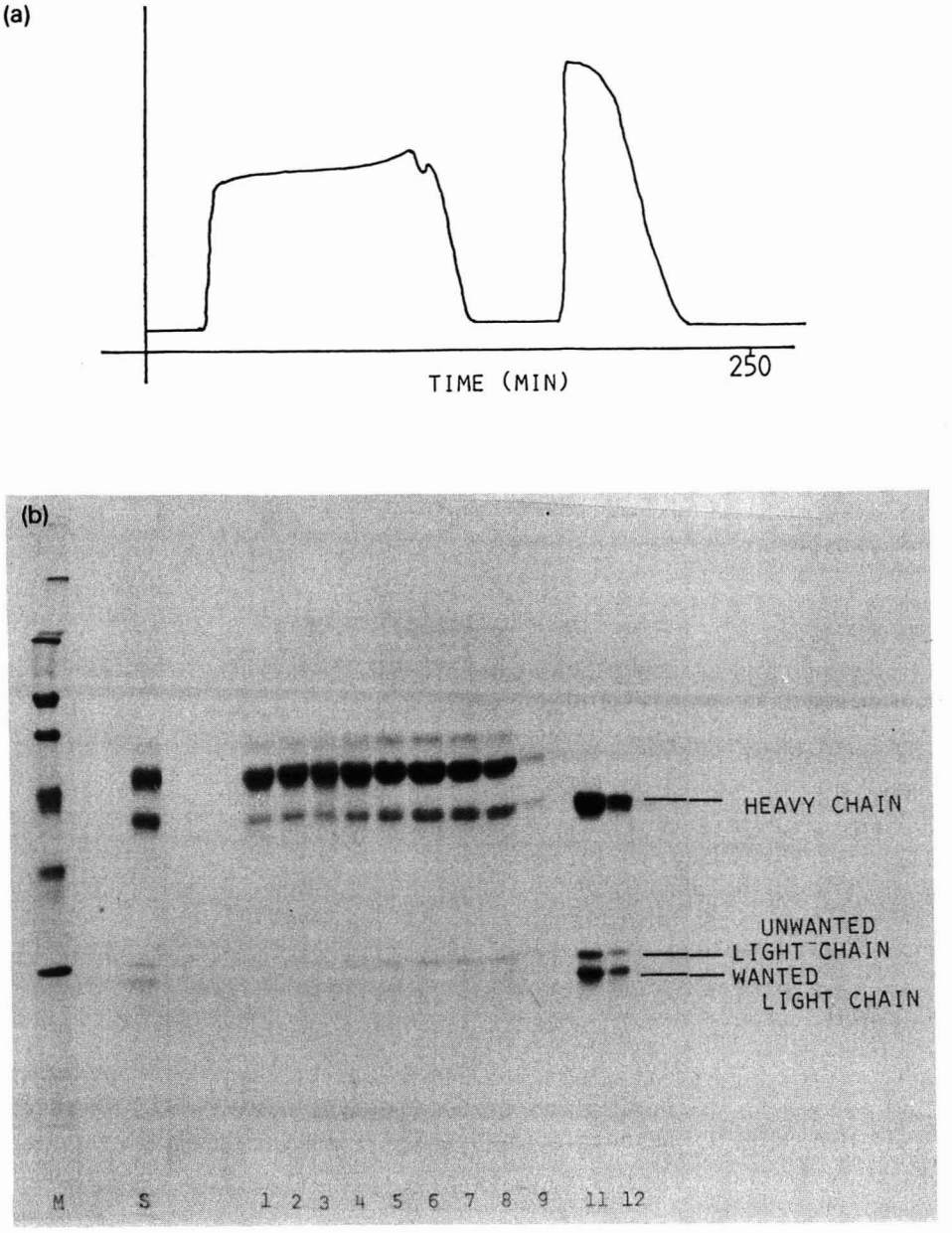

Fig. 2. Purification of anti-paraquat antibody on an immobilised paraquat column. Adsorption carried out in the presence of salt. A buffer wash was started at 90 min, followed by acid elution at 150 min. (a) Spectrophotometer reading at 280 nm as a function of time (arbitrary units). (b) Gel electrophoresis of samples corresponding vertically to the respective position of the optical density trace. M = Molecular weight markers 205, 116, 97, 66, 45 and 29 kilodaltons; S = Starting material; 1–8 = unadsorbed material; 11,12 = eluted peak. Antibody at 0.5 mg/ml was applied at a flow-rate of 0.5 ml/min to a 3-ml column of paraquat immobilised on Sepharose 4B. The eluted peak contained 18 mg of purified antibody.

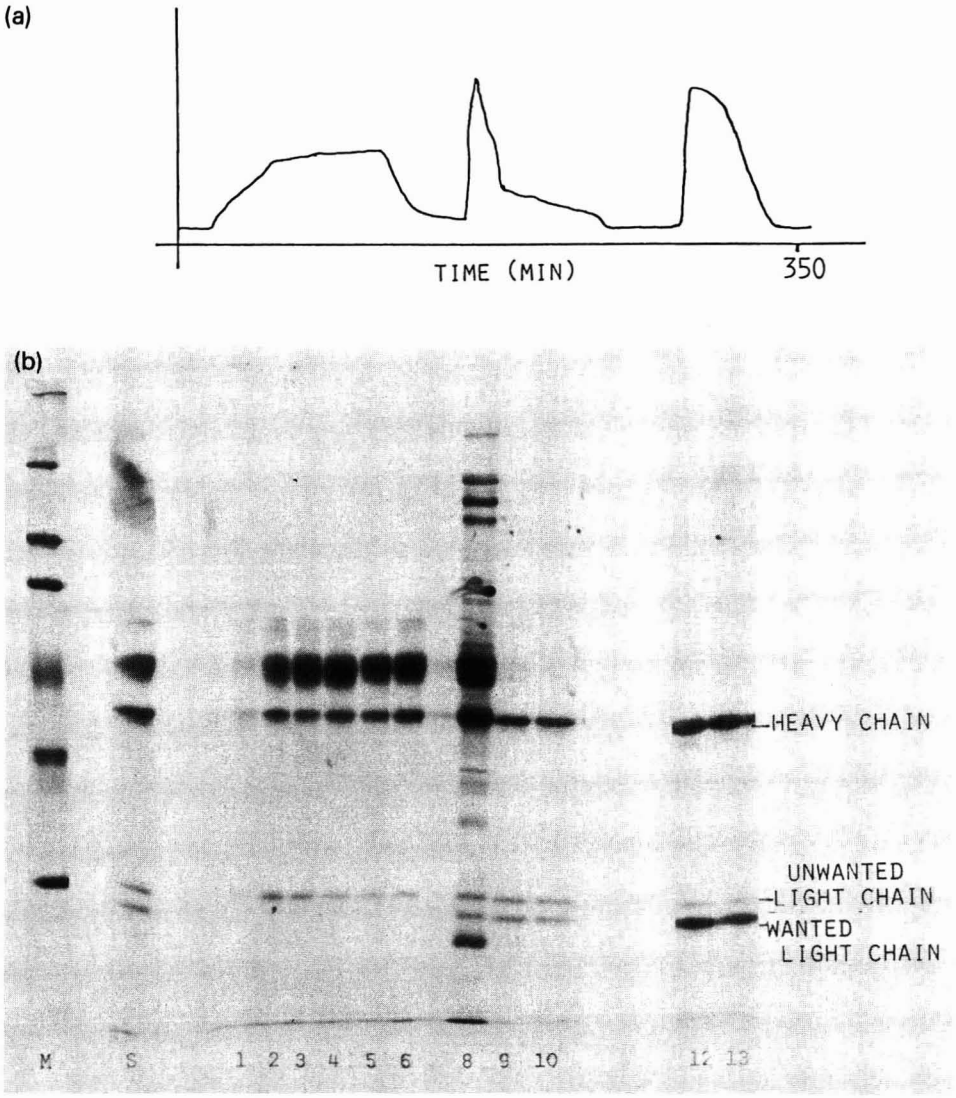

Fig. 3. Purification of anti-paraquat antibody on an immobilised paraquat column. Adsorption carried out in phosphate-buffered saline, followed by washing with 1 *M* NaCl. A buffer wash was started at 90 min, followed by the salt wash at 135 min, a futher buffer wash at 195 min, and acid elution at 255 min. (a) Spectrophotometer reading as a function of time (arbitrary units). (b) Gel electrophoresis of samples corresponding vertically to the respective position on the optical density trace. M = Molecular weight markers, 205, 116, 97, 66, 45 and 29 kilodaltons; S = starting material; 1–6 = unadsorbed material; 8 = components removed immediately by salt wash; 9, 10 = components removed by extended salt wash; 12, 13 = eluted peak. Antibody at 0.5 mg/ml was applied at a flow-rate of 0.5 ml/min to a 3-ml column of paraquat immobilised on Sepharose 4B. The eluted peak contained 13 mg of purified antibody.

recognition site for antigen. The Fab fragments still retain their specific binding sites, and can still bind antigen, but Fab fragments that originate from the myeloma parent of the monoclonal will not recognise paraquat. Therefore, if the mixture of digested antibody is applied to a column of immobilised paraquat, then the Fc fragments and the Fab fragments corresponding to the myeloma parent will pass straight through, and only the paraquat specific Fab fragment will bind. As the light chains are unaffected by the papain digestion, comparison of the tracks corresponding to purified antibody with those for unadsorbed and eluted material from the digestion, on an SDS-PAGE gel, shows which light chain is which. Such analysis with this antibody showed that it is the smaller of the two light chains that is paraquat specific (result not shown).

Comparison of the size of the eluted peaks for the two purification runs on SDS-PAGE shows that the quantity of the unwanted light chain is considerably reduced during the method where a separate salt wash step was used. This is because monovalent antibody molecules are removed from the column during the salt wash and are no longer adsorbed on the column at the start of elution. From Fig. 3a it can be seen that as the salt wash is applied to the column, initially there is a large peak which indicates that most contaminants are removed immediately by the salt, but the peak has a "shoulder" showing that some material is removed only slowly. Examination of the corresponding gel tracks, track 8 (the initial peak) shows that indeed many proteins are eluted at the start of the salt wash. The tracks corresponding to the shoulder (tracks 9 and 10), however, contain only three bands, and represent pure antibody. As in the eluted peak, there are two bands indicating two different light chains, but here they are equal in intensity, suggesting that only the monovalent antibody with one light chain of each type is being removed by the prolonged salt wash. Affinity adsorption between paraquat and a paraquat binding site via a single monovalent interaction does not appear to be particularly strong, as paraquat-specific Fab fragments adsorbed to the column could also be removed by an extended salt wash. In the absence of salt, antibody molecules are adsorbed to the column by a combination of affinity and ion exchange interactions. In the presence of salt, the ion exchange interactions are abolished, and the strength of the adsorption is consequently weakened. The bivalent antibody binds more strongly than the monovalent antibody in the presence of salt, as the former species is not eluted with a salt wash. This suggests that the bivalent antibody is actually bound to the column using both antigen binding sites. Although the monovalent antibody is removed from the column by a salt wash, it is still significantly retarded due to the affinity interactions involving the single antigen-binding site. When ascites fluid is applied to the column in the presence of salt followed by a buffer wash, a considerable amount of monovalent antibody is still retained by the column, as this protocol does not contain a long enough irrigation of the column with salt to result in complete removal of the monovalent antibody. The monovalent antibody is then adsorbed more strongly during the subsequent buffer wash as additional ion-exchange interactions can now occur which also prevent its removal from the column. The purified antibody still contains some monovalent antibody. In order to effect complete removal of the monovalent antibody, a longer salt wash would be required. As a result of improved cell-line selection methods, in subsequent batchs of ascites fluid, the contamination with light chain variants was not as great, and this protocol proved to be sufficient. The apparent increased

recovery of antibody observed during the method involving adsorption in the presence of salt may be due substantially to the presence of increased quantities of the adsorbed monovalent antibody, rather than resulting from an increase in the capacity of the column for antibody in the absence of ion-exchange interactions.

The analysis by FPLC (result not shown) also confirmed the complete separation of the purified antibody from other proteins, as only a single peak was observed. The monovalent antibody molecule does not appear to be separated from the bivalent antibody during ion-exchange chromatography. The presence of monovalent antibodies in ascites fluid has been noted elsewhere[7]. In order to effect resolution of the light chain variants, high performance liquid chromatography on hydroxyapatite and gradient elution were employed.

It was possible to effect elution of anti-paraquat antibodies from the immobilised antigen simply by lowering the pH, without resorting to the use of chaotropic salts, or other methods. Even at pH 2.5, the elution process is slow, requiring about three column volumes of eluent. Despite being broad the eluted peak does not display the long tailing usually observed in such systems, and the tailing edge of the peak was observed to drop fairly sharply (see Figs. 2 and 3).

To ensure that the antibody is not denatured by the elution conditions, a purification run was carried out and then the eluted peak dialysed against PBS and re-applied to the column. No protein passed straight through the column, and only a tiny fraction was eluted with a salt wash, the remainder being eluted with acid as before. This shows that the antibody still retains its full antigen binding activity.

Immobilised paraquat also proved to be very stable, as during this work a single column of paraquat–Sepharose was used repeatedly (approx 50 times) and over the course of several years without a noticeable drop in performance.

CONCLUSION

Affinity purification of monoclonal anti-paraquat from ascites fluid using immobilised antigen proved to be a successful single step method for purification to protein homogeneity. As salt wash was required, during the protocol, due to the presence of positive charges on the paraquat molecules, giving the adsorbent ion-exchange properties. The purification method had the added advantage that it resulted in separation of antibody that had two paraquat-specific binding sites from antibody that had only one. Such separation would not have been possible by methods such as ion-exchange chromatography.

ACKNOWLEDGEMENTS

This work was supported by the Science and Engineering Research Council, Great Britain, and by ICI Pharmaceuticals Division. We are grateful for both the materials and information supplied by Dr. Wright of ICI Corporate Bioscience Group.

REFERENCES

1 *Monoclonal Antibody Markets, Report No. 772*, Theta Corporation, November 1987.
2 M. D. Scott, *Trend Biotechnol.*, 3 (1985) 170.
3 S. J. Tarnowski, R. A. Liptak, *Adv. Biotechnol. Proc.*, 2 (1983) 271.
4 C. Ostlund, *TibTech*, 4 (1986) 288.
5 S. W. Burchiel, J. R. Billman, T. R. Alber, *J. Immunol. Methods*, 69 (1984) 33.
6 J. W. goding, *J. Immunol. Methods*, 20 (1978) 241.
7 L. H. Stanker, M. Vanderlaan and H. Juarez-Salinas, *J. Immunol. Methods*, 76 (1985) 157.
8 R. Ehrnstrom and B. Gustavsson, *Am. Lab.*, 19, No. 4 (1987) 78.
9 B. J. Horstmann and H. A. Chase, *Chem. Eng. Res. Des.*, 67, May (1989) 243.
10 Z. Niewola, C. Hayward, B. A. Symington and R. T. Robson, *Clin. Chim. Acta*, 1 (1985) 149.
11 C.-M. Yang and G. T. Tsao, in A. Fiechter (Editor), *Advances in Biochemical Engineering*, Vol. 25, Springer, New York, 1982, pp. 19, 42.
12 H. A. Chase, *J. Gen. Microbiol.*, 117 (1980) 211.
13 J. W. Goding, *Monoclonal Antibodies: Principles and Practice*, Academic Press, London, 1983.
14 J. Kaye and C. A. Janeway, *J. Exp. Med.*, 159 (1984) 1397.

Journal of Chromatography, 516 (1990) 442–445
Elsevier Science Publishers B.V., Amsterdam

CHROM. 22 601

Note

Analysis of the pesticide flufenoxuron in apples and kiwifruit by high-performance liquid chromatography

WENDY A. HOPKINS* and DENIS R. LAUREN
MAFTech, Ruakura Agricultural Centre, Private Bag, Hamilton (New Zealand)
(First received February 5th, 1990; revised manuscript received May 10th, 1990)

Flufenoxuron, 1-{4-[2-chloro-4-(trifluoromethyl)phenoxy]-2-fluorophenyl}-3-(2,6-difluorobenzoyl)-urea, is an acylurea compound currently being evaluated for control of insects and mites attacking a range of important crops[1,2]. The compound is a slow-acting growth regulator[3] which inhibits the synthesis of chitin[1,4] in these pests causing death without producing a detrimental effect on important predatory mites[2].

As part of efficacy trials, we were required to measure residues on fruit harvested at varying times after spray application.

The methods available were laborious[5–7]. Sample extraction was followed by a multi-step clean-up involving three or four evaporations plus either multiple partitions or a solid-phase clean-up cartridge, plus fractionation by reversed-phase high-performance liquid chromatography (HPLC). Final analysis was achieved using an alternative HPLC system.

This report describes a very simple and rapid method which limits clean-up to a single liquid–liquid partition and evaporation. This has been achieved by changing the extraction solvent and by using a more selective partition solvent. The extracts are analysed by reversed-phase HPLC producing good recoveries (81–117%) and low detection limits ($\leqslant$ 0.005 mg/kg).

EXPERIMENTAL

Chemical standards

A sample of flufenoxuron (97.6%) was obtained from Shell Research (Sittingbourne, U.K.). A stock solution of the standard was made accurately in methanol at about 200 μg/ml, and stored at 2°C. Dilute solutions at 10 and 1 μg/ml in methanol were made and stored similarly at 2°C. These dilute solutions were used for spiking samples and for the preparation of analytical standards which were prepared in methanol–water (80:20).

Reagents

Solvents were HPLC grade. Water was distilled in glass then passed through a Millipore Milli-Q water purifier.

0021-9673/90/$03.50

Apparatus

HPLC was performed using a Shimadzu LC-6A gradient liquid chromatography system with variable-wavelength UV absorption detector, set to 254 nm, and autosampler. Data aquisition was by peak height from a Shimadzu Chromatopac C-R3A. The analytical column, a 5-μm Zorbax ODS (25 cm × 4.6 mm I.D.) (DuPont, Wilmington, DE, U.S.A.), was preceded by a 2-μm in-line filter (Rheodyne, Cotati, CA, U.S.A.) and an MPLC RP-8 guard column (Brownlee Labs., Santa Clara, CA, U.S.A.).

Sample extraction and clean-up

Samples (fresh fruit) were stored deep frozen (−15°C) prior to analysis. The thawed fruit was finely diced and mixed in a Hobart food chopper. A subsample (50 g) was macerated with methanol (100 ml) for 4 min and filtered through a Buchner funnel and glass fibre filter paper (Whatman GFA). An aliquot (15 ml) of the filtrate (which is in approximately 10:4 methanol–water due to the water contribution from fresh fruit) was pipetted into a clean test tube. Water (10 ml) and hexane (10 ml) were added to the test tube which was stoppered and shaken. An aliquot (4 ml) of the upper hexane layer was blown to dryness with nitrogen at 50°C. The residue was dissolved in methanol (0.8 ml) and water added (0.2 ml).

The calculation factor required inclusion of both the water contribution from the fresh fruit (mean dry matter content 16%, range 13–19%), and the volume contractions (*ca.* 2.8%) caused by mixing methanol and water. The final analysis solution was thus calculated to be equivalent to 2.17 g of fresh fruit per ml of solution.

HPLC conditions

The mobile phase was acetonitrile–water (74:26) run at 1 ml/min. The detector was set at 254 nm. Injection size was 100 μl for standards and samples. Flufenoxuron retention time was 11.3 min (capacity factor, $k' = 4.5$), and a 0.1 μg/ml standard solution gave 20% of full scale deflection at 0.005 a.u.f.s. Kiwifruit samples were run in groups of three with injections at 12.5-min intervals; the third followed by a solvent programme to flush late eluting peaks from the column. In this case the solvent was changed to 100% acetonitrile over 5 min and held there for 5 min until reset to initial conditions. The apple samples had no late eluting peaks and were run isocratically.

RESULTS AND DISCUSSION

The method for sample extraction and clean-up was chosen after several options were tested, including the use of different absorbants in clean-up columns and alternative solvent combinations for extraction and single step partition. The resultant chromatograms after column clean-up were unsatisfactory due to impurities interfering with the peak of interest. They also contained a number of late eluting peaks.

The best results were obtained from a methanol extraction with the addition of water and partition of the flufenoxuron into hexane. The ratio of water to methanol was found to be a critical factor in determining the percentage of flufenoxuron recovered in the hexane layer. Spiked solutions were made with an increasing volume of water to methanol, enabling the percentage recovery to be manipulated from 3.7%

TABLE I

PERCENTAGE RECOVERIES OF FLUFENOXURON INTO HEXANE PARTITION FROM SPIKED METHANOL–WATER MIXTURES

Ratio of methanol–water (v/v)	*Recovery of flufenoxuron in hexane partition (%)*
9:1	4
3:1	26
2:1	49
1:1	98
1:2	103

(methanol–water, 9:1) to near 100% (methanol–water, 1:1) as illustrated in Table I. Substituting water with saline solution (10%, w/v) did not improve the recoveries, and chromatograms of fruit extracts showed no reduction of co-extracted components. The chosen partition conditions employ a methanol–water ratio of approximately 1:1.4.

The HPLC conditions elute flufenoxuron clear of co-extracted components for both apple and kiwifruit extracts. Recoveries for replicate spiked samples of both apples and kiwifruit from several analytical runs were between 81–93% (0.1 mg/kg), 86–101% (0.05 mg/kg) and 84–117% (0.01 mg/kg).

Fig. 1 illustrates the analysis of apple extracts. Analysis of a field-treated sample with 0.005 mg/kg of flufenoxuron is shown in Fig. 1c. This peak represents a solution

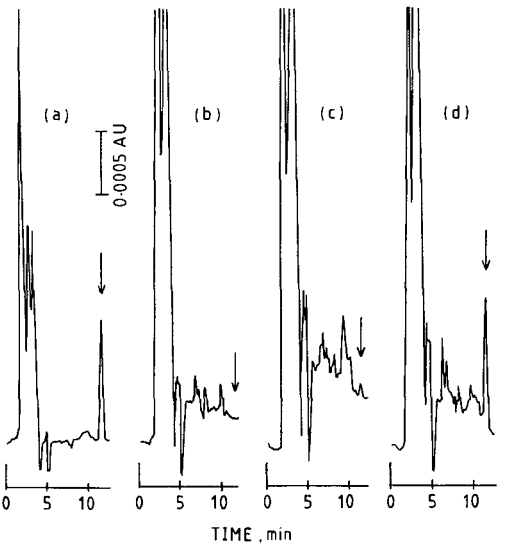

Fig. 1. Analysis of flufenoxuron in apple extracts. (a) Standard solution of flufenoxuron (0.1 μg/ml) in methanol–water (8:2); (b) extract of untreated apple; (c) extract of field-treated apple containing 0.005 mg/kg of flufenoxuron; and (d) extract of untreated apple spiked at 0.05 mg/kg flufenoxuron (95% recovery). Chromatographic conditions as in text including detection at 254 nm and 0.005 a.u.f.s. The arrow indicates the retention time of flufenoxuron.

concentration of 0.01 μg/ml and is close to the detection limit of the method (ca 2% f.s.d. at 0.005 a.u.f.s.; signal-to-noise ratio of at least 10), although estimates of lower levels were generally possible. Fig. 1b shows the analysis of apples untreated with flufenoxuron.

This procedure provides the basis for a sensitive, rapid and versatile method for the analysis of flufenoxuron in fruit. It illustrates the use of a simplified extraction and clean-up which should be suitable for residue analysis of similar acylurea compounds.

REFERENCES

1 M. Anderson, J. P. Fisher, J. Robinson and P. H. Debray, *Proc. Br. Crop Prot. Conf.—Pest Dis.*, 1 (1986) 89.
2 G. Perugia, C. Inglesfield and J. D. Tipton, *Proc. Br. Crop Prot. Conf.—Pest Dis.*, 1 (1986) 315.
3 B. W. Blair, *Crop Prot.*, 8 (1989) 212.
4 V. E. Deacon, M. A. van den Berg and B. Sutherland, *Ann. Appl. Biol.*, 114 (Suppl.) (1989) 6.
5 *Sittingbourne Analytical Method Series, SAMS 432-2*, Shell Sittingbourne, August, 1986.
6 *Sittingbourne Analytical Method Series, SAMS 432-3*, Shell Sittingbourne, July, 1987.
7 *Sittingbourne Analytical Method Series, SAMS 454-1*, Shell Sittingbourne, May, 1987.

Journal of Chromatography, 516 (1990) 446–449
Elsevier Science Publishers B.V., Amsterdam

CHROM. 22 549

Note

Small-scale method for the determination of organophosphorus insecticides in tea using sulphuric acid as clean-up reagent

HAIBIN WAN
Tea Research Institute, Chinese Academy of Agricultural Sciences, Hangzhou (China)
(First received November 23rd, 1990; revised manuscript received April 9th, 1990)

Some organophosphorus pesticides, such as malathion, fenitrothion and quinalphos, are regarded as suitable pesticides for tea plantation use because of their relatively low mammalian toxicity, low persistence on tea plants and high loss rate during the tea manufacturing process[1]. Many methods for determining residues of organophosphorus pesticides on crops have been reported[2,3]. Generally a volume of several hundred millilitres solvent is needed for the analysis of one sample in these methods, which makes them expensive. Sulphuric acid has been used successfully in the determination of some organochlorine pesticides and pyrethroids on tea[4,5]. This paper reports a simple and inexpensive method for the determination of organophosphorus pesticides in tea in which sulphuric acid as a clean-up reagent.

EXPERIMENTAL

Materials

Toluene, methanol and sulphuric acid (98%) were all of analytical-reagent grade and were used as received. Florisil (60–100 mesh) was heated at 600°C for 6 h and then deactivated by mixing with 5% (w/w) of distilled water.

The chromatographic mini-column (12 × 0.5 cm I.D.) used, with a solvent reservoir (5 ml) was of a similar size to of a Pasteur pipette.

A Hewlett-Packard HP-5790A gas chromatograph equiped with a nitrogen–phosphorus detector and a glass column (1.2 m × 2 mm I.D.) packed with 6% OV-101 on Chromosorb W (80–100 mesh) was used for residue analysis.

Method

Tea (10 g) was blended for 4 min with 100 ml of toluene–methanol (3:1, v/v) and the slurry obtained was filtered by suction through filter-paper on a Buchner funnel. The filtrate was shaken vigorously and an aliquot (10 ml) was transferred immediately into a 20-ml test-tube. After distilled water (1 ml) and sulphuric acid (1 ml) had been added, the test-tube was stoppered and shaken vigorously ten times and then allowed

0021-9673/90/$03.50

to stand for 10 min to effect phase separation. The upper (toluene) phase was transferred to the chromatographic mini-column or a Pasteur pipette packed with Florisil (1 g), using a Pasteur pipette. The test-tube was washed with toluene (1 ml) and the washings were added to the column. The column was then eluted with toluene–acetone (98:2, v/v; *ca.* 3 ml) until 10 ml of the eluate had been collected. The eluate was analysed by gas chromatography under following conditions: column temperature, 200°C; injector temperature, 230°C; detector temperature, 250°C; carrier gas (nitrogen) flow-rate, 50 ml/min; air flow-rate, 80 ml/min; and hydrogen flow-rate, 1.5 ml/min.

The retention times of dimethoate, fenitrothion, malathion and quinalphos were 1.9, 3.6, 3.9 and 5.7 min, respectively. The detection limit was 0.01 mg/kg for quinalphos and 0.02 mg/kg for malathion and fenitrothion.

Recovery test

Dimethoate, malathion, fenitrothion and quinalphos dissolved in benzene (1 μg/ml) were added to tea (10 g) at the level of 0.1–0.3 mg/kg. The fortified samples were extracted and analysed immediately after the fortification, following the above procedure.

Field test and sample analysis

Fenitrothion (50% emulsifiable concentrate) was sprayed on tea plants at 900 g active ingredient per ha. Tea shoots were collected at random over the test plot (300 m^2) at various intervals, and processed to green tea by the commonly used methods.

The green tea samples were analysed by the above method. To investigate the extraction efficiency, the residue from the blending extracted samples was Soxhlet extracted with 100 ml of chloroform–methanol (9:1, v/v) for 6 h with about six solvent exchanges per hour. The extract was concentrated to *ca.* 1 ml at 50°C, and then dissolved in 10 ml of toluene–methanol (3:1, v/v). The solution was transferred into a 20-ml test tube and analysed following the procedure described above.

RESULTS AND DISCUSSION

Recoveries of pesticides

The recoveries of dimethoate, malathion, fenitrothion and quinalphos are given in Table I.

TABLE I

RECOVERIES OF PESTICIDES

Means of four replicate determinations.

Pesticide	*Recovery ± S.D. (%)*	*Fortified level (mg/kg)*
Dimethoate	21.9 ± 9.2	0.3
Fenitrothion	97.2 ± 0.8	0.1
Malathion	94.4 ± 7.1	0.3
Quinalphos	96.1 ± 8.1	0.3

Fenitrothion, malathion and quinalphos all showed recoveries above 90%, but dimethoate was nearly totally lost, suggesting that fenitrothion, malathion and quinalphos were satisfactorily stable to the sulphuric acid treatment but dimethoate was not.

Extraction efficiency

The tea samples collected during the field test were first analysed by the blending method, and then Soxhlet extracted. The results are given in Table II.

TABLE II

FENITROTHION RESIDUES ON TEA SAMPLES COLLECTED DURING THE FIELD TEST

Means of two replicate determinations: (A) by blending method; (B) by Soxhlet extraction.

Days after spraying	*Residues (mg/kg)*		*Ratio B/A*
	A	*B*	
0	9.46		
2	1.27	0.017	0.013
5	0.20	0.002	0.010
8	0.09	0.012	0.13
15	0.02	0.007	0.35

The ratio of the residues extracted by Soxhlet extraction to that given by the blending method was proportional to the period of time the sample had weathered in the field. It has been reported that the recoveries of organophosphorus pesticides were best when Soxhlet extraction with chloroform–methanol (9:1, v/v) was used[6]. The present results suggest that most of the fenitrothion residues in tea were removed by the blending method.

Clean-up effect

The coextractives were mainly caffeine and polyphenols. Caffeine has a very similar polarity to those of many non-polar organophosphorus pesticides. Its retention behaviour and detection limit are also very close to those of malathion and fenitrothion, making the gas chromatographic determination of these two pesticides very difficult by commonly used residue methods.

The present method was able to remove caffeine completely from the extract, while still giving good recoveries of non-polar organophosphorus pesticides. The chromatograms showed no impurity peaks which would affect the analysis. After over 50 injections the response and the baseline of the gas chromatograph were still steady, which indicates that the clean-up of the samples was adequate.

REFERENCES

1 Z. Chen and H. Wan, *Pestic. Sci.*, 23 (1988) 109.
2 H. A. Moye (Editor), *Analyis of Pesticide Residues*, Wiley, New York, 1981, p. 263.
3 J. Sherma, *Anal. Chem.*, 61 (1989) 153.
4 Z. Chen, H. Han, H. Wan and R. Yue, *Acta Sci. Circumstantiae*, 6 (1986) 278.
5 H. Wan, *Pesticides*, 2 (1989) 27.
6 M. C. Bowman, M. Beroza and D. B. Leuck, *J. Agric. Food Chem.*, 16 (1968) 796.

Journal of Chromatography, 516 (1990) 450–455
Elsevier Science Publishers B.V., Amsterdam

CHROM. 22 529

Note

Chemiluminescence detection of free fatty acids by high-performance liquid chromatography with immobilized enzymes

HIDEKI KAWASAKI*, NORIO MAEDA and HIDETAKA YUKI
Department of Clinical Chemistry, School of Pharmaceutical Sciences, Toho University, Miyama 2–2–1, Funabashi, Chiba 274 (Japan)
(First received October 10th, 1989; revised manuscript received April 10th, 1990)

Recently, the assay of free fatty acids (FFA) has become important in biochemical and clinical investigations. Although high-performance liquid chromatography (HPLC) is widely used for this purpose, most of these methods involve the formation of derivatives having ultraviolet or fluorescent groups[1,2]. Fatty acids themselves generally do not show strong absorption in the ultraviolet region, so that direct detection is not suitable for trace analysis. In the clinical field, an enzymatic method has been used for the determination of total fatty acids in serum[3,4] by spectrophotometry, using an acyl-CoA synthetase (ACS) and acyl-CoA oxidase (ACO) reaction system:

$$\text{RCOOH} + \text{CoA} + \text{ATP} \xrightarrow{\text{ACS, } Mg^{2+}} \text{acyl-CoA} + \text{AMP} \quad (1)$$

$$\text{Acyl-CoA} + O_2 \xrightarrow{\text{ACO}} \text{2,3-}\textit{trans}\text{-enoyl-CoA} + H_2O_2 \quad (2)$$

Chemiluminescence detection:

$$H_2O_2 + \text{luminol} \xrightarrow{\text{mPOD, } OH^-} \text{aminophthalate} + N_2 + \text{light} \quad (3)$$

of the hydrogen peroxide formed by the same reaction system has also been reported[5]. As these methods are carried out in a test-tube reaction system, the differential analysis of constituents of the fatty acids is difficult. However, this problem can be approached by coupling the HPLC system with immobilized enzyme reactors in the similar manner to that described by Koerner and Nieman[6], in which the glucosides were determined by HPLC using immobilized enzyme reactors and a chemiluminescence detector. Lawrence and Charbonneau[7] reported a simple HPLC method with a post-column ion-pair extraction and detection system; however, the enzymatic method has the advantage of selectivity. Therefore, in this paper, we describe a novel HPLC method

0021-9673/90/$03.50

for the detection of individual fatty acids without the labelling procedure, using the immobilized ACS–ACO system, coupled with chemiluminescence detection of hydrogen peroxide catalysed by microperoxidase (mPOD).

EXPERIMENTAL

Materials

Luminol was of analytical-reagent grade from Tokyo Kasei Kogyo (Tokyo, Japan) and microperoxidase (MP-11) was a product of Sigma (St. Louis, MO, U.S.A.). N,N′-Dicyclohexylcarbodiimide (DCC), N-hydroxysuccinimide (for peptide synthesis) and standard fatty acids were products from Nacalai Tesque (Kyoto, Japan). Acyl-CoA synthetase (type III) and acyl-CoA oxidase (type II) were purchased from Toyobo (Osaka, Japan). Coenzyme A (CoA) and adenosine 5′-triphosphate (ATP) were products of Khojin (Tokyo, Japan). Carboxyl-controlled-pore glass (carboxyl-CPG, CBX-500, 120–200 mesh) was obtained from Electro-Nucleonics (Fairfield, NJ, U.S.A.) and polyoxyethylene(10)octyl phenyl ether (Triton X-100) was obtained from Wako (Osaka, Japan). Other reagents were of analytical-reagent grade. Desalted, distilled water was used throughout.

High-performance liquid chromatography

The high-performance liquid chromatograph used was a Shimadzu (Kyoto, Japan) Model LC-6A and the high-pressure sample injector was a Shimamura (Tokyo, Japan) Model EIE-005. The separation column was LiChroCART Superspher 60 RP-8 (25 mm × 4 mm I.D.) (Merck, Darmstadt, F.R.G.). The post-column reactor consisted of double plunger pump (Simamura Keiki, Tokyo, Japan) for reagent delivery and an immobilized enzyme column (50 mm × 3 mm I.D.) (Omnifit minicolumn). The flow cell of the detector was a laboratory-made spiral-shaped PTFE tube (290 μl). The light emitted was measured with a Niti-On (Tokyo, Japan) photometer. The recorder was a Shimadzu Chromatopak C-R3A. The arrangement of the manifolds used is shown in Fig. 1.

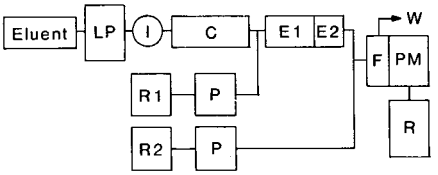

Fig. 1. Schematic diagram of the HPLC system and the manifold for chemiluminescence detection. LP = Liquid chromatograph pump; I = injector; C = LiChroCART Superspher 60 RP-8 (HPLC column); E1 and E2 = immobilized ACS and ACO column, respectively; F = flow cell; R1 = reagent R1; R2 = reagent R2; P = pump; PM = photometer; R = recorder–integrator; W = waste.

Immobilization of enzymes

Immobilization of enzymes was performed as follows. Carboxyl-CPG (0.2 g) was added to 10 ml of a dioxane solution of 0.1 *M* N-hydroxysuccinimide and 0.1 *M* N,N′-dicyclohexylcarbodiimide and the mixture was stirred for 120 min at room temperature. The CPG was washed with 20 ml of dioxane, 10 ml of methanol and 10 ml

of dioxane successively under suction and then dried. The imidoester-CPG thus obtained was reacted with ACO (10 mg, 10 units/mg) dissolved in 5 ml of phosphate buffer solution (pH 5.5) below 4°C. After 6 h it was washed extensively with 0.1 *M* phosphate buffer solution (pH 7.4), the same buffer solution containing 1 *M* NaCl and water for three cycles, and was kept below 4°C. ACS (5 mg, 1.47 units/mg) was added to 5 ml of 0.1 *M* phosphate buffer solution (pH 8.0) and treated in a similar manner to ACO. The immobilization yields of the enzymes were calculated from the protein concentration of the solution determined by the Lowry method[8] before and after the reaction.

Separation and detection of fatty acids

The HPLC mobile phase was methanol–phosphate buffer solution (pH 8.0) (1:1), and was degassed by ultrasonication for 10 min prior to use. The flow-rate was 0.3 ml/min. Reagent R1 (flow-rate 0.45 ml/min) was 20 m*M* phosphate buffer solution (pH 7.6) containing 0.5 m*M* $MgCl_2$, 0.05 m*M* CoA, 0.1 m*M* ATP and 0.25% Triton X-100. Reagent R2 (flow-rate 0.75 ml/min) was 50 m*M* carbonate buffer solution (pH 10.5) containing 10 μM luminol and 0.8 μM microperoxidase. The lengths of the immobilized ACS and ACO columns were 35 and 15 mm, respectively. The sample solution of fatty acids injected was 10 μl of a methanol–phosphate buffer solution (pH 7.6) (1:1) containing 1 nmol of each fatty acid. The output from the photometer was recorded with the C-R3A.

RESULTS AND DISCUSSION

The chemiluminescence detection system with a flow cell unit was devised and reported previously[9]. In this work, the system was used with the enzyme reactor inserted in front of the detection unit and with a slightly modified flow cell, in which the volume was increased from 75 to 290 μl so as to detect as much of the light emitted from the samples as possible. The whole apparatus for fatty acid detection is shown schematically in Fig. 1. Each fatty acid eluted from the HPLC column was mixed with reagent R1 and subjected to enzymatic reaction in the immobilized ACS–ACO column to form hydrogen peroxide, which was mixed with the chemiluminescence reagent R2 and the light emitted in the flow cell was detected by the photomultiplier.

Optimization of the reaction conditions for the detection of hydrogen peroxide was carried out by a flow-injection method without the HPLC column. The effect of the concentrations of luminol and microperoxidase in reagent R2 on the chemiluminescence intensity was first examined by injecting 450 pmol of hydrogen peroxide. The concentrations examined for luminol and microperoxidase were in the ranges 10 n*M*–100 μM and 0.2–2.0 μM, respectively, and maximum intensity was obtained at 10 μM for luminol and 0.8 μM for microperoxidase. The variations in chemiluminescence intensity and background noise level with changes in the pH of reagent R2 were examined in the pH range 5–10.5, and the best result was obtained at pH 10.5. Under the optimized conditions, a linear calibration graph for hydrogen peroxide was obtained in the range 12.5–200 pmol. The limit of detection was 5 pmol (10-μl injection, signal-to-noise ratio = 2, relative standard deviation = 1.6%, n = 5).

The immobilization of ACS and ACO has not been reported previously, so the methods for immobilization of these enzymes were examined first. As the detection

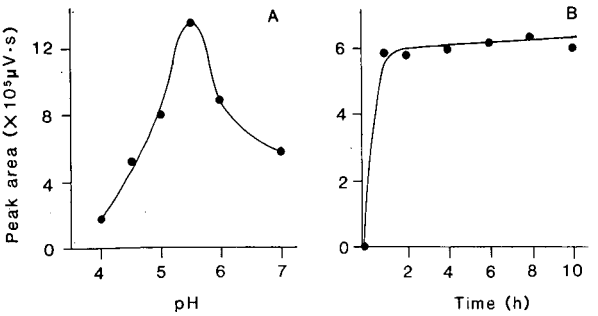

Fig. 2. (A) Optimum pH for immobilization and (B) time course of immobilization reaction of acyl-CoA oxidase. Experimental conditions as described in the text.

system was operated under high pressure, controlled-pore glass beads were used as the support. First, immobilization of the enzymes with the glutaraldehyde method was attempted, but this method did not give a reproducible activity of the immobilized enzymes. However, the use of DCC and N-hydroxysuccinimide gave good results. Therefore, the conditions for the immobilization of enzymes were investigated further using this method. The optimum pH for immobilization of ACO was examined in the range 4.0–7.0, and the maximum activity was obtained at pH 5.5 (Fig. 2A). The activity of immobilized ACO was measured with the flow-injection system, injecting 0.2 μmol of palmitoyl-CoA as a sample. The immobilization reaction was allowed to proceed for 6 h at 4°C, which was adequate for the reaction (Fig. 2B). The immobilization yield was 67%. The optimum pH for immobilization of ACS was examined in the range 5.5–8.5, and pH 7.6 was found to give the best results. As ACS was labile during the immobilization reaction, even if the enzyme was treated at the optimum pH, the yield obtained was only 7.6%.

The enzyme reactor consisted of two columns, packed with the immobilized ACS and ACO. The flow-injection method with these columns was used for optimization of the reaction conditions. The effect of the concentration of CoA in reagent R1 on the chemiluminescence was examined up to 0.075 mM, injecting 5 nmol of palmitic acid as a sample. As shown in Fig. 3A, 0.01 mM gave the maximum response, and it decreased slowly as the concentration was increased further. This is

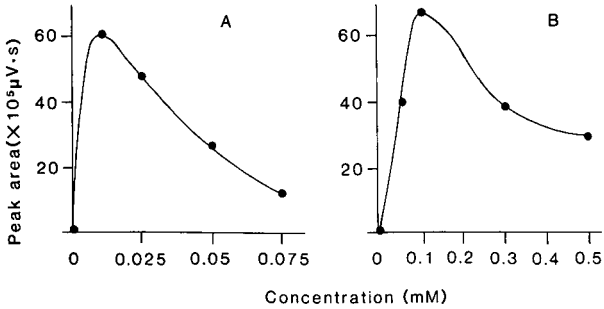

Fig. 3. Effect of the concentration of (A) coenzyme-A and (B) ATP on the immobilized enzyme reaction. Experimental details as described in the text.

probably due to the effect of the SH group of CoA remaining, but this effect can be avoided by the use of N-ethylmaleimide if the remaining CoA extremely interferes with the detection. Therefore, 0.05 m*M* was chosen as an excess amount for the enzyme reaction. Fig. 3B shows the effect of ATP concentration between 0 and 0.5 m*M*, the maximum response being obtained at 0.1 m*M*. The concentration of Mg^{2+} had little effect on the reaction of ACS, so 0.5 m*M* $MgCl_2$ was used.

The ratio of ACS to ACO was also examined, and it was found that the sensitivity was constant at ratios above 3:2. In view of sample dispersion, a shorter column affords compact and sharp peaks, *i.e.*, higher sensitivity. Therefore, the two immobilized enzymes were packed in a single column of length 50 mm; a 35-mm length of ACS followed by a 15-mm length of ACO showed the highest sensitivity.

Under the optimized conditions specified above, the relationship between the chain length of saturated fatty acids and the chemiluminescence response was examined. Fatty acids from C_8 to C_{10} showed a strong response, and as the carbon number increased further a lower response was obtained. However, fatty acids up to C_{17} were definitely detected (Fig. 4).

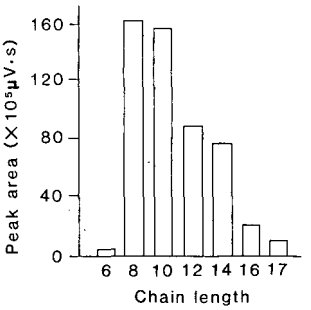

Fig. 4. Specificity of immobilized acyl-CoA synthetase and acyl-CoA oxidase on chain length of fatty acids. The samples were methanol–phosphate buffer solutions (pH 7.6) (1:1) of *n*-caproic acid (C_6), *n*-caprylic acid (C_8), *n*-capric acid (C_{10}). lauric acid (C_{12}), myristic acid (C_{14}), palmitic acid (C_{16}) and margaric acid (C_{17}). The sample volume was 10 μl, containing 5 nmol of the fatty acid.

The HPLC separation of fatty acids was examined with RP-18, RP-8 and RP-4 reversed-phase columns. On the RP-18 column, fatty acids were so strongly retained that the retention time was impractical for analysis. The RP-4 column did not show the features of a reversed-phase packing but of ion exclusion at higher pH. Of these columns examined, LiChroCART Superspher 60 RP-8 gave the best separation of the fatty acids. The effect of the pH of the eluent on retention times was examined between 6 and 8.5, and it was found that fatty acids were more retained as the pH was decreased, but there was almost no effect above pH 7.6. An eluent pH of 8.0 was chosen. The methanol concentration in eluent was also examined in the range 40–55%, and 50% was chosen as 55% methanol lowered the luminescence strength.

Fig. 5 shows the separation and detection of fatty acids in 3 h under the above conditions. Each fatty acid was well separated, except parmitoleic ($C_{16:1}$) and linolenic ($C_{18:3}$) acids. The retention times of oleic ($C_{18:1}$) and stearic ($C_{18:0}$) acid were so long that their detection was difficult because of the broadening of the peaks. The

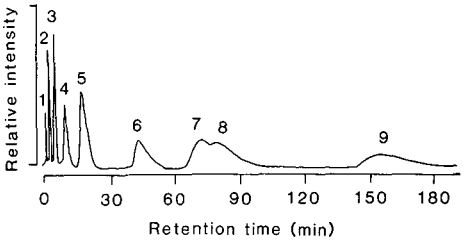

Fig. 5. Chromatogram of the authentic fatty acids. HPLC conditions as described in the text. Peaks: 1 = *n*-caprylic acid ($C_{8:0}$); 2 = *n*-capric acid ($C_{10:0}$); 3 = dodecenoic acid ($C_{12:1}$); 4 = lauric acid ($C_{12:0}$); 5 = myristoleic acid ($C_{14:1}$); 6 = myristic acid ($C_{14:0}$); 7 = linolenic acid ($C_{18:3}$); 8 = palmitoleic acid ($C_{16:1}$); 9 = linoleic acid ($C_{18:2}$).

calibration graph for *n*-capric acid was linear in the range 0.4–2.0 nmol. The resolution of the RP-8 column was maintained during 2 months of these experiments (more than 100 injections), provided that the column was filled with methanol between experiments. Usually higher concentrations of methanol (80–100%) are employed in the separation of fatty acids by reversed-phase HPLC for a faster separation. However, high concentrations of methanol inactivate the enzymes immobilized in the column and so could not be used in the present method.

In conclusion, fatty acids were selectively detected by a chemiluminescence method without labelling using an immobilized ACS–ACO column. Unfortunately, the method requires a long chromatographic separation, has a limited linear range, is not suitable for $C_{18:0}$ and $C_{18:1}$ fatty acids and the organic content of the mobile phase is restricted.

REFERENCES

1 W. Voelter, R. Huber and K. Zech, *J. Chromatogr.*, 217 (1981) 491.
2 Y. Shimomura, S. Sugiyama, T. Takemura, T. Kondo and T. Ozawa, *J. Chromatogr.*, 383 (1986) 9.
3 S. Shimizu, Y. Tani, H. Yamada and T. Murachi, *Anal. Biochem.*, 107 (1980) 193.
4 K. Mizuno, M. Toyosato, S. Yabumoto, I. Tanimizu and H. Hirakawa, *Anal. Biochem.*, 108 (1980) 6.
5 Y. Uji, H. Okabe, Y. Sakai, A. Noma, M. Maeda and A. Tsuji, *Clin. Chem.*, 35 (1989) 325.
6 P. J. Koerner, Jr. and T. A. Nieman, *J. Chromatogr.*, 449 (1988) 217.
7 J. Lawrence and C. Charbonneau, *J. Chromatogr.*, 445 (1988) 189.
8 O. Lowry, N. Rosebrough, A. Farr and R. Randall, *J. Biol. Chem.*, 193 (1951) 265.
9 H. Yuki, Y. Azuma, N. Maeda and H. Kawasaki, *Chem. Pharm. Bull.*, 36 (1988) 1905.

Journal of Chromatography, 516 (1990) 456–460
Elsevier Science Publishers B.V., Amsterdam

CHROM. 22 528

Note

Reversed-phase high-performance liquid chromatographic study of the formation of complexes of nucleotides and oligonucleotides with Lu(III)

ALEXANDER SIGALOV
U.S.S.R. Research Centre for Preventive Medicine, Petroverigsky Street 10, 101953 Moscow (U.S.S.R.)
(First received February 28th, 1989; revised manuscript received May 1st, 1990)

High-performance liquid chromatography (HPLC) is widely used in the analysis of nucleoside–nucleotide mixtures and in the isolation of synthetic oligonucleotides[1–3]. As shown previously[4,5], the presence of Mg(II) ions in the mobile phase greatly affects the retention times of the nucleotides, and in some instances allows the separation time to be considerably reduced and the process to be simplified.

This paper reports investigations on the reversed-phase HPLC of deoxynucleosides, deoxynucleotides and oligodeoxynucleotides in standard systems of solvents in the presence of lutetium chloride ($LuCl_3$). This lanthanide has the smallest radius among the rare earth elements and so possesses the maximum ability to form complexes with different n- and π-donors.

EXPERIMENTAL

Materials and apparatus

Deoxynucleosides and deoxynucleotides were obtained from SKTB BAV (Novosibirsk, U.S.S.R.). [γ-^{32}P]ATP (3000 Ci/mmol) was obtained from Amersham (Amersham, U. K.). UV spectra were recorded on a Specord M40 spectrophotometer.

HPLC procedures

Reversed-phase HPLC was carried out at 25°C on a Gilson liquid chromatograph equipped with a UV detector (254 nm). For the separation of the deoxynucleosides and deoxynucleotides, a column (250 × 4 mm I.D.) with LiChrosorb RP-18 (LKB, Bromma, Sweden), particle size 10 μm, as the stationary phase was used; the mobile phases were (A) 0.05 *M* KH_2PO_4 (or 0.05 *M* $HCOONH_4$)–methanol (89:11, v/v), pH 4.2, and (B) 0.05 *M* CH_3COONH_4–methanol (89:11, v/v), pH 6.2, with or without 80 μM $LuCl_3$. The flow-rate was 2 ml/min. For the analysis of a crude 20-mer oligodeoxynucleotide and a slab gel-purified 20-mer oligodeoxynucleotide, a column (250 × 4 mm I.D.) with LiChrosorb RP-8 (LKB), particle size 10 μm was used; the mobile phases were 0.05 M CH_3COONH_4 (pH 6.2), with or without 80 μM $LuCl_3$,

0021-9673/90/$03.50

with a stepped acetonitrile gradient from 0 to 60% (0–8 min, 0–8%; 8–10 min, 8%; 10–15 min, 8–15%; 15–20 min, 15%; 20–25 min, 15–30%; 25–30 min, 30%; 30–35 min, 30–60%; and 35–40 min, 60% acetonitrile). The flow-rate was 1 ml/min. The capacity factor, k', is defined by $k' = (V_R - V_0)/V_0$, where V_R is the retention volume of the substance of interest and V_0 that of an unretarded substance (usually the solvent).

Oligonucleotide synthesis

The oligodeoxynucleotides CCAGCCCTAGGGATTGAG (I), CTTATGTGCACGATGCACCT (II) and AACGAGGGTACCAACGGCTA (III) were synthesized by a solid-phase phosphoramidate method according to a previously described procedure[6]. Aminopropyl-CPG-550Å (Fluka, Buchs, Switzerland) was used as a polymeric carrier. As soon as the synthesis and last detritylation had been accomplished, the P-methoxy protecting groups were removed by the treatment with thiophenol–dioxane–triethylamine (1:3:1, v/v/v) at 20°C for 45 min. Subsequently, the carrier was washed with ethanol and diethyl ether and dried. The splitting of the oligodeoxynucleotides from the carrier was performed with 25% ammonia solution at 20°C for 3 h; thereafter the carrier was filtered off and the solution sealed in an ampoule and maintained for 20 h at 60°C. The crude mixture was separated by preparative 20% polyacrylamide slab gel electrophoresis under denaturated conditions. The zone containing the desired product was cut off and the transfer of oligodeoxynucleotide was performed on DEAE-cellulose by electroelution. The oligodeoxynucleotide was then eluted with a minimum volume 1.5 *M* aqueous lithium perchlorate solution for 10 h at 37°C, precipitated with 2% lithium perchlorate in acetone, washed with acetone and ethanol–water (80:20) and dried.

Analysis of a crude 20-mer oligodeoxynucleotide

The crude 20-mer oligodeoxynucleotide (II) was analysed by reversed-phase HPLC under the above conditions. The fractions were collected, evaporated, dissolved in water and precipitated with 2% lithium perchlorate in acetone by the described technique. All fractions were radiolabelled using T4 polynucleotide kinase and [γ-^{32}P]ATP (3000 Ci/mmol) in a standard reaction mixture[7]. An aliquot of each sample was loaded onto 20% polyacrylamide slab gel. After electrophoresis, the gel was fixed and then dried. Autoradiography was performed at −70°C using an intensifying screen for 1 h.

RESULTS AND DISCUSSION

The results (Table I) showed that in buffer A at pH 4.2 in the presence of 80 μM $LuCl_3$ the capacity factors (k') for both the deoxynucleosides and deoxynucleotides decrease. This phenomenon may be explained by the formation of Lu(III) complexes with the heterocyclic bases, which leads to some increase in hydrophilicity. The latter was observed for protein molecules during the isolation of α-interferon by HPLC when $LaCl_3$ was added to the mobile phase[8]. Similar retention behaviour was also observed for the deoxynucleosides on applying buffer B (pH 6.2) (Table I).

The effect of Lu(III) is much more noticeable with deoxynucleotides when buffer B is used. The capacity factors for these compounds increase considerably, prob-

TABLE I

CAPACITY FACTORS OF DEOXYNUCLEOSIDES AND DEOXYNUCLEOTIDES IN REVERSED-PHASE HPLC WITH (k'_{Lu}) AND WITHOUT (k') 80 μM $LuCl_3$

Compound	*Buffer A (pH 4.2)*[a]			*Buffer B (pH 6.2)*[a]		
	k'	k'_{Lu}	k'_{Lu}/k'	k'	k'_{Lu}	k'_{Lu}/k'
dA	11.53	7.73	0.67	13.84	11.65	0.84
dG	3.42	2.41	0.70	3.89	3.42	0.88
dC	1.03	0.77	0.75	1.26	1.14	0.90
dT	3.95	2.87	0.73	4.28	3.77	0.88
dCMP	0.40	0.39	0.98	0.19	1.25	6.58
dGMP	0.95	0.86	0.91	0.63	4.47	7.10
dAMP	2.03	1.45	0.71	1.42	11.33	7.98
dADP	0.83	0.63	0.76	0.74	6.68	9.02
dATP	0.53	0.39	0.74	0.40	4.62	11.55

[a] See *HPLC procedures.*

ably owing to the formation of Lu(III)–deprotonated phosphate group complexes. The existence of such complexes is also confirmed by the increase in the capacity factors for deoxynucleotide as the number of phosphate groups increases. Thus, the k'_{Lu}/k' ratio is 11.55, 9.02 and 7.98 for dATP, dADP and dAMP, respectively, and the retention order is dAMP < dADP < dATP (Table I). The retention order for these deoxynucleotides with a mobile phase not containing Lu(III) is dATP < dADP < dAMP. There is evidence[4,5] that Mg(II) ions form strong complexes with deprotonated phosphate groups when Mg(II) salts are added to the mobile phase at a concentration $8.1 \cdot 10^{-4}$ M, which results in a decrease in the capacity factors of nucleotides in anion-exchange and reversed-phase HPLC. The reasons for the decrease are not clear. In this work, probably the formation of a strong complex of Lu(III) with the deprotonated phosphate groups and the bases results in phosphate charge neutralization and a decrease in hydrophilicity. Correspondingly, an increase in the retention indices of the deoxynucleotides is observed in reversed-phase HPLC with the addition of $8.0 \cdot 10^{-5}$ M Lu(III) to the mobile phase.

The chromatographic behaviour of the oligodeoxynucleotides in the presence of Lu(III) was studied by using a slab gel-purified 20-mer oligodeoxynucleotide (I). The capacity factor appears to increase in the presence of 80 μM $LuCl_3$ and the ratio k'_{Lu}/k' is 1.47. The analysis of the crude mixture obtained by the synthesis of the oligodeoxynucleotide II under the same conditions of separation indicates that the presence of 80 μM $LuCl_3$ induces a change in the general separation pattern and an improvement in the purification of the desired product (Fig. 1, top). The k'_{Lu}/k' ratio is 1.81–2.10 (depending on the gradient profile of acetonitrile) for the zone containing the principle amount of the desired oligodeoxynucleotide (up to 90%, determined by slab-gel electrophoresis of the radiolabelled collected fractions and subsequent autoradiography). In addition, the application of the above buffer containing 80 μM $LuCl_3$ permits the flow-rate to be increased from 1 to 2 ml/min without worsening the separation pattern (data not shown).

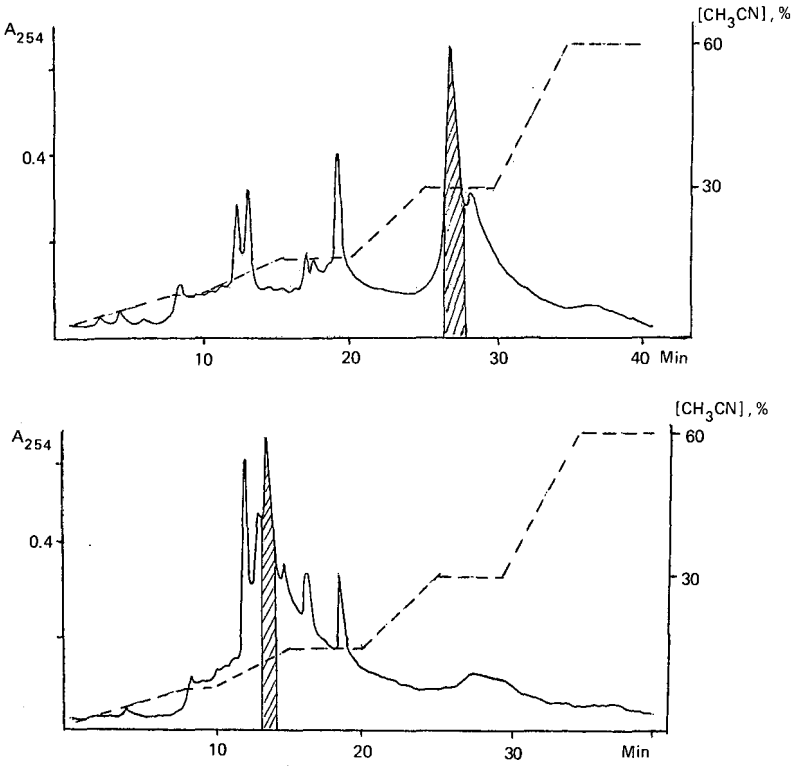

Fig. 1. Reversed-phase HPLC of crude 20-base oligodeoxynucleotide CTTATGTGCACGATGCACCT. Column, LiChrosorb RP-8 (250 × 4 mm I.D.). Mobile phase: gradient of acetonitrile concentration (broken line) in 0.05 *M* ammonium acetate (pH 6.2), (top) with and (bottom) without 80 μM $LuCl_3$. Flow-rate, 1 ml/min. The shaded area is that containing the major amount (up to 90%) of the desired product.

Hence the addition of 80 μM $LuCl_3$ to the mobile phases usually used in reversed-phase HPLC leads to a pronounced increase in the capacity factors for compounds with deprotonated phosphate groups (deoxynucleotides and oligodeoxynucleotides).

The UV spectra of the oligodeoxynucleotide III at various concentrations were measured to investigate the mechanism of the interaction of Lu(III) with oligodeoxynucleotides in aqueous solutions. Fig. 2 illustrates that the change in the molar absorption coefficient is 12–17% at λ_{max} = 260.4 nm, whereas the $LuCl_3$-to-phosphate molar ratio ranges from 0.7 to 7.0. This effect may be associated with a disturbance of the "stacking" interaction between the heterocyclic oligodeoxynucleotide bases caused by the formation of the Lu(III) complexes with both the phosphate groups and the heterocyclic bases. A change in the oligodeoxynucleotide structure seems to be another reason for the increase in the capacity factors of the oligodeoxynucleotides in the presence of 80 μM $LuCl_3$.

An interesting analogy is observed by comparison of the above results with

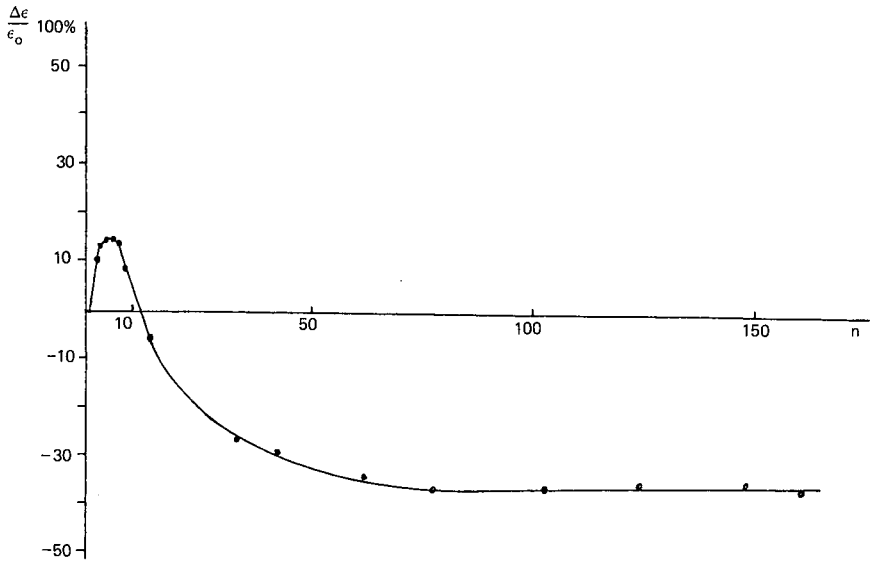

Fig. 2. Relationship between $\Delta\varepsilon/\varepsilon_0$ [ε_0 = molar absorption coefficient at $\lambda_{max} = 260.4$ nm of the initial oligodeoxynucleotide (III)] and the molar ratio of $LuCl_3$ to phosphate groups of oligodeoxynucleotide.

those from a study of the fluorescence of Tb(III) complexes with nucleic acids[9]. The Tb(III) fluorescence appeared to increase considerably from 0.4–0.6 with increase in the Tb(III)-to-phosphate group molar ratio up to $n = 2.8$ in the presence of a single-stranded RNA ($rC_{75}G_{75}$). Unfortunately, the Tb(III) fluorescence at $n > 2.8$ was not investigated, and therefore we cannot compare the titration curve in our study with the corresponding[9] characteristic over the entire range of n values.

In conclusion, the results presented here show that the formation of strong Lu(III) complexes with deoxynucleotides and oligodeoxynucleotides in aqueous solutions results in alterations of both the optical characteristics and the chromatographic behaviour of these compounds.

ACKNOWLEDGEMENTS

The author is grateful to N. Petcheritsa and V. Pedchenko for assistance.

REFERENCES

1 S. A. Standard, P. Vaux and C. M. Bray, *J. Chromatogr.*, 318 (1985) 433.
2 B. Allinquant, C. Musenger and E. Schuller, *J. Chromatogr.*, 326 (1985) 281.
3 C. R. Becker, J. W. Efcavitch, Ch. R. Heiner and N. F. Kaiser, *J. Chromatogr.*, 326 (1985) 293.
4 E. Grushka and F. K. Chow, *J. Chromatogr.*, 199 (1980) 283.
5 A. S. Cohen and E. Grushka, *J. Chromatogr.*, 318 (1985) 221.
6 S. M. Gryasnov, V. K. Potapov, V. G. Metelev, A. A. Elov, A. A. Purmal and Z. A. Shabarova, *Bioorg. Khim.*, 12 (1986) 988.
7 T. Maniatis, E. F. Fritisch and J. Sambrook, *Molecular Cloning: a Laboratory Manual*, Cold Spring Harbor Laboratory, Cold Spring Harbor, NY, 1982.
8 H. J. Friesen, S. Stein, M. Evinger, P. C. Familletti, J. Moshera, J. Meinhofer, J. Shively and S. Pestka, *Arch. Biochem. Biophys.*, 206 (1981) 432.
9 M. D. Topal and J. R. Fresco, *Biochemistry*, 19 (1980) 5531.

Journal of Chromatography, 516 (1990) 461–466
Elsevier Science Publishers B.V., Amsterdam

CHROM. 22 542

Note

Modification of a horizontal sandwich chamber for thin-layer chromatography

TADEUSZ H. DZIDO* and EDWARD SOCZEWIŃSKI
Department of Inorganic and Analytical Chemistry, Medical Academy, Staszica 6, 20-081 Lublin (Poland)
(First received November 6th, 1988; revised manuscript received May 8th, 1990)

Thin-layer chromatography (TLC) is still commonly used, and new analytical applications and recent developments have been reported[1–5]. In recent years sandwich chambers have become more popular than conventional cylindrical or rectangular containers in which the plate is placed in an approximately vertical position. In sandwich chambers much less eluent is consumed; the eluent is poured into a narrow trough and is delivered to the adsorbent layer by various methods[6–8], *e.g.*, by a wick made of filter-paper, felt or a frit. In another construction[9], the role of the wick is played by a long porous strip placed in the eluent trough under the plate with the adsorbent layer underneath; the development starts when the reservoir (trough) is elevated so that the strip is pressed against the adsorbent layer. In Soczewiński's chamber[10–12], the eluent is delivered by a capillary siphon to a flat horizontal slit formed between the distributor beneath the cover-plate and the margin of the carrier plate cleaned of adsorbent; development is started by shifting the distributor (a thin strip of glass) over the edge of adsorbent layer. In the Camag linear developing chamber[3], the eluent is delivered from the trough to the edge of the plate through a narrow slit formed between the vertical wall of the trough and an adjacent glass plate.

Horizontal sandwich chambers have several advantages over conventional saturated chambers, *e.g.*, the horizontal position of the plate accelerates the migration of the mobile phase, the consumption of eluent is much lower and the sample can be applied as a band for micropreparative separations. Their disadvantage is a more complex construction and a correspondingly higher price.

In this paper a modified sandwich chamber is described.

CONSTRUCTION OF THE CHAMBER

The modified construction of the horizontal sandwich chamber developed in this laboratory[13,14] is relatively simple (Fig. 1). Fig. 1a shows its cross-section before development: the glass plate (1) covers a shallow (1 mm deep) rectangular reservoir (2) with the eluent (3). The precoated chromatographic plate (4) is placed (adsorbent layer downwards) on two parallel 1-mm ledges (6) (in Fig. 1 one is visible) on its longer edges, several millimetres from the eluent reservoir.

0021-9673/90/$03.50

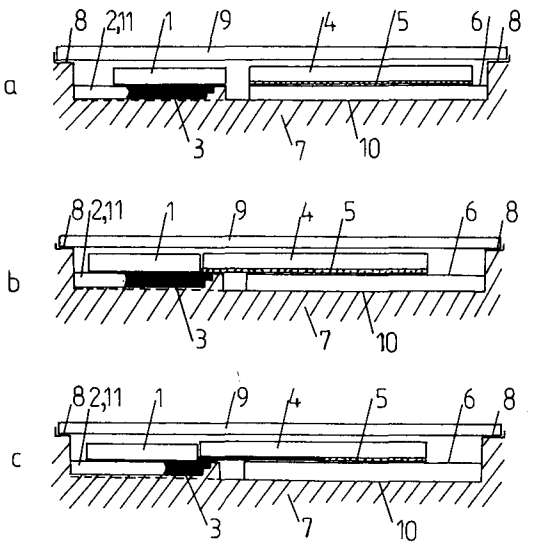

Fig. 1. Principle of action of modified sandwich chamber with a horizontal bottom of the eluent reservoir. 1 = Glass cover-plate; 2 = eluent reservoir; 3 = solvent; 4 = chromatographic plate; 5 = (dotted area) thin layer of adsorbent; 6 = ledge supporting the TLC plate; 7 = body of the chamber; 8 = rectangular depression; 9 = glass cover-plate of the chamber; 10 = bottom; 11 = edges of the eluent reservoir. (a) Original position; (b) beginning of development; (c) advanced development.

The chromatographic process is started by shifting the chromatographic plate 4 to the left (together with the cover-plate 1) so that its edge rests on the threshold of the reservoir and comes into contact with the eluent 2 along a narrow (*ca.* 1 mm) zone. Because the eluent reservoir is shallow (*ca.* 1 mm), a vertical meniscus is formed between its bottom and the cover-plate; the meniscus shifts to the right as the eluent is absorbed by the thin layer of adsorbent (Fig. 1c). To the right, the bottom is shallower, in the form of a step; the surface tension accumulates the last drops of eluent between this step and the adsorbent layer to the end, thus securing uniform delivery of eluent on the whole width of the adsorbent layer.

Another design which is advantageous owing to the sucking of the eluent by capillary forces in the direction of the edge of the chromatographic plate is to use a reservoir with a slanted bottom with the depth varying, *e.g.*, from 2 to 0.5 mm on the side of the plate, as illustrated in Fig. 2 for situations analogous to that in Fig. 1: (a) preliminary position; (b) beginning of development; and (c) partly developed plate with diminished volume of eluent in the reservoir.

Another version of development, suitable also for less stable self-made layers, consists in putting the plate 4 from the beginning in position (b) (Figs. 1 and 2) in a dry chamber. The reservoir is covered with the cover-plate 1, leaving a 4 mm gap between the latter and the chromatographic plate 4. A suitable volume of eluent is introduced into the reservoir and then the cover-plate is shifted to the right to close the gap and to start development.

A detailed view of the chamber for standard 50 × 100 mm glass plates is

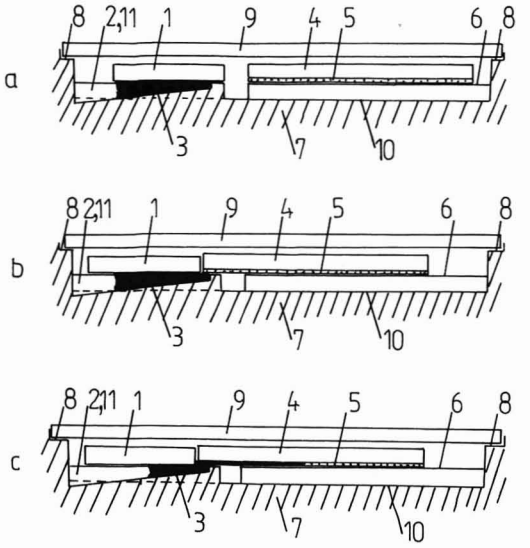

Fig. 2. Modified construction with slanted bottom of the reservoir. Notation as in Fig. 1.

presented in Fig. 3 in three projections: (a) overhead, (b) parallel to the shorter edge and (c) parallel to the longer edge. The chamber is made of polytetrafluoroethylene (PTFE) and consists of a PTFE plate (7) with a 1-mm deep depression (8) for the rectangular glass cover-plate (9). The bottom (10) of the chamber is 6 mm below the

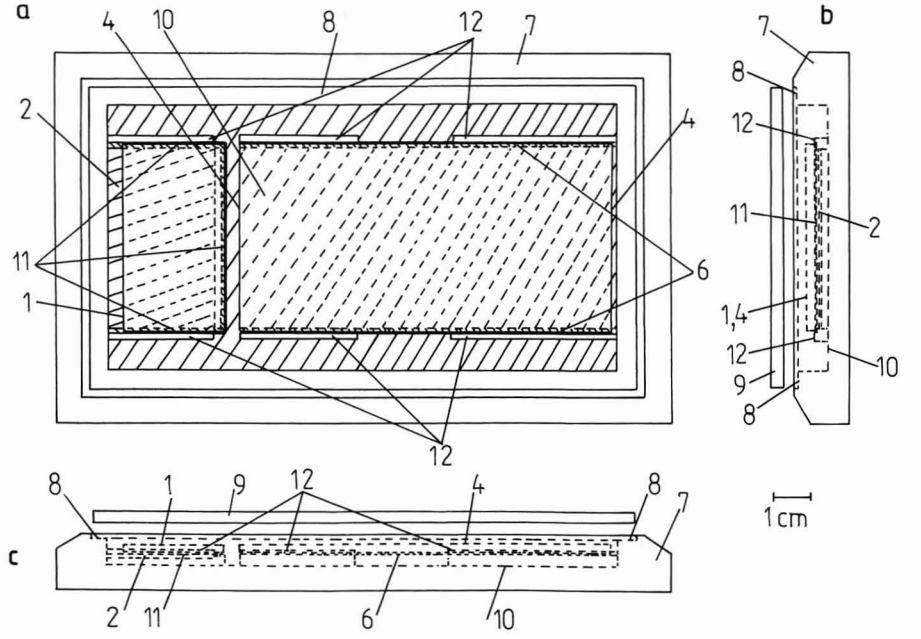

Fig. 3. Detailed design of the chamber for single precoated Merck plate (50 × 100 mm). Notation as in Fig. 1; 12 = vertical walls holding the plate in place.

upper surface of the plate; in parallel, another rectangular depression (2) (30 × 48 mm) forms the reservoir of the eluent, 1 mm deep. Along the right-hand edge, adjacent to the chromatographic plate, the reservoir is only 0.5 mm deep (the step is 1 mm wide) to facilitate uniform absorption of the last drops of the eluent. The edges of the reservoir (2) are on the same level as two parallel ledges (6), 1 mm wide, on which the chromatographic plate is placed; the ledges have low vertical walls (12) which prevent the chromatographic plate and the glass plate covering the reservoir from shifting across the chamber. The glass cover-plate of the reservoir is shorter by 5 mm from the shorter edge (11) of the reservoir. The above construction permits the development of a single plate.

Another construction with two reservoirs of eluent on the opposite sides of the chamber (Fig. 4) permits the simultaneous development of two chromatograms (on two separate plates).

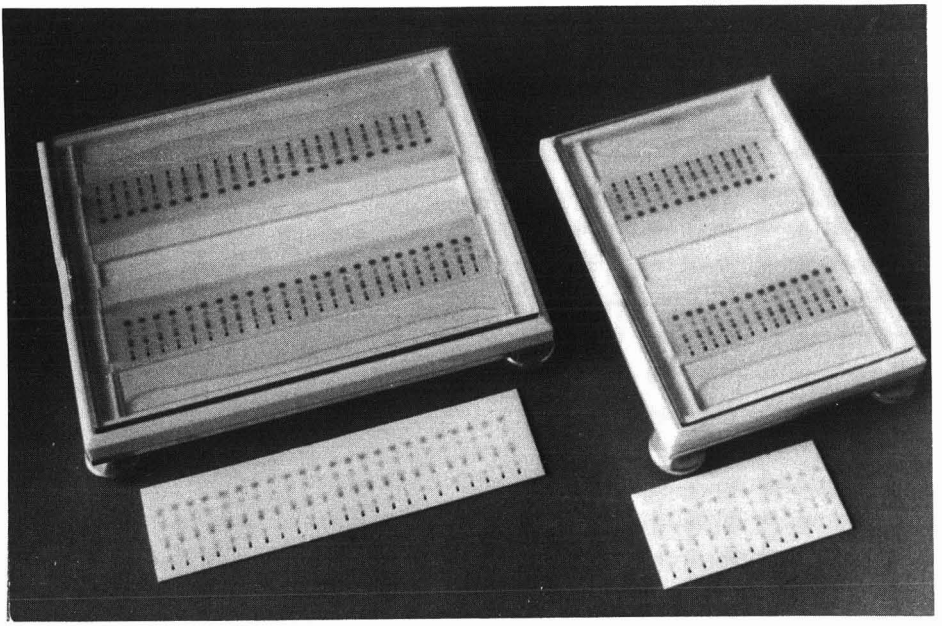

Fig. 4. Twin chambers for 10- and 20-cm wide plates during the development process. Manufacturer and distributor: Modin, Lublin, Poland.

The design of the chamber is suitable for the development of precoated or laboratory-made glass plates which can be placed (adsorbent layer downward) in the chamber with visual control of the process.

SPECIAL APPLICATIONS

Owing to complete absorption of the eluent from the reservoir, stepwise gradient elution is possible by stagewise introduction of eluent fractions of increasing eluent strength (as in ref. 15, Fig. 2) or by absorption of solvent vapour from the bottom of the

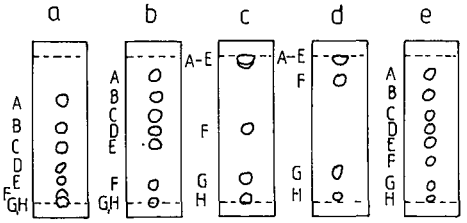

Fig. 5. Thin-layer chromatograms obtained with the chamber. (a–d) Isocratic elution; (e) gradient elution (see text). 10 × 10 cm TLC plates with silica (Merck). Samples: A = 4-chloro-4′-dimethylaminoazobenzene; B = fast yellow; C = 2-nitroaniline; D = 1-(2-methoxyphenylazo)-2-naphthol; E = 4-nitroaniline; F = 1-(4-hydroxyphenylazo)-2-naphthol; G = iodoeosin; H = phenol red.

chamber (ref. 1, Figs. 149–151) as in the well known chambers of Geiss and Schlitt[6], De Zeeuw[8] and Kaiser[16] and the linear Camag chamber.

Fig. 5 shows examples of chromatograms obtained using the horizontal chamber and isocratic elution with pure solvents, (a) toluene, (b) methylene chloride, (c) ethyl acetate, (d) acetone and (e) three-step gradient elution with (1) 1 cm^3 of methylene chloride, (2) 0.25 cm^3 of ethyl acetate and (3) 0.25 cm^3 of acetone, each portion of solvent being delivered into the solvent reservoir with a syringe, after complete absorption of the previous portion by the adsorbent layer. It can be seen that the horizontal chamber is suitable for the gradient chromatographic resolution of mixtures that cannot be completely separated by isocratic development.

The complete absorption of the eluent from the reservoir also permits the zonal application of large volumes of the sample for micropreparative separations, as in the equilibrium sandwich chamber with a glass distributor; the introduction of the sample from the edge of the layer (frontal + elution chromatography) greatly improves the separation capacity[2].

Fig. 6 shows an example of zonal application of a mixture on the TLC plate in a horizontal chamber with two reservoirs. The mixture was introduced into the first reservoir and the eluent (toluene) into the second. The chromatographic plate was brought into contact with the mixture to develop the TLC plate a distance of 2 cm (Fig. 6a). The development was then interrupted and the plate was left in the chamber to absorb the remainder of the mixture from the edge of the TLC plate. The

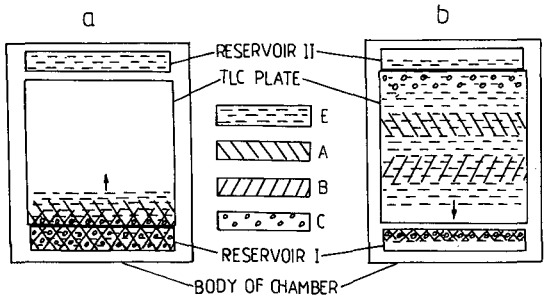

Fig. 6. Zonal application of the mixture using a twin chamber. A = 4-Chloro-4′-dimethylaminoazobenzene; B = 2-nitroaniline; C = 1-(4-hydroxyphenylazo)-2-naphthol; E = toluene (eluent).

chromatographic plate with the wide starting zone was then turned through 180° and developed with the eluent from the second reservoir. Fig. 6b shows the situation on the plate in the last stage of development of the micropreparative chromatogram.

The construction of the chamber is simpler than that of other chambers of this type. Its depth is only 6 mm so that the manufacture of the chamber is simplified[13,14].

REFERENCES

1 F. Geiss, *Fundamentals of Thin Layer Chromatography*, Hüthig, Heidelberg, Basle, New York, 1987.
2 E. Soczewiński, in R. E. Kaiser (Editor), *Planar Chromatography*, Vol. 1, Hüthig, Heidelberg, Basle, New York, 1986, p. 79.
3 *TLC 88, Catalogue*, Camag, Muttenz, Switzerland.
4 D. E. Jaenchen and H. J. Issaq, *J. Liq. Chromatogr.*, 11 (1988) 1941.
5 J. Donovan, M. Gould and R. E. Majors, *LC · GC*, 5 (1987) 1024.
6 F. Geiss and H. Schlitt, *Chromatographia*, 1 (1968) 309.
7 M. Brenner and A. Niederwieser, *Experientia*, 17 (1961) 237.
8 R. A. De Zeeuw, *Anal. Chem.*, 40 (1968) 2134.
9 P. Buncak, *Fresenius' Z. Anal. Chem.*, 318 (1984) 291.
10 E. Soczewiński, *Pol. Pat.*, 100 849 (1978) and 103 834 (1978).
11 E. Soczewiński, *Chem. Anal. (Warsaw)*, 23 (1978) 515.
12 E. Soczewiński, *J. Chromatogr.*, 138 (1977) 443.
13 T. H. Dzido, *Pol. Pat. Appl.*, 280 087, 1989.
14 T. H. Dzido and E. Soczewiński, *Pol. Pat. Appl.*, 281 231, 1989.
15 G. Matysik and E. Soczewiński, *J. Chromatogr.*, 369 (1986) 19.
16 R. E. Kaiser, in A. Zlatkis and R. E. Kaiser (Editors), *HPTLC —High Performance Thin-Layer Chromatography*, Elsevier, Amsterdam, and Institute of Chromatography, Bad Dürkheim, 1977, p. 73.

Journal of Chromatography, 516 (1990) 467–472
Elsevier Science Publishers B.V., Amsterdam

CHROM. 22 534

Note

Trifluoroacetic anhydride–sodium iodide as a reagent for the selective detection of nitroso compounds by thin-layer chromatography

ANDRZEJ KOTYŃSKI
Institute of Chemistry, Faculty of Pharmacy, Medical Academy of Łódź, Narutowicza 120 A, 90-151 Łódź (Poland)
and
ZBIGNIEW H. KUDZIN* and ROMUALD SKOWROŃSKI
Institute of Chemistry, University of Łódź, Narutowicza 68, 90-136 Łódź (Poland)
(First received February 22nd, 1990; revised manuscript received May 2nd, 1990)

Nitroso compounds show great activity and considerable diversity of action[1,2], especially as carcinogens[3,4]. For this reason their occurrence[5], whether as synthetic derivatives[2,6], natural products[2] or accidental products in food processing[7] or tobacco smoke[2], is of significant environmental concern. Consequently, there are numerous methods for the detection and determination of nitroso compounds[2,8–10]. However, their selective determination in thin-layer chromatographic systems (TLC) is limited to a narrow range of detection reagents. Preussmann and co-workers[11,12] described the silica gel TLC of wide variety of N-nitrosamines; detection was achieved using a 5:1 mixture of 1.5% of diphenylamine in ethanol and a 0.1% solution of palladium(II) chloride in 0.2% sodium chloride, and a solution of 0.5% sulphanilic acid and 0.05% α-naphthylamine in 30% acetic acid (Griess reagent[13]), followed by UV irradiation. These reagents and also ninhydrin reagent (0.2–0.3%, ethanolic) were applied by Kroeller[14] and Sen *et al.*[15] for the detection and identification of nitrosamines in foodstuffs and tobacco smoke.

Yasuda and Nakashima[16] accomplished the TLC detection of several aromatic nitroso compounds by heating the plates sprayed with acidic 2-naphthol solution [1% 2-naphthol in methanol–ethylene glycol–35% hydrochloric acid (10:8:2)]. Results for the TLC detection of nitrosamines with several common spray reagents were given in a comprehensive paper by Reio[17].

In some procedures nitrosamines were derivatized to compounds exhibiting higher detectability (strong absorbance or chemiluminiscence), prior to their chromatographic separation and subsequent determination. Thus, nitrosamines were prereduced to the corresponding hydrazines, followed by acylation with 4-nitroazobenzene-4′-carboxylic chloride[18], or by coupling with anthranil-[19,20] or 5-nitrosalicylaldehyde[21]. Nitrosamines were also prereduced to amines and subsequently

dansylated[22,23] or treated with N-(8-methoxy-5-quinolinesulphonyl)aziridine[24]. Direct derivatization of nitrosamines was accomplished by treatment with 1-chloro-4-nitrobenzofuran[25] or 7-chloro-4-nitrobenzo-2-oxa-1,3-diazole[26].

In previous papers we have reported procedures for the determination[27] and detection of sulphoxides and sulphimides[28] and nitroxide radicals and nitrones[29] using tifluoroacetic anhydride–sodium iodide (TFAA–I) reagent. We have found that this reagent also reacts with various nitroso compounds with simultaneous release of iodine. In this paper we present results for the application of the TFAA–I reagent to the detection of nitroso compounds in TLC.

EXPERIMENTAL

Materials

Acylating agents (TFAA, acetyl chloride, acetic anhydride), 2,3-dichloro-5,6-dicyano-1,4-benzoquinone, tetrachlorobenzoquinone (chloranil), cupferron, 1-nitroso-2-naphthol, N,N-dimethyl-4-nitrosoaniline, sulphanilic acid and 2-naphthol were purchased from Aldrich (Milwaukee, WI, U.S.A.). Other nitroso compounds were prepared according to Ref. 30 and were all of the purity previously reported.

Reagents and solutions

The concentrations of nitroso compounds **1–5** (see Table II) were *ca.* $5 \cdot 10^{-2}$–10^{-3} *M* in anhydrous acetone. A 0.8 *M* solution of sodium iodide in anhydrous acetone and 0.8 *M* solution of TFAA in anhydrous acetone (prepared immediately before use) were used. Other acylating agents solutions were all 0.8 *M* in anhydrous acetone. Dragendorff reagent (Bi) was a 2% solution of potassium bismuth tetraiodide in 0.01 *M* hydrochloric acid. DDQ reagent was a 2% 2,3-dichloro-5,6-dicyano-1,4-benzoquinone solution in benzene. TCBQ reagent was a 2% tetrachlorobenzoquinone solution in benzene. Griess reagent (Gr R) was a solution of 0.5% sulphanilic acid and 0.05% α-naphthylamine in 30% acetic acid. Other solutions were 2% iron(III) chloride (Fe) and 0.1% potassium permanganate (Mn).

Thin-layer chromatography

Precoated silica gel 60 F_{254} aluminium sheets and precoated aluminium oxide 60 F_{254} aluminium sheets (10 cm × 5 cm), with a 0.2-mm thick layer (Merck, Darmstadt, F.R.G.), were used in all TLC experiments. The plates were spotted with an appropriate amount of compound (see tables), developed for a distance of 8 cm with acetone, air-dried and sprayed with sodium iodide solution and subsequently with TFAA solution. Nitroso compounds appeared almost immediately as brown spots on a white background, and were stable for more than 20 min.

RESULTS AND DISCUSSION

The results of the application of the various acylating agent–halide salt systems for the detection of nitroso compounds by TLC are presented in Table I. The most sensitive are TFAA–I and acetyl chloride–sodium iodide reagents. Subsequent modification of the reagent system by replacement of the halide salt or acetylating agent leads to differentiation of their detection selectivity. Thus, the use of the mild

TABLE I

COMPARISON OF VARIOUS ACYLATING AGENT–HALIDE SALT SYSTEMS FOR THE DETECTION OF NITROSO COMPOUNDS **1–3** AND **5** BY TLC

Silica gel plates. Solvent, acetone. −, Not detected; +/−, spot is detectable; +, distinct detection; ++, strong detection. Ac_2O = acetic anhydride; AcCl = acetyl chloride.

Compound applied			*Ac_2O–NaI*	*AcCl–NaI*	*Ac_2O–LiBr*	*AcCl–LiBr*	*TFAA–I*
No.	*Structure*[a]	*Amount (μg/spot)*					
		1	−	−	−	−	−
1b	$(i\text{-}Bu)_2N\text{-}NO$	10	−	−	−	−	−
		50	−	+	−	−	+
		1	−	−	−	−	−
1d	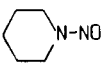	10	−	+	−	−	+
		50	−	+	−	−	+
		1	−	−	−	−	+
1f	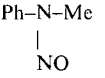	10	−	+	−	+	++
		50	−	+	−	+	++
		1	−	+/−	−	−	−
1g	$Ph_2N\text{-}NO$	10	+[b]	+[c]	+[c]	+[c]	+[b]
		50	+[b]	++[c]	++[c]	++[c]	++[b]
		1	+	+	−	−	+/−
2	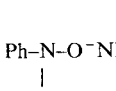	10	++	+	−	−	+
		50	++	++	+	+/−	++
		1	+[d]	+[d]	−	−	+[d]
3	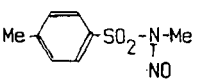	10	+[d]	+[d]	−	−	++[d]
		50	+[d]	+[d]	−	−	++[d]
		1	−	−	−	−	−
5a	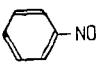	10	−	−	−	−	−
		50	−	+/−	−	−	−
		1	−	+	−	−	+
5b	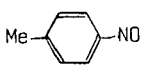	10	+/−	+	−	−	++
		50	+	++	−	+/−	++

[a] i-Bu = Isobutyl; Me = methyl; Ph = phenyl.

[b] Blue-brown spots after preheating to *ca.* 150°C, turning yellow after spraying with the reagent.

[c] Blue-brown spots after preheating to *ca.* 150°C, turning blue-navy after spraying with LiBr, turning green after additional spraying with acetyl chloride.

[d] Yellow spots after spraying with sodium iodide solution.

acetic anhydride–sodium iodide reagent allows the detection of N-nitroso-N,N-diphenylamine, N-nitroso-N-hydroxyphenylamine and N-nitrosamide **3**, whereas the acetic anhydride–lithium bromide reagent detects only N-nitroso-N,Ndiphenylamine. The more reactive systems based on TFAA and acetyl chloride detect a much wider range of nitroso compounds.

Results for the application of TFAA–I for the detection of nitroso compounds are summarized in Table II. It is evident that the detection limits of nitroso derivatives are strongly dependent on their structure. Thus, the detection limits of N-nitrosamines vary from 1 μg (per spot) for diaryl- and arylalkyl-N-nitrosamines (**1f** and **1g**) through 5–10 μg cyclic aliphatic N-nitrosamines (**1c–e**) to *ca.* 50 μg for acyclic aliphatic N-nitrosamines (**1a** and **1b**). N-Nitrosophenylhydroxylamine (**2**) (cupferron) and N-nitrosoamides **3** and **4** exhibit detection at *ca.* 1–5 μg.

Detection of C-nitroso compounds was even more influenced by structural factors. Thus, *p*-nitrosodimethylaniline (**5c**) and 1-nitroso-2-naphthol (**5d**) exhibit strong molecular absorbance themselves and they are detectable as yellow spots at levels lower than 0.5 μg in both the UV and visible light regions. Therefore, their reaction with TFAA–I cannot be applied to their detection.

Large differences in detection limits were observed for nitrosobenzene (**5a**) and

TABLE II

DETECTION LIMITS FOR NITROSO COMPOUNDS **1–5** WITH UV DETECTION (360 nm) AND USING TFAA–I AS THE DETECTION REAGENT

Compound applied		*SiO_2*			*Al_2O_3*		
No.	*Structure*[a]	*Detection limit (μg)*		R_F	*Detection limit (μg)*		R_F
		UV	*TFAA-I*		*UV*	*TFAA-I*	
1a	$(i\text{-}Pr)_2N\text{–}NO$	50	50	0.72	50	50	0.85
1b	$(i\text{-}Bu)_2N\text{–}NO$	50	50	0.72	50	50	0.78
1c	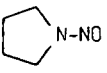	50	10	0.61	50	50	0.78
1d	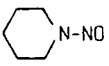	50	10	0.52	50	50	0.80
1e	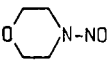	5	5	0.50	10	10	0.78
1f	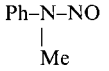	5	1	0.66	10	3	0.80
1g	$Ph_2N\text{–}NO$	3	1	0.58	10	1	0.85
2	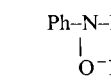	5	1	0.56	10	1	0.81
3	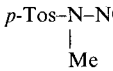	50	1	0.67	50	1	0.81
4	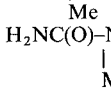	50	5	0.62	50	50	0.80
5a	Ph–NO	50	–	0.69	50	–	0.83
5b	*p*-Tol–NO	1	5	0.69	10	10	0.84

[a] i-Pr = Isopropyl; i-Bu = isobutyl; Ph = phenyl; Me = methyl; Tos = tosyl; Tol = tolyl.

TABLE III

COMPARISON OF REAGENTS FOR THE DETECTION OF NITROSO COMPOUNDS BY TLC

Compound applied[a]		*Detection reagent*								
No.	*Amount (μg/spot)*	*UV (360 nm)*	*I_2*	*Bi*	*Fe*	*Mn*[b]	*TFAA–I*	*DDQ*	*TCBQ*	*Gr-R*
1b	5	−	−	−	−	−	−	−	−	+[c]
	25	+	+	−	−	−	−	−	−	+[c]
1e	5	+/−	+	−	−	−	+	−	−	+[c]
	25	+	+	−	−	−	+	−	−	+[c]
1f	5	+/−	+/−	−	+[d]	+/−	++	−	−	+[e]
	25	+	+	−	+[d]	+	++	−	−	+[e]
1g	5	+	+	−	+[f]	+	+	+[g]	−	+[e]
	25	+	+	−	+[f]	+	+	+[g]	−	+[e]
2	5	−	+	−	+/−[h]	+/−	+	+[i]	−	+/−[c]
	25	−	+	−	+[h]	+	+	+[i]	−	+[c]
3	5	−	+	−	−	−	+	−	−	+[c]
	25	+/−	+	+/−[j]	−	+/−	++	−	+/−[k]	+[c]
5a	5	−	−	−	−	−	−	−	−	−
	25	+	−	−	−	+/−	−	−	−	−
5b	5	+	−	−	−	−	+	−	−	+[l]
	25	+	−	−	−	+/−	++	−	−	+[l]

[a] For structures, see Table II.
[b] Grey-green spots.
[c] Pink-violet spots.
[d] Yellow-brown spots, turning green after preheating to *ca.* 150°C.
[e] Grey-green spots after UV irradiation.
[f] Navy blue spots, turning green after preheating to *ca.* 150°C.
[g] Grey-red spots.
[h] Orange spots.
[i] Red-brown spots turning green after saturation with ammonia vapour.
[j] Orange spots after preheating to *ca.* 150°C.
[k] Lilac spots.
[l] Yellow-brown spots turning red brown.

p-nitrosotoluene (**5b**), apparently owing to the induction effect caused by the methyl substituent. Thus, whereas nitrosobenzene was undetectable even at a level of 50 μg on both silica gel and aluminium oxide plates, *p*-nitrosotoluene had detection limits of 5 μg (silica gel) to 10 μg (aluminium oxide).

A similar effect was observed with azoxybenzene derivatives. Thus, whereas azoxybenzene was not detected using TFAA–I even at a level of 50 μg per spot, its 2,2′-dimethoxy and 2,2′-dicarboxylic analogue were detectable at levels of 1 μg (acetyl chloride–sodium iodide) to 5 μg (TFAA–I) (silica gel plates).

Results are given in Table III for the evaluation of TFAA–I reagent in comparison with other spray reagents for the detection of representative nitroso compounds.

ACKNOWLEDGEMENT

This project was partially supported by the Polish Academy of Sciences, Grant CPBP 01.13.

REFERENCES

1 J. H. Boyer, in H. Feuer (Editor), *The Chemistry of the Nitro and Nitroso Group*, Interscience, New York, 1969.
2 L. Fishbein, *Chromatography of Environmental Hazards*, Vol. I, Elsevier, Amsterdam, 1972, pp. 37–64.
3 P. N. Magee and J. B. Barnes, *Brit. J. Cancer*, 10 (1956) 114.
4 P. N. Magee and J. B. Barnes, *Adv. Cancer Res.*, 10 (1967) 163.
5 L. Fishbein, *Sci. Total Environ.*, 13 (1979) 157.
6 H. Zimmer, L. F. Audrieth, M. Zimmer and R. A. Rowe, *J. Am. Chem. Soc.*, 77 (1955) 790.
7 N. T. Crosby, J. K. Foreman, J. F. Palframan and R. Sawyer, *Nature (London)*, 238 (1972) 342.
8 J. M. Kruse, in G. A. Streuli and P. R. Averell (Editors), *The Analytial Chemistry of Nitrogen and Its Compounds*, 28 (2), Wiley-Interscience, New York, 1970, pp. 431–439.
9 M. R. Smyth and W. F. Smyth, *Analyst (London)*, 103 (1978) 529.
10 T. A. Gough, *Analyst (London)*, 103 (1978) 785.
11 R. Preussmann, D. Daiber and H. Hengy, *Nature (London)*, 201 (1964) 502.
12 R. Preussmann, G. Neurath, G. Wulf, D. Daiber and H. Hengy, *Fresenius' Z. Anal. Chem.*, 202 (1964) 187.
13 P. Griess, *Chem. Ber.*, 12 (1879) 427.
14 E. Kroeller, *Dtsch. Lebensm.-Rundsch.*, 63 (1967) 303.
15 N. P. Sen, D. C. Smith, L. Schwinghamer and J. J. Marleau, *J. Assoc. Off. Anal. Chem.*, 52 (1969) 47.
16 K. Yasuda and K. Nakashima, *Bunseki Kagaku*, 17 (1968) 732; *Anal. Abstr.*, 18 (1970) 1743.
17 L. Reio, *J. Chromatogr.*, 88 (1974) 119.
18 W. J. Serfentein and P. Hurter, *Nature (London)*. 209 (1966) 1238.
19 G. Neurath, B. Pirman and M. Dunger, *Chem. Ber.*, 97 (1964) 1631.
20 K. W. Kim and E. V. Brown, *Anal. Lett.*, 5 (1972) 293.
21 N. J. Sarfontein and H. Smit, *Nature (London)*, 214 (1967) 169.
22 G. F. Zhukova V. V. Pimenova and F. A. Medvedev, *Zh. Anal. Khim.*, 34 (1979) 1621.
23 Y. L. Kostyukovski, D. B. Medvedev and A. A. Pokrovskii, *Zh. Anal. Khim.*, 33 (1978) 808.
24 I. N. Gracheva, G. F. Zhukova, I. R. Kovelman, W. W. Pimenova and A. I. Totchilkin, *Zh. Anal. Khim.*, 41 (1986) 356.
25 Y. L. Kostyukovski and D. B. Malmed, *Zh. Anal. Khim.*, 34 (1979) 1358.
26 H. J. Klimsch and L. J. Stadler, *J. Chromatogr.*, 90 (1974) 223.
27 W. Ciesielski, W. Jędrzejewski, J. Drabowicz, Z. H. Kudzin and R. Skowroński, *Talanta*, 35 (1988) 969.
28 J. Drabowicz, A. Kotyński and Z. H. Kudzin, *J. Chromatogr.*, 447 (1988) 225.
29 J. Drabowicz, A. Kotyński, Z. H. Kudzin and R. Skowroński, *J. Chromatogr.*, 473 (1989) 287.
30 E. Muller (Editor), *Methoden der Organischen Chemie (Houben–Weyl)*, Georg Thieme, Stuttgart, 1958; H. Soll, Vol. XI-2, p. 178; W. Seidenfaden, Vol. X-1, p. 1021; B. Eistert, M. Regitz, G. Heck and H. Schwall, Vol. X-4, p. 475.

Journal of Chromatography, 516 (1990) 473–477
Elsevier Science Publishers B.V., Amsterdam

CHROM. 22 538

Note

Determination of trimetaphosphate in pyrophosphate by capillary isotachophoresis

PAVEL JANOŠ
Research Institute of Inorganic Chemistry, 400 60 Ústi nad Labem (Czechoslovakia)
(First received December 19th, 1989; revised manuscript received May 7th, 1990)

Pyrophosphates, like other phosphates, have many applications, including uses in the foodstuffs industry. On the other hand, condensed cyclic polyphosphates are considered to be potentially detrimental to health. Hence a requirement has arisen for the selective determination of cyclic triphosphate (trimetaphosphate) in foodstuff-grade pyrophosphate.

A number of procedures for the determination of phosphates have been described, including gravimetric, titrimetric and spectrophotometric[1] methods. These, however, do not permit individual types of phosphates to be determined selectively. Paper[1,2], thin-layer[1,3], ion-exchange[1,4,5] and ion chromatography[6] make it possible in some instances to separate and identify the phosphates but they are inadequate when a small amount of one type of phosphate is to be determined in the presence of a large excess of other phosphates.

Papers dealing with the determination of various phosphates by capillary isotachophoresis have been published (*e.g.*, refs. 7–9).

Yagi *et al.*[10] have described the separation of different phosphorus oxo acids, together with trimetaphosphate and pyrophosphate, using capillary isotachophoresis. The separation and determination of trimetaphosphate in a mixture with other phosphates has been reported[11,12].

In the above studies chloride served as the leading ion in most instances and a histidine buffer solution was used to maintain the required pH value. In this system the effective mobility of the trimetaphosphate anion is close to that of the leading ion, which makes detection and identification difficult. Motooka *et al.*[13] were successful in altering the effective mobility of condensed cyclic phosphates by the addition of bivalent inorganic cations (cations of alkaline-earth elements). In this study we have attempted to influence the effective mobility of the separated ions by addition of organic cations (quaternary ammonium bases) with the objective of developing a method for the determination of trimetaphosphate in pyrophosphate.

0021-9673/90/$03.50

EXPERIMENTAL

Apparatus

The measurements were carried out on an Agrofor isotachograph (JZD Odra, Krmelín, Czechoslovakia) equipped with a PTFE separation capillary (300 × 0.4 mm I.D.), a 20-μl sampling valve and a conductimetric detector connected to a TZ 4620 line recorder (Laboratorní přístroje, Prague, Czechoslovakia). The pH of the solutions was checked with an OP-211/1 pH meter (Radelkis, Budapest, Hungary) with an Orion 81-02 combined electrode.

Chemicals

The leading electrolytes were prepared by combining the following stock solutions in appropriate proportions: 0.1 mol/l hydrochloric acid (Merck, Darmstadt, F.R.G.), 0.1 mol/l hydrobromic acid (Lachema, Brno, Czechoslovakia), 0.1 mol/l tetrabutylammonium hydroxide (Fluka, Buchs, Switzerland) and 0.01 mol/l cetyltrimethylammonium bromide in methanol, 1% poly(vinyl alcohol) (purified on a mixed ion exchanger). The solutions containing cetyltrimethylammonium bromide were always prepared a day in advance and were filtered prior to use.

As terminating electrolytes 0.1 mol/l solutions of 2-thio-6-azathymine, caproic acid (Serva, Heidelberg, F.R.G.) and potassium hydrogentartrate (Lachema) were used.

Histidine (Reanal, Budapest, Hungary) was adopted for adjusting the pH value of solutions.

All the chemicals used [except poly(vinyl alcohol)] were of analytical-reagent-grade. Water deionized on a mixed-bed ion-exchange column served for preparing the solutions.

RESULTS AND DISCUSSION

Trimetaphosphoric acid is a comparatively strong acid. At pH > 3 it is dissociated almost completely to the third degree of dissociation. Therefore, it is not possible to influence the effective mobility of the trimetaphosphate ion by the method that is most commonly applied in isotachophoresis, *i.e.*, by a change in the pH of the leading electrolyte. This may be demonstrated with published isotachophoretic indices[14]. Within the pH range 3–10 the relative detector response ($R_E = R_X/R_{Cl}$) ranges from 1.088 to 1.061, *i.e.*, it differs from the R_E value of the chloride ion less than required for a successful separation[14] ($\Delta R_E > 0.15$).

In spite of this, it has been demonstrated[10–12] that trimetaphosphate can be determined in the normal HCl–histidine system, provided that the content of the analyte in the sample is not too high. According to Hirokawa *et al.*[15], the effective mobility of the trimetaphosphate anion decreases owing to the formation of an ion pair with the histidine cation. In spite of this, however, difficulties were encountered when working with this system, as proper functioning of the Agrofor instrument requires that there should be a sufficiently large difference between the effective mobilities of the leading ion and of the first of the separated ions.

The effective mobility of cyclic polyphosphates can be influenced by addition to the leading electrolyte of, *e.g.*, Ca^{2+}, Mg^{2+}, Sr^{2+} or Ba^{2+}[13]. If, however, in addition

to the trimetaphosphate that is being determined, the sample also contains a large amount of pyrophosphate, there is a risk of precipitation of sparingly soluble salts of these elements[16].

We examined the effect of the presence of quaternary ammonium bases in the leading electrolyte on the isotahophoretic behaviour of trimeta-, pyro- and orthophosphate anions. Tributylammonium cation (TBA^+) and cetyltrimethylammonium cation ($CTMA^+$) were selected as they are frequently used in ion-pair reversed-phase chromatography (see, *e.g.*, ref. 17). The measurements with TBA^+ were carried out in an operating system employing Cl^- as the leading ion and those with $CTMA^+$ in a system with Br^- as the leading ion in 25% (v/v) methanol (because of the limited solubility of CTMA-Br in water).

It was found that TBA^+ does not affect the migration of ortho- and pyrophosphates; only in with the trimetaphosphate anion at concentrations of TBA^+ higher than about 3 mmol/l was a certain decrease in effective mobility observed (Fig. 1).

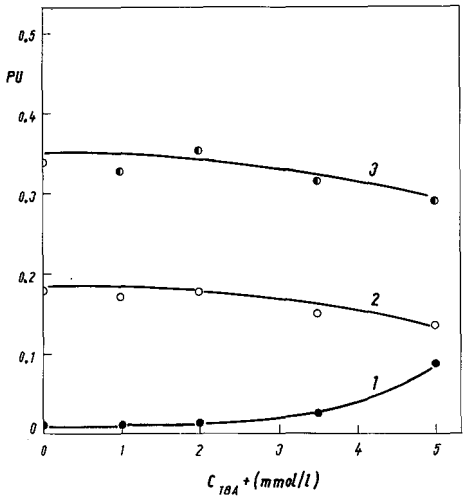

Fig. 1. Effect of TBA^+ concentration on the *PU* values of separated ions. Leading electrolyte (LE): 0.01 mol/l Cl^- + TBA^+ + histidine + 0.05% poly(vinyl alcohol), pH = 5.5. Terminating electrolyte (TE): 0.01 mol/l 2-thio-6-azathymine. *PU* = potential units[14] calculated from responses of the conductimetric detector; $PU = (R_X - R_L)/(R_T - R_L)$. R_X, R_L and R_T are zone heights of the analyte, leading and terminating ions, respectively. 1 = Trimetaphosphate; 2 = pyrophosphate; 3 = orthophosphate.

It is probable that the trimetaphosphate anion, $P_3O_9^{3-}$, forms an ion-pair with TBA^+ in a similar manner to the histidine cation[15], whereas ortho- and pyrophosphate anions do not form ion-pairs.

It can be seen in Fig. 2 that trimeta-, pyro- and orthophosphates can be separated effectively in the HBr–histidine system in 25% (v/v) methanol. The influence of $CTMA^+$ is more pronounced than that of TBA^+ and manifests itself at $CTMA^+$ concentrations as low as 0.5–1 mmol/l. Fig. 3 shows the isotachophoretic separation of trimeta-, pyro- and orthophosphate in the presence of TBA^+. It can be seen in Fig. 4

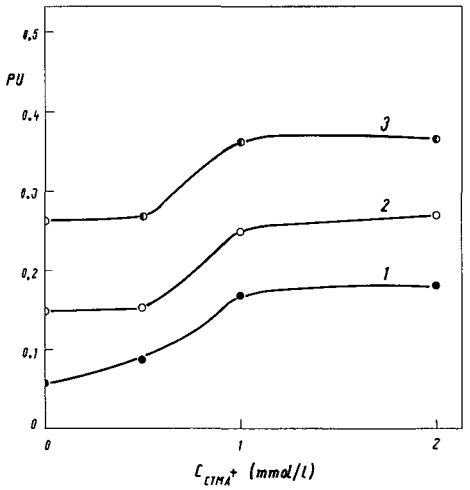

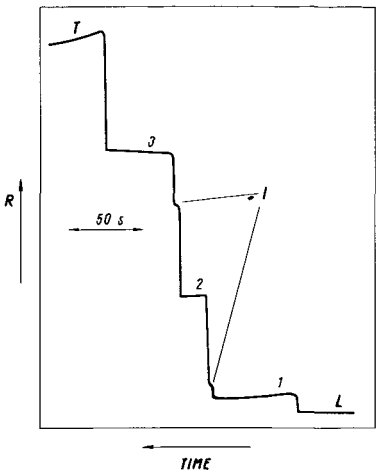

Fig. 2. Effect of $CTMA^+$ concentration on the *PU* values of separated ions. LE: 0.01 mol/l Br^- + $CTMA^+$ + histidine + 0.05% poly(vinyl alcohol) in 25% (v/v) methanol, pH = 5.3. TE: 0.01 mol/l 2-thio-6-azathymine. 1 = Trimetaphosphate; 2 = pyrophosphate; 3 = orthophosphate.

Fig. 3. Isotachopherogram of the separation of a model mixture of trimeta-, pyro- and orthophosphates (system with TBA^+). LE: 0.01 mol/l Cl^- + 0.004 mol/l TBA^+ + histidine + 0.05% poly(vinyl alcohol), pH = 5.5. TE: 0.01 mol/l caproic acid. Driving current intensity during recording = 60 μA. 1 = Trimetaphosphate; 2 = pyrophosphate; 3 = orthophosphate; I = unidentified impurities. R = Resistance.

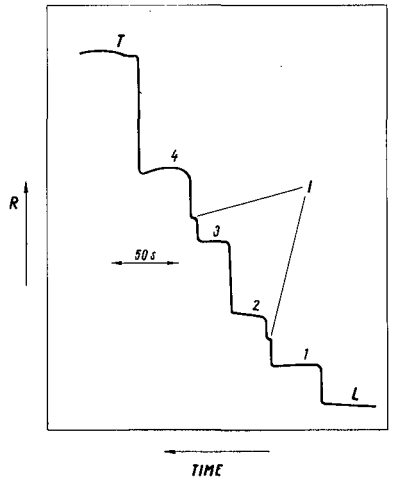

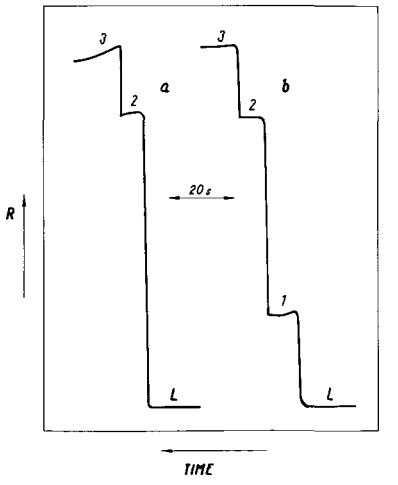

Fig. 4. Isotachopherogram of the separation of a model mixture of sulphate and trimeta-, pyro- and orthophosphates (system with $CTMA^+$). LE: 0.01 mol/l Br^- + 0.001 mol/l $CTMA^+$ + histidine + 0.05% poly(vinyl alcohol) in 25% (v/v) methanol, pH = 5.3. TE: 0.01 mol/l caproic acid. Driving current intensity during recording = 60 μA. 1 = Sulphate; 2 = trimetaphosphate; 3 = pyrophosphate; 4 = orthophosphate; I = unidentified impurities.

Fig. 5. Analysis of commercial pyrophosphate. LE: as in Fig. 3. TE: 0.01 mol/l potassium hydrogentartrate. Sample: (a) $Na_2H_2P_2O_7$ (Ladensburg, F.R.G.), 0.2 g per 100 ml; (b) same as (a), spiked with *ca.* 0.5% of trimetaphosphate. Driving current intensity during recording = 60 μA. 1 = Trimetaphosphate; 2 = tartrate; 3 = terminating zone, mixed zone of tartrate and pyrophosphate.

that trimeta-, pyro- and orthophosphates are separated very effectively in a system with $CTMA^+$ in a mixed aqueous–methanolic medium. This system can be considered optimum for separating the above phosphates together with sulphates (which can serve as an internal standard). In this instance probably both the influence of the mixed solvent and the formation of ion-pairs of the ions to be separated with $CTMA^+$ are combined to give this final effect. A disadvantage of this system for practical use in the limited stability of the leading electrolyte solution.

Therefore, we adopted the system with TBA^+ for routine determinations of trimetaphosphate in pyrophosphate. Tartrate was chosen as the terminating electrolyte. Its effective mobility in the given system is close to that of pyrophosphate and hence the terminating zone during an analysis is formed by a mixed zone of tartrate with pyrophosphate. The selection of the faster moving tartrate (compared with hexanoate) makes it possible to use a higher intensity of the driving current and thus shorten the duration of analysis. The composition of the leading electrolyte is 0.01 mol/l Cl^- + 0.004 mol/l TBA^+ + 0.05% poly(vinyl alcohol), pH = 5.5, adjusted with histidine.

An example of the analysis of commercial pyrophosphate used in the foodstuffs industry as an additive to baking powders is shown in Fig. 5. Under the conditions specified trimetaphosphate in pyrophosphate can be determined at concentration levels down to 0.1%, which satisfied the given application.

The equation of the linear calibration graph for the determination of trimetaphosphate is $y = 0.0340x - 0.0089$, where y (s) is the zone length (at a driving current of 60 μA) and x (mg/l) is the concentration of trimetaphosphate for an injection of 20 μl (correlation coefficient = 0.9996, $n = 9$). The detection limit, established under the conditions specified in Fig. 5 and defined according to ref. 18 as the absolute amount of the analyte that will give a zone passing through the detector during 1 s, is *ca.* 0.5 μg.

REFERENCES

1 S. Greenfield and M. Clin, *Analytical Chemistry of the Condensed Phosphates*, Pergamon Press, Oxford, 1975.
2 T. Ando and J. Ito, *Bull. Chem. Soc. Jpn.*, 25 (1952) 78.
3 N. Takai, T. Iida and J. P. W. Houtman, *Fresenius' Z. Anal. Chem.*, 244 (1969) 38.
4 J. Beukenkamp and W. Rieman, *Anal. Chem.*, 26 (1954) 505.
5 D. Lúčanský, *Chem. Prům.*, 26 (1976) 514.
6 F. C. Smith and R. C. Chang, *The Practice of Ion Chromatography*, Wiley, New York, 1983, p. 46.
7 D. Lúčanský, V. Bátora, J. Polonský and J. Garaj, in F. M. Everaerts (Editor), *Analytical Isotachophoresis (Analytical Chemistry Symposium Series*, Vol. 6), Elsevier, Amsterdam, 1981, p. 147.
8 F. Mikkers, W. van Gils and W. Roos, in F. M. Everaerts (Editor), *Analytical Isotachophoresis (Analytical Chemistry Symposium Series*, Vol. 6), Elsevier, Amsterdam, 1981, p. 91.
9 P. Boček, B. Kaplanová, M. Deml and J. Janák, *J. Chromatogr.*, 153 (1978) 287.
10 T. Yagi, K. Kojima, H. Nariai and I. Motooka, *Bull. Chem. Soc. Jpn.*, 55 (1982) 1831.
11 T. Hirokawa, S. Kobayashi and Y. Kiso, *J. Chromatogr.*, 318 (1985) 195.
12 I. Motooka, K. Nakazaki, H. Nariai and M. Tsuhako, *J. Chromatogr.*, 367 (1986) 271.
13 I. Motooka, H. Nariai, K. Nakazaki and M. Tsuhako, *J. Chromatogr.*, 295 (1984) 533.
14 T. Hirokawa, M. Nishino, N. Aoki, Y. Kiso, Y. Sawamoto, T. Yagi and J. Akiyama, *J. Chromatogr.*, 271 (1983) DI.
15 T. Hirokawa, S. Kobayashi and Y. Kiso, *J. Chromatogr.*, 410 (1987) 279.
16 J. R. van Wazer, *Phosphorus and its Compounds*, Vol. 1, Interscience, New York, 1958, pp. 628–630.
17 P. R. Haddad and A. L. Heckenberg, *J. Chromatogr.*, 300 (1984) 357.
18 I. Valášková, I. Zelenský, V. Zelenská, A. Komarnicki and D. Kaniansky, *Collect. Czech. Chem. Commun.*, 53 (1988) 515.

Journal of Chromatography, 516 (1990) 478–479
Elsevier Science Publishers B.V., Amsterdam

CHROM. 22 539

Book Review

Protein–dye interactions: development and applications, edited by M. A. Vijayalakshmi and O. Bertrand, Elsevier Applied Science, London, New York, 1989, XIII + 342 pp., price £ 42.80, ISBN 1-85166-316-9.

This book contains papers presented at the *First International Conference on "Modern Aspects of Protein–Dye Interactions: Role in Downstream Processing"*, held at the University of Compiègne, France, in July 1988.

The ever-increasing use of dye-based affinity techniques in many fields of biomedical research and biotechnology is reflected in the 34 contributions from a worldwide gathering of experts. A short historical review of the interactions between dyestuffs and biological matter is presented by J. Porath in the introductory section. Chapter 1 reviews the dye structures and their relevance to protein recognition. C. R. Lowe, in the first report in this chapter, describes many advantages of using dye-ligands, particularly for large-scale applications. Compared with biological ligands, dye-ligands are inexpensive materials available in tonnage quantities worldwide. There is a wide range of chromophores available which are dye-based biologically, chemically and photochemically stable adsorbents potentially sterilizable *in situ* with no degradation of the ligand itself. Because they are reactive materials, they are very easily immobilized to hydroxyl-polymers, generally by a single-step process. Such adsorbents have a high capacity, a very broad binding capability in terms of the complimentary proteins and they are easily re-usable. Several thousand different types of proteins can interact with an immobilized textile dye. Examples are oxidoreductases, phosphokinases and nearly all coenzyme-dependent enzymes, hydrolases, various transferases, a number of proteins which interact with mono- and polynucleotides, synthetases, hydroxylases, nearly all of the glycolytic enzymes, phosphatases, a whole variety of blood proteins and other non-enzyme proteins. A number of studies using classical enzyme kinetics, circular dichroism, affinity labelling, X-ray diffraction and other techniques have been utilized to demonstrate the specificity of dye binding to active sites of proteins. The computer-aided study of the interaction between proteins and dye chromogens presented in the second paper in Chapter 1 ("Structure, preparation and chemistry of reactive dyes", by C. V. Stead) could be interesting to many readers. The last paper of Chapter 1 is about dye fragments in protein-dye interactions (F. Cadelis *et al.*).

A valuable piece of information to readers who want a better understanding of the mechanism of interactions of proteins with different triazine dyes will certainly be Chapter 2, "Physico-chemical aspects of dye–protein interactions". The uses of dye-ligand adsorbents in chromatographic systems are described in Chapter 3. R. K. Scopes shows the advantages of using biospecific elution in purifying proteins from dye-ligand adsorbents. The influence of matrices on dye–protein interactions are described in several contributions. The last paper in Chapter 3 is about the use of dyes in affinity ligand and protein immobilization.

Chapter 4 contains up-to-date contributions on newly developed dye-based affinity methods such as affinity partition, affinity ultrafiltration or affinity precipitation. The roles of added ions (mostly metal ions) in dye–protein interactions are the main topic in Chapter 5. The uses of dye-ligand affinity chromatography for the purification of blood proteins and plant proteins are the subjects of Chapters 6 and 7, respectively.

The last Chapter, 8, is devoted to dyes in molecular biology. The influence of dye binding on the integrity and function of nucleic acids and nucleoproteins, in particular the complexation of polysomes with Coomassie Blue and the progressive unfolding of the conformational states of transfer RNA and ribosomal 5S RNA by methylene blue binding, are described by M. R. Ven Murthy *et al.*

The last part of the book is an Epilogue written by M. A. Vijayalakshmi. Summarizing, she states that it is "stimulating and promising to see that the dye-ligand affinity systems have developed in different spheres and this domain is becoming one of the milestones in the progress of downstream processing in biotechnology". But she goes on to say that, "only very little information is available on the toxicological aspects of the eventual traces of dye molecules or their fragments present in the final product. This situation is undoubtedly an obstacle to a real industrial exploitation of this fast developing field". This has helped to trigger plans for future work, and the topic will be one of the priorities in future meetings on dye–protein interactions.

Prague (Czechoslovakia) JAROSLAVA TURKOVÁ

Journal of Chromatography, 516 (1990) 480–481
Elsevier Science Publishers B.V., Amsterdam

CHROM. 22 597

Book Review

Selectivity and detectability optimizations in HPLC, edited by S. Ahuja, Wiley, New York, 1989, XIII + 610 pp., price US$ 97.75, ISBN 0-471-62645-7.

Accomplishing a separation with the desired selectivity and detectability is obviously a primary goal for practising chromatographers. This book is intended to treat complex problems pertaining to these basic aspects of chromatographic analysis.

In the first chapter, the scope of selectivity and detectability optimization in high-performance liquid chromatography (HPLC) is outlined, including some basic theoretical considerations and classification of some methods used for the optimization of the mobile phase in HPLC. The second chapter, contributed by L. R. Snyder, gives a clear, concise theoretical survey of the physico-chemical phenomena underlying the retention in various modes of HPLC. The next chapter tries to treat the separation mechanism in some more detail, presents some equations used to describe the retention as a function of mobile phase composition and surveys correlations between the retention data and other quantities, such as water–1-octanol partition coefficients, solubility and some structural descriptors. Possibilities of using retention and interaction indices for the calibration of a retention scale as a means of characterizing HPLC columns and the influence of the stationary phase on the selectivity and dynamics of chromatography are discussed. The survey of methods used for the investigation of retention mechanisms in HPLC systems given here is far from being complete and the treatment lacks a discussion and comparison of the relative merits of the individual methods.

Chapter 4 deals with the "conventional" approaches to column and mobile phase selection, based on the properties of sample or solute structures and gives some useful hints for this purpose. The effects of the experimental parameters and of the solute structure on chromatographic behaviour in adsorption, reversed- and normal-bonded-phase chromatography and ion-pair and ion-exchange systems are briefly discussed.

The next four chapters present the theory, separation mechanisms, column packings, solvent selection, mobile phase and solute structure effects on separation and give numerous application examples of separations using normal-phase, reversed-phase, ion-exchange and ion-pair HPLC. Chapter 9 describes specific methods used for the separation of macromolecules (almost exclusively biopolymers; synthetic polymers are hardly mentioned) and Chapter 10, probably the best written, deals with separations of optical isomers by HPLC using both chiral additives to mobile phases and chiral columns of the Pirkle, protein and cavity or inclusion type. These chapters represent the core of the book and contain a considerable amount of information. Unfortunately, the material in the individual chapters is not arranged in a systematic manner and there is significant overlap of the contents of the individual sections on stationary phases, theory and retention mechanism, mobile phase effects, mobile phase selection and optimization and applications, with some unnecessary repetition.

Some of the applications are representative, but many other seem to have been selected and arranged rather arbitrarily, giving too much detail without critical evaluation to offer a good assessment of the most important current trends in the individual modes of HPLC, and on the other hand still lacking some important information to allow the methods described to be used without resorting to the original literature. The reader will find orientation in the material difficult. For example, the chapter on ion-pair separations contains some applications of argentation chromatography, of secondary mobile phase equilibria using the formation of metal chelates or complexes with crown ethers and of improving the separation in reversed-phase chromatography by masking the residual silanol groups in the bonded stationary phase.

There are some omissions, errors and incorrect statements; *e.g.*, it is not true that "reversed-phase chromatography requires a non-polar mobile phase" and that "on silica gel, the elution is essentially independent of molecular weight"; the Henderson–Hasselbach equation (7.6) is given incorrectly; in ion-exchange chromatography, the temperature affects not only the efficiency, but also the selectivity and absolute retention (Table 7.5).

Computer optimization of selectivity is treated in Chapter 11 in 40 pages, which is surprisingly short in comparison with the size of the book. From a great variety of optimization methods, some of the more common are selected and described here: the window diagram method, simplex optimization, interactive methods, overlapping resolution mapping (inaccurately classified as a simplex method), optimization of gradient elution and the commercially available computerized procedures "Dry Lab" and "PESOS" (a grid-search method). Iterative and predictive optimization methods are mentioned only marginally. Some important points, such as peak recognition during the optimization, advantages and disadvantages of various optimization criteria or expert systems for developing a chromatographic separation, are not addressed here. The part describing the "critical band" method is incomprehensible, obviously because of the omission of important parts of the text reproduced from Schoenmakers' "Optimization of Chromatographic Selectivity", p. 206. Eqn. 11.3 for the chromatographic response function (CRF) is wrong and in the subsequent discussion the highest value of CRF means the best and not the worst response.

Chapter 12 lists the properties and some application possibilities for the commonly used HPLC detectors and the last chapter, dealing with detectability optimization, gives the rules for selecting adequate chromatographic conditions to minimize the detection limits and various possible instrumental sources of noise in ultraviolet and fluorescence detectors. Some possibilities for pre- and post-column derivatization are mentioned here and problems connected with indirect photometric detection and on-column laser-induced fluorimetric detection in capillary HPLC are discussed, together with the possibilities for improving peak shape by using various mobile phase additives. There is an error in eqn. 13.10 for the detector contribution to band spreading.

On the whole, this book probably does not offer a significant amount of new information on selectivity and detectability optimization in HPLC in comparison with earlier books and review articles, such as the aforementioned book by Schoenmakers and "Quantitative Analysis Using Chromatographic Techniques", edited by E. Katz. Maybe someone looking for references to the original literature describing applications of various modes of HPLC will find this book of some use.

Pardubice (Czechoslovakia) PAVEL JANDERA

Author Index

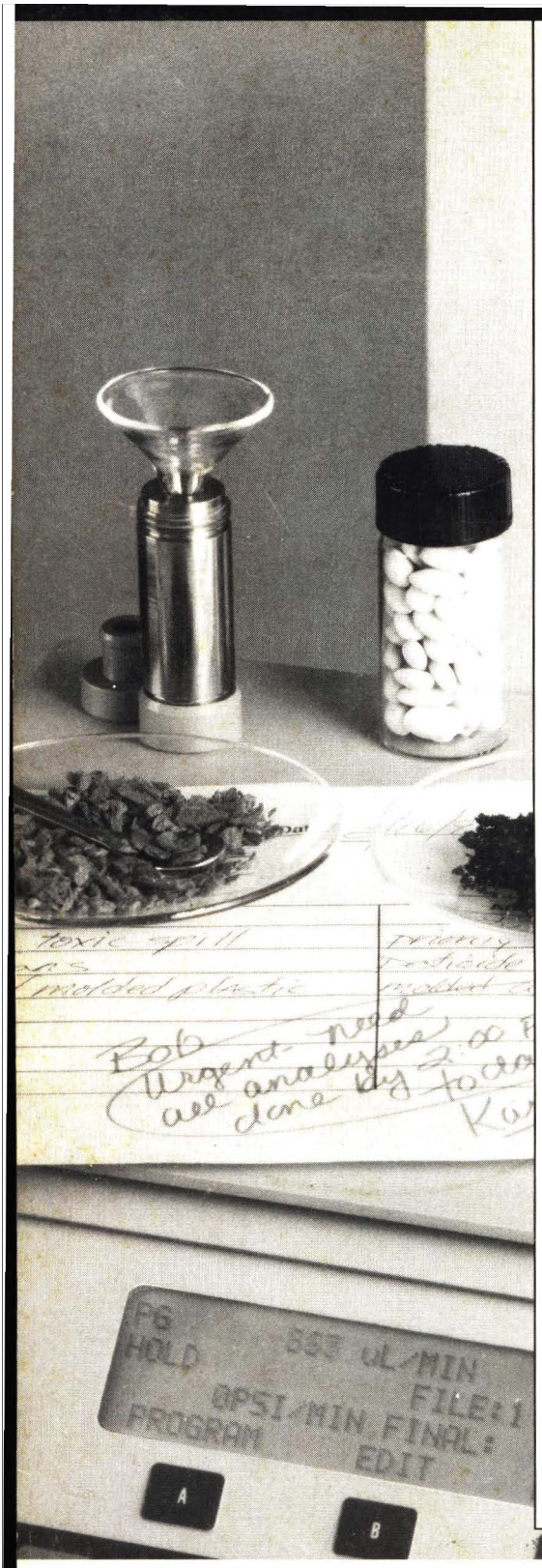

New SFE system extracts your samples in minutes, not days

Say goodbye to tedious liquid-extraction sample prep for GC, HPLC, and UV-vis analyses. Supercritical fluid extraction (SFE) is faster and more efficient; uses inexpensive, nontoxic solvents like CO_2; and allows easy control of selectivity via fluid pressure/density.

And with Isco's new extraction system, SFE just became even more powerful and accessible.

- The SFX™ 2-10 extractor uses quick-load sample cartridges up to 10 ml. Dual-chamber design gives you efficient, continuous operation.
- Capture extractants off-line in minimal solvent volume for immediate analysis.
- New Model 260D pump handles any SFE or SFC technique: flow range is 1 µl to 40 ml/min at up to 7500 psi.
- Digital pump controller lets you quickly set up and recall extraction conditions.

Ask today for details.

Isco, Inc., P.O. Box 5347
Lincoln NE 68505, U.S.A.
Tel. **(800)228-4250**

Isco Europe AG, Bruschstr. 17
CH8708 Mannedorf, Switzerland
Fax: **(41-1)920 62 08**

ISCO

Distributors • **Australia:** Australian Chromatography Co. • **Austria:** INULA • **Belgium:** SA HVL NV • **Canada:** Canberra Packard Canada, Ltd. • **Denmark:** Mikrolab Aarhus **Finland:** ETEK OY • **France:** Ets. Roucaire, S.A. • **Germany:** Colora Messtechnik GmbH • **Hungary:** Lasis Handelsges. mbH • **Italy:** Analytical Control Italia S.p.A. • **Japan:** JSI Co. Ltd. • **Korea:** Sang Chung, Ltd. • **The Netherlands:** Beun-de Ronde B.V. • **Norway:** Dipl. Ing. Houm A.S. • **Spain:** CHEMICONTROL, S.L. • **Sweden:** SAVEN AB • **Switzerland:** IG Instrumenten-Gesellschaft AG • **U.K.:** Life Science Laboratories, Ltd. •

PUBLICATION SCHEDULE FOR 1990

Journal of Chromatography and Journal of Chromatography, Biomedical Applications

MONTH	J	F	M	A	M	J	J	A	S	O	N	D[a]
Journal of Chromatography	498/1 498/2 499	500 502/1	502/2 503/1 503/2 504/1	504/2 505/1	505/2 506 507 508/1	508/2 509/1 509/2 510	511 512 513	514/1 514/2 515	516/1 516/2 517 518/1	518/2 519/1	519/2 520 521/1 521/2	
Cumulative Indexes, Vols. 451–500		501										
Bibliography Section		524/1		524/2		524/3		524/4		524/5		
Biomedical Applications	525/1	525/2	526/1	526/2 527/1	527/2	528/1 528/2	529/1	529/2 530/1	530/2	531 532/1	532/2 533	

[a] The publication schedule for further issues will be published later.

INFORMATION FOR AUTHORS

(Detailed *Instructions to Authors* were published in Vol. 513, pp. 413–416. A free reprint can be obtained by application to the publisher, Elsevier Science Publishers B.V., P.O. Box 330, 1000 AH Amsterdam, The Netherlands.)

Types of Contributions. The following types of papers are published in the *Journal of Chromatography* and the section on *Biomedical Applications:* Regular research papers (Full-length papers), Notes, Review articles and Letters to the Editor. Notes are usually descriptions of short investigations and reflect the same quality of research as Full-length papers, but should preferably not exceed six printed pages. Letters to the Editor can comment on (parts of) previously published articles, or they can report minor technical improvements of previously published procedures; they should preferably not exceed two printed pages. For review articles, see inside front cover under Submission of Papers.

Submission. Every paper must be accompanied by a letter from the senior author, stating that he is submitting the paper for publication in the *Journal of Chromatography*. Please do not send a letter signed by the director of the institute or the professor unless he is one of the authors.

Manuscripts. Manuscripts should be typed in double spacing on consecutively numbered pages of uniform size. The manuscript should be preceded by a sheet of manuscript paper carrying the title of the paper and the name and full postal address of the person to whom the proofs are to be sent. As a rule, papers should be divided into sections, headed by a caption (*e.g.*, Abstract, Introduction, Experimental, Results, Discussion, etc.). All illustrations, photographs, tables, etc., should be on separate sheets.

Introduction. Every paper must have a concise introduction mentioning what has been done before on the topic described, and stating clearly what is new in the paper now submitted.

Abstract. Full-length papers and Review articles should have an abstract of 50–100 words which clearly and briefly indicates what is new, different and significant. (Notes and Letters to the Editor are published without an abstract.)

Illustrations. The figures should be submitted in a form suitable for reproduction, drawn in Indian ink on drawing or tracing paper. Each illustration should have a legend, all the *legends* being typed (with double spacing) together on a *separate sheet*. If structures are given in the text, the original drawings should be supplied. Coloured illustrations are reproduced at the author's expense, the cost being determined by the number of pages and by the number of colours needed. The written permission of the author and publisher must be obtained for the use of any figure already published. Its source must be indicated in the legend.

References. References should be numbered in the order in which they are cited in the text, and listed in numerical sequence on a separate sheet at the end of the article. Please check a recent issue for the layout of the reference list. Abbreviations for the titles of journals should follow the system used by *Chemical Abstracts*. Articles not yet published should be given as "in press" (journal should be specified), "submitted for publication" (journal should be specified), "in preparation" or "personal communication".

Dispatch. Before sending the manuscript to the Editor please check that the envelope contains four copies of the paper complete with references, legends and figures. One of the sets of figures must be the originals suitable for direct reproduction. Please also ensure that permission to publish has been obtained from your institute.

Proofs. One set of proofs will be sent to the author to be carefully checked for printer's errors. Corrections must be restricted to instances in which the proof is at variance with the manuscript. "Extra corrections" will be inserted at the author's expense.

Reprints. Fifty reprints of Full-length papers, Notes and Letters to the Editor will be supplied free of charge. Additional reprints can be ordered by the authors. An order form containing price quotations will be sent to the authors together with the proofs of their article.

Advertisements. Advertisement rates are available from the publisher on request. The Editors of the journal accept no responsibility for the contents of the advertisements.